If art is long, science is much longer, and of all sciences Zoology makes the greatest drafts on time for securing synthetic results. …Even if every conclusion it expresses should turn out to be untenable, there are times when it is useful to throw the windows of the mind wide open.

Walter Garstang (1928), Presidential Address to the British Association for the Advancement of Science, Section D

****

ギリヤークじんはなぜひろいドウロをあるかないでもりのぬかるみをあるくのか。
…ドウロがべんりでもギリヤークじんたちはドウロからはなれてもりをあるいたほうがラクだ。ドウロをあるくにはあるくことをはじめからつくりなおさなくてはならない。あるくことをつくりなおすとほかのこともつくりなおさなくてはならない。
…もりではきをつけるように。だいじなものはもりのなかにありもりにはリトル・ピープルがいる。リトル・ピープルからガイをうけないでいるにはリトル・ピープルのもたないものをみつけなくてはならない。

WHY DO THE GILYAKI WALK THROUGH THE BOGS AND REFUSE TO TAKE THE TRAIL.
…THE GILYAKI HAVE AN EASIER TIME WALKING THROUGH THE FOREST OFF THE TRAIL NO MATTER HOW INCONVENIENT. YOU HAVE TO REINVENT WALKING FROM SCRATCH TO WALK ON A PATH. YOU HAVE TO REIVENT OTHER THINGS TO REINVENT WALKING.
…BE CAREFUL IN THE FOREST. IMPORTANT THINGS ARE IN THE FOREST AND IN THE FOREST LURK THE LITTLE PEOPLE. TO PROTECT YOURSELF FROM THE LITTLE PEOPLE YOU MUST FIND WHAT THE LITTLE PEOPLE HAVE NOT.

Haruki Murakami (2009), 1Q84
(Fukaeri's letter translated by T. M.)

University of Alberta

Comparative Analysis of the Anatomy of the Myxinoidea
and the Ancestry of Early Vertebrate Lineages

by

Tetsuto Miyashita

A thesis submitted to the Faculty of Graduate Studies and Research
in partial fulfillment of the requirements for the degree of

Master of Science
in
Systematics and Evolution

Department of Biological Sciences

Fall 2012
Edmonton, Alberta

ABSTRACT

The question of whether a hagfish is a true vertebrate or not has profound implications about the ancestry of the clade. New anatomical evidence allows a test of their systematic position. With dissections and serial sections of original specimens, and with a literature review, a comparative analysis revealed homologues in the chondrocranium and musculature of hagfish shared with lampreys, gnathostomes, and extinct jawless vertebrates. The analysis also identified intermediate characters that foreshadow gnathostomes, including a possible precursor of the synovial joint and tendon-like pseudocartilages. However, the hierarchical organization of the homologues presented an enormous challenge to recovering a phylogenetic signal. The traditional morphological view of the vertebrate head was overturned to formulate new evolutionary models for the ancestry of vertebrates and the origin of the gnathostome jaw. A phylogenetic analysis placed hagfish more basal than other living vertebrates, and a new definition was proposed for the clade Vertebrata.

ACKNOWLEDGEMENTS

I have so much to owe to my two wonderful graduate advisors, Rich Palmer and Philip Currie. Both scientifically and personally, they are great examples by which I always wish to live. I thank Rich for opening up my eyes to the diversity of animals and for patiently guiding me at every stage of my academic development since 2007. I thank Philip for being my academic father — for taking me under his wings when I moved to Drumheller in 2003 and for training me to become a researcher ever since. Above all, I appreciate both for giving me freedom to pursue my interests even when they did not exactly align with their own. Their partners, Lois Hammond and Eva Koppelhus, have been equally helpful and supportive. If not for Eva, I would have turned into someone much less capable and much less responsible.

This thesis is a tribute to two great schools of zoology that my two advisors represent. The Romer school would use everything they could — anatomy and development, fossils and embryos, labs and fields — to the finest possible details, and would typically mess up a beautiful phylogeny in an inspiring manner. I made my best efforts in the main body of the thesis to follow that Romer tradition traced back to Thomas Henry Huxley and Francis Maitland Balfour (who descended from Johannes Müller, the first anatomist to describe hagfish morphology, via Albert von Kölliker, Carl Gegenbaur, Ernst Haeckel, and Anton Dohrn) and passed down the line through Henry Fairfield Osborn, William King Gregory, Alfred Sherwood Romer, and Robert Lynn Carroll to Philip. Although cut from this thesis in order to reduce its length, an investigation of handed behaviours in chordates (T. M. and A. R. Palmer in review; the American Naturalist) was originally the other half of the thesis. It is a tribute to another great school in zoology founded by Evelyn Hutchinson and passed down via Alan Kohn, Frederick Smith, Richard Strathmann, and Robert Paine to Rich. I will remain an admirer of their knack in turning curious natural historical observations into sophisticated evolutionary and ecological insights. Education in these two great schools of zoology has been a fortune that I will always appreciate.

I am grateful to my last committee member Brian Hall (Dalhousie University) and other mentors who educated me. In particular, Richard Strathmann (Friday Harbor Laboratories) helped me realize exactly what sort of research I wanted to do. Shigeru Kuratani (RIKEN) and — although I have never personally met — Philippe Janvier (Muséum National d'Histoire Naturelle) had a tremendous influence on the development of my ideas. The following people have been significant sources of information and encouragement: Ted Allison, Greg Goss, Rob Holmes, Takuya Konishi, Sally Leys, Richard Moses, Alison Murray, the late Joe Nelson, Heather Proctor, and Mark Wilson (University of Alberta); Jason Anderson (University of Calgary); Don Brinkman, Dave Eberth, Jim Gardner, Don Henderson, Andy Neuman, Mike Newbrey, Darren Tanke, and François Therrien (Royal Tyrrell Museum of Palaeontology); Mike Coates (University of Chicago); David Evans (Royal Ontario Museum); Tim Higham (University of California Riverside); Hans Larsson (McGill University); Erin Maxwell (Museum für Naturkunde Berlin); Tsutomu Miyake (Jikei Medical University); Michael Ryan (Cleveland Museum of Natural History); Tamaki Sato (Tokyo Gakugei University); and Lawrence Witmer (Ohio University).

I am lucky to have great colleagues with whom I always had stimulating discussion: past and present members of the Palmer, Currie, Murray, Caldwell, Wilson, and Leys labs (University of Alberta); Karen Chan and Danny Grümbaum (University of Washington); Federico Fanti (University of Bologna); Ariana Paulina Carabajal (Museo Carmen Funes); and Eric Snively (Ohio University). I thank the following people for technical assistance at various stages of the research (with no particular order): the late Randy Zohner, Dave Riddell, Janice Pierce, Shirley Pakula, Katie Gale, Emy Montgomery, AJ Chapelski, Bruce Cameron, Tao Eastham, Dane Stabel (Bamfield Marine Sciences Centre); Victoria Arbour, Marjan Barazandeh, Mike Burns, Miriam Reichel, Al Lindoe, Clive Coy, Amanda Kahn, Wanda Vivequin, Neel Doshi (University of Alberta); and Stacey Markman (Friday Harbor Laboratories). In particular, Arlene Oatway (University of Alberta) trained me with basic histological techniques. Wei Liu and Benedikt Hallgrímsson (University of Calgary) performed the microCT scan on hagfish.

Staff at the University of Alberta Cameron Library tracked down numerous obscure references and delivered them to me in a timely manner. Without them, this thesis would not be the same. I prepared all photographs and illustrations in this thesis unless otherwise noted.

My graduate program (this thesis and other projects not included here) was supported by Alberta Ingenuity Fund Graduate Scholarship, Lerner Gray Memorial Grant, Bamfield Marine Sciences Centre WCUMSS Award (2), Dinosaur Research Institute Student Projects (3), Rene Vandervelde Award, Jurassic Foundation Research Grant, Friday Harbor Laboratories Student Scholarship (sponsored by Dennis Willows), Canadian Society of Zoologists Travel Grant, the Society of Vertebrate Paleontology and Jackson T. School of Geology Travel Grant, and Okinawa Institute of Science and Technology Travel Fund to me, and by a NSERC Discovery Grant to Rich Palmer. Animals were captured, maintained, and studied under the protocols approved by the animal care committees at Bamfield Marine Sciences Centre and the University of Alberta.

I thank my friends and family home, here, and elsewhere for being a cause for my hard work. Though too numerous to name, they know who they are, and this includes those who went to Ohwada Elementary School, Dai-ichi Junior High School, and Hinodai Senior High School with me. Brent, Dolores, and Bryna Andressen, Ariana Paulina Carabajal, Federico Fanti and Mariastella Paderni, Kazuhiro Magome, Hisao Nakagawa, Miyuki Tajima, Lida Xing, and Nana Wong deserve special mention and acknowledgement. My grandparents, Takeshi and Kimie Miyashita, Chizuko Kuroda, and the late Hidehiko Kuroda, have always watched over me. My parents, Junichi and Kanae Miyashita, have supported me all the way through, even when it meant that they saw me off to a rural town in a foreign land before even graduating from a high school. Finally, Kesia Andressen Miyashita is the most patient human being I know. I can’t think of anyone else remotely capable of tolerating three straight months of my writing this thesis, and she tolerated it while writing her own! Her support, care, and love sustain all that I do as a scientist, and it is my wish to help her as much in return.

TABLE OF CONTENTS

Comparative Analysis of the Anatomy of the Myxinoidea and the Ancestry of Early Vertebrate Lineages

LIST OF TABLES

LIST OF FIGURES

ABBREVIATIONS

Some elements may overlap in terminology between different taxa, even though homology between the elements is tentative. In some other cases, different elements that are unlikely homologues of each other have been traditionally labeled with the same term (e.g. cornual process in hagfish and lampreys). To avoid confusion, different labels are used in each of the taxa for the overlapped, potentially non-homologous terminology as noted in parentheses.

a.an	Anlage of annular cartilage
acp	Acrochordal process
a.cp	Anlage of cornual plate
adp	Anterior dorsal plate
a.hy	Anlage of hyoid skeleton
a.ling	Anlage of lingual apparatus
a.lpa	Anlage of anterior lateral plate
a.lpp	Anlage of posterior lateral plate
a.mvc	Anlage of medioventral cartilage
anc	Annular cartilage
apc	Apical cartilage
a.pis	Anlage of piston cartilage
arc	Arcualia
a.stc	Anlage of styliform cartilage
a.stl	Anlage of stylet cartilage
a.vl	Anlage of velar skeleton
b	Brain
bc	Basal cartilage
bcl	Lateral wall of braincase
bra	Branchial arch
brb	Branchial basket
brc	Ceratobranchial
brca	Branchial canal
brda	Afferent branchial duct
brde	Efferent branchial duct
bre	Epibranchial
brh	Hypobranchial
brp	Pharyngobranchial
brx	Extrabranchial
brxh	Extrabranchial cartilage (hagfish)
bs	Branchial slit
bsc	Branchial superficial constrictors
cap	Capillary

ch	Cardinal heart
coc	Copular cartilage
cop	Cornual process (hagfish)
cp	Cornual plate (lamprey)
cpr	Cornual process (lamprey)
da	Dental apparatus
dalb	Lateral basal plate of dental apparatus
dalp	Anterior lateral process of midline plate
dap	Apical tooth plate
ddm	Dorsal median tooth
ddmp	Periodontal tissue for dorsal median tooth
dlb	Dosolateral blastema
dlbp	Lateral basal plate of dental apparatus
dlp	Lateral tooth plate
dlpp	Lateral posterior process of lateral basal plate
dmb	Dorsal midline bar
dmbp	Medial basal plate of dental apparatus
dmp	Medial tooth plate
dmpp	Medial posterior process of lateral basal plate
dp	Dental papilla
dplp	Posterior lateral process of midline plate
dsl	Dorsum sellae
dsp	Suprapical tooth plate
ebc	Extrabranchial cartilage (gnathostomes)
ehy	Extrahyal
epke	Epipokal epithelial layer
epm	Epaxial myotomes
es	Esophagus
f	Facial segment
ff	Facial foramen
fph	Fold of pharynx for velum
gp	Gill pouch
gpf	Foramen for glossopharyngeal nerve
hf	Hypophyseal fenestra
hmf	Hyomandibular fenestra
hmn	Hyomandibular nerve (VII)
hph	Hyoid and post-hyoid domains
hsc	Hyoid superficial constrictors
hyo	Hyoid domain
iel	Inner epithelial layer
if	Intermediate fibre
ifs	Interfenestral strut

ima	Intermandibularis
IX	Glossopharyngeal nerve
ks	Keratinous sheath
lab	Labial muscles
lal	Ventral longitudinal arch
lau	Dorsal longitudinal arch
lcal	Anterolateral lingual cartilage
lcam	Anteromedial lingual cartilage
lcdl	Ventral distal lingual cartilage
lcdu	Dorsal distal lingual cartilage
lcm	Middle lingual cartilage
lcp	Posterior lingual cartilage
lep	Lens placode
lf	Lingual foramen
lig	Ligament
ling	Lingual apparatus
llb	Lateral longitudinal bar
llc	Lower lip cartilage
llf	Foramen for lateral line
lmp	Lateral mouth plate
lpa	Anterior lateral plate
lpp	Posterior lateral plate
m.abd	M. adductor branchialis dorsalis
m.abv	M. adductor branchialis ventralis
m.am	M. adductor mandibulae
m.ams	M. adductor mandibulae superficialis
man	Mandibular domain
m.ang	M. annuloglossus
m.ann	M. annularis
max	Maxillary process
m.bag	M. basilariglossus
m.bas	M. basilaris
m.bca	M. buccalis anterior
m.bcs	M. buccalis superficialis
m.cap	M. cardioapicalis
m.cb	M. constrictor buccalis
m.cbe	M. constrictor branchialis externus
m.cbi	M. constrictor branchialis internus
m.cbr	M. constrictor branchialis
m.cbs	M. constrictor branchialis superficialis
mcc	Mucocartilage
m.ccs	M. constrictor cornualis superficialis

m.cgi	M. constrictor glossus internus
m.cgl	M. cornuoglossus
m.cgo	M. copuloglossus obliquus
m.cgr	M. copuloglossus rectus
m.ch	M. constrictor hyoideus
m.cl	M. craniolingualis
m.coa	M. cornual labialis
m.cob	M. coracobranchialis
m.coh	M. coracohyoideus
m.com	M. coracomandibularis
m.coi	M. cornual lingualis
m.con	M. cornealis
m.cp	M. constrictor pharyngis
m.crt	M. cornuotaenialis
m.cuc	M. cucullaris
m.dev	M. depressor veli
mec	Meckel’s cartilage
m.elb	M. elevator labialis ventralis
m.epb	M. epibranchialis
meso	Oral mesenchyme
m.hyb	M. hypobranchialis (lamprey)
m.ibr	M. interbranchialis
m.ihy	M. interhyoideus
m.imd	M. intermandibularis
m.lhm	M. levator hyomandibulae
m.lpq	M. levator palatoquadratus
m.lt	M. lingual tentacularis
mna	Mandibular adductors
m.na	M. nasalis
m.nl	M. nasolingualis
m.ob	M. obliquus
m.oba	M. obliquus anterior
m.obp	M. obliquus posterior
m.ol	M. otic lingualis
mp	Midline plate of dental apparatus
m.pa	M. parietalis
m.par	M. parietalis (lamprey)
m.pal	M. palatolabialis
m.pc	M. palatocoronarius
m.pdl	M. protractor dentalis lateralis
m.pdm	M. protoractor dentalis medialis
m.pha	M. pharyngicus anterior
m.php	M. pharyngicus posterior
m.plp	M. palatolingualis profundus
m.pls	M. palatolingualis superficialis

mpo	Perioptic membrane
m.por	M. preorbitalis
m.prb	M. prebranchialis
m.prp	M. perpendicularis
m.prv	M. protractor veli
m.rdl	M. retractor dentalis lateralis
m.rdm	M. retractor dentalis major
m.re	M. rectus
m.rea	M. rectus anterior
m.rei	M. rectus inferior
m.rep	M. rectus posterior
m.res	M. rectus superior
m.rl	M. retractor lingualis
m.rld	M. retractor labialis dorsalis
m.rlv	M. retractor labialis ventralis
m.rpa	M. retractor papillaris
m.sbe	M. sphincter branchialis externus
m.sbi	M. sphincter branchialis internus
msc	Mandibular superficial constrictors
m.snp	M. subnasalis profundus
m.sns	M. subnasalis superficialis
m.so	M. subocularis
m.spc	M. spinocopularis
m.spo	M. supraocularis
m.spr	M. spiracularis
m.sta	M. styloapicalis
m.stt	M. stylotectalis
m.tcl	M. tectolateralis
m.tap	M. tendinoapicalis
m.tp	M. tentacularis posterior
m.tsa	M. tectospinosus anterior
m.tsp	M. tectospinosus posterior
m.vad	M. craniovelar anterior dorsalis
m.vav	M. craniovelar anterior ventralis
mvc	Medioventral cartilage
m.vcr	M. velocranialis
m.vhy	M. velohyoideus
m.vp	M. craniovelar posterior
m.vs	M. spinovelaris
m.vth	M. velothyroideus
na	Nasal arch
na1r	Nasohypophyseal rim of first nasal arch
nap	Posterior-most nasal arch
nap2	Second-most posterior nasal arch

nbl	Lower nasohypophyseal barbell
nbs	Nasobuccal shelf
nbu	Upper nasohypophyseal barbell
nc	Nasal capsule
ncb	Nasal capsule basket
ncbl	Longitudinal bar of nasal capsule basket
nch	Notochord
nchs	Sheath for notochord
ncpb	Nasopharyngeal bar of nasal capsule basket
ncr	Roof of nasal capsule
nhc	Nasohypophyseal complex
np	Nasal papilla
npb	Nasopharyngeal bar of nasal capsule basket
npd	Nasopharyngeal duct
npp	Nasopharyngeal plate
ns	Nasal sac
nt	Nasal tube
oc	Otic capsule
occ	Foramen for occulomotor nerve
oe	Olfactory epithelium
oel	Outer epithelial layer
olp	Olfactory placode
on	Olfactory neuron
oni	Innervation by olfactory neuron
onl	Orbitonasal lamina
or	Orbital cartilage
orc	Oral cavity
ore	Oral epithelium
ota	Otic-trigeminal arch
pa	Palatal arch
PA1…	Pharyngeal arch number
pac	Palatal commissure
pcc	Pericardial cartilage
pc	Perichondrium
pch	Parachordal domain/skeleton
pchc	Parachordal cartilage
pcpl	Perichondral extension of posterior lingual cartilage
pdp	Posterior dorsal plate
pern	Perforating nerve (V_2)
ph	Pharynx
phcd	Pharyngocutaneous duct
pia	Pilla antotica
pisc	Piston cartilage
pkc	Pokal cell

pkca	Precursor of pokal cell
pkcn	Pokal cone
plae1	First external pharyngolingual arch
plae2	Second external pharyngolingual arch
plai1	First internal pharyngolingual arch
plai2	Second pharyngolingual arch
plc	Polar cartilage
plf1	First pharyngolingual fenestra
plf2	Second pharyngolingual fenestra
pq	Palatoquadrate
prf	Prootic fenestra
prm	Premandibular domain
prr	Preoptic root for orbital cartilage
ps	Pharyngeal slit
pz	Proliferation zone
r	Rostrum
r1, 2...	Rhombomere number
rap	Rathke's pouch (hypophyseal placode)
rf	Red fibre
sap	Suprapical cartilage
sc	Spinal cord
se	Sensory epithelium
sen	Sensory neuron
slg	Slime gland
snc	Subnasal cartilage
soa	Subocular arch
soac	Commissure of subocular arch
sob	Suotic blastema
spr	Spiracle
ssc	Semicircular canal
stc	Styliform cartilage
stl	Stylet cartilage
t	Tooth
taa	Anterior transverse arch
tap	Posterior transverse arch
tc	Cornu trabeculae
tcl	Lateral tentacular cartilage
tclr	Labial ramus of lateral tentacular cartilage
tco	Oral tentacular cartilage
tcpp	Perioral process of lateral tentacular cartilage
trpr	Paranasal ramus of lateral tentacular cartilage
tcpt	Paranasal tuber of lateral tentacular cartilage

tcup	Upper nasohypophyseal process of lateral tentacular cartilage
tea	Anterior tectal cartilage
tep	Posterior tectal cartilage
tf	Trigeminal fenestra
tk	Keratinous tooth
t.na	Tendon of m. nasalis
tp	Terminal process
t.pdl	Tendon for m. protractor dentalis lateralis
t.pdm	Tendon for m. protractor dentalis medialis
tr	Trabecula
trc	Trabecular commissure
trcl	Foramen for trochlear nerve
t.rdm	Tendon of m. retractor dentalis major
trp	Trabecular plate
trr	Trematic ring
ulc	Upper lip cartilage
V_1	Trigeminal nerve, ophthalmic branch
V_2	'Maxillomandibullar' trigeminal nerve*
V_{2m}	Motor component of 'maxillomandibular' trigeminal nerve*
V_{2p}	Posterior branch of 'maxillomandibular' trigeminal nerve*
V_{2s}	Sensory component of 'maxillomandibular' trigeminal nerve*
Vg	Trigeminal ganglion
VII	Facial nerve
vlb	Lower longitudinal bar
vlf	Velar fenestra
vlk	Velar knob
vll	Lateral velar cartilage (hagfish)
vllb	Lateral velar bar (lamprey)
vlm	Medial velar cartilage (hagfish)
vlmb	Medial velar bar (lamprey)
vlp	Velar process
vls	Velar skeleton
vlspa	Anterior suprapharyngeal process
vlspp	Posterior suprapharyngeal process
vsp	Visceral plate
wf	White fibre
X	Vagus nerve

Chapter 1 – Introduction: Historical Review of Living Jawless Fishes and Early Vertebrate Phylogeny

You reproach me with unbelief: "You see, but you don't believe."
But, my friend, I am not alone in that, all of us there are stirred up now,
and it all comes from your science.
Fyodor Dostoevsky (1880), The Brothers Karamazov

1.1. HAGFISH AS A KEY TO UNDERSTAND EARLY VERTEBRATE EVOLUTION

Of all questions pursued in zoology today, few topics are as controversial and as puzzling as the origin and early evolution of vertebrates. Hagfish are central to this long-standing scientific endeavor, because they appear to sit at the boundary that sets vertebrates apart from invertebrates. Do they form an outgroup to vertebrates or represent a lineage derived from the most basal vertebrates? If the former is true, hagfish likely document a crucial evolutionary stage that bridges vertebrates and invertebrate chordates such as lancelets and tunicates. In this case, any character present in all vertebrates and absent in hagfish would likely be a vertebrate synapomorphy. If the latter hypothesis is true, hagfish constrain possible character states for the vertebrate ancestor. Under this scenario, hagfish somehow lost vertebrate synapomorphies (such as true arcualia and two semicircular canals) that all other vertebrates conserved, and/or lampreys independently evolved these structures. Such a radical pattern of character evolution challenges a more static view of early vertebrate evolution as a step-wise transition toward jaw-bearing vertebrates (gnathostomes). Either way, hagfish are closer in form to the evolutionary root of vertebrates than any other living taxon — with a possible exception of lampreys — and as such, comparative morphology of hagfish could reveal what makes a vertebrate a vertebrate.

I set out to examine the chondrocranium and cranial musculature in a representative taxon, the northeastern Pacific hagfish (*Eptatretus stoutii*). This new information is then combined with a detailed comparative analysis of the cranial anatomy of other hagfish species, lampreys, and gnathostomes. The purpose of this analysis is to address the following key questions regarding the origin and early evolution of vertebrates: 1) Does morphological evidence support cyclostome (hagfish + lamprey) monophyly? 2) Do hagfish have evolutionary precursors to gnathostome-specific characters that could later allow the evolution of jaws? 3) Do fossil jawless vertebrates show osteological correlates for structures homologous between hagfish and lampreys? 4) Does phylogenetic inference of morphological characters support the view of early vertebrate evolution as step-wise acquisitions of gnathostome conditions? 5) What evolutionary scenario for early vertebrates can reconcile morphological and developmental evidence? Following a brief review of the major taxa that were the focus of this study, I lay out a more detailed rational with specific hypotheses that were tested.

1.2. LIVING CYCLOSTOMES

Hagfish (Myxinoidea) and lampreys (Petromyzontiformes) represent two surviving lineages of jawless fish (Appendix 1.1 for phylogenetic and anatomical terminology). They resemble each other in having elongate bodies, horny teeth, and single nasohypophyseal apertures, and lacking bones, jaws, and paired fins. Phylogenetically, these cyclostomes are consistently placed near the root of vertebrates (in the broad sense). Lampreys are used to constrain the node of Vertebrata, whereas hagfish act as a wildcard taxon at the base of the vertebrate tree. Detailed anatomical description of each is presented in subsequent chapters. Here, I provide brief overview of hagfish and lampreys, with some curious natural historical or cultural references.

1.2.1 Hagfish

Six living genera of hagfish are known (*Eptatretus*, *Myxine*, *Nemamyxine*, *Neomyxine*, *Notomyxine*, and *Paramyxine*), and collectively occur in all oceans, all climatic zones, and depths ranging from 10 to 2,000 m (Fernholm 1998; Cavalcanti and Gallo 2008). Among these genera, *Eptatretus* and *Myxine* are each a monophyletic and stable genus, whereas other genera, especially *Paramyxine*, may represent a polyphyletic assemblage or a lineage within either *Eptatretus* or *Myxine* (Kuo et al. 2003). *Eptatretus* is distinguished from *Myxine* in retaining marginally functional, photosensitive eyes and having an external pore for each gill pouch (Fernholm 1998). The consensus is that *Eptatretus* is morphologically more plesiomorphic with respect to *Myxine* (Fernholm 1998; Martini 1998). This thesis therefore focuses on the northeastern Pacific hagfish *Eptatretus stoutii*, although comparisons are made to the Atlantic hagfish *Myxine glutinosa*, the South African inshore hagfish *Eptatretus hexatrema*, and the Japanese inshore hagfish *Eptatretus burgeri*.

The external appearance of hagfish is striking in the absence of general vertebrate characteristics such as jaws, bones, or paired fins. A single median fin is restricted to the caudal region. Four pairs of barbels develop around the aperture of the nasohypophyseal canal and the mouth. The eyes are greatly reduced and lack lenses, and are either covered with skin in *Eptatretus* or buried underneath the trunk musculature in *Myxine*. Nonetheless, the lens placode does appear during development (Kuratani and Ota 2008). The gills are wrapped within a series of isolated pouches in mid-trunk rather than set between cartilaginous arches. Slime glands develop along both sides of the body, one pair per segment. These glands secrete copious amounts of slime, which can clog the gills of other fish in a laboratory setting (Lim et al. 2006) and has been observed to deter predatory fish in the wild (Zintzen et al. 2011). They are quite sedentary in captivity, often resting in place over a week (T.M. pers. obs.). Coupled with their low metabolism, perhaps their ability to absorb amino acids from the skin and gills accounts for the inactivity (Glover et al. 2011). Although they are generally considered benthic scavengers, the

majority of stomach contents consist of benthic invertebrates such as polychaetes (Strahan 1963; Martini 1998). Such documented predatory behavior in the wild confirms that hagfish are more than just carrion feeders (Zintzen et al. 2011). Because of the elongate body shape and the lack of a hard skeleton, hagfish are extremely flexible. They can even tie themselves in a knot to tear flesh from potential food or to wash themselves of their own slime (Worthington 1905; Adam 1960).

My personal experiences with hagfish slime include one individual filling a 25L bucket with slime in less than a minute. According to an anecdote around Bamfield, British Columbia, Canada, hagfish slime can substitute for egg albumen when making scones. In fact, students of Bamfield Marine Sciences Centre allegedly made scones using hagfish slime in 2005. A Google search recovered the recipe in the blog "*The Museum of Awful Food*" (Appendix 1.2). In Japan, hagfish are occasionally fried or barbecued. Skewered and barbecued hagfish are a delicacy in Niigata Prefecture along the coast of the Sea of Japan and believed among locals as male tonic (Honma 1998). In the Korean Peninsula, both slime and meat are used for a variety of dishes that add to the rich cuisine of the region, including hagfish stir-fry, kkomjangeo bokkeum (Y. Ito pers. comm. 2009).

1.2.2. Lampreys

Ten genera of lampreys from three families are known, and they occur in freshwater and marine systems in temperate zones of all continents except Africa. Each family appears to represent a valid clade (geotriids, mordaciids, and petromyzontids), the first two of which occur in the southern hemisphere and the last of which is a large monophyletic clade restricted to the northern hemisphere (Gill et al. 2003; Renaud 2011). In this thesis, the sea lamprey *Petromyzon marinus* and the European river lamprey *Lampetra fluvialis* are used for comparison with hagfish.

Lampreys lack general vertebrate characteristics such as mineralized skeletons, jaws, and paired fins (reviewed by Janvier 1996a). However, the cartilaginous skeleton is better developed in lampreys than in hagfish. In particular, the cartilaginous branchial bars are complete whereas they are lacking in hagfish.

Lamprey adults have functional, image-forming eyes with extraocular muscles. The nasohypophyseal canal is a blind tube. In addition to the caudal fin, a dorsal fin develops along the midline. Vertebral elements form beside the notochord. These seemingly derived characters are absent from hagfish. For this reason, lampreys have always been considered 'true' vertebrates (Janvier 2008).

Lampreys are either anadromous or strictly freshwater. The larvae, the distinctive ammocoetes, are filter-feeders and undergo metamorphosis (Nelson 2006). The eyes are fully developed and the body is elongate and cylindrical. The mouth sits within a large funnel with horny teeth, with which they bore into other fish and suck blood. The adults of some genera (*Eudontomyzon*, *Geotria*, and *Lampetra*) are either non-parasitic predators or non-feeding (Renaud 2011). The blood-sucking ectoparasitic lifestyle has been long appreciated by humans to the extent that convicted slaves were thrown into a pond of lampreys during the Roman Empire. According to Seneca (40), Caesar released a slave who was almost executed in Vedius Pollio's lamprey pond, and Augustus later punished Vedius for the cruelty. Plutarch (976) recorded an event in which the senator Dmitius teased Crassus the orator about crying over his deceased pet lampreys despite the fact that Crassus buried "three wives without ever shedding a tear." Von Hofmannsthal (1902) included the same episode as described by Aelian and Macrobius in *The Letter of Lord Chandos*. This fictional letter dated 1603 and addressed to Francis Bacon notes:

> "And in my mind I compare myself from time to time with the orator Crassus, of whom it is reported that he grew so excessively enamoured of a tame lamprey — a dumb, apathetic, red-eyed fish in his ornamental pond — that it became the talk of the town; and when one day in the Senate Domitius reproached him for having shed tears over the death of this fish, attempting thereby to make him appear a fool, Crassus answered, "Thus have I done over the death of my fish as you have over the death of neither your first nor your second wife.""

Lampreys are important food for humans worldwide. The most cerebrated example of this delicacy is a pie of lamprey baked in syrup favored in the English court (reviewed in Stradley 2004). The city of Gloucester would send a lamprey pie to the monarch every Christmas until the 19th century. It upset the medieval tradition in 2012 when local lampreys were so scarce that the Royal Family was forced to import lampreys from Lake Huron: not only monarchs no longer dine on English lampreys, but the import only has a 50:50 chance of being a Commonwealth lamprey that grew up in Canadian water (Taylor 2012). King John charged 40 marks in the city of Gloucester because they failed to "pay him sufficient respect in the matter of his lampern" (Doherty 1971). Queen Elizabeth II's coronation pie in 1953 was made from lampreys baked by the Royal Air Force, and so was her jubilee lamprey pie (British Broadcast 2012). In an extreme case of royal fondness for lampreys, Henry of Huntington posthumously reported that King Henry I died of food poisoning for eating "a surfeit of lampreys", which became the title of a British crime novel (Marsh 1941). Charles Dickens (1852) described King Henry I in *A Child's History of England*: "When he had reigned upward of thirty-five years, and was sixty-seven years old, he died of an indigestion and fever, brought on by eating, when he was far from well, of a fish called Lamprey, against which he had often been cautioned by his physicians."

1.2.3. Systematic History of Living Jawless Fishes

Lampreys have always been unanimously treated as vertebrates. As for hagfish, though, their vertebrate status remains contentious. The lack of vertebrate characteristics, their primitive appearance, and their scavenging behavior compelled Linnaeus (1758) to classify hagfish as intestinal worms within Vermes, a class within which he included non-arthropod invertebrates such as molluscs and echinoderms. In retrospect, this classification is now deemed curious because Linnaeus clearly recognized morphological similarities between hagfish and lampreys such as the presence of a notochord and general body shape (Janvier 2008). However, to a

naturalist in the 18th century who set out to categorize organisms without knowledge of evolution, no distinction could have been made between primitive and degenerate features. Linnaeus's (1758) classification of animals heavily relies on distinct body plans dictated by appendages (legs or fins), integument, and the presence of eyes (his first five classes of the Kingdom Animalia are Mammalia [including bats], Aves, Amphibia [including non-avian reptiles], Pisces [non-tetrapod fishes], and Insecta [including all other arthropods]). Thus, the sixth animal class Vermes seems to have served as a wastebasket group for Linnaeus to include all animals that fell out of his five other classes. For the near absence of eyes and the absence of other typical vertebrate characteristics, Linnaeus's classification of hagfish at least agrees with his principles.

Although Linnaeus's (1758) treatment of hagfish was incorrect, a similar approach is still in practice. The question of degeneracy lingers for almost all early lineages of chordates including cephalochordates, urochordates, myxinoids, petromyzontiforms, and their fossil relatives. Because comparative methods in morphology and molecular genetics both require an outgroup, any interpretation is influenced by a choice of preconceived phylogenetic models. But this approach could lead to a circular reasoning if the phylogenetic model itself is based on the same interpretation of comparative morphology. As such, it is difficult to determine whether a given feature of the lineage truly represents a primitive condition or a unique modification of a basal state. This is a recurring theme in this thesis.

Half a century later, the intestinal worms of Linnaeus were grouped together with lampreys based on similarity to vertebrates, and less so on the absence of vertebrate traits (Abildgaard 1792; Duméril 1806). Duméril (1806) coined Cyclostomi as a group of fish consisting of hagfish and lampreys. Fitting for Duméril (1812) who sought relations between genera, he interpreted hagfish as a possible intermediate form between polychaetes and vertebrates (Janvier 2008). Many comparative morphologists followed this scheme for nearly a century (Müller 1836; Parker 1883; Cole 1905, 1907, 1909). On the other hand, Dohrn (1875) maintained that cyclostomes were degenerate descendants of teleost fishes.

In the work that continues to influence systematic terminology of vertebrates today, Cope (1898) grouped cyclostomes and ostracoderms (extinct jawless fishes) in Agnatha in parallel with Pisces, or Gegenbaur's (1874) Gnathostomata. A neoclassical cladistic interpretation of this is that both hagfish and lampreys were removed from the ancestral stock of gnathostomes. Kiaer (1924) split ostracoderms into anaspids, coleolepids, heterostracans, and osteostracans and placed the latter three closer to gnathostomes than to cyclostomes. Stensiö (1927, 1932, 1958, 1964, 1968), on the other hand, associated hagfish with heterostracans and lampreys with anaspids and osteostracans, respectively, suggesting that these two living cyclostome lineages *sensu* Duméril (1806) had two independent origins in the Agnatha. Many fossil 'agnathan' lineages are now widely regarded as stem gnathostomes as in Kiaer (1924), although their exact phylogenetic positions remain uncertain (Janvier 2007, 2008, 2010). Importantly, living jawless fish formed a group of fish that excluded gnathostomes in the first half of the 20th century in all of these phylogenetic hypotheses during this time (Obruchev 1964; Romer 1945; Halstead 1973). Dissent from this view came from comparative morphology (Goodrich 1909; Brodal and Fänge 1963) but was never formulated as a phylogenetic hypothesis.

This trend was disrupted by Løvtrup (1977) who placed lampreys closer to gnathostomes than to hagfish, thus implying that cyclostomes are paraphyletic. Janvier (1978) recovered hagfish and lampreys closer to the origin of vertebrates than either osteostracans or heterostracans, and followed Løvtrup (1977) in placing lampreys closer to gnathostomes than hagfish. As a result, agnathans no longer form a clade but are reduced to a paraphyletic assemblage between the nodes of vertebrates and gnathostomes. Janvier (1981) restored Craniata in the current cladistic sense as outlined in Appendix 1.1.

Since the publication of Løvtrup's (1977) extensive phenotypic data set, the status of cyclostomes as a clade has become a major focus of debate over vertebrate origins. The paraphyly of cyclostomes received massive support from analyses of morphological and physiological data with or without fossil taxa (Løvtrup 1977; Janvier 1978, 1981, 1996a, b, 2007; Dingerkus 1979; Hardisty 1979, 1982; Janvier

and Blieck 1979; Forey 1984, 1995; Jefferies 1986; Maisey 1986; Gagnier 1993; Forey and Janvier 1993; Donoghue et al. 2000; Donoghue and Smith 2001; Gess et al. 2006; Near 2009). Molecular data tends to recover a monophyletic Cyclostomata (Stock and Whitt 1992; Lanfranchi et al. 1994; Lipscomb et al. 1998; Mallatt and Sullivan 1998; Kuraku et al. 1999; Hedges 2001; Mallatt et al. 2001; Delarbre et al. 2002; Furlong and Holland 2002; Takezaki et al. 2003; Blair and Hedges 2005; Delsuc et al. 2006; Kuraku and Kuratani 2006; Mallatt and Winchel 2007; Yu et al. 2008; Near 2009). Notable exceptions among the morphological phylogenetic studies are Schaeffer and Thomson (1980) who supported cyclostome monophyly based on the pouched gills and their endodermal origin in cyclostomes, and Yalden (1985) who reached the same conclusion based on purported homology of the hagfish and lamprey lingual apparatus.

Cyclostome monophyly has recently gained increasing support. Heimberg et al.'s (2010) phylogeny based on miRNA explicitly supported the hagfish-lamprey clade, whereas their accompanying phenotypic data set was almost equivocal between the monophyly and paraphyly of Cyclostomata, with the latter only being one step shorter than the former. Furthermore, developmental anatomy of hagfish has revealed vertebrate-like neural crest origin and vertebra-like cartilaginous elements derived from sclerotomes (Ota et al. 2007, 2011); the supposed lack of these characters had previously been used to support the more basal position of hagfish than lampreys. These results caused early proponents of cyclostome paraphyly to accept the accumulating support for cyclostome monophyly and to re-consider the once dismissed degeneracy of hagfish (Janvier 2010, 2011).

1.2.4. Rationale for the Test of Cyclostome Relationships

The focus of this thesis is a test of cyclostome monophyly through anatomical description of the hagfish head. This test is important for three reasons. First, the choice between monophyletic and paraphyletic cyclostomes greatly alters character states predicted at the origin of vertebrates. With monophyletic cyclostomes, reconstructed character states at the root of Vertebrata are either those shared

between hagfish, lampreys, and gnathostomes (unequivocal), or those constrained to the root by optimized character transformation or by addition of fossil data (equivocal). With paraphyletic cyclostomes, on the other hand, hagfish and lampreys bracket the main stem between these two lineages and constrain character states along it. In this case, any character that hagfish lack but lampreys and gnathostomes have is likely a vertebrate synapomorphy. Second, neontological morphological data are essential in formulating characters for the phylogeny of fossil jawless fishes. Extremely unstable interrelationships among extinct jawless fishes are partly because plesiomorphic states are not constrained along the main stem of early vertebrate evolution. In addition, osteological or skeletal correlates of soft tissues can be only identified in living taxa. Therefore, an updated anatomy and phylogeny of living jawless fishes could greatly improve information available for extinct jawless fishes.

Third, detailed anatomical description and mapping of characters can reveal how a cascade of homologues affects phylogenetic reconstruction. Vertebrate synapomorphies consist of evolutionary novelties such as the neural crest, cranial nerves, and the vertebral column. Those of the Gnathostomata include the origin of jaws and a bilateral pair of nasal cavities. Between these two nodes, paired fins, dermal skeleton, teeth, bony braincase, and other vertebrate features arose. Each of these innovations accompanies a number of novel characters, thereby forming a cascade of homologues in which a novel trait is dependent on the presence of another trait that has broader phylogenetic distribution. These innovations are collectively recognized as a distinct body plan and each used as a reliable systematic character; but these are precisely the characters that are difficult to compare with outgroups because complete homology breaks down (Gegenbaur 1898; Mitgutschi 2003; Kuratani 2004). For example, it is possible to compare the presence and absence of jaws by identifying a homologue of the precursor of the jaws in jawless vertebrates. Can such homology be extended to the musculature in the mandibular region between gnathostomes and non-gnathostome fish? Is the head homologous between a vertebrate with neural crest and a basal chordate without neural crest? Outgroup comparison of a set of key innovations characterizing a major evolutionary transition

often leads to an inflated number of synapomorphies mapped onto the ingroup branch. The distribution does not mean that these characters appeared from nowhere. The cluster of synapomorphies results partly from interdependence of the characters (e.g., jaw muscles require the presence of jaws), and partly from the difficulty of recognizing the characters in any way other than as present or absent. At the same time, the cascade structure of homologues should be reflected in a phylogenetic analysis. The presence of many such characters depends on the body plan characterizing the ingroup clade; therefore, a biased signal caused by the interdependence should be removed from the data set. I will explore phylogenetic information of incomplete homologues in early vertebrate evolution in Chapter 4.

For the resolution of cyclostome relationships, the lack of congruence between genotypic and phenotypic data is frustrating because they each support the topology predicted from problems associated with data types. Phenotypic data are problematic because absence of characters is often treated as a basal condition. Translated into coding in a data matrix, taxa that lost important synapomorphies of the clade may appear more primitive than their phylogenetic position. This bias influences tree topology because absence of a trait is one step shorter as a result of plesiomorphy rather than as a result of subsequent reduction. This phenotypic model would favor successive acquisitions of vertebrate characteristics, and this is indeed the topology that most phylogenetic analyses using morphological data support.

On the other hand, molecular data may be vulnerable to the problem of long-branch attraction in which random correspondence between independently changing sequences overwhelms true phylogenetic signal and causes nearby, long and independent lineages to cluster as a monophyletic group. Among living vertebrates, hagfish, lampreys, and gnathostomes each represent a long lineage, although gnathostomes are characterized by a unique set of genes and many gene duplication events. The long branches of hagfish and lampreys are rooted closer to the vertebrate origin than each terminal gnathostome branch. Therefore, hagfish and lampreys are more likely to form a clade with each other due to stronger long-branch attraction than with other terminal branches, and this is precisely the topology that most

molecular phylogenetic analyses support. This explains the fact that model-informed analyses such as Bayesian analysis strongly support cyclostome monophyly (Near 2009).

If a similar, strong phylogenetic signal existed in both morphological and molecular data sets, this result would contradict the intuitions in one of the two data types. In other words, cyclostome monophyly would become a robust phylogenetic hypothesis if a morphological analysis also lent support. In the same sense, molecular evidence would be particularly welcome for cyclostome paraphyly.

In this spirit, the cranial connective tissues are examined in detail, as the lingual apparatus was used to support cyclostome monophyly (Yalden 1985). The cranial skeleton of hagfish is described and compared first with that of lampreys and then with gnathostomes to provide a framework to map cranial musculature (Chapter 2). If any combination of skeletal elements holds as a potential homologue, muscle attachments can be compared between these taxa. The cranial musculature of hagfish is then described and compared with that of lampreys and gnathostomes (Chapter 3). Finally, a comprehensive phylogenetic analysis is performed based on the morphological data assembled in the course of the thesis, and from the literature, with an aim to test cyclostome monophyly (Chapter 4).

1.2.5. Phylogenetic and Developmental Frameworks for Early Vertebrate Evolution

In this thesis, I accept urochordates as a sister-group to vertebrates. However, congruence between multiple outgroup taxa are used to determine character polarity and plesiomorphic conditions where possible. In contrast to many early authors, I will not treat any of the existing lineages as an *a priori* ancestral model. The poor resolution of deuterostome phylogeny and long branch lengths for almost all the lineages render such an assumption a risky strategy. This precaution also precludes the use of ontogenetic information and the deployment of an archetype to polarize characters. For example, a series of head cavities may appear ancestral to the absence of head cavities in vertebrates based on elasmobranch embryology (Balfour 1878;

Goodrich 1918). The series of metameristic posterior pharyngeal slits used for respiration may support the assumptions that the mandibular arch was specialized after the origin of vertebrates or that the premandibular arch existed (Jarvik 1980). Ancestral chordates may have developed a mouth asymmetrically as in living cephalochordates (Jefferies 1986; Lacalli 2010). The notochord may have extended to the anterior end of the head in basal chordates, and thus the prechordal region may be a "new head" added at the origin of vertebrates (Gans and Northcutt 1983; Northcutt and Gans 1983; Gans 1993; Northcutt 2005). These speculations are seductive, but they introduce unnecessary weight on certain characters, or assumptions that are not testable. The review of vertebrate origins presented here reveals that there is either a) no positive evidence that supports these claims or b) significant counterevidence that contradicts these predictions (Gee 1996; Kuratani 2004).

Similarly, I make no assumption either that the ammocoetes larvae of lampreys represent basal conditions or that the larval stage is secondarily inserted within the lineage. Hypotheses are tested after a comparative analysis.

1.3. SUMMARY AND PROSPECTS

Resolving early vertebrate relationships has implications far beyond the simple question of whether hagfish are vertebrates. The phylogenetic position of hagfish and character transformations along this lineage could root vertebrates, reveal true vertebrate synapomorphies, and establish polarity of vertebrate characters. Without that, a transition from basal chordates to vertebrates remains shrouded in phylogenetic uncertainties, and reconstruction of a vertebrate ancestor has no choice but to rely on the archetypes provided by previous comparative morphologists such as Goodrich (1930), de Beer (1937), Holmgren (1940, 1943), Bjerring (1977), and Jarvik (1980).

The great challenge to any resolution of cyclostome relations is not just the conflict between morphological and molecular analyses that support alternative

topologies, but the fact that both data types consistently support the topologies that each data type would favor because of long branches leading to the living terminal taxa. Therefore, the strength and robustness of each phylogenetic hypothesis cannot be measured by the consistency of results within each data type. The incongruence calls for a re-analysis of characters and tests of alternative interpretations. In that sense, the head is an interesting anatomical region because apparent homologies between hagfish and lamprey cranial musculature seemingly support cyclostome monophyly, a topology rarely supported by analyses using more extensive morphological data. In this thesis, I will provide a comprehensive description of the hagfish cranial skeleton and skeletal muscles. The skeleton is compared with those of other vertebrates, including lampreys and gnathostomes, to provide an anatomical framework to assess attachment sites of the skeletal muscles. Then the muscular system is described, with an intention to assess homology with equivalent muscles in lampreys and gnathostomes.

Finally, I present a new phylogenetic analysis of basal vertebrates and chordate outgroups that incorporates results from these anatomical descriptions. Character definitions and polarities are modified to reflect the modular nature of morphological characters. In reviews presented in this chapter, I outline problems associated with morphological data, the most significant of which are incomplete homologies and transcendental, archetypical assumptions for a common ancestor. The latter generates *ad hoc* explanations for each phylogenetic hypothesis and has influenced character definitions. A choice of outgroups or ancestral model, along with the choice of the most reliable characters, alters not just the optimal tree topology but also interpretations of characters that form a basis for testing relationships. No morphological analysis is free from this partly circular argument. In this thesis, I will use character congruence among outgroups to identify plesiomorphic conditions, and remove as much character interdependence as can be identified from character definitions and coding, where plesiomorphy is not testable.

1.4. LITERATURE CITED

Abildgaard, P. C. 1792. Kurze anatomische beschreibung des Säugers (*Myxine glutinosa*). Schriften der Gesellschaft naturforschender Freunde zu Berlin 10:193-200.

Adam, H. 1960. Different types of body movement in the hagfish, *Myxine glutinosa*. Nature 188:595-596.

Balfour, F. M. 1878. The development of the elasmobranchial fishes. Journal of Anatomy and Physiology 11:405-706.

de Beer, G. 1937. The Development of the Vertebrate Skull. Oxford University Press, London. 554 pp.

Bjerring, H. C. 1977. A contribution to structural analysis of the head of craniate animals. Zoologica Scripta 6:127-183.

Blair, J. E., and S. B. Hedges. 2005. Molecular phylogeny and divergence times of deuterostome animals. Molecular Biology and Evolution 22:2275–2284.

British Broadcast. 2012. Gloucester lamprey pie is fit for the Queen. BBC News. April 20, 2012. [http://www.bbc.co.uk/news/uk-england-gloucestershire-17791695] with a movie.

Brodal, A., and R. Fänge. 1963. The Biology of *Myxine*. Universitetesforlaget, Oslo. 588 pp.

Cavalcanti, M. J., and V. Gallo. 2008. Panbiogeographical analysis of distribution patterns in hagfishes (Craniata: Myxinidae). Journal of Biogeography 35:1258-1268.

Cole, F. J. 1905. A monograph on the general morphology of the myxinoid fishes, based on a study of *Myxine*. Part I. The anatomy of the skeleton. Transactions of the Royal Society of Edinburgh 41:749-791.

Cole, F. J. 1907. A monograph on the general morphology of the myxinoid fishes, based on a study of *Myxine*. Part II. The anatomy of the muscles. Transactions of the Royal Society of Edinburgh 45:683-757.

Cole, F. J. 1909. A monograph on the general morphology of the myxinoid fishes, based on a study of *Myxine*. Part III. Further observations on the skeleton. Transactions of the Royal Society of Edinburgh 46:669-681.

Cope, E. D. 1889. Synopsis of the families of Vertebrata. The American Naturalist 23:1-29.

Delarbre, C., C. Gallut, V. Barriel, P. Janvier, and G. Gachelin. 2002. Complete mitochondrial DNA of the hagfish, *Eptatretus burgeri*: the comparative analysis of mitochondrial DNA sequences strongly supports the cyclostome monophyly. Molecular Phylogenetics and Evolution 22:184–192.

Delsuc, F., H. Brinkmann, D. Chourrout, and H. Philippe. 2006. Tunicates and not cephalochordates are the closest living relatives of vertebrates. Nature 439:965–968.

Dickens, C. J. H. 1852. A Child's History of England. [Public domain]

Dingerkus, G. 1979. Chordate cytogenetic studies: an analysis of their phylogenetic implications with particular reference to fishes and the living coelacanth. California Academy of Sciences Occasional Papers 134:111-127.

Doherty, R. H. 1971. Royal Cookbook. Favorite Court Recipes from the World's Royal Families. Parents' Magazine Press.

Dohrn, A. 1875. Der Ursprung der Wirbelthiere und das Princip des Functionswechsels. Genealogische Skizzen. Wilhelm Engelmann, Leipzig. 87 pp.

Donoghue, P. C. J., P. L. Forey, and R. J. Adridge. 2000. Conodont affinity and chordate phylogeny. Biological Review 75:191-251.

Donoghue, P. J. C., and M. P. Smith. 2001. The anatomy of *Turinia pagei* (Powrie) and the phylogenetic status of the Thelodonti. Transactions of the Royal Society of Edinburgh (Earth Science Series) 92:15-37.

Duméril, A. M. C. 1806. Zoologie Analytique, ou Méthode Naturelle de Classification des Animaux. Didot, Paris.

Duméril, A. M. C. 1812. Dissertation sur la Famille des Poissons Cyclostomes, pour Démontrer leurs Rapports avec les Animaux sans Vertébres. Didot, Paris.

Fernholm, B. 1998. Hagfish systematics. Pages 33-44 in J. M. Jørgensen, J. P. Lonholt, R. E. Weber, and H. Malte, eds. The Biology of Hagfishes. Chapman, London.

Forey, P. L. 1984. Yet more reflections on agnathan-gnathostome relationships. Journal of Vertebrate Paleontology 4:330-343.

Forey, P. L. 1995. Agnathans recent and fossil, and the origin of jawed vertebrates. Reviews in Fish Biology and Fisheries 5:267-303.

Forey, P. L., and P. Janvier. 1993. Agnathans and the origin of jawed vertebrates. Nature 361:129-134.

Furlong, R. F., and P. W. H. Holland. 2002. Bayesian phylogenetic analysis supports monophyly of Ambulacraria and of cyclostomes. Zoological Science 19:593–599.

Gagnier, P.-Y. 1993. *Sacabambaspis janvieri*, Vertébré ordovicien de Bolivie. 2. Analyse phylogéenétique. Annales de Paléontologie (Vertébrés) 79:119-166.

Gans, C. 1993. Evolutionary origin of the vertebrate skull. Pages 1-35 in J. Hanken and B. K. Hall, eds. The Skull. Volume 2. Patterns of Structural and Systematic Diversity. The University of Chicago Press. Chicago.

Gans, C., and R. G. Northcutt. 1983. Neural crest and the origin of vertebrates: a new head. Science 220:268-274.

Gee, H. 1996. Before the Backbone. Chapman & Hall, London. 346 pp.

Gegenbaur, C. 1874. Grundriss der Vergleichenden Anatomie. Verlag von Wilhelm Engelmann, Leipzig.

Gegenbaur, C. 1898. Vergleichende Anatomie der Wirbelthiere mit Berücksichtung der Wirbellosen. Verlag von Wilhelm Engelmann, Leipzig.

Gess, R. W., M. I. Coates, B. S. Rubidge. 2006. A lamprey from the Devonian of South America. Nature 443:981-984.

Gill, H. S., C. B. Renaud, F. Chapleau, R. L. Mayden, and I. C. Potter. 2003. Phylogeny of living parasitic lampreys (Petromyzontiformes) based on morphological data. Copeia 2003:687-703.

Glover, C. N., C. Bucking, and C. M. Wood. 2011. Adaptations to *in situ* feeding: novel nutrient acquisition pathways in an ancient vertebrate. Proceedings of the Royal Society B 278:3096-3101.

Goodrich, E. S. 1909. Vertebrata Craniata. I. Cyclostomes and Fishes. R. E. Lankester, ed. Treatise on Zoology. Black, London.

Goodrich, E. S. 1918. On the development of the segments of the head in *Scyllium*. Quarternary Journal of Microscopical Science 63:1-30.

Goodrich, E. S. 1930. Studies on the Structure and Development of Vertebrates. The Macmillan Company, London.

Halstead, L. B. 1973. The heterostracan fishes. Biological Reviews 48:279-332.

Hedges, S. B. 2001. Molecular evidence for the early history of living vertebrates. Pages 119-134 in P. E. Ahlberg, ed. Major Events in Early Vertebrate

Evolution: Paleontology, Phylogeny, Genetics and Development. Taylor & Francis, London.

Heimberg, A. M., R. Cowper-Sal-lari, M. Sémon, P. J. C. Donoghue, and K. J. Peterson. 2010. microRNAs reveal the interrelationships of hagfish. Lampreys, and gnathostomes and the nature of the ancestral vertebarate. Proceedings of the National Academy of Sciences 107:19379-19383.

von Hofmannsthal, H. 1902. The Letter of Lord Chandos. [Public domain]

Holmgren, N. 1940. Studies on the head of fishes. Part. I. Development of the skull in sharks and rays. Acta Zoologica 21:51-266.

Holmgren, N. 1943. Studies on the head of fishes. Part. IV. General morphology of the head in fish. Acta Zoologica 24:1-188.

Honma, Y. 1998. Asian hagfishes and their fisheries ecology. Pages 45-56 in J. M. Jørgensen, J. P. Lonholt, R. E. Weber, and H. Malte, eds. The Biology of Hagfishes. Chapman, London.

Janvier, P. 1978. Les nageoires paires des Ostéostracés et la position systématique des Céphalaspidomorphes. Annales de Paléontologie (Vertébrés) 64:113-142.

Janvier, P. 1981. The phylogeny of the Craniata, with particular reference to the significance of fossil 'agnathans'. Journal of Vertebrate Paleontology 1:121-159.

Janvier, P. 1993. Patterns of diversity in the skull of jawless fishes. Pages 131-188 in J. Hanken and B. K. Hall, eds. The Skull. Volume II. Patterns of Structural and Systematic Diversity. The University of Chicago Press, Chicago.

Janvier, P. 1996a. Early Vertebrates. Oxford Monographs on Geology and Geophysics, 33. Clarendon Press, Oxford. 393 pp.

Janvier, P. 1996b. The dawn of the vertebrates: characters versus common ascent in the rise of current vertebrate phylogenies. Palaeontology 39:259-287.

Janvier, P. 2007. Homologies and evolutionary transitions in early vertebrate history. Pages 57-121 in J. S. Anderson and H. D. Sues, eds. Major Transitions in Vertebrate Evolution. Indiana University Press, Bloomington.

Janvier, P. 2008. Early jawless vertebrates and cyclostome origins. Zoological Science 25:1045-1056.

Janvier, P. 2010. microRNAs revive old views about jawless vertebrate divergence and evolution. Proceedings of the National Academy of Sciences 107:19137-19138.

Janvier, P. 2011. Comparative anatomy: all vertebrates do have vertebrae. Current Biology 21:R661-R663.

Jarvik, E. 1980. Basic Structure and Evolution of Verebrates. 2 Volumes. Academic Press, London.

Jefferies, R. P. S. 1986. The Ancestry of the Vertebrates. 376 pp. British Museum (Natural History), London.

Johnston, J. B. 1905. The morphology of the vertebrate head from the viewpoint of the functional divisions of the nervous system. Journal of Comparative Neurology and Psychology 15:175-273.

Kiaer, J. 1924. The Downtonian fauna of Norway. I Anaspida. Norsk Videnskaps-Akedemi Skrifter 1924:1-139.

Kuo, C.-H., S. Huang, and S.-C. Lee. 2003. Phylogeny of hagfish based on the mitochondrial 16S rRNA gene. Molecular Phylogenetics and Evolution 28:448-457.

Kuraku, S., and S. Kuratani. 2006. Time scale for cyclostome evolution inferred with a phylogenetic diagnosis of hagfish and lamprey cDNA sequences. Zoological Science 23:1053–1064.

Kuraku, S., D. Hoshiyama, K. Katoh, H. Suga, and T. Miyata. 1999. Monophyly of lampreys and hagfishes supported by nuclear DNA-coded genes. Journal of Molecular Evolution 49:729–735.

Kuratani, S. 2004. [Evolutionary Morphology: Bauplan and Embryonic Development of Vertebrates]. The University of Tokyo Press, Tokyo. 611 pp. [In Japanese]

Kuratani, S., and K. G. Ota. 2008. Primitive versus derived traits in the developmental program of the vertebrate head: views from cyclostome developmental studies. Journal of Experimental Zoology B 310:294-314.

Lacalli, T. C. 2010. The emergence of the chordate body plan: some puzzles and problems. Acta Zoologica 91:4-10.

Lanfranchi, G., A. Pallavicini, P. Laveder, and G. Valle. 1994. Ancestral hemoglobin switching in lampreys. Developmental Biology 164:402–408.

Lim, J., D. S. Fudge, N. Levy, and J. M. Gosline. 2006. Hagfish slime ecomechanics: testing the gill-clogging hypothesis. Journal of Experimental Biology 209:702-710.

Linnaeus, C. 1758. Systema Naturae per Regna Tria Naturae. Regnum Animale. Laurentii Salvii, Stockholm.

Lindström, T. 1949. On the cranial nerves of the cyclostomes with special reference to n. trigeminus. Acta Zoologica 30:315-458.

Lipscomb, D. L., J. S. Farris, M. Kallersjo, and A. Tehler. 1998. Support, ribosomal sequences and the phylogeny of the eukaryotes. Cladistics 14:303–338.

Løvtrup, S. 1977. The Phylogeny of the Vertebrata. Wiley, New York. 330 pp.

Mallatt, J., and J. Sullivan. 1998. 28S and 18S rDNA sequences support the monophyly of lampreys and hagfishes. Molecular Biology and Evolution 15:1706–1718.

Mallatt, J., and C. J. Winchell. 2007. Ribosomal RNA genes and deuterostome phylogeny revisited: more cyclostomes, elasmobranchs, reptiles, and a brittle star. Molecular Phylogenetics and Evolution 43:1005–1022.

Mallatt, J., J. Sullivan, and C. J. Winchell. 2001. The relationship of lampreys to hagfishes: a spectral analysis of ribosomal DNA sequences. Pages 106–118 in P. E. Ahlberg, ed. Major Events in Early Vertebrate Evolution: Paleontology, Phylogeny, Genetics and Development. Taylor & Francis, London.

Marsh, N. 1941. Surfeit of Lampreys. Harper Collins, London.

Martini, F. H. 1998. The ecology of hagfishes. Pages 57-77 in J. M. Jørgensen, J. P. Lonholt, R. E. Weber, and H. Malte, eds. The Biology of Hagfishes. Chapman, London.

Maisey, J. G. 1986. Heads and tails: a chordate phylogeny. Cladistics 2:201-256.

Mitgutsch, C. 2003. On Carl Gegenbaur's theory on head metamerism and the selection of taxa for comparisons. Theory in Biosciences 122:204-229.

Müller, J. 1836. Vergleichende anatomie der Myxinoiden, der Cyclostomen mit durchbohrtem Gaumen. Osteologie und Myologie. Abhandlungen der Königlichen Akademie der Wissenschaften zu Berlin 1834:65-340.

Near, T. J. 2009. Conflict and resolution between phylogenies inferred from molecular and phenotypic data sets from hagfish, lampreys, and gnathostomes. Journal of Experimental Zoology B 312:749-761.

Nelson, J. S. 2006. Fishes of the World (4th edition). John Wiley & Sons, New York. 624 pp.

Northcutt, R. G. 2005. The new head hypothesis revisited. Journal of Experimental Zoology B 304:274-297.

Northcutt, R. G., and C. Gans. 1983. The genesis of neural crest and epidermal placodes: a reinterpretation of vertebrate origins. Quarterly Review of Biology 58:1–28.

Obruchev, D. V. 1964. [Agnathan and Fishes]. I. A. Orlov, ed. [Fundamentals of Palaeontology]. Volume 11. Nauka, Moscow. 522 pp.

Ota, K. G., S. Kuraku, and S. Kuratani. 2007. Hagfish embryology with reference to the evolution of the neural crest. Nature 446:672-675.

Ota, K. G., S. Fujimoto, Y. Oisi, and S. Kuratani. 2011. Identification of vertebra-like elements and their possible differentiation from sclerotomes in the hagfish. Nature Communications 2:373. 6 pp.

Parker, W. K. 1883. On the skeleton of the marsipobranch fishes. Part I. The myxinoids (*Myxine* and *Bdellostoma*). Philosophical Transactions of the Royal Society of London 174:373-409.

Plutarch. L. M. 976. On the Intelligence of Animals. [English translation; Public domain]

Renaud, C. B. 2011. Lampreys of the world. An annotated and illustrated catalogue of lamprey species known to date. Food and Agriculture Organization Species Catalogue for Fishery Purposes 5:1-109.

Romer, A. S. 1945. Vertebrate Palaeontology (2nd edition). University of Chicago Press, Chicago. 687 pp.

Shaeffer, B., and K. S. Thomson. 1980. Reflections on agnathan–gnathostome relationships. Pages 19-33 in L. L. Jacobs, ed. Aspects of Vertebrate History. Museum of Northern Arizona Press, Flagstaff.

Schlosser, G. 2005. Evolutionary origins of vertebrate placodes: insights from developmental studies and from comparisons with other deuterostomes. Journal of Experimental Zoology B 304:347-399.

Seneca, L. A. 40. Book III. To Novatus On Anger. [English translation; Public domain]

Stensiö, E. A. 1927. The Devonian and Downtonian vertebrates of Spitsbergen. Part I. Family Cephalaspidae. Skrifter om Svalbard og Nordishavet 12:1-391.

Stensiö, E. A. 1932. The Cephalaspids of Great Britain. Trustees of the British Museum, London. 220 pp.

Stensiö, E. A. 1958. Les Cyclostomes fossiles ou Ostracodermes. Pages 173-425 in P. P. Grassé, ed. Traité de Zoologie. Volume 13. Masson et Cie, Paris.

Stensiö, E. A. 1964. Les Cyclostomes fossiles ou Ostracodermes. Pages 96-383 in J. Piveteau, ed. Traité de Paléontologie, Volume 4. Masson et Cie, Paris.

Stensiö, E. A.1968. The cyclostomes with special reference to the diphyletic origin of the Petromyzontida and the Myxinoidea. Pages 13-71 in T. Ørvig, ed. Current Problems in Lower Vertebrate Phylogeny. Almqvist and Wiksell, Stockholm.

Stock, D. W., and G. S. Whitt. 1992. Evidence from 18S ribosomal RNA sequences that lampreys and hagfishes form a natural group. Science 257:787-789.

Stradley, L. 2004. History of lamprey pie. What's Cooking America. [http://whatscookingamerica.net/History/PieHistory/LampreyPie.htm] Retrieved May 15, 2012.

Strahan, R. 1963. The behaviour of myxinoids. Acta Zoologica 44:1-30.

Swalla, B. J., and A. B. Smith. 2008. Deciphering deuterostome phylogeny: molecular, morphological and palaeontological perspectives. Philosophical Transactions of the Royal Society B 363:1557-1568.

Takezaki, N., F. Figueroa, Z. Zaleska-Rutczynska, and J. Klein. 2003. Molecular phylogeny of early vertebrates: monophyly of the Agnathans as revealed by sequences of 35 genes. Molecular Biology and Evolution 20:287–292.

Taylor, L. C. 2012. Great Lakes rescues Queen's traditional Jubilee lamprey pie. Toronto Star. April 24, 2012.

Worthington, J. 1905. Contribution to our knowledge of the myxinoids. The American Naturalist 39:625-663.

Yalden, D. W. 1985. Feeding mechanisms as evidence for cyclostome monophyly. Zoological Journal of the Linnean Society 84:291-300.

Yu, S.-Y., W.-W. Zhang, L. Li, H.-F. Huang, F. Ma, and Q.-W. Li. 2008. Phylogenetic analysis of 48 gene families revealing relationships between hagfishes, lampreys, and Gnathostomata. Journal of Genetics and Genomics 35:285–290.

Zintzen, V., C. D. Roberts, M. J. Anderson, A. L. Stewart, C. D. Struthers, and E. S. Harvey. 2011. Hagfish predatory behaviour and slime defence mechanism. Scientific Reports 1:131. 6 pp.

1.5. FIGURE

Figure 1-1. Phylogenetic trees of chordates showing early vertebrate lineages and the controversy over cyclostome relationships. (A) Conventional phylogenetic tree used as a comparative framework in this thesis. The tree is simplified from Janvier (2007) and Swalla and Smith (2008). The relationships shown here represent the current consensus. The red line is based on cyclostome monophyly, whereas the blue line depicts the topology for cyclostome paraphyly in which the node Craniata precedes the node Vertebrata. A revised phylogenetic analysis suggests an alternative topology in which thelodonts shift closer to lampreys, conodonts to hagfish, and arandaspids to heterostracans. However, optimized character evolution in the revised phylogenetic analysis does not significantly differ from this consensus tree, and the consensus is presented without modification. Simplified cladograms in the lower right corner showing the three surviving vertebrate lineages arranged according to cyclostome paraphyly (B) or cyclostome monophyly (C).

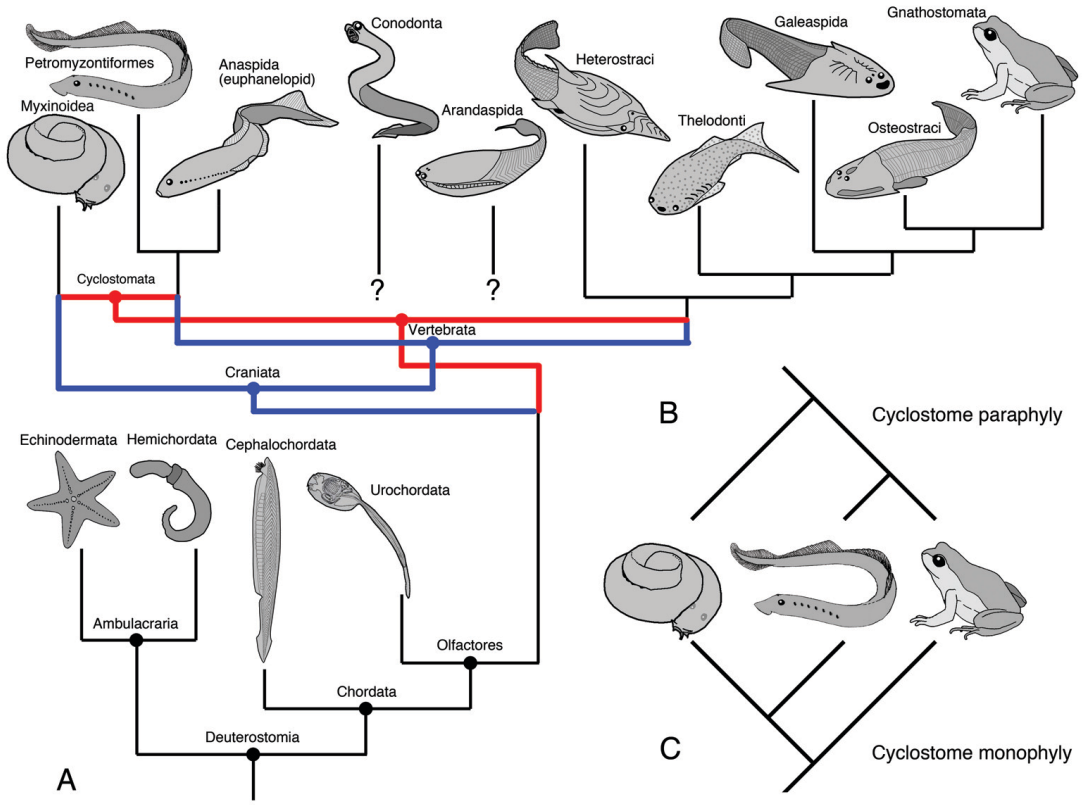
Petromyzontiformes
Myxinoidea
Anaspida
(euphanelopid)
Conodonta
Arandaspida
Heterostraci
Galeaspida
Thelodonti
Gnathostomata
Osteostraci
Cyclostomata
?
?
Vertebrata
Craniata
Echinodermata
Hemichordata
Cephalochordata
Urochordata
Ambulacraria
Olfactores
Chordata
Deuterostomia
A
B
Cyclostome paraphyly
C
Cyclostome monophyly

Figure 1-1.

Appendix 1.1 Phylogenetic and Anatomical Terminology

In this thesis, I adhere to a clade-based definition of phylogenetic terminology unless necessary to do otherwise (Figure 1-1). Vertebrata as a formal taxon refers to the clade (Gnathostomata + Petromyzontiformes), whereas Craniata designates the clade (Vertebrata + Myxinoidea). If Vertebrata and Craniata converge on a single node due to the clade Cyclostomata (Myxinoidea + Petromyzontiformes) with an exclusion of Gnathostomata, Vertebrata takes precedence over Craniata (Figure 1-1). It should be noted, however, that the terms 'vertebrates' and 'craniates' have been used interchangeably in the literature. For this reason, hagfish are loosely treated as vertebrates in all textbooks of vertebrate zoology. Recent evidence also suggests that hagfish do have homologues of vertebrate synapomorphies that were previously considered lacking (Ota et al. 2007, 2011; Kuratani and Ota 2008). To reduce confusion, I minimize the usage of Craniata and refer to "other vertebrates" rather than to "other craniates" when hagfish are compared with vertebrates. The clade (Vertebrata + Urochordata) is Olfactores (Swalla and Smith 2008). Throughout the thesis, several paraphyletic grades are used for the purpose of convenience. These are:

Basal chordates (=non-vertebrate chordates). All chordates closer to urochordates or cephalochordates than to vertebrates.

Cyclostomes. Hagfish (Myxinoidea) and lampreys (Petromyzontiformes). If they are sister group to each other, the clade Cyclostomata is the valid terminology. If they are not, cyclostomes are a paraphyletic grade of jawless fish.

Fish. All members of the total group Vertebrata closer to teleosts or lungfish than to urochordates or cephalochordates, excluding tetrapods.

Jawless vertebrates (agnathans). All non-gnathostome vertebrates.

Living jawless fish (=cyclostomes). Hagfish (Myxinoidea) and lampreys (Petromyzontiformes).

Stem gnathostomes. All non-gnathostome vertebrates closer to the crown-group Gnathostomata than to Petromyzontiformes.

Stem vertebrates. All non-vertebrate chordates closer to the crown-group Vertebrata than to the crown-group Urochordata or Cephalochordata.

Cranial nerves are numbered from I to XII, but only the cranial nerves I-X are relevant because the accessory and hypoglossal nerves (XI and XII) are enclosed within the occiput only in gnathostomes. The terminology is: I, olfactory; II, optic; III, oculomotor; IV, trochlear; V, trigeminal; VI, abducens; VII, facial; VIII, vestibulocochlear; IX, glossopharyngeal; X, vagus. Among these nerves, cranial nerves I, II, and VIII are entirely sensory (to nasal capsule, eye, and inner ear, respectively), cranial nerves III, IV, and VI are entirely motor and restricted to innervating the extraocular muscles, and cranial nerves V, VII, IX, and X (branchiomeric nerves) contain both sensory and motor components and innervate the visceral part of the head.

The trigeminal nerve has two ganglia, one being the ophthalmic ganglion and the other being the maxillomandibular ganglion, whereas other cranial nerves have one ganglion each. The maxillomandibular ganglion splits into the maxillary and mandibular branches in gnathostomes, but the homology for each of the branches remains uncertain with respect to the branches of the trigeminal nerve in hagfish and lampreys (Johnston 1905; Lindström 1949). All the ganglia for the cranial nerves with sensory component (I, II, V, VII-X) are induced by ectodermal placodes (reviewed by Schlosser 2005). Particularly, trigeminal placodes are associated with the trigeminal ganglia, and a series of epibranchial placodes correspond to a series of ganglia for the cranial nerves VII-X. Those for the branchiomeric nerves (VII, IX, and X) are referred to as geniculate, petrosal, and nodose, respectively. This thesis makes occasional reference to the geniculate placode.

In vertebrate zoology, pharyngeal arches are numbered from anterior to posterior and the anterior-most arches have specific terms (reviewed by Goodrich 1930). However, the designation of pharyngeal arches varies among authors. A

premandibular domain likely never was a distinct pharyngeal arch, and there is good evidence that a mandibular domain only became a serial homologue of branchial arches (pharyngeal arches 2 to 6) at the origin of gnathostomes (Chapter 3). Therefore, I refer to the anterior pharyngeal regions as domains.

Premandibular domain. The domain of head anterior to the hypophyseal fenestra, which generally sits in front of or above the mouth. It contains the nasal cavity and the capsule and is innervated by the ophthalmic branch of the trigeminal nerve (V_1).

Mandibular domain. The domain of the head lateral to the oral cavity, which is innervated by the maxillomandibular branches of the trigeminal nerve (V_2 in jawless vertebrates; V_{2+3} in gnathostomes). In gnathostomes, the mandibular domain represents the anterior-most pharyngeal arch. The jaw belongs to this domain.

Hyoid domain. The domain of the head between the hyomandibular pouch (the first lateral diverticulum of the pharynx) and the first branchial slit. The domain is the anterior-most branchial arch, and it is innervatied by the facial nerve.

Post-hyoid domain. A series of pharyngeal arches posterior to the hyoid domain. The first post-hyoid domain is innervated by the glossopharyngeal nerve, whereas all arches behind it are innervated by the vagus nerve.

Appendix 1.2. Recipe for Hagfish Slime Scones

(adopted from "The Museum of Awful Food" by a writer with the handle name "an icky fish"; entry dated March 21, 2006; retrieved on May 25, 2012; http://ewewgross.blogspot.ca/2006/03/hagfish-slime-scones.html)

Note by T.M.: the author has not attempted making this scone, but the recipe is herein preserved for posterity. This curious culinary adventure should excite future generations of zoologists, and is too good to let go into obscurity along with the website.

4 cups all-purpose flour
2 tablespoons baking powder
4 teaspoons sugar
1/2 teaspoon salt
1 cup (two sticks) chilled unsalted butter, cut into 1/2-inch cubes
2 cups (packed) coarsely grated extra-sharp yellow cheddar cheese (about 9 ounces), or a mix of 6 ounces cheddar and 3 ounces gruyere.
1-1/2 cups chilled heavy whipping cream
6 tablespoons hagfish slime

Preheat oven to 375F

In a food processor, blend flour, baking powder, sugar, and salt. Cut in the butter using quick pulses until the mixture resembles coarse meal. Add cheese and cut in using quick pulses. In a small bowl, whisk together the cream and hagfish slime. With the food processor running, add cream mixture through feed tube. Process until dough just holds together – don't overmix!

Turn dough out onto a lightly floured work surface. Gather the dough together and divide into quarters. Pat each quarter into a round just short of 1 inch high (it should

be about 6-7 inches in diameter). Using a clean, sharp knife, cut each round into six wedges. Transfer half the wedges to ungreased baking sheets lined with parchment paper, spacing them about 2 inches apart.

Bake the first batch of scones until the edges just start to brown and a toothpick comes out clean, about 20 minutes. Transfer them, still on their parchment paper, to a wire rack to cool at least 10 minutes, during which time put in the second batch of scones.

Serve warm or at room temperature. The scones will stand for about 8 hours. Do not refrigerate. If you want to reheat them, warm them in a 350F oven for about 5 minutes.

Chapter 2 – The Skull of the Northeastern Pacific Hagfish *Eptatretus stoutii* and Early Evolution of the Vertebrate Head

You may think I'm only kidding but inside my notochord
I feel these changes coming and teeth growing like a horde…
Your pelagic upper class has had it good too long
Don't forget we're not just suckers for you to string along.
Roger Lethbridge (1981), The Socialist Lamprey

2.1. INTRODUCTION

Hagfish have always posed a paradox to zoologists. They lack many traits that set vertebrates apart from invertebrates, including a mineralized skeleton, multiple semicircular canals, and extraocular muscles; they have many others that do not occur in any other vertebrate groups, such as the hypertrophied lingual apparatus, slime glands, and cardinal and caudal hearts. These are testaments of the deep origin and long branch-length of the lineage within the chordate tree. Hagfish are the only vertebrates or stem vertebrates that Linnaeus (1758) failed to recognize as such in his groundbreaking work of animal taxonomy. In fact, their status as vertebrates still remains a central question in vertebrate zoology. If hagfish fall outside the lamprey + gnathostome clade, they would form a sister group to vertebrates. On the other hand, hagfish may be a highly specialized lineage of the monophyletic cyclostome vertebrates — therefore a sister-group to lampreys. At the heart of this debate is a conflict of morphological and molecular data, but both data sets consistently result in phylogenetic hypotheses expected from problems inherent to the type of data: cyclostome paraphyly supported mostly by morphological characters, which may underestimate secondary loss of vertebrate characters; and cyclostome monophyly supported mostly by molecular data, which is prone to long branch attraction (reviewed in Chapter 1).

Recently, developmental and anatomical evidence has revealed that some hagfish characters previously interpreted as primitive may represent secondary

loss or artifacts of observation during experimental procedures. The developmental origin of the neural crest in hagfish is identical to that in other vertebrates (Ota et al. 2007), and the skeleton of the caudal fin derived from sclerotomes in hagfish may be a homologue of vertebra (Ota et al. 2011). These results do not necessarily support cyclostome monophyly because potential homologues are widespread across vertebrates. Instead, they highlight the fact that the comparative morphology of hagfish remains poorly understood. Indeed, morphological comparisons of hagfish with various vertebrate lineages based on original material have languished since the description of two embryos of the Atlantic hagfish *Myxine glutinosa* (Holmgren 1946). Subsequent authors mostly used second-hand observations from earlier anatomical studies (for skeletons, Müller 1834; Parker 1883a; Ayers and Jackson 1901; Cole 1905, 1909; Holmgren 1946; Marinelli and Strenger 1956).

This hiatus presents an obstacle to an urgently needed re-interpretation of hagfish morphology in an evolutionary context for several reasons. First, the early descriptions are not always accurate enough to allow detailed comparison. Skeletal proportions and shapes of elements in the early reconstructions sometimes depart significantly from those in the original specimens used in the descriptions. Second, intraspecific and interspecific variation are not clearly distinguished because each description tended to rely on a few specimens, and artifacts in illustrations often went unnoticed. Third, variation within the Myxinoidea remains unexplored. This is problematic not only for generic or specific diagnostics within the group, but also for phylogenetic comparison because it is hard to tell whether a character is unique to a particular taxon of hagfish or a general feature of the group. Fourth, the descriptions have long been outdated and many of them are not readily accessible.

There is an obvious need for detailed, original description of hagfish morphology, a topic that spawned, but then was left behind the recent progress in developmental anatomy and paleontology on early vertebrate evolution (succinctly summarized in Janvier 2007). Developmental, paleontological, and anatomical evidence that became available in the last half a century allows a

revival of that approach. This paper presents a detailed description of the skull of the northeastern Pacific hagfish (*Eptatretus stoutii*) and comparison in phylogenetic context. *E. stoutii* is one of the best-studied species of hagfish (see Jørgensen et al. 1998a) and likely retains plesiomorphic conditions with respect to its Atlantic relative, *M. glutinosa* (Fernholm 1998; Martini 1998; Chen et al. 2006). In the vertebrate body, the head is the most complex and has more vertebrate-specific novelties than any other body part. So a detailed morphological comparison of the head emerges as a priority. The description focuses on the skeleton and major nerves within the hagfish head as a foundation for a subsequent description of the musculature (Chapter 3; Figure 2-1).

2.2. MATERIALS AND METHODS

More than 100 adult specimens of northeastern Pacific hagfish (*Eptatretus stoutii*) were trapped from approximately 80 m deep in Barkley Sound, British Columbia, Canada (latitude: N 48° 84’ 96.37”; longitude: W 125° 13’ 18.01”) and held in the aquarium at Bamfield Marine Sciences Centre, Bamfield, British Columbia from May 2010 to November 2011. Among these adults, 11 euthanized individuals of varying sizes were used to study the skeleton. Of these 11 specimens, five individuals (body lengths of 275 mm to 450 mm) were dissected. Three individuals were decapitated, fixed in 4% neutrally buffered formalin for one week, and preserved in 75% ethanol. One of the three formalin-fixed specimens (body length approx. 320 mm) underwent paraffin sectioning at the thickness of 7.5 μm, for which two to four of every 50 slices were retained and stained with eosin and hematoxylin. The rest of the formalin-fixed specimens (body length of approximately 400 mm) were scanned using μCT scanner (CT = X-ray computed tomography) after either four days or two weeks of exposure to 1% IKI solution as a contrast-staining agent (Metscher 2009). Unfortunately, cartilages and muscles have similar densities, and hagfish adults are substantially larger than various vertebrate embryos scanned by Metscher (2009) and do not evenly absorb the contrast-staining agent deep within tissues. Due to extensive noise and

inability to contrast cartilages against muscles, resulting images were never clear enough to allow accurate three-dimensional reconstruction of the entire skull except for some cartilages around which little muscle exists (Figure 2-2F, G). To avoid excessive smoothing, extrapolation, and deformation during reconstruction, I treated each raw CT micrograph as a separate radiograph and used a combination of them and images obtained by other preparation methods to manually trace and superimpose outlines of the cartilages (Figure 2-1). The skull was also digitally reconstructed using standard CT analytical software (OsiriX) by tracing reconstructed and aligned images of μCT sections.

Finally, cartilages were extracted from three individuals of *E. stoutii* of similar size to those used for dissection (body length of 250 mm to 450 mm). These specimens were digested in a solution of 50 mg/ml cyanogen bromide (CNBr: Sigma-Aldrich, St. Louis) in 70% formic acid for 24 hours at room temperature (20 °C) and for one hour at 60 °C, following Robson et al. (2000).

The cartilaginous skull of hagfish is soft and flexible. Extraction of the cartilages, fixation of the head, histological sectioning, and even contact with an object or substrate can substantially deform or distort *in situ* natural shape of the skeleton. That no method is free of this problem justifies a combination of variously prepared specimens in reconstructing the skull. The outline of the head was assembled (Figure 2-1) from dissection and μCT radiographs, whereas the cartilages were drawn and described using digital reconstruction of μCT data, manually assembled μCT radiographs, extracted cartilages, dissections, stained histological sections, and photographs during life. Nerves and other soft tissues were identified during dissection and in histological sections.

2.3. DESCRIPTION

The hagfish skull consists of ten major units: nasal skeleton; tentacular skeleton; nasopharyngeal plate; facial skeleton; parachordal skeleton; pharyngolingual arches; velar skeleton; dental apparatus; lingual apparatus; and branchial cartilages. These anatomical units are for convenience based on position within

the head and functions, although elements within each unit may not necessarily share the same developmental origin. The notochord extends anteriorly into the cartilaginous sheath between the otic capsules. I exclude the notochord and postcranial cartilaginous elements from this description because these elements have already been described in detail elsewhere (Ayers and Jackson 1901; Cole 1905; Marinelli and Strenger 1956; Welsch et al. 1998; Ota et al. 2011). Each skeletal region is described morphologically based on *Eptatretus stoutii* (Figures 2-1), compared with other myxinoids (Figure 2-2), and reviewed for its developmental background (Figure 2-3). Based on all of this information, I attempt to assess similarities of the skeletal elements by comparison with lampreys and gnathostomes (Figures 2-4, 2-14).

2.3.1. Nasal Skeleton

2.3.1.1. Morphology

The nasal skeleton consists of the nasal arches (na) and the nasal capsule basket (ncb) (Figures 2-1, 2-5). The nasal arches form the dorsal roof and lateral walls of the nasal tube (nt) and provide structural support in the snout. Approximately half the transverse width of the snout, the nasal tube has a single external aperture at the anterior end of the head and leads to the nasal capsule posteriorly and the nasopharyngeal duct posteroventrally. Because of the large diameter relative to the head and because of the absence of a sphincter, the nasal tube always maintains an open passage.

The number of nasal arches varies among individuals. Specimens of *Eptatretus stoutii* that I examined for this study either had nine or ten nasal arches in total (at least three out of five specimens had ten nasal arches). In addition, Ayers and Jackson (1901) report the occasional occurrence of individuals with only eight nasal arches in the same species. This variation is likely independent of body size, as one of the individuals with ten nasal arches fell among the smallest specimens with a body length less than 300 mm. In at least five of the 11 specimens, the first two independent arches are closer to each other than other

arches are. These two arches may be connected by the dorsal midline bar in some individuals (Ayers and Jackson 1901).

In the specimen with ten nasal arches (Figures 2-1, 2-5), the first five are fused to the lateral longitudinal bar (llb) at the ventral ends. The number of the arches connected to the longitudinal bar is four in specimens with nine nasal arches. The right and left longitudinal bars extend anteromedially below the first nasal arch as terminal processes (tp, Figure 2-5E) and are bridged by a thin cartilaginous connection that forms the ventral margin of the nasohypophyseal aperture. This cartilaginous connection is thinner than 20 μm and hardly detectable in μCT scan or CNBr-digested specimens. Another bilateral pair of terminal processes extends anteriorly below the longitudinal bars from the bases of the third nasal arch.

The first nasal arch is inclined anterodorsally at an angle of approximately 45°, whereas the other arches are nearly vertical. A cartilaginous sheet thinner than 20 μm forms the anterior margin of the dorsoventrally flattened top of the first nasal arch, forming the dorsal margin of the nasohypophyseal aperture (na1r, Figure 2-5E). The cartilaginous sheet is perforated by a bilateral pair of fenestrae and so thin that it is half transparent and not detectable in a μCT scan. A clear boundary between the sheet and the main arch due to difference in thickness indicates that the sheet is not a simple extension from the first nasal arch but likely represents secondary chondrification of the membrane that connects the anterior margin and the dorsal midline process of the first nasal arch.

A dorsal midline bar connects the first and second nasal arches. The nasal tube is transversely narrower and dorsoventrally taller at the third nasal arch than it is anterior to this point. The following three independent nasal arches lack support of the lateral longitudinal bar, and the last two nasal arches (the ninth and tenth in individuals with ten nasal arches) are connected to the anterior transverse arch of the nasal capsule basket by the dorsal midline bar. The second last arch is inclined posterodorsally near the top of the nasal tube in nearly 75% of the individuals observed, whereas the last arch is transverse in all specimens. The ventral base of the second last nasal arch has a posteriorly oriented, hook-shaped

terminal process. These free-ended terminal processes may variably connect to the last nasal arch or even the anterior transverse arch of the nasal capsule basket in *Myxine glutinosa* (Cole 1905). The dorsal midline contact between the last two arches is individually variable (Ayers and Jackson 1901). In individuals in which the last two nasal arches are nearly parallel, they may fuse partially or nearly entirely along the margins, or may connect to each other via the dorsal midline bar. In individuals with the posterodorsally inclined second last nasal arch, the arches fuse to each other where the margins contact near the top of the nasal tube with or without perforations along the contact line, or they may connect via the dorsal midline (dmb; Figure 2-5B, E). There is no apparent trend in this variation with respect to body size or sex. The last nasal arch is connected to the anterior transverse arch of the nasal capsule basket via the upper and lower longitudinal bars across this junction. The lower longitudinal bar extends posteriorly to fuse to the posterior transverse arch and the nasopharyngeal bar.

A basket of cartilaginous bars covers the nasal capsule dorsally. The posterior transverse arch of the basket (tap; Figure 2-5E) marks the position of the olfactory fenestra, and the total of nine longitudinal bars bridge the anterior and posterior transverse arches. Each of the six intermediate and one midline longitudinal bars (ncbl) supports a ventrally suspended longitudinal sheet of the olfactory epithelium (se; Figure 2-5C, D). The lower longitudinal bar (vlb) is more robust than the midline and intermediate longitudinal bars and has a plate-like outgrowth dorsally and ventrally. At the lateroventral corner of the nasal capsule, the posterior transverse arch, lower longitudinal bar, and nasopharyngeal bar (npb) meet to form a junction. The nasopharyngeal bar extends posteroventrally to fuse to the acrochordal process of the nasopharyngeal plate.

2.3.1.2. Taxonomic comparison

In *E. stoutii*, variation exists among individuals in the number of nasal arches, in the thin cartilaginous sheet that forms the anterior margin of the first nasal arch, and in the mode of fusion between nasal arches. Similar variation occurs among illustrated skulls of three species of hagfish (Müller 1834; Parker

1883a; Ayers and Jackson 1901; Cole 1905; Marinelli and Strenger 1956; Robson et al. 2000). The number of nasal arches varies from eight to ten in *E. stoutii*. In *E. hexatrema*, the number appears to be ten (Figure 2-2A; Müller 1834, 1838) or eleven (Figure 2-2C; Parker 1883a), but more sampling is required to determine the range of variation. In *M. glutinosa*, the number agrees at eleven in all published first-hand observations (Figure 2-2E; Parker 1883a; Cole 1905, 1909; Holmgren and Stensiö 1936; Marinelli and Strenger 1956; Robson et al. 2000). Although Cole (1905) thought that Parker (1883a) overlooked the first nasal arch, and suggested that the real count was therefore twelve, he likely misinterpreted exaggeration of the anterior terminal process of the first nasal arch illustrated by Parker (1883a) as the part of the dorsal midline bar. Confusion appears to result from Parker's oversight (1883a) of the thin cartilaginous sheet along the anterior margin of the first nasal arch, but not the first nasal arch itself, because most anterior nasal arch of Parker (1883a) is in the position expected for the first nasal arch that supports the dorsal margin of the nasohypophyseal aperture.

The specimens of *E. stoutii* examined for this study show no ontogenetic trend in the number of the arches. However, an ontogenetic change in the number of nasal arches remains possible. Ayers and Jackson (1901) reported bifurcation at both the right and left ventral ends of a nasal arch in one individual, with its right half forming an incipient arch. In *M. glutinosa*, the seventh and eighth nasal arches tend to coalesce toward their ventral bases but remain separate at the dorsal midline. *E. stoutii* shows a similar tendency, but the fusion occurs at the dorsal midline and the ventral bases are separate. Likewise, the sixth and seventh nasal arches of *E. hexatrema* are bridged by the dorsal midline bar (Figure 2-2C; Parker, 1883a).

The right and left ventral bases of the nasal arches are widely separated in all specimens of *E. stoutii* examined for this study (npb; Figure 2-5C). Cole (1905) reports two small specimens of *M. glutinosa* (approximate body lengths of 65 mm and 250 mm) in which the right and left ventral ends of the nasal arches approach the ventral midline or even overlap with the counterpart ventral to the nasal tube.

The bilateral fenestrae in the first nasal arch seem to be absent in *E. hexatrema* (Müller 1834, 1838) and *M. glutinosa* (Parker 1883a; Cole 1905; Robson et al. 2000), although the fenestra is illustrated asymmetrically on the left side of *E. hexatrema* (Figure 2-2C; Parker 1883a). However, the thin cartilaginous sheet along the anterior margin of the first nasal arch was not clearly identified in either of these descriptions, which leaves uncertainty about whether this character was recognized.

A pair of small, free cartilages between the first and second nasal arches of *M. glutinosa* illustrated in Cole (1905, 1909; Figure 2-12I) are the cartilages that support the papillae. Cartilaginous support for the nasal papilla is absent in *E. stoutii*, but this sensory structure shows a wide range of variation among hagfish. The papilla may have small cartilaginous support, and may be paired, single, or two in tandem on the midline either on the floor or roof of the anterior nasal tube (Mok 2001). Unlike other hagfish, the nasal papillae occur posteriorly in front of the nasal capsule in *E. stoutii* (np; Figure 2-5B). The dorsal and ventral midline papillae bifurcate distally, whereas the lateral papillae are paired.

In *M. glutinosa*, the number of the anterior nasal arches connected by the longitudinal bar at the ventral base varies from four (Cole 1905; Figure 2-12I) to nine (Robson et al. 2000). In *E. stoutii*, this number is either four or five, depending on the total count of the nasal arches (nine or ten). The number of the posterior nasal arches connected to the nasal capsule basket also varies from two (Robson et al. 2000) to three (Cole 1905). Parker (1883a; Figure 2-2C) illustrated that *E. hexatrema* has only the most posterior nasal arch connected to the anterior transverse arch of the nasal capsule basket by the dorsal midline bar. The connection between the posterior nasal arches and the anterior transverse arch seems to be absent in the description of *E. hexatrema* (Müller 1834, 1838), but this area is not clearly illustrated.

These characters are potentially taxonomically significant at the species or generic level. In particular, the number of the nasal arches appears to be fixed at eleven in *M. glutinosa*. The larger number in this taxon than in *E. stoutii* reflects the relatively longer snout of *M. glutinosa*. *Myxine* may be further distinguished

from *Eptatretus* by the absence of the perforation in the first nasal arch and the tendency to coalesce the seventh and eighth nasal arches toward the ventral bases. But these characters may be subject to intraspecific variation or be artifacts introduced during tissue preparation and illustration, and therefore should be treated with caution. Chondrification of thin connective membranes could easily escape detection during dissection. These obscure cartilaginous elements include the bilateral connection between the anterior terminal process of the lateral longitudinal bar below the nasohypophyseal aperture, the chondrifaction along the anterior margin of the first nasal arch, and the number of nasal arches connected at the ventral base by the longitudinal bars.

2.3.1.3. Development

In embryos of hagfish (Figure 2-3; *E. stoutii*: Dean 1899; Neumayer 1938; *M. glutinosa*: Holmgren 1946), chondrification of the nasal skeleton is delayed with respect to other cartilaginous elements in the head. Similar to the nasohypophyseal placode in lampreys, an unpaired olfactory placode forms at the anteroventral end of hagfish embryos (Ota and Kuratani 2008). By Neumayer's Stage II, a bilateral pair of rods arises from the otic capsule at the parachordal level and extends anteroventrally with one transverse bridge in front of the notochord (acrochordal commissure in this paper). The paired rods extend farther anteriorly and give rise to: 1) the anlage of the nasopharyngeal bar (npb); 2) paired rods that are part of the diffuse commissure of mesenchyme below the nasopharyngeal bar (vlb); and 3) another bilateral pair of rods that join anteriorly as the anlage of the nasal skeleton in front of the nasal capsule (na; Figure 2-3B$_{2, 3}$; Neumayer 1938; Holmgren 1946). The middle element that forms the diffuse commissure has been labeled as the trabecular commissure (Figure 2-3B, asterisk) by Holmgren (1946) and Kuratani and Ota (2008).

There is confusion in the literature largely introduced by Neumayer (1938) as to the origin and fate of the "trabecular commissure". Neumayer (1938) recognized the paired bases of the trabecular commissure (his figure 8-20) but reconstructed them as connecting to the palatal commissure at stage II (his plates

4-5). By his stage III, the paired bases disappear so that the elements never contribute to the nasal skeleton (his plates 6-9). Curiously, at the same stage, the cartilaginous elements appear in the same location, but this time as extending from the nasopharyngeal bar independent of the palatal commissure. These elements are chondrifications of the trabecular commissure of (Holmgren 1946) and the anlage for the pre-nasal capsule nasal skeleton. The embryo of Neumayer (1938) at stage IV indicates that Holmgren's trabecular commissure corresponds to the lower longitudinal bar of the nasal capsule basket (his plate 13), a fate unlikely for the mesenchymal population below the nasopharyngeal duct (Holmgren 1946). Importantly, at no point in development does the transverse connection of the right and left bases of the trabecular commissure arise as a chondrocranial element because the commissure consists of the connective mesenchyme and never chondrifies (Holmgren 1946). Having described this element and mesenchymal population, Holmgren (1946) appears to have been predisposed to the idea of the gnathostome trabecular homologue and probably interpreted the position of the mesenchyme under the nasopharyngeal duct to infer that the trabecular commissure entirely disappears in the adult skull.

However, the partial misinterpretation of hagfish chondrocranial development by Neumayer (1938) suggests an alternative view. That is, the lower longitudinal bar of the nasal capsule basket arises in the ectomesenchyme that wraps around the nasopharyngeal duct. It chondrifies into a bilateral pair of rods along the lateroventral wall of the nasopharyngeal duct, a position conserved throughout ontogeny in adults (Figure 2-3), and joins the nasal capsule basket subsequently. Neumayer (1938) did not recognize the ectomesenchyme and erroneously reconstructed the element as part of the palatal commissure nearby at stage II, but correctly observed its morphology once it chondrified at stage III. On the other hand, Holmgren (1946) over-interpreted the mesenchymal connection, even though this is just a part of the connective mesenchymal sheet around the nasopharyngeal duct and nasal tube.

These observations lead to the following new interpretations: 1) anterior extensions of the parachordal skeleton beyond the anlage of the nasopharyngeal

plate (acrochordal commissure) are prechordal, and originate in the ectomesenchyme in the premandibular domain (npb, vlb, na) or laterally overlapping the premandibular domain (pa); 2) the most posterior pair of skeletal rods is an anlage of the nasopharyngeal bar of the nasal capsule basket (npb); 3) the next pair of skeletal rods is an anlage of the lower longitudinal bar of the nasal capsule basket (vlb); and 4) the anterior-most extension is an anlage of the nasal skeleton in front of the nasal capsule basket (na; Figure 2-3B_{1-3}).

By Neumayer's Stage III, all longitudinal bars of the nasal capsule basket initiate from the posterior transverse arch (Figure 2-3D), and the timing and direction of the anterior extension agree with the formation of nasal folds and the longitudinal extension of the olfactory epithelium (Dean 1899; Figure 2-5C, D). Here, the chondrification appears to be induced at the epithelial-mesenchymal interface in each nasal fold under the placode, just as in skeletonization around the nasal capsule in other vertebrates. The difference is that no invagination occurs in the olfactory placode of hagfish, and the nasohypophyseal complex is endodermal in origin (Gorbman 1983, 1997). Therefore, the interaction is not with the invaginated ectodermal epithelium as in other vertebrates (Parsons 1959; Romanoff 1960; Croucher and Tickle 1989; Kardong 2006), but with the epithelium of the preoral gut derivative. At this stage, the anterior transverse arch is represented by a series of small anlagen (Figure 2-3D_2). Meanwhile, the nasal tube is wrapped around by the premandibular ectomesenchyme, presumably from both preoptic and postoptic domains of the trigeminal neural crest cells (Holmgren 1946). The dorsal half of the mesenchymal sheet chondrifies with perforations, which continues to extend anteriorly as an anlage for the nasal arches along with the nasal tube (Figure 2-3E; Neumayer 1938). The anterior end of the sheet develops processes parallel with the terminal processes of the paranasal tentacular cartilages and the sensory ophthalmic branch of the trigeminal nerve toward the snout tip (Neumayer 1938). The positions and orientations of the processes are consistent with the terminal processes of the lateral longitudinal bar of the anterior nasal arches, and suggest that these terminal

processes did not result from the interaction with the endodermal nasal tube as in the nasal arches.

2.3.1.4. Homology

The endodermal nature of the nasohypophyseal complex makes an assessment of similarity problematic. At the level of the chondrogenic premandibular ectomesenchyme underneath the dorsal surface of the prechodal head (Holmgren 1946), the elements of the hagfish nasal skeleton topologically and functionally correspond to those that arise from the premandibular ecotomesenchyme in vertebrates. This includes the ethmoidal elements of the nasal capsule, and the interorbital and nasal septa in gnathostomes (onl, r, trc; Figure 2-4E, H; de Beer 1937). Possibly, hagfish may have ancestrally co-opted the preoral gut derivative in the absence of ectodermal invagination to induce the nasohypophyseal complex and the nasal skeleton.

The nasal capsule basket has an obvious topographical and functional counterpart in the skeletal nasal capsule in lampreys and gnathostomes (Figure 2-4; de Beer 1937; Holmgren 1940, 1943, 1946; Johnels 1948; Marinelli and Strenger 1954, 1956; Langille and Hall 1988). The nasal capsule in hagfish sits in front of the forebrain and is innervated by the olfactory nerves as in all vertebrates. The nasal capsule of all living vertebrates accompanies skeletal support originating in the chondrocranium, and the chondrification initiates in the premandibular ectomesenchyme (de Beer 1937; Parsons 1959; Hall and Hörstadius 1988; Schultze 1993; Trueb 1993; Rieppel 1993; Zusi 1993; Novacek 1993), again consistent with potential homology. The hagfish nasal capsule basket uniquely consists of multiple cartilaginous rods rather than a capsule, and the olfactory region is endodermal.

These difficulties can be explained by the lack of ectodermal invagination in the olfactory placode. Because the olfactory neurons and epithelia are induced as longitudinal folds into the nasal capsule directly underneath the placode, and because the nasopharyngeal duct is directly beneath the nasal capsule, the mesenchyme cannot invade over or underneath the nasal capsule from the side.

The chondrification of the mesenchyme would then occur: 1) along the margin of the olfactory fenestra (posterior transverse arch; tap; Figure 2-5E); 2) into the folds of the olfactory epithelium (midline and intermediate longitudinal bars; ncbl; Figure 2-5D); 3) along the lateral wall of the nasal capsule (lower longitudinal bar; vlb; Figure 2-5E); and 4) over the boundary between the nasal capsule and the nasal tube (anterior transverse arch; taa; Figure 2-5E). The anterior end of the forebrain, the anterior end of the notochord, and the presence of the placode anterior to the forebrain all constrain the ectomesenchyme in this region as the premandibular domain (Goodrich 1930; de Beer 1937; Holmgren 1946; Johnels 1948; Hall and Hörstadius 1988; Couly et al. 1993; Horigome et al. 1999; Kuratani et al. 2004, 2012; Kuratani 2005, 2012; Kuratani and Ota 2008; Hall 2009; Wada et al. 2011). The endodermal epithelium in the anterior head induces chondrification of the prechordal cranium in vertebrates (Couly et al. 1998, 2002). Even in highly derived vertebrates as birds, *Shh* signaling from the foregut endoderm is necessary to induce the ventral part of the nasal capsule (Benouaiche et al. 2008). A crucial role of the preoral gut as a patterning agent in the preoral development is not restricted to vertebrates. In cephalochordates, the preoral gut diverticula differentiates into a variety of coelomic tissues, one of which is the externally open Hatschek's pit, a potential homologue for the vertebrate adenohypophysis (Hatschek 1881; Wiley 1894; Boorman and Shimeld 2002). Given the topographical identity of the chondrifying ectomesenchyme, and given the conserved skeletogenic role of the anterior head endoderm, the nasal capsule basket can be considered as a homologue of the lamprey and gnathostome nasal capsules.

The anlage of the lower longitudinal bar (vlb; Figure 2-3B_2) has been labeled as the trabecular commissure by Holmgren (1946) and Kuratani and Ota (2008). If the delineation between the parachordal part of the skull and the true trabecula in hagfish embryo by Kuratani and Ota (2008) is correct, however, the primordial nasopharyngeal bar, not the lower longitudinal bar, is the topographical homologue of the gnathostome trabecular cranii (tr; Figure 2-4H). This is because the nasopharyngeal bars are a pair of prechordal longitudinal

cartilaginous rods that delineate the anteroventral extreme of the forebrain. Rejecting problematic identification of the hypophyseal fenestra in hagfish (see the rationale for this in 2.3.3.4. Homology) also rules out the homology between the hagfish lower longitudinal bar and the gnathostome trabecular commissure. This is because the bar no longer forms the margin of the hypophyseal fenestra as reconstructed by Holmgren (1946) and Kuratani and Ota (2008).

As for a homologue of gnathostome trabecula in lampreys, Kuratani (2012) suspects that a population of the premandibular ectomesenchyme cells that would otherwise form trabecula in gnathostomes migrate into the upper lip and give rise of some of the skeletal elements in that region. In a metamorphosing lamprey, the dorsolateral blastema appears in the region close to the gnathostome trabecula and the hagfish nasopharyngeal bar, anteroventral to the nasal capsule, as a part of the mucocartilage, and disappears without chondrifying (dlb; Figure 2-4F; Johnels 1948). The dorsolateral blastema undoubtedly belongs to the premandibular region as it arises anterior to the otic-trigeminal rod and ventromedial to the supraorbital nerve. Therefore, this is a good candidate for the true trabecular homologue in lampreys.

The nasal arches pose a different issue, even though they clearly result from chondrification of the premandibular ectomesenchyme around the endodermally derived sac (Holmgren 1946). There is no readily identified topographical and functional counterpart for the nasal arches in other vertebrates. In lampreys, the nasohypophyseal duct does not accompany skeletonization other than the nasal capsule (Parker 1883b; Damas 1944; Johnels 1948; Marinelli and Strenger 1954; Janvier 1993). In gnathostome chondrocrania, the ethmoidal plate sits in this region (ncr, r, tc; Figure 2-4H) but the element separates, and may wrap around, each of paired olfactory passages (de Beer 1937) rather than simply hang over the top of the undivided passage as in hagfish. In addition, the extension of the endodermal nasal tube to the tip of the snout in hagfish has no comparable condition in other vertebrates (von Kupffer 1899; Gorbman 1983; Gorbman and Tamarin 1985; Wicht and Northcutt 1995). As such, a specific homology cannot be established. Even at the level of a possible precursor,

chondrification of the premandibular ectomesenchyme anterior to the nasal capsule only establishes topographical identity. There is no evidence based on lampreys and fossil vertebrates that the chondrification in this domain of the head is conserved across vertebrates. At this time, the nasal arches have no structural resemblance among any known chondrocranial elements in other vertebrates. Topographically, the roof of the prenasal sinus in heterostracans suggests a tempting comparison with the nasal arches in hagfish for parallel development between the nasohypophyseal complex and oral cavity and for proximity between the nasohypophyseal aperture and mouth (Stensiö 1927, 1964, 1968; Janvier 1974, 1975, 1993, 1996, 2007; Blieck 1984). However, this region in heterostracans is a part of the exoskeleton and histologically unique to the clade with aspidin in pteraspids (Halstead Tarlo 1963). If any homology could potentially be established between hagfish and heterostracans in this region, it would be on similarities in the overall patterning of the nasohypophyseal complex and the surrounding oral region, but not between the specific skeletal elements.

2.3.2. Tentacular Skeleton

2.3.2.1. Morphology

As in all hagfish, *E. stoutii* has four pairs of barbels, two bilateral pairs each for the nasohypophyseal aperture and for the mouth. Each of these pairs is supported by distinct cartilaginous elements (Figures 2-1, 2-6). The labial ramus of the lateral tentaticular cartilage (tclr) is the longest, sigmoid portion of the lateral tentacular cartilage, and is more than five times the length of the paranasal ramus (tcpr; Figure 2-6). The labial ramus extends anterodorsally from the anterolateral lingual cartilage within the dorsoventrally thick perichondral tissue (Figure 2-6C) and passes medial to the cornual process of the facial skeleton. Medial to the anterior tip of the cornual process, the perioral process splits from the labial ramus ventrally. The labial ramus continues its course anterodorsally and terminates anterodorsally in the paranasal tuber (tcpt), from which the paranasal ramus extends anteriorly (Figure 2-6A, B). The paranasal ramus bridges the labial ramus and the upper nasohypophyseal process (tcup), which extends

anterodorsally to support the upper nasohypophyseal barbel. The process also extends ventromedially into a handle for the tentacular muscles to attach to and contract against. The labial and paranasal rami are round in cross section, whereas the cartilages supporting the barbels (the upper nasohypophyseal and perioral processes) are transversely flattened. The lateral tentacular cartilage is anchored to the lateral surface of the nasal tube between the first and third nasal arches by tendons of m. nasalis.

There is a bilateral pair of isolated anchor-shaped cartilages beside the mouth (tco; Figure 2-1, 2-6). They have no spatial association with any other cartilages. These are the oral tentacular cartilages that are normally folded medially onto the ventral surface near the mouth. The dorsal rod of each is a site of insertion for m. lingual tantacularis and m. cornual labialis. Contraction of these muscles causes the oral and perioral barbels to open anteriorly during feeding.

The subnasal cartilage originates from the level just behind the palatal commissure and extends anteriorly underneath the nasal tube (snc; Figure 2-1, 2-6). At the ventral margin of the nasohypophyseal aperture, the cartilage forks into a bilateral pair of prongs anterolaterally. These prongs extend into and support the lower nasohypophyseal barbels. The proximal contact with the palatal commissure is via ligaments, and the elements are independent from each other (Figure 2-6C).

2.3.2.2. Taxonomic comparison

Generally, *M. glutinosa* has an anteroposteriorly longer and dorsoventrally lower snout than *E. stoutii*. Several characters in the tentacular skeleton reflect this difference. The labial ramus of the lateral tentacular cartilage is dorsoventrally taller and more strongly bowed dorsally in *E. stoutii* in a gentle sigmoidal shape than it is in *M. glutinosa* (Figure 2-2E). The paranasal ramus of the lateral tentacular cartilage is nearly as long as the distance between the dorsal tuber and the base of the perioral process in *E. stoutii*, whereas the distance is nearly two times longer than the paranasal ramus in *M. glutinosa*. The subnasal

cartilage is relatively shorter anteroposteriorly in *E. stoutii* (extending below nine to ten nasal arches) than in *M. glutinosa* (extending below eleven nasal arches). Phylogenetic distribution of these differences in skeletal proportions is not clear. Although *Eptatretus* appears to have a shorter snout than *Myxine*, *E. hexatrema* is the only other species of the genus for which the tentacular skeleton is described (Müller 1834; Parker 1883a; Figure 2-2, A-D). In their illustrations, the terminal process of the lateral tentacular cartilage supports the lower pair of the nasohypophyseal barbels, whereas that of the subnasal cartilage supports the upper. The perioral barbel, along with the perioral process, is oriented anteriorly. The subnasal cartilage is relatively short in extending below seven nasal arches, whereas the palatal commissure is far anterior to the nasal capsule. Unique to this taxon, the oral tentacular cartilage is comparable in size with the perioral process of the tentacular cartilage and connected to the lingual cartilage. Müller (1834) and Parker (1883a) disagree on the relative proportions of the labial ramus with respect to the base of the perioral process. It is not clear whether these illustrations accurately represent the morphology of the taxon. If they are, the skeletal proportions in *E. hexatrema* resemble *E. stoutii*, suggesting that these characters are useful at the generic level.

2.3.2.3. Development

Multiple condensations of the chondrifying ectomesenchyme are present in the anteroventral end of the head of a hagfish embryo by stage II of Neumayer (1938) (Figure 2-3C). The labial ramus of the lateral tentacular cartilage is present as the anterior extension of the anterolateral lingual cartilage. The condensations below or at the level with this rod eventually form components of the lateral tentacular cartilage (tcl), whereas those above this rod become the cornual process (cop) of the facial skeleton and the subnasal cartilage (snc). In the embryo of *M. glutinosa* at the comparable, or slightly earlier, stage of development (Holmgren 1946) shows distinction among these elements (Figure 2-3B). The components of the lateral tentacular cartilage are connected to one another. The horizontally inverted F-shape of the lateral tentacular cartilage is reminiscent of the shape of

this cartilage in adults of *E. hexatrema* (Müller 1834; Parker 1883a). The subnasal cartilage and the cornual process are parallel to each other, with the latter on the lateral side and posterior to the upper portion of the lateral tentacular cartilage. The oral tentacular cartilage is not described in this embryo.

At later stages near hatching and coinciding with the anterior extension of the nasal tube (Figure 2-3, D-E), the nasohypophyseal portion of the tentacular skeleton migrate anterodorsally to where the nasal tube opens externally, whereas the oral portion of the skeleton remains at the anteroventral site where the mouth forms. This indicates two zones of induction and growth, one around the nasohypophyseal aperture and the other around the mouth.

The innervation of the upper nasohypophyseal, perioral, and oral barbels by the external trigeminal nerve raises the possibility that the lateral tentacular cartilage belongs to the mandibular domain (V_2). The innervation of the lower nasohypophyseal barbel by the ophthalmic trigeminal nerve suggests that the subnasal cartilage develops in the premandibular domain (V_1; Figure 2-1C). The external trigeminal nerve shares a ganglion with the velobuccal and dental trigeminal nerves and originates in the V_2 lobe along with the motor and sensory branches that innervate the pharynx (Müller 1838; Allis 1903; Worthington 1906; Lindström 1949; Nishizawa et al. 1988; Ronan 1988; Wicht and Nieuwenhuys 1998; this study). There is a good reason to draw the premandibular-mandibular boundary between the ophthalmic and external trigeminal domains, even though the trigeminal nerve of hagfish is not exactly comparable to those of lampreys and gnathostomes. At the level of the trigeminal placodal cells, the ophthalmic (V_1) and 'maxillomandibular' (V_2) domains are intrinsically distinct from each other because removal of cephalic neural crest cells results in a clear separation of the ophthalmic and 'maxillomandibular' lobes of the trigeminal ganglion (Hamburger 1961; Moody and Heaton 1983a, b; Stark et al. 1997). Experimental ablation of the trigeminal placodes and inhibition of coalescence of the trigeminal placodal cells both indicate that cephalic neural crest cells take on the domain identity of the placodal cells in contact to project axons into the periphery (Hamburger 1961; Moody and Heaton 1983b; Baker and Bronner-Fraser 2001; Shigetani et al. 2008).

In addition to originating from a separate ganglion (V_1), the ophthalmic trigeminal nerve is the only one of the trigeminal trunks in hagfish that does not pass through the trigeminal fenestra (Figure 2-7; Worthington 1906; Jansen 1930; Lindström 1949; this study). This nerve consistently innervates the region anterior to the eye, the most anterior domain that the trigeminal crest cells could migrate and occupy from embryo to adults (Lindström 1949; Wicht and Northcutt 1995). Therefore, in the traditional terminology, the ophthalmic trigeminal trunk in hagfish corresponds to that in vertebrates and defines the premandibular domain, and all other trigeminal trunks innervate the mandibular domain just posterior to that. The caveat here is that the premandibular-mandibular boundary by the trigeminal axon paths may not depend on the target (Scott and Atkinson 1999). Therefore, distinction between the domains in the head is unlikely to exist before migration of trigeminal crest cells, and the boundary may not always sit in exactly the same position relative to the underlying mesoderm across vertebrates.

The mandibular affinity of the lateral tentacular cartilage has two implications. First, the mouth opens in the mandibular region in hagfish, indicating clearly that there is no premandibular arch in front of the mandibular arch. The theory of vertebrate head segmentation has long assumed one or two independent premandibular arches as an ancestral state (Balfour 1878; Marshall 1881; van Wijhe 1882, Platt 1891; Goodrich 1918, 1930; de Beer 1937; Holmgren 1940; Bjerring 1970, 1972, 1977, 1984; Jarvik 1980; Jefferies 1986), but no living or fossil vertebrate shows such a structure or supports its presence as an ancestral state (Kingsbury 1926; Romer 1972; Northcutt 1990, 1993, 2008; Kuratani et al. 1999; Kuratani 2003, 2004a, 2005a, 2008; Kimmel and Eberhart 2008).

The second implication of the mandibular affinity of the lateral tentacular cartilage is possible anterior extension of the mandibular domain similar to that in lamprey development. If the ophthalmic and external trigeminal nerves can be treated as approximate markers each for the premandibular and anterior mandibular ectomesenchyme domains, the anterodorsal portion of the lateral tentacular cartilage is lateral to the premandibular region defined by the subnasal cartilage. This topographical relationship indicates that the mandibular domain

overlapped the premandibular domain from the posterolateral side, just as the upper and lower lips primarily arising from the cheek process migrate anteriorly in lampreys (Figure 2-4 D-F; Horigome et al. 1999; Kuratani et al. 1999, 2001, 2004, 2012; Kuratani 2005b, 2012). Because the upper lip of a lamprey contains the premandibular mesoderm at its anterior tip, the anterior extension is not restricted to the mandibular domain in that taxon (Kuratani et al. 1999, 2001; Kuratani 2012). It remains unknown whether this is also the case in hagfish. In addition, the parallel development of the subnasal cartilages and other tentacular skeletal elements in hagfish indicates that the mandibular domain already overlapped laterally before the onset of chondrification, whereas the migration of the upper lip cartilages occurs during metamorphosis in lampreys (Johnels 1948). Still, the lateromedial topography of the premandibular and mandibular domains is consistent between the two taxa.

Early authors (Ayers and Jackson 1901; Cole 1905) suggested that the terminal processes of the subnasal cartilage are originally a bilateral pair of independent cartilaginous rods, and that they are free from the main cartilage in individuals less than 10 cm in length both in *E. stoutii* and *M. glutinosa*. However, the embryonic anlage of this element is continuous (Neumayer 1938; Holmgren 1946). The element may not be fully chondrified in hatchlings. Alternatively, the separation of the cartilages may be an artifact because the ventral periphery of the nasohypophyseal aperture is delicate.

2.3.2.4. Homology

Although the possible anterior extension of the mandibular domain in hagfish leaves the possibility that the potential homologue of the lateral tentacular cartilage may exist in the perioral region of lampreys, element-to-element correspondence is not obvious. Topographical correspondence is difficult to trace because of extensive remodeling of the lamprey skull during metamorphosis, and none of the cartilaginous elements in lampreys is functionally equivalent to the tentacular skeleton in hagfish (Sewertzoff 1917; Tretjakoff 1926; Johnels 1948). Holmgren (1946) homologized the anterior lateral plate of lampreys with the

lateral tentacular cartilage of hagfish based on the fact that the sensory branch of the 'maxillomandibular' trigeminal trunk (V_2) passes lateral to the element in both taxa. If this relationship were to be established, it forces topographical correspondence between the hagfish perioral process and the lamprey stylet cartilage, and between the hagfish oral tentacular cartilage and the lamprey annular cartilage. These elements do not resemble each other in shapes, and the anteroposterior positions differ slightly. The hagfish lateral tentacular cartilage extends into the preoral region, whereas the lamprey anterior lateral plate remains dorsolateral to the mouth. The hagfish perioral process is lateral with respect to the oral tentacular cartilage, whereas the lamprey stylet cartilage is behind the annular cartilage. Nevertheless, the potential homology between these elements has some additional support. The lateral tentacular cartilage appears to develop as an anterior extension of the anterior lateral lingual cartilage (Figure 2-3, B-F; Neumayer 1938; Holmgren 1946), and the anterior lateral plate develops within the lower part of the mucocartilage and connects the anlagen of lingual apparatus and annular cartilage (Figure 2-4 D-F; Johnels 1948). The muscles in this region have similar functions and topographical relationships to the skeletons (Chapter 3). Therefore, the labial ramus of the lateral tentacular cartilage is tentatively accepted as corresponding to the anterior lateral plate. For similar reasons and for close association with the mouth, the hagfish perioral tentacular process and oral tentacular cartilage are functionally and anatomically comparable to the stylet and annular cartilages of lampreys, respectively.

Although the subnasal cartilage has no obvious topographical correspondence with any element in the adult lamprey skull, the upper process of the mucocartilage in an ammocoete larva wraps around the anterior edge of the nasal capsule and forms the posterodorsal plate, which eventually becomes the posterior tectal cartilage in the adult skull (Figure 2-4, D-F; Johnels 1948). This position approximately coincides with the dorsal limit of where the premandibular ectomesenchyme is expected within the upper lip (Horigome et al. 1999; Kuratani et al. 1999, 2001, 2004; Kuratani 2012). The element borders the anterodorsally oriented nasohypophyseal canal anteriorly, a position similar to the subnasal

cartilage with respect to the longitudinal axis of the canal. The cutaneous innervation around the cartilages is by the deep sensory branch of the ophthalmic trigeminal nerve in both taxa (Figure 2-1C; Allis 1903, 1925; Lindstöm 1949; Nishizawa et al. 1988; Ronan 1988).

In lamprey ammocoetes, the anterior tectal cartilage develops over the anterior lateral plate at the anterodorsal tip of the upper mucocartilage (Johnels 1948). Although the element coincides with the anterior lateral plate as the subnasal cartilage parallels the lateral tentacular cartilage in hagfish, the element is unlikely to be a homologue of the subnasal cartilage. The anterior tectal cartilage expands laterally to overhang the annular cartilage and anterior lateral plate in lamprey adults rather than remaining along the midline, and the nasohypophyseal canal does not pass anterior to the mouth as the nasal tube in hagfish.

Some heterostracans have lateroventral subrostral grooves interpreted as the impressions of the barbels in the region corresponding to the lower nasohypophyseal barbels in hagfish (Stensiö 1958, 1964; Janvier 1974). Such barbels would have had cartilaginous support comparable to the subnasal cartilage in hagfish.

2.3.3. Nasopharyngeal Plate

2.3.3.1. Morphology

The nasopharyngeal plate (Figure 2-7) is an elongate midline element in the nasobuccal shelf that sets apart the nasopharyngeal duct dorsally from the oral cavity. Although this element is commonly called the hypophyseal plate (e.g., Cole 1905, 1909), the terminology is misleading because the plate neither forms part of the neurocranium nor contacts the adenohypophysis. Anteriorly, the plate forks into a bilateral pair of terminal processes toward the palatal commissure, thereby forming the posterior limit of the periodontal tissue of the dorsal median tooth. Posteriorly the plate forms the anterior margin of the choana where the posterior terminal processes hooks anterolaterally in the shape of a U, just anterior to the proximal end of the velar skeleton.

The plate is suspended from the parachordal skeleton by the acrochordal process (acc) from the dorsomedial margin of the trigeminal fenestra. The plate expands laterally in this region, and the right and left acrochordal processes form an M-shaped commissure in dorsal view. The nasopharyngeal bar of the nasal capsule basket fuses to the dorsal surface of the acrochordal process, not the main body of the nasopharyngeal plate.

2.3.3.2. Taxonomic comparison

The nasopharyngeal plate of *M. glutinosa* differs from that of *E. stoutii* as it lacks the anterior terminal processes, tapers anteriorly and posteriorly, and has two midline perforations (Figure 2-12J; Cole 1905, 1909; Marinelli and Strenger 1956). In addition, the posterior terminal processes of *M. glutinosa* are oriented posteriorly and are only slightly wider transversely than the main body. Although the illustrations and descriptions of *E. hexatrema* are inadequate to assess if any of the traits are consistent at the generic level, at least the anterior and posterior terminal expansions occur in this taxon (Figure 2-2D) and it is likely a morphological character that sets *Eptatraitus* spp. apart from *M. glutinosa* (Müller 1834; Parker 1883a). The nasopharyngeal plate is not perforated in either species of *Eptatretus*.

The lack of the acrochordal suspension of the nasopharyngeal plate in *E. hexatrema* (Müller 1834) is likely an artifact, but the direct connection between the laterally expanded plate and the parachordal skeleton reconstructed by Parker (1883a) is equally misleading (Figure 2-2D). Müller (1834) draws a partial acrochordal process as a medial projection from the parachordal skeleton; thus the acrochordal connection probably exists in this taxon. Cole (1905) originally reconstructed the root of the nasopharyngeal bar in the main body of the plate, but the connection is at the acrochordal process (Cole 1909).

2.3.3.3. Development

In the chondrocranium of a hagfish embryo, a transverse commissure between the right and left parachordal skeletons in front of the anterior tip of the notochord develops into the nasopharyngeal plate (npp; Figure 2-3 B, C; Neumayer 1938; Holmgren 1946). This acrochordal commissure marks the anterior end of the parachordal skeleton. Therefore, the anterior extensions from the parachordal skeletons beyond this point belong to the prechordal region, and should be treated separately from the parachordal skeleton (Kuratani and Ota 2008). The nasopharyngeal plate migrates ventrally as the nasopharyngeal duct extends posteriorly to pass between the anterior and posterior commissures and join the pharynx (von Kupffer 1899; Neumayer 1938; Gorbman 1983; Gorbman and Tamarin 1985; Wicht and Northcutt 1995). The anteroposterior extension of the plate within the nasobuccal shelf does not occur until Neumayer's stage III, and likely correlates with the contact with the epithelium of the nasopharyngeal duct. It is debatable whether the nasopharyngeal plate derives entirely from the parachordal mesoderm. The anterior extension of the plate below the nasal skeleton suggests that the prechordal tissue may contribute to the plate.

2.3.3.4. Homology

The posterior commissure between the parachordal rods in a hagfish embryo is most comparable to the acrochordal commissure (traditionally called trabecular commissure) in lampreys (Holmgren 1946; Kuratani and Ota 2008). The lamprey acrochordal commissure develops as the anterior extreme of the cranial parachordal skeleton in the mesoderm and is therefore not homologous with the gnathostome trabecula (Koltzoff 1902; Johnels 1948; Kuratani et al. 2001, 2004). Indeed, the commissures in both lamprey and hagfish embryos border the anterior ends of the notochord posteriorly. In the gnathostome chondrocranium, the dorsum sella or acrochordal cartilage agrees with these elements in the topology with respect to the hypophysis anteriorly and the notochord posteriorly (dsl; Figure 2-4H), although actinopterygian chondrocrania often lack this element (de Beer 1937; Holmgren 1940, 1943, 1946).

Although the space between the acrochordal commissure and the anlage of the ventral longitudinal bar in the embryonic hagfish chondrocranium is labeled as hypophyseal fenestra by Kuratani and Ota (2008), the terminology is misleading because the hypophysis does not settle into this fenestra. First, the fenestra never forms in the chondrocranium because the trabecular commissure of Holmgren (1946) is likely a part of the mesenchymal sheet and never chondrifies. Furthermore, the relationship with the forebrain suggests that the nasopharyngeal bar, not the lower longitudinal bar, corresponds better to the gnathostome trabecula. Finally, the ventral migration of the nasopharyngeal plate and the dorsal elevation of the nasal capsule basket (Figure 2-3) orient the fenestra to face anteriorly, over which the nasopharyngeal duct passes. The adenohypophysis develops on the dorsal roof of the duct posterior to the fenestra. Therefore, no homology with the vertebrate pituitary fossa or hypophyseal fenestra (hf; Figure 2-4H) should be assumed for this space. On similar grounds, one potential difficulty of the homology between the nasopharyngeal plate in hagfish and acrochordal elements in other vertebrates is that the nasopharyngeal duct extends above the nasopharyngeal plate. In contrast, the functionally equivalent nasohypophyseal canal or nasal cavity is below or anterior to the acrochordal elements in lampreys and gnathostomes. Because these tubes are not exactly homologues with each other, however, the homology of the nasopharyngeal plate with the acrochordal cartilage is still valid.

2.3.4. Facial Skeleton

2.3.4.1. Morphology

The facial skeleton constitutes the largest component of the hagfish skull (Figures 2-1, 2-7). It consists of the cornual process, palatal commissure, palatal, dorsal longitudinal, and ventral longitudinal arches, and visceral plate. Except for the palatal commissure, all of these cartilages are bilaterally paired. As a whole, the facial skeleton suspends the dental apparatus, nasobuccal shelf, lingual and velar cartilages, oral epithelium, and pharynx ventrally via various skeletal contacts and connective tissues.

The bilateral cornual processes (cop) arise from the lateral ends of the palatal commissure anterolaterally (Figure 2-1A, B). In the absence of surrounding tissues, the relaxed cornual processes are level with the palatal cartilage and apart from each other at an approximate angle of 140 degrees. In life, however, the processes are warped ventrally and medially by the facial muscles from the lingual and subnasal cartilages so that the anterior halves of the processes are ventral with respect to the palatal cartilage and parallel longitudinally with the lateral tentacular cartilage in dorsal and ventral views. The anterior tip of the cornual process is attached to the labial ramus of the lateral tentacular cartilage via ligaments.

The palatal commissure (pac) bridges the right and left palatal arches (pa) in a U-shape in dorsal view, and provides substrate for the proximal contact of the subnasal cartilage and for the periodontal tissue of the dorsal median tooth (Figure 2-6A, C). The palatal arch has the largest diameter among rod-like elements in the skull of *E. stoutii*. The arch bows posteroventrally below the eye and joins the junction of the otic-trigeminal (ota), dorsal longitudinal (lau), and ventral longitudinal arches (lal; Figure 2-1A, B). The dorsal longitudinal arch is approximately level with the palatal arch and forms the ventral margins of the trigeminal fenestra and facial foramen. It meets with the interfenestral strut and fuses to the visceral plate near the upper end of it. The ventral longitudinal arch is gently concave posterodorsally and fuses to the lower end of the visceral plate. The dorsal and ventral longitudinal arches delineate the anterior margins of a large triangular opening, the hyomandibular fenestra (hmf; Figures 2-1A, B, 2-7).

The visceral plate (vp) is a transversely flat, dorsoventrally tall cartilage that forms the posterior margin of the facial foramen (ff) and contacts the otic capsule (oc) farther dorsally (Figures 2-1A, 2-7). It forms the posterior margin of the hyomandibular fenestra and anterior margin of the first pharyngolingual fenestra (plf1). The plate develops the velar process (vlp) anteromedially into the hyomandibular fenestra, which forms a tooth that fits into the lateral concavity at the base of the lateral velar cartilage. Posteriorly, the plate develops a planar

expansion. At the level of the dorsal and longitudinal arches, the pharyngolingual arches fuse to the visceral plate near the upper and lower ends.

2.3.4.2. Taxonomic comparison

The facial skeleton of *E. stoutii* can be distinguished from that of *M. glutinosa* based on several differences (Figures 2-1, 2-2E, 2-12I, J). First, the right and left palatal arches are parallel in *E. stoutii*, whereas the arches converge anteriorly toward the midline in a shallow angle in dorsal view in *M. glutinosa.* Related to this difference, the palatal arch is gently bowed dorsally in the former and nearly horizontal in the latter. The lower half of the visceral plate is anteroposteriorly longer than the otic capsule in *M. glutinosa*. Also in that taxon, the lower margin of the ventral longitudinal arch has a rugose process extending towards the dental apparatus (described as a palatoquadrate process by Holmgren 1946; Figure 2-2E). The growth of the lower part of the facial skeleton is moderate in *E. stoutii*.

It is difficult to evaluate the facial characters in *E. hexatrema* due to imprecision of the illustrations. According to illustrations by Müller (1834), the facial skeleton of this taxon is horizontal as in *M. glutinosa* and the visceral plate lacks the velar and posterior processes. In Parker (1883a), the facial skeleton is gently sinuous in lateral view as in *E. stoutii* and the velar process and the smaller posterior process of the visceral plate are present. In both works, the visceral plate is anteroposteriorly shorter than the otic capsule and has a smooth ventral margin, suggesting a closer affinity with *E. stoutii*.

2.3.4.3. Development

The facial skeleton is treated separately from the parachordal cartilage because these two regions are likely developmentally distinct. Allis (1903) reported that the otic-trigeminal arch and the dorsal longitudinal arch are independent from each other in a juvenile of *E. stoutii* with a smaller body length than 20 mm, although Cole (1905) saw no such dissociation in his equally small specimens. In addition, the facial skeleton consistently lies lateral to the

trigeminal and facial nerves and form the anterior region of what Cole (1905) termed the pharyngeal basket. The lateral position of the facial skeleton suggests that it does not develop within the parachordal mesoderm; instead, the neural crest-derived ectomesenchyme likely plays a role in patterning the skeleton. If this view is correct, the question then is whether or not the premandibular, mandibular, and hyoid domains can be delineated in the facial skeleton.

Possible candidates for the premandibular component of the facial skeleton are the cornual process, palatal commissure, and palatal arch (Kuratani and Ota 2008). On the other hand, the path of the external trigeminal nerve largely parallels the palatal arch and cornual process on the medioventral side, and the anterior branch of the motor trunk of the trigeminal nerve innervates the muscles attached to these cartilages (Chapter 3). The anlage of the cornual process develops just posterior to that of the lateral tentacular cartilage, and behind the anlage of the cornual process is that of the palatal arch (Figure 2-3; Holmgren 1946). The cornual process eventually extends to the lateral side of the lateral tentacular cartilage, and the palatal arch follows behind the bow of the latter. Even setting aside the problematic homology of the element, there is enough evidence that the lateral tentacular cartilage belongs to the mandibular domain. Given that the mandibular domain of the head overlaps the premandibular domain laterally in hagfish, the cornual process and the palatal arch are mandibular. The palatal commissure is below the subnasal cartilage, a position medial enough for the presumptive premandibular domain. Still, the commissure is continuous with the palatal arch throughout the development of the skull (Neumayer 1938; Holmgren 1946), and the possibility of it being a simple median extension of the palatal arch cannot be ruled out.

The dorsal and ventral longitudinal arches are clearly within the mandibular domain, except for their contacts with the visceral plate. The trigeminal ganglion equivalent to the maxillomandibular trunk in gnathostomes sits above the dorsal longitudinal arch (Figures 2-1C, 2-7). By similar reasoning, the visceral plate is continuous with the otic capsule and hosts the facial foramen near its dorsal end, which strongly suggests that the plate is in the hyoid domain.

Indeed, the facial nerve is either just medial to or posterior to the plate. All of the elements in the facial skeleton, with the exception of the palatal commissure, define the lateral extremes of the skull and do not contact the gut or oral cavity. By conventional definitions, then, these elements are external elements in the mandibular and hyoid arches (Holmgren 1946). The hyomandibular fenestra seems to coincide topographically with the hyomandibular cleft that appears early in the development of hagfish (Dean 1899; Stockard 1906; Wicht and Northcutt 1995). This provides further support that the visceral plate belongs to the hyoid arch.

2.3.4.4. Homology

An apparent correspondence exists between the hagfish visceral plate and the lamprey styliform cartilage (compare vsp in figure 2-1A to stc in 2-4E, F). Both elements are ventrally oriented pillars from the otic capsule and external with respect to the major trunks of nerves or blood vessels, and the facial nerve passes posterior to them (Holmgren 1946; Johnels 1948). In lampreys, the styliform cartilage forms the lateral velar skeleton, the internal counterpart of which belongs to the mandibular domain. However, the styliform cartilage in lampreys is best interpreted as an element forming in the hyoid arch because its mucocartilaginous anlage forms together with the anlage for the external hyoid arch, penetrated by the hyomandibular trunk of the facial nerve (hmn; Figure 2-4F) and posterolateral to the medial velar skeleton (Johnels 1948). The anterior migration of the anlage for the styliform cartilage allows the split from the extrahyal arch, and it assumes position lateral to the medial velar skeleton, but the cartilage and the hyomandibular nerve are still closely associated (Figure 2-4E, F; Johnels 1948; Lindström 1949). In the lamprey skull, the styliform cartilage continues ventromedially to the cornual plate that functions as a base for the velar skeleton. Therefore, the association and ventrolateral position with respect to the velar skeleton suggest that the cornual plate potentially corresponds to the velar process of the visceral plate in hagfish.

In addition to the cornual plate, two elements — otic-trigeminal cartilage (ota; traditionally called trabecula) and subocular arch (soa; Figure 2-4A) — extend anteriorly from the styliform cartilage in the lamprey skull. The lamprey otic-trigeminal cartilage is mesodermal in origin (Koltzoff 1901; Johnels 1948; Kuratani et al. 2004) and has a counterpart in the hagfish skull (parachordal skeleton, discussed in 2.3.5). On the other hand, the subocular arch can correspond to either the dorsal or ventral longitudinal arches of the hagfish facial skeleton plus the palatal arch. The suborbital trigeminal nerve closely parallels the subocular arch and eventually passes ventrally and medially from the dorsal side of the arch (Johnels 1948; Lindström 1949). This is more consistent with the dorsal longitudinal arch than with the ventral one. Although the subocular arch does not form the trigeminal fenestra as in the dorsal longitudinal arch of a hagfish, it calls into question the homology of the trigeminal fenestra between the two taxa, but not that of the dorsal longitudinal and subocular arches (discussed in 2.3.5.4). The transverse commissure of the arch is right below the mucocartilaginous anlage of the tectal cartilages, which likely comes from the premandibular ectomesenchyme. This implies that the palatal commissure in hagfish may arise from the premandibular domain.

In lampreys, the anterior extension of the subocular arch eventually differentiates into the posterior lateral plate and anterior tectal cartilage. The anterior tectal cartilage replaces the anterodorsal mass of the mucocartilage in the premandibular domain and forms the roof of the upper lip in front of the posterior dorsal plate (Johnels 1948). There is no element in the hagfish skull that topographically or anatomically corresponds to the anterior tectal cartilage. On the other hand, the posterior lateral plate compares well with the cornual process of hagfish. The plate lies lateral to the suborbital branch of the trigeminal nerve, forms part of the attachment for the muscle that suspends the lingual cartilages, and proximally contacts the subocular arch.

The extensive remodeling of the mandibular and hyoid arches in gnathostomes makes it difficult to identify similarities in the skeleton of these arches in gnathostomes with the facial skeleton of hagfish and lampreys (Janvier

2007). Clearly, the gnathostome mandibular and hyoid arches have neural crest-derived skeletons that support them. Similarity beyond that point breaks down (discussed in 2.4.1.3). There is evidence that inhibition of the endothelin signaling in lamprey ammocoetes results in skeletal defects in the lateral mouth plate of the mucocartilage (Yao et al. 2011), which in the adult skull is the lamprey counterpart of the hagfish facial skeleton. Yao et al. (2011) went even further to imply possible homology between the plate and the gnathostome Meckel's cartilage. However, the endothelin signaling does not necessarily imply such homology. The signaling from the mesoderm specifies the lower part of the pharyngeal arches in gnathostomes (Kurihara et al. 1994; Clouthier et al. 1998, 2000; Yanagisawa et al. 1998; Kempf et al. 1998; Kimmel et al. 2003; Nair et al. 2007). The polarity would be prerequisite in dorsoventral differentiation of any skeletogenic cells in the region, and lampreys do express genetic cascades for gnathostome-like dorsoventral polarization of the mandibular domain (Cerny et al. 2010). The signal specifying the ventral portion of pharyngeal arches could be similar between lampreys and gnathostomes, but that does not necessarily point to homology between specific elements beyond the observation that both develop in the equivalent portion of the arch.

2.3.5. Parachordal Skeleton

2.3.5.1. Morphology

The parachordal skeleton consists of the otic-trigeminal arch (ota), interfenestral strut (ifs), otic capsule (oc), and parachordal cartilage (nchs; Figure 2-1, 2-7). The otic-trigeminal arch forms a partial floor lateroventral to the brain and passes ventromedial with respect to the first ('ophthalmic') and second ('maxillomandibular') trigeminal ganglia and the ganglion of the facial nerve, forming the dorsomedial margins of the trigeminal fenestra and the facial foramen. The arch connects the palatal arch of the facial skeleton with the otic capsule. The acrochordal process of the nasopharyngeal plate fuses to the arch on the medial side of the trigeminal fenestra. The interfenestral strut between the

fenestra and the facial foramen bridges between the otic-trigeminal arch and the dorsal longitudinal arch of the facial skeleton.

Posteromedial to the facial foramen, the otic capsule houses the inner ear (Figure 2-7). The inner ear of hagfish only has a single semicircular canal (Retzius 1881). The longitudinal axis of the canal is oriented anterolaterally at 30° with respect to the sagittal plane, and the plane of the canal is tilted laterodorsally also at 30° with respect to the horizontal plane so that it can detect all three major planes of rotation (pitch, yaw, roll) (McVean 1991, 1998). The endolymphatic sac is also enclosed within the otic capsule (Jørgensen 1998; Jørgensen et al. 1998b). Between the right and left otic capsules is the parachordal cartilage below the brain. The cartilage has a dorsally open slot into which the notochord terminates anteriorly in adult hagfish.

2.3.5.2 Taxonomic comparison

There is no apparent morphological variation in the parachordal skeleton between species of hagfish. The otic capsule tends to be illustrated in parallel with the sagittal plane in early descriptions (Parker 1883a; Ayers and Jackson 1901; Cole 1905). The parasagittal longitudinal orientation of the capsule is erroneously reconstructed.

2.3.5.3. Development

In the development of a hagfish skull, the parachordal skeleton is among the first cartilages to appear (Figure 2-3A; Neumayer 1938). The otic capsules bridge over the notochord, which extends beyond the future parachordal cartilage at Neumayers stage I. The hyoid and mandibular components of the facial skeleton are also present at this time. The anterior extensions from the base of the otic capsule pass the lateral and medial sides of the facial and trigeminal ganglia and join anteriorly; of these the medial rod belongs to the parachordal skeleton. The notochord penetrates the future parachordal cartilage anteriorly into the late stages of embryonic development (Figure 2-3B; Neumayer 1938; Holmgren 1946). Because of the close association with the notochord, the parachordal

skeleton is assumed to arise in the paraxial mesoderm in the head (Koltzoff 1901; Johnels 1948; Kuratani 2004b; Kuratani et al. 2004). Contribution from the trigeminal crest cells is possible, but no experimental evidence is available for this hypothesis.

2.3.5.4. Homology

Functional and topographical correspondence is clear in the cranial parachordal skeletons of hagfish and other vertebrates. The otic capsule is treated as a homologue across vertebrates because it houses the same sensory structure innervated by the same cranial nerve (the vestibulocochlear nerve associated with the facial nerve) in all of them. Indeed, the otic capsule may be the most conservative and easily identifiable element in the vertebrate skull. The otic-trigeminal arch has long been labeled as trabecular in both hagfish (e.g., Holmgren 1946) and lampreys (e.g., de Beer 1937). This arch bridges the otic capsule and the facial skeleton or subocular arch, extends under the roots of the trigeminal and facial nerves along the lateral wall of the braincase, and forms the lateroventral wall of the braincase in both hagfish and lampreys. As for lampreys, Koltzoff (1901) and Johnels (1948) correctly observed that the 'trabecular' rod arises at the same anteroposterior level with the first aortic arch and therefore represents the parachordal component, not prechordal as in the true gnathostome trabecular (Kuratani et al. 2004). The same is true for the corresponding element in the hagfish skull (Kuratani and Ota 2008).

Related to the homology of the otic-trigeminal arch is the homology of trigeminal fenestra and facial foramen between hagfish and other vertebrates. In hagfish, the cartilaginous braincase is dorsally open and lacks the lateral wall. The trigeminal and facial nerves pass ventrally through the trigeminal fenestra (tf) and facial foramen (ff; Figure 2-7). In all other vertebrates including lampreys, the more medial opening through the chondrocranium for these nerves occurs in the lateral wall of the braincase. If the trigeminal fenestra and facial foramen were homologous across hagfish and all other vertebrates, it requires either of two scenarios in the lineage of hagfish: 1) the lateral wall of the braincase unfolded

laterally and the roots of the nerves overrode the inverted wall of the braincase laterally and penetrated it ventrally; or 2) the lateral wall of the braincase formed via dorsomedial folding of the parachordal skeleton, thereby shifting the opening from beside the floor of the braincase to the lateral wall. Given that the similarity can be established in the parachordal skeletons and the upper component of the facial skeletons between hagfish and lampreys, however, a much simpler explanation is that the lateral wall of the braincase is absent in hagfish, and the trigeminal fenestra and facial foramen secondarily formed in the rest of vertebrates upon the formation of the lateral wall of the braincase.

The parachordal cartilage is a chondrification around the notochord between the otic capsules, and therefore corresponds to the parachordal cartilages in lampreys and gnathostomes (Kuratani and Ota 2008). The wide conservation of the parachordal skeleton is due developmentally to the proximity between the notochord and the paraxial mesoderm and skeletogenic potential in signaling from the notochord (Couly et al. 1993), and due functionally to the need for skeletal separation between the enlarged vertebrate brain and pharynx.

2.3.6. Pharyngolingual Arches

2.3.6.1. Morphology

Previous literature always referred to the cartilaginous loops in the posterior part of the hagfish skull as branchial arches, although they identified different elements as the first and second branchial arches (Müller 1834; Parker 1883a; Ayers and Jackson 1901; Cole 1905, 1909; Holmgren and Stensiö 1936; Luther 1938; Holmgren 1946; Marinelli and Strenger 1956). These arches do not support any branchial structure, and no evidence exists to suggest that they did ancestrally. Therefore, the term branchial arch is inadequate, and these arches are termed pharyngolingual arches in this description.

There are two pairs each of external and internal pharyngolingual arches (plae1, 2, plai1, 2, Figures 2-1A, 2-8A, E). The internal arches form a basket along the lateral wall of the pharynx, whereas the external arches suspend the lingual apparatus from the basket. The first internal arch is complete and is shorter

dorsoventrally than the visceral plate by approximately a quarter. The second internal pharyngolingual arch may be complete or incomplete in different individuals, but the dorsal and ventral rami approach each other even in those without a complete arch. The first pharyngolingual fenestra (plf1) is approximately twice as long anteroposteriorly as the second (plf2; Figures 2-1A, 2-8A). The first external pharyngolingual arch originates from the dorsal ramus of the first internal pharyngolingual arch, splits the first pharyngolingual fenestra in half, overlaps the ventral ramus of the internal arch, fuses with the second external pharyngolingual arch and then to the posterolateral corner of the middle lingual plate. The second external pharyngolingual arch contacts the ventral ramus of the second internal pharyngolingual arch and parallels the first external arch on the medial side.

2.3.6.2. Taxonomic comparison

In *M. glutinosa*, the first pharyngolingual fenestra is shorter anteroposteriorly than in *E. stoutii* such that the fenestra is more round than elliptical. Also in *M. glutinosa*, the second internal pharyngolingual arch appears to be incomplete in all individuals, and in some the second external pharyngolingual arch does not contact the internal arch (Figures 2-2E, 2-12I; Cole 1905, 1909; Holmgren and Stensiö 1936; Holmgren 1946; Marinelli and Strenger 1956). Although the arch is incomplete in some individuals of *E. stoutii* with body lengthes shorter than 300 mm, *M. glutinosa* is different from *E. stoutii* in that the dorsal and ventral rami of the arch parallel each other, leaving the second pharyngolingual fenestra open posteriorly (Ayers and Jackson 1901). The complete or almost complete second internal pharyngolingual arch may be a diagnostic feature of *E. stoutii* at the level of species, because the congeneric *E. hexatrema* resembles *M. glutinosa* in having an incomplete second internal arch (Figure 2-2A, C; Müller 1834; Parker 1883a). Another character that sets apart *E. hexatrema* from *E. stoutii* is that the second external pharyngolingual arch does not appear to contact the internal pharyngolingual skeleton (Müller 1834; Parker 1883a). On the other hand, the anteroposteriorly elongate first pharyngolingual

fenestra is consistent between these species of *Eptatretus*, which suggests a potential utility in contrasting *Eptatretus* and *Myxine*.

2.3.6.3. Development

Designation of the external and internal arches depends on observations by Holmgren (1946) on the embryo of *M. glutinosa* between stages I and II of Neumayer (1938) that the anlagen of the internal arches form right along the lateral wall of the pharynx, whereas those of the external arches are removed laterally from this position and associated with the lingual skeleton (plai, plae; Figure 2-3B$_1$). The same observations can be made based on illustrations in Neumayer (1938). However, this topographical relationship only applies for the basal parts of the external arches (process lateralis in Neumayer 1938); the upper portions of the external arches develop near the wall of the pharynx. Later in life, the internal and external arches are at similar parasagittal plane (Figure 2-8E). The first external pharyngolingual arch remains lateral to the ventral ramus of the first internal pharyngolingual arch, but the second external arch fuses to the medial side of the ventral ramus of the second internal arch. At that stage, no major muscles, nerves or vessels clearly set apart the external and internal arches.

At stage I of Neumayer (1938), the first internal arch chondrifies to the extent of almost closing the pharyngolingual fenestra, and below and lateral to the element is the anlage of the first external arch. At stage II, the first internal and first external arches are complete, with the incipient dorsal and ventral rami of the second internal arch. All arches form by stage III.

2.3.6.4. Homology

The previous terminology of branchial arches for pharyngolingual arches assumes homology with branchial arches in lampreys and gnathostomes (Figure 2-4A, G). Two problems inherent to this assumed homology are the incongruence in the homology of branchial arches between lampreys and gnathostomes and the assumption that these arches ancestrally supported gills. As in the hyomandibular fenestra, the pharyngolingual fenestrae appear consistent in position with the

lateral diverticula from the pharynx at early stages of development, and these clefts from the diverticula later become reduced (Dean 1899; Stockard 1906). The implication is that the pharyngolingual arches represent a serial homologue as the pharyngeal skeleton, just as in the branchial arches of lampreys and gnathostomes. On the other hand, no positive evidence exists that these arches ancestrally supported gills in the lineage of hagfish. A posterior series of the diverticula from the pharynx derive gill pouches by folding the epithelium, but no part of this process occurs in the anterior series associated with the skull (Stockard 1906). The diverticula from the pharynx need not always form gills in vertebrates (e.g., mandibular and hyoid arches of living vertebrates do not support gills). This issue is further complicated by the incongruence of the branchial anatomy between lampreys and gnathostomes (discussed in 2.4.1.3). The gill pouches form medial to the branchial arches in lampreys as outpockets and folds of the gut epithelium; the branchial nerves and vessels are also medial to the arches (Goette 1901; Schaeffer and Thomson 1980; Janvier 2007). In gnathostomes, these structures form on the lateral side of the main branchial arches. In this paper, the branchial arches in lampreys are interpreted as chondrification of the neural crest-derived cells lateral to the head mesoderm, whereas those in gnathostomes are treated as chondrification at the interface of the mesoderm and endoderm in the head on the medial side.

The most intuitive explanation is that the external pharyngolingual arches in hagfish correspond to the branchial arches in lampreys, and the internal arches to the internal branchial skeleton in gnathostomes (Holmgren 1946). Difficulty with this interpretation lies in the absence of gills and any substantial mesodermal derivative between the external and internal pharyngolingual arches in hagfish. Among the muscles that attach to or lie near the external pharyngolingual arches, m. otic lingualis originates from the otic capsule and passes medial to the dorsal ramus of the first internal arch before it overlaps the ventral ramus of the internal arch laterally (Chapter 3). M. constrictor pharyngis and m. protractor dentalis lateralis are more superficial than the external arches. The pharynx has a lateral outpocket that approaches the upper portions of the external arches (Figure 2-8E).

The protractors and retractor of the lingual and dental apparatus likely extend from more posterior positions (Holmgren 1946), so they are not relevant in determining relative positions of the external arches.

Taken together, available anatomical evidence is equivocal in upholding the homology of the external pharyngolingual arches with the branchial arches in lampreys. The fact that the basal parts of the external pharyngolingual arches develop in association with the lingual skeleton suggests that at least these parts of the arches may belong to the lateral component of the ectomesenchyme, but the proximity of the upper portions of the external arches to the pharynx suggests that that parts of the external arches may be patterned by induction from the gut endoderm as in the pharyngeal skeleton of gnathostomes (Couly et al. 2002; Cerny et al. 2004a). There is no question that the internal arches in hagfish and lampreys are associated with the pharynx, and they can be viewed as developmentally equivalent to the branchial skeleton in gnathostomes.

In extinct jawless vertebrate lineages, some exceptional fossils preserve impressions for the support of the branchial arches (heterostracans) or tubers at the edge of the branchial cavity (galeaspids and osteostracans) (Stensiö 1927, 1932, 1958, 1964; Wangsjö 1952; Halstead Tarlo and Whiting 1965; Halstead 1973a, b; Janvier 1981b, 1984, 1985, 1993, 1996, 2007; Blieck 1984; Gai et al. 2011). These anatomical correlates for branchial support indicate that branchial support may be cartilaginous in these fishes and lateral to the gills and their associated mesoendodermal derivatives.

2.3.7. Velar Skeleton

2.3.7.1. Morphology

The velar skeleton is responsible for ventilation and consists of the cartilaginous arches and processes that extend posteriorly within the dorsal fold of the pharynx (vls; Figures 2-1, 2-8). The longitudinal cartilaginous bars support the velar scroll — the lateral portions of the longitudinal double membrane suspended in the pharynx — and the suprapharyngeal processes anchor the velar complex to the roof of the pharynx. The velar cartilages are highly mobile within the hagfish

head. The muscles attached to the velar cartilages are responsible for dorsoventral flexion of the velum to create respiratory current (Strahan 1958). The velar cartilages also suspend the pharynx within the pharyngeal cavity in the area of high activity and ensure an open passage through the pharynx. The anterior pharynx is pulled forward as the dental apparatus is everted, and backward as the food item passes through the oral cavity. The nasopharyngeal duct joins the pharynx below the proximal end of the velar skeleton as well.

The lateral velar cartilage (vll; Figure 2-8A, B, E) extends posteriorly behind the facial and pharyngolingual skeletons, supporting the free lateral portion of the velar scroll. The anterior end of the cartilage curls laterally to form the velar knob (vlk). The velar knob is visible in lateral view of the skull behind the anterior margin of the visceral plate. The knob serves as a site of attachment anteriorly, for m. craniovelar anterior dorsalis and ventralis, posterodorsally, for m. spinovelaris, and posteromedially, for m. craniovelar posterior. The velar knob and the velar process of the visceral plate (vlp) contact each other by sandwiching the cardinal heart (ch; Figure 2-8D). The muscular activity in this area presumably drives the pulsation of the cardinal heart.

On the medial side of the first external pharyngolingual arch, the medial velar cartilage (vlm; Figure 2-8A, B, E) fuses to the lateral velar cartilage. Both lateral and medial cartilages support the velar scroll. The lateral cartilage is slightly longer than, and dorsal with respect to, the medial cartilage. The medial cartilage bows medially along the medial margin of the velar scroll before meeting the anterior and posterior transverse cartilage to enclose the velar fenestra (vlf; Figures 2-1B, 2-8A). The velar fenestra is transversely wider anteriorly than it is at the posterior margin. The medial velar cartilage terminates posteriorly at the junction with the posterior transverse cartilage and the lateral scroll process (tp; Figure 2-8A) that extends posterolaterally for approximately the same distance as the anteroposterior length of the velar fenestra.

The anterior transverse velar cartilage is the base for the anterior and posterior suprapharyngeal processes at the midline (vlspa, vlspp; Figures 2-1B, 2-8A). The anterior suprapharyngeal processes are bilaterally paired and without

hooks or forks, and extend anterodorsally above the pharynx to attach to the connective tissue associated with the notochord dorsally near the dorsal aorta. This part of the anterior suprapharyngeal process sits on the dorsal roof of the pharynx and suspends the velar cartilages within the pharynx. The anterior suprapharyngeal process extends anteriorly to the split between the first external and internal pharyngolingual arches. Also extending to the suprapharyngeal path, the posterior suprapharyngeal process is a single midline element and as long posteriorly as the anterior suprapharyngeal process. The posterior cartilage extends posteriorly beyond the posterior margin of the fenestra. At the posterior end, it has a squamous perforated plate. The posterior transverse cartilage has a posterior process along the midline. This process is posteriorly shorter than the lateral terminal process and directly below the posterior end of the posterior suprapharyngeal process.

2.3.7.2. Taxonomic comparison

The velar skeleton of *M. glutinosa* can be distinguished from that of *E. stoutii* by the following several characters (Figures 2-1B, 2-2B, D, 2-8, 2-12I, J; Parker 1883a; Cole 1905, 1909; Marinelli and Strenger 1956; Strahan 1958; Robson et al. 2000). The posterior suprapharyngeal process is incipient, and the anterior suprapharyngeal processes are hooked and forked. The velar fenestra is square. The lateral terminal process is strongly hooked dorsally. There are several posterior processes extending from the posterior transverse cartilage. *E. hexatrema* also has the square velar fenestra and the anterior suprapharyngeal rod that splits into anterior and posterior terminal processes, but the velar skeleton of this taxon is similar to that of *E. stoutii* in having the elongate posterior suprapharyngeal process and the single-rooted process from the posterior transverse bar (Müller 1834; Parker 1883a). Therefore, the latter two characters may set *Eptatretus* apart from *Myxine*. *E. stoutii* is unique in having the posteriorly tapering velar fenestra, a terminal expansion on the posterior suprapharyngeal process, and a simple, undivided anterior suprapharyngeal process.

Because the velar skeleton is flexible, it is illustrated in various positions. Cole (1905) drew attention to the parallel relationships between the lateral and medial velar cartilages in *Eptatretus* spp., but the lateral velar cartilage is more dorsal than the medial velar cartilages and does cross over to the medial side of the medial cartilages in this taxon, depending on the degree of flexibility in the skeleton. Therefore, this is not a reliable character. Similarly, the lack of an interlocking contact at the proximal end of the velar skeleton in *E. stoutii* (as noted by Ayers and Jackson [1901] and used by Cole [1905]) is also likely an omission, if not intraspecific variation, because this contact is often concealed from lateral view.

2.3.7.3. Development

The velar skeleton forms a posteriorly oriented V within the dorsal fold of the pharynx below the notochord by stage II (Holmgren 1946). The lateral and medial velar cartilages (vll, vlm) split, and the transverse bars connect the right and left medial velar cartilage to define the velar fenestra by stage III (Figure 2-3C, D). At the same stage of development, the anlagen for the suprapharyngeal processes form above the rest of the velar skeleton and subsequently fuse with the anterior transverse bar. Reconstruction of the skull of an embryo gives an impression that the velar skeleton is closely associated with the pharyngolingual skeleton (Neumayer 1938), but the two are separated by the pharynx.

Coupled with a close association between the velar knob and the visceral plate, the position of the velar skeleton below the otic capsule (vls; Figure 2-3B_1) appears to suggest that it derives from the hyoid arch (Kuratani and Ota 2008). However, the velar skeleton is likely mandibular in origin. The dorsal fold of the pharynx that houses the velar skeleton begins below the trigeminal ganglia as a medially invaginated lateral wall of the pharynx. Anterior to this point is the pouch into which the dental apparatus is tucked, and this is a derivative of the mandibular pouch, or the first lateral outpocket of the pharynx. The reduced hyomandibular pouch is posterior to the origin of the dorsal fold (Stockard 1906; Wicht and Northcutt 1995). In the embryo of Holmgren (1946), the dorsolateral

wing of the hyomandibular pouch separates the visceral plate and the lateral velar cartilage. Even in adults, the velar skeleton and the visceral plate are set apart by the cardinal heart (Figure 2-8D). The internal carotid artery originates posterior to the velar knob, and indicates that the proximal portions of the velar skeleton is still within the mandibular domain. The internal carotid artery enters the braincase through the hypophyseal fenestra in gnathostomes (Goodrich 1930; de Beer 1937), and thus can be used as a marker relative to the mandibular domain. Furthermore, the musculature in the velar skeleton is innervated by a branch of the motor trunk of the trigeminal nerve. These observations suggest that the velar skeleton and its connective tissues originate in the mandibular domain as mesenchyme and extend posteriorly into the pocket between the mandibular and hyomandibular pouches. There is no contribution from postcranial somites to the velar skeleton, as shown by the fact that the velar tissues do not receive innervation by spinal nerves. The skeletonization in the velum is likely to be induced by the wall of the pharynx, but the close proximity of the suprapharyngeal anlage to the notochord suggests that the suprapharyngeal processes may develop from chordal induction.

It remains uncertain if the velar skeleton is a chondrification of mesoderm-derived or neural crest-derived cells. It is tentatively assumed as derived from the trigeminal neural crest-derived ectomesenchyme, because all chondrocranial elements closely associated with endodermal derivatives (and known to be induced by the endodermal epithelium) originate from the neural crest cells (Noden 1992; Couly et al. 2002; David et al. 2002; Ruhin et al. 2003; Crump et al. 2004; Haworth et al. 2004, 2007; Graham et al. 2005; Brito et al. 2006; Benouaiche et al. 2008). Regardless of developmental origin, the medial position of m. craniovelar posterior with respect to the lateral velar cartilage indicates that the velar skeleton represents a skeletal component lateral to the head mesoderm. Anterior and medial to the velar knob, the muscle passes below the trigeminal ganglia and consistently separates the velar skeleton from the nasopharyngeal duct and pharynx. Even within the dorsal fold, the muscle is between the skeleton and the midline ridge of the pharyngeal epithelium. These anatomical

observations indicate that the velar skeleton forms on the lateral side of the mandibular mesoderm, and is thus external.

2.3.7.4. Homology

Cephalochordates and lampreys also have a velum, although the homology of the velum across chordates is uncertain. Cephalochordates are excluded from the analysis of similarity because the cephalochordate velum lacks skeletal support and because the current through the velum is driven by cilia, not by muscles. Coupled with the absence of vertebrate synapomorphies such as the neural crest, it is difficult to compare the cephalochordate velum with those in vertebrates based on anatomical evidence alone.

In lampreys, the velum has a skeletal rod that supports it. The velar skeleton develops below the otic-trigeminal rod and medial to the styliform cartilage and above the cornual plate, along the lateral wall of the pharynx (Figure 2-4C; Johnels 1948). The musculature attached to the medial velar plate is innervated by the motor branch of the trigeminal nerve as in hagfish (Lindström 1949) and lateral with respect to the medial bar (ammocoete) or medial plate of the velar skeleton regardless of life stages (Marinelli and Strenger 1954; Mallatt 1996). These similarities suggest that at least the lateral bar of the lamprey velar skeleton is a strong candidate for a homologue with the lateral velar cartilage in hagfish. It is unknown if the medial velar cartilage in hagfish represents an internal skeletal component of the mandibular arch like the medial velar plate in lampreys.

Gnathostomes lack a velum. Because the hagfish velar skeleton forms on the lateral side of the mandibular mesoderm, it is not comparable with the gnathostome jaw, whose serial homologue (branchial arch) is medial with respect to the mesoderm within pharyngeal arches. The medial position and mandibular origin of the lamprey velar skeleton raises the possibility that at least the medial part of it represents the internal component of the skeleton of the mandibular arch as in the gnathostome palatoquadrate and/or in Meckel's cartilages (Mallatt 1996). This is an attractive hypothesis, but that is not necessarily to say that the same

chondrocranial element is conserved in lampreys as the medial velar skeleton and in gnathostomes as the palatoquadorate and/or Meckel's cartilages. The homology between the lamprey velum and the gnathostome jaw has not received support from the morphology of the trigeminal nerve. The peripheral pathways of the trigeminal nerve do not necessarily indicate correspondence between the lamprey velar nerve and the gnathostome mandibular nerve (Lindström 1949; Kuratani et al. 1997; Barreiro-Iglesias et al. 2008). The immunohistochemistry of the velar nerve is distinct from other trigeminal motor neurons innervating the upper and lower lips in lampreys in having tubulin-ir/DCX-positive fibers (Barreiro-Iglesias et al. 2011). The origin of jaws has to incorporate the dorsoventral patterning within the mandibular arch and form the jointed upper and lower skeletal components (Depew et al. 2001, 2005; Shigetani et al. 2002, 2005; Cerny et al. 2004b, 2010; Depew and Simpson 2006; Kuratani 2004b, 2012; Yao et al. 2011; Kuratani et al. 2012). Such a dorsoventral patterning need not only affect one skeletal element in the arch, it likely also affects all visceral skeletal elements in it. Indeed, the gnathostome palatoquadrate is best viewed as the composite of the premandibular and mandibular ectomesenchyme (Cerny et al. 2004b). The heterotopic theory of the origin of jaws holds that the posterior shift of the induction site for the oral epithelium is a prerequisite (Shigetani et al. 2002, 2005; Kuratani 2004b, 2012; Kuratani et al. 2012). Interestingly, the velar skeleton is medially and posteriorly the deepest skeletal element within the mandibular arch in both hagfish and lampreys, so such a posterior position brings the mouth and the presumptive jaw joint close to where the velum would otherwise form. Although a complete homology cannot be established between the velar skeletons of hagfish and lampreys and the mandibular skeletons of gnathostomes, it is reasonable to hypothesize that a homologue of the hagfish and lamprey velar skeletons is incorporated within the gnathostome mandibular skeleton.

No osteological correlates of the velum have been identified in fossil jawless vertebrates. However, the most anterior impression of the gill lamellae in heterostracans is lateral to the semicircular canals; the most anterior branchial

cavity is likewise lateral to the semicircular canals in galeaspids; and the prebranchial cavity is identified in the mandibular domain in osteostracans (Stensiö 1927, 1932, 1958, 1964; Wangsjö 1952; Halstead 1973a, b; Janvier 1981b, 1984, 1985, 1993, 1996, 2007; Blieck 1984; Gai et al. 2011). These observations suggest that the mandibular arch did not form a gill at any point in early vertebrate evolution, and that the mandibular domain in these animals served a different function than respiration, likely one analogous to the velum in hagfish and lampreys.

2.3.8. Dental Apparatus

2.3.8.1. Morphology

The dental apparatus consists of the midline plate, and two bilateral pairs of basal plates and tooth plates (Figure 2-9). The dorsal median tooth is fixed and not involved in the dental apparatus, but is discussed in this section. All of these elements, with the exception of the dorsal median tooth, form a mobile, butterfly-shaped complex that sits within the oral cavity. The dental apparatus is gently folded toward the midline at rest. When the protractors are contracted, the dental apparatus is everted ventrally in a fashion analogous to a pulley and unfolded laterally. This eversion and lateral unfolding of teeth is quite similar to what is observed in a gastropod radula, which is also used for rasping.

Anteriorly, the midline plate (mp) is the site of attachment for the protractors of the dental apparatus (m.pdm, m.pdl; Figure 2-9A, D). Posteriorly, the plate has two processes posterolaterally on each side. The anterior lateral process (dalp) fuses to the anteromedial margin of the lateral basal plate at the point adjacent to the lateral margin of the midline plate. The posterior lateral process (dplp) extends farther posterolaterally to arch over and parallel the medial margin of the lateral basal plate and fuses to the plate at the base of the medial posterior process.

The lateral basal plate (dlbp; Figure 2-9A, D) is the largest element in the dental apparatus that sits beside the midline plate and the medial basal plate (dmbp). The plate is thin dorsoventrally and is concave dorsally. Posteriorly, the

plate splits into the lateral and medial posterior processes that have approximately the same lengths. Whereas the lateral posterior process (dlpp) is free, the medial posterior process (dmpp) attaches to the lateral wing of the medial basal plate (dmbp).

The medial basal plate has a ventrally convex gentle arch on each side and is M-shaped in anterior view. Because of this arch, the medial basal plate is lower in position than the lateral basal plate or the midline plate. The tip of the lateral wing attaches to the medial posterior process of the lateral basal plate. The tendon from m. retractor dentalis major (t.rdm) inserts onto the dorsal surface of the plate. The dental apparatus lies flat in normal position, but posterior retraction of the medial basal plate causes the tailing edge of the lateral basal plates to fold. The lateral wings of the medial basal plate are pulled posteromedially, and the dental apparatus is retracted through the mouth back into the oral cavity.

The dental apparatus is connected to the skull by m. retractor dentalis lateralis and by sheets of ligamentous tissues. On the dorsal surface, the ligamentous membrane from the nasopharyngeal plate suspends the apparatus along the midline and along the posterior margin. The ligamentous membrane from the palatal commissure and subnasal cartilage connect the apparatus along its lateral margin. On the ventral side, the ligamentous membrane from the bilateral longitudinal ridges (pcpl; Figure 2-10A) extends posterodorsally to the dental apparatus.

A bilateral pair of keratinous lateral and medial tooth plates sits on the dorsal sides of the lateral basal plates (Figure 2-9 A-C, E, F). The cusps are elevated from the plane of the basal plate at an angle of 35 to 45° when the dental apparatus is everted. As the apparatus is folded and retracted through the mouth, the cusps also fold toward the midline, which would be effective in trapping preys or food items within the oral cavity. When in life position, the lateral and medial tooth plates form a posteriorly open arc, with each cusp pointing toward the split of the right and left posterior lateral process of the midline plate. The lateral tooth plate has ten cusps, the first three of which are fused to each other; the medial tooth plate has ten or eleven cusps, the first two of which are fused to each other.

The rest of the cusps have sutures between them. The cusps are stouter and less strongly curved in the lateral tooth plate than in the medial tooth plate. Within the same tooth plate, the second to sixth cusps are the tallest, widest at the base, and are less strongly curved. The first cusp is smaller than the second one, and the cusps beyond the sixth progressively become shorter, narrower, and more strongly recurved than their anterior neighbors. The eleventh cusp of the medial tooth plate is incipient and easily detached from the rest of the tooth plate. Therefore, it cannot be accurately determined whether the cusp number varies asymmetrically, ontogenetically, or individually. All cusps are hollow inside and filled with papillae.

The dorsal median tooth (ddm; Figure 2-1A) hangs from the space between the ventromedial surface of the palatine commissure and the anterior terminal processes of the nasopharyngeal plate. The cusp is slender and more strongly curved than those in the lateral tooth plates. Histologically, the tooth is similar to those in the tooth plates. Functionally, it is fixed at the roof of the oral cavity, presumably to prevent prey from escaping the cavity.

2.3.8.2. Taxonomic comparison

In *M. glutinosa*, the posterior lateral process of the midline plate fuses to the lateral basal plate more proximally than in *E. stoutii*. Furthermore, the right and left lateral basal plates are transversely nearly the same width as the medial basal plate, whereas they are significantly wider in *E. stoutii* (Cole 1905; Marinelli and Strenger 1956). In the illustration of the dental apparatus of *E. hexatrema* by Parker (1883a), the posterior lateral process fuses to the medial basal plate. This is likely an error, because no such connection is observed in illustration of the same species by Müller (1834).

The total number of cusps in the tooth plates and the number of the fused cusps are both taxonomically significant (Fernholm 1998). Both meristic traits tend to be conservative within species, although the magnitude of intraspecific variation in the total cusp number may be up to eight in two out of 35 species of *Eptatretus* recognized by Fernholm (1998). Although *E. stoutii* is listed to have

ten cusps each in the lateral and medial tooth plates (total *n* = 40) (Fernholm 1998), the specimens from Barkley Sound tend to have an incipient eleventh cusp in the medial tooth plate (total *n* = 40 to 42). One specimen collected off the shores of California was identified as *E. stoutii* and was illustrated by Clark and Summers (2012) as having eleven cusps in both the lateral and medial tooth plates. In the illustration of *E. stoutii* collected off the shores of California by Ayers and Jackson (1901), the lateral tooth plate on the right side has thirteen cusps, whereas the number is eleven on the left. However, the rough drawing suggests that the variation could be an artifact. This variation may be geographical, and it is not warranted to establish a new taxon based on the count of cusps alone. No variation is observed in the cusp number within each of the species of *Myxine*, *Nemamyxine*, *Neomyxine*, and *Notomyxine* (Fernholm 1998). Across myxinoids, the total number of cusps varies from 27 (*M. pequenoi*; Wisner and McMillan 1995) to 71 (*E. carlhubussi*; McMillan and Wisner 1984).

2.3.8.3. Development

The dental apparatus (da) is one of the last elements in the hagfish skull to chondrify (Figure 2-3D). The cartilaginous anlage cannot be confirmed until stage IV. Holmgren (1946) described a pad of mesenchyme in his palatoquadrate anlage as an anteroventral projection from the ventral longitudinal arch of the facial skeleton (Figure 2-3B_1) in the embryo of *M. glutinosa* between Neumayer's stages I and II. If their observations are correct, the dental apparatus develops in the mandibular domain between the mandibular and hyoid pouches (Stockard 1906). The ligamentous connection with the anterior and middle lingual cartilages and the trigeminal innervation support this view. In later embryos, the oral cavity is M-shaped in cross section (Wicht and Northcutt 1995). The lateral and medial basal plates appear to develop along the ventral wall of the cavity. The pouch within the oral cavity that houses the mature dental apparatus corresponds in position with the earlier mandibular pouch, and these two may be equivalent.

2.3.8.4. Homology

There is a nearly perfect anatomical, topological, and functional counterpart of the hagfish dental apparatus in lampreys. The lingual tooth plate of lampreys (dsp) sits on the supralingual cartilage (sap), which forms a dental apparatus along with the apical teeth (dap). It is pulled forward and outward by the retraction of m. protractor dentalis and backward by the retraction of m. retractor dentalis (Figure 2-4B; Holmgren 1946; Marinelli and Strenger 1956; Yalden 1985; Janvier 1993). In the absence of a cyclostome-like lingual apparatus, identification of a homologue in the gnathostome skull is challenging. The definite origin in the mandibular domain, coupled with the close association of the mesenchyme with that of the facial skeleton (Holmgren 1946), suggests that skeletal components of the oral apparatus derived from the mandibular arch are homologous at that level across vertebrates. At a finer level, however, an element-to-element complete homology with the hagfish dental apparatus cannot be determined in gnathostomes with morphological evidence alone because similarities of the anatomical correlates of the dental apparatus are also uncertain. The association with the ventral longitudinal arch of the facial skeleton suggests that the dental apparatus may belong to the ventral component of the mandibular domain. However, that does not mean that a homologue of the dental apparatus has been conserved across vertebrates. Although the dental apparatus has been termed as 'jaw' apparatus for functional reasons (Dawson 1963; Yalden 1985), even that designation is misleading, as no gnathostome oral apparatus functions in the pulley-like motion that involves the protractors below and retractors above basal elements on which the apparatus sits. Therefore, the dental apparatus can only be compared with the gnathostome jaw as a functional unit of the oral apparatus; a homologue may exist, but it cannot be determined as such with the anatomical information available at hand.

It is possible to seek functional and anatomical correspondence in the oral plates of heterostracans and osteostracans and in euconodont elements of conodonts (Figures 2-15, 2-16 A-C). Although the histology of the oral plates is unknown, these oral plates may have functioned in an analogous way with the

tooth plates in hagfish, especially in heterostracans (Janvier 1974). On the other hand, the plates sustain no significant wear along the edge but only on the ventral surface in heterostracans (White 1935; Purnell 2002). This falsifies an important prediction if the plates were used for highly mobile, predatorial functions similar to the dental apparatus in hagfish. Furthermore, the oral plates in both groups are from the dermal skeleton and positioned along the buccopharyngeal opening. Unlike the tooth plates of hagfish, they could not be tucked inside the oral cavity, attached to mobile substrate tissue, or associated with the underlying skeleton over which they glide. Coupled with the ventral position, these characteristics of the oral plates are more reminiscent of the infraoral lamina in lampreys, to which no anatomical correlate exists in hagfish (Marinelli and Strenger 1954; Hillard et al. 1985; Kawasaki and Rovainen 1988; Rovainen 1996). So hagfish tooth plates and heterostracan and osteostracan oral plates can be compared at the level of functional units (oral apparatus), but anatomical evidence for specific homology at the level of element (tooth plates, basal plates, or midline plate) cannot be established.

Various types of euconodont elements each show specialization toward grasping, mashing, grinding, or cutting (Purnell 1994, 1995; Purnell and von Bitter 1992; Purnell and Donoghue 1997; Goudemand et al. 2011; Jones et al. 2012). Although histological characters reveal a number of differences between hagfish tooth plates and conodont teeth (discussed in 2.3.11.5), the structures associated with conodont teeth may have been almost identical to those associated with hagfish tooth plates. Biomechanical analyses predict partial, forward eversion and posteroventrally rotating retraction of the anterior longitudinal teeth called S elements (Purnell and Donoghue 1997; Goudemand et al. 2011), similar to the pulley motion in hagfish and lampreys (Hillard et al. 1985; Yalden 1985; Kawasaki and Rovainen 1988; Rovainen 1996). Such a motion would require the presence of a basal cartilage, protractors, and retractors arranged identically to the oral apparatus in hagfish and lampreys (Figure 2-16 A-C; Aldridge et al. 1995; Purnell and Donoghue 1997, 1998; Goudemand et al. 2011). The presence of basal bodies in conodont tooth crowns also suggests an attachment to a substrate

(Sansom et al. 1992). Regardless of the homology of the hagfish tooth plates and conodont S elements, the oral apparatuses of these animals on the whole are functionally and anatomically equivalent. A functional comparison of the oral apparatuses in hagfish, lampreys, conodonts, heterostracans, and osteostracans requires comprehensive description of the hagfish musculararature, and is thus given a treatment in Chapter 3.

2.3.9. Lingual Apparatus

2.3.9.1. Morphology

The lingual cartilages underlie the oral cavity and form the lingual apparatus in conjunction with the protractors and retractors of the dental apparatus (Figures 2-1, 2-10). They consist of the anterolateral, anteromedial, middle, and lower distal lingual cartilages, and the posterior lingual and upper distal lingual pseudocartilages (histologically distinct from other cartilages).

The anterolateral lingual cartilage (lcal) is the only bilaterally paired element and forms the lateral wall of the oral cavity. Much of the cartilage in the periphery of the mouth consists of a perichondral connective tissue, or pseudocartilage of Cole (1905) (Figure 2-12G; histological description in 2.3.11.1). The hard cartilage that makes up the posterior three quarters of the plate extends anteriorly within the perichondral pseudocartilage, and this is the proximal portion of the lateral tentacular cartilage.

The anteromedial lingual cartilage (lcam) is approximately half the transverse width of the middle lingual cartilage. Anteriorly, it forms a shallow notch at the posterior margin of the mouth and, posteriorly, encloses the anterior half of the lingual foramen (lf; Figure 2-10A). It has ligamentous contact along the lateral margin with the anterolateral lingual cartilage and at the posterior end with the middle lingual cartilage. The contact is stronger with the middle lingual cartilage than with the anterolateral lingual cartilage such that extraction of the hagfish skull usually results in detachment of the latter.

The middle lingual cartilage (lcm) is approximately 1.5 times longer anteroposteriorly than wide transversely. Anteriorly, the cartilage encloses the

posterior part of the lingual foramen. Posteriorly, the lingual apparatus is suspended at the posterolateral corner by the first and second external pharyngolingual arches. In the anterior third, the cartilage is thinnest along the midline (less than one fifth the thickness of the lateral part), which forms a transversely wide, V-shaped trough to accommodate the medial basal plate of the dental apparatus. Posteriorly, the cartilage is thicker so that the trough is shallower and U-shaped. The tendon for the dental apparatus (t.rdm) extends above this trough and between the anterior extensions of the perichondrium of the posterior lingual cartilage (pcpl; Figure 2-10C).

The posterior lingual cartilage is the longest and largest unit in the hagfish skull (lcp; Figures 2-1A, 2-10D, G-J). As in the perichondral tissue of the anterolateral lingual cartilage, the cartilage consists entirely of pseudocartilage (Figure 2-12E). The cartilage has a deep midline trough through which the tendon of m. retractor dentalis major passes to insert to the dental apparatus. The cartilage also extends anteriorly in a pair of ridges onto the middle lingual cartilage on both sides of the tendon (pcpl; Figure 2-10A, C). Laterally, the main part of the element serves as the site of attachment for the protractors of the dental apparatus.

Two distal lingual skeletal elements lie near the posterior end of the lingual apparatus. The upper distal lingual cartilage (lcdu) is dorsoventrally flattened at the top of the lingual apparatus near the posterior end and its ventral surface is the origin of m. perpendicularis (Figure 2-10E). Histologically, this tissue cannot be distinguished from perichondrium or peseudocartilage. The rod-like lower distal lingual cartilage (lcdl) is anteroposteriorly longer than the upper element, circular in cross section, and a true cartilage (Figure 2-10F). It provides the sites of attachment for m. perpendicularis and m. retractor dentalis major; the latter is the largest muscle in the apparatus.

2.3.9.2. Taxonomic comparison

Descriptions of the hagfish skeleton disagree over how many elements exist in the anterior and middle segments of the lingual skeleton. Müller (1834), Parker (1883a), and Clark and Summers (2012) illustrated the anteromedial

lingual cartilage as a bilateral pair for each of *E. hexatrema*, *M. glutinosa*, and *E. stoutii*, respectively. The anteromedial cartilage is undoubtedly a single element in the adults of *M. glutinosa* and *E. stoutii*. The anterior portion of the cartilage has a bilateral pair of processes of hard cartilage embedded within the pseudocartilaginous matrix, which may have been misinterpreted as suture. However, the posterior half of the cartilage is entirely hard cartilage, and no suture exists along the midline. The middle lingual cartilage is unanimously described as paired (Müller 1834; Parker 1883a; Ayers and Jackson 1901; Cole 1905; Holmgren 1946; Clark and Summers 2012). Indeed, the cartilage is much thinner along the midline than in the lateral side. However, no suture is observed in histological sections of the adult *E. stoutii*. The cartilaginous matrix is continuous, and chondrocytes distribute on and across the midline. This may be a result of fusion between bilateral counterparts, but by the time body length reaches 250 mm, the cartilage is decidedly a single element.

2.3.9.3. Development

The lingual skeleton appears as continuous condensations of ectomesenchyme between Neumayer's stages I and II (Figure 2-3; Neumayer 1938; Holmgren 1946). This matrix probably consists of the pseudocartilage, and chondrification of hard cartilage proceeds within this matrix. At stage II, the middle and posterior lingual cartilages are single, whereas chondrification for the anteromedial lingual cartilage is represented by paired incipient processes between the anterolateral lingual cartilages (Figure 2-3C_2). The boundaries among the segments of the lingual cartilage appear to correlate with the pharyngeal arches. The anterolateral and anteromedial cartilages correspond to the position of the mandibular pouch, and the middle lingual cartilage to the hyomandibular pouch (Stockard 1906; Wicht and Northcutt 1995). The anterolateral lingual cartilage extends anterodorsally, and becomes the lateral tentacular cartilage.

2.3.9.4. Homology

There is an apparent similarity in the lingual apparatuses of hagfish and lampreys (Figures 2-1A, 2-4B, 2-10; Yalden 1985). As in hagfish, the lingual apparatus consists of three segments of cartilages in lampreys, from anteriorly: apical, copular, and piston cartilages (apc, coc, and pisc; Figure 2-4B). The largest of the three is a posterior median element that serves as an attachment for protractors of the dental apparatus, and the anterior element provides a pulley for it to slide over.

Although the use of a jaw apparatus instead of a lingual apparatus (e.g., Dawson 1963) assumes a functional correspondence between the cyclostome lingual apparatus and the gnathostome jaw, it is difficult to compare these structures beyond functional similarities. The gnathostome jaw requires an upper and lower component, but the cyclostome lingual apparatus lies on the ventral side of the head. The skeleton of the gnathostome lower jaw does not have three anteroposteriorly segmented units as in the lingual apparatus. No gnathostome is known to have a pulley at the anterior end of the jaw or oral apparatus. Crucially, the Heterotopic Theory (Shigetani et al. 2002, 2005; Kuratani 2004b, 2012; Kuratani et al. 2004, 2012) suggests that the induction of oral epithelium shifted posteriorly at the origin of the jaw. The implication is that significant remodeling set apart non-gnathostomes and gnathostomes in this region of the head. This does not preclude homology, but it is difficult to identify it on the basis of anatomical information alone. The ventral longitudinal groove in heterostracans is interpreted as an imporession of the lingual apparatus (Janvier 1996), and a biomechanical analysis of conodont teeth implies the presence of the lingual apparatus-like structure in conodonts (Goudemand et al. 2011). These observations suggest that at least a functional analogue existed in these animals, but evidence for the homology is circumstantial at best.

2.3.10. Branchial Cartilages

2.3.10.1. Morphology

Branchial cartilages in *E. stoutii* have two types: extrabranchial cartilage and extra-pharyngocutaneous cartilage (Figure 2-11). The extrabranchial cartilage wraps around the distal portion of the efferent branchial duct near the external pore. It is semilunate in shape when extracted. The main body is attached to the posterolateral surface of the duct, whereas its two arms, if present, encircle the duct. The extra-pharyngocutaneous cartilage only occurs on the left side, as it is attached to the left-sided pharyngocutaneous duct. The shape is variable (Ayers and Jackson 1901), and the most differentiated specimen as described in that paper is reproduced here. It has three arms, two medially oriented and one laterally oriented, and hosts a large foramen along its anterior margin.

2.3.10.2. Taxonomic comparison

The efferent branchial ducts join with one another into a common external duct on the right side and further with the pharyngocutaneous duct in *M. glutinosa*. Accordingly, the branchial cartilages form around the common efferent ducts on both sides (Cole 1905). On the right side, the main body of the extrabranchial cartilage lies underneath the first two ducts and encircles the common duct with a slender terminal process; on the left side, the tetraradiate extra-pharyngocutaneous cartilage connects with the extrabranchial cartilage, which lacks the ventral arm from the main body (Cole 1905). In both *E. stoutii* and *M. glutinosa*, the shapes of these cartilages are highly variable (Ayers and Jackson 1901; Cole 1905), as some specimens lack arms or perforations and others develop a contact between the arms. Therefore, the specific morphology of the cartilages is not as important as the distribution and location. The conditions in *E. stoutii* demonstrate that the cartilages have the main body on the posterior side of each of the efferent branchial ducts, an outer component of the endodermal epithelium (Stockard 1906), and are lateral with respect to the pharyngeal mesoderm and branchial arteries. The difference with *M. glutinosa* is that the cartilages are fused into a loop around the common external passage, but the

relatively lateral position is the same. Cole (1905) reported that in at least one specimen of *M. glutinosa*, the extrabranchial loop and the extra-pharyngocutaneous cartilage were still separate, which supports the idea that the cartilaginous precursors are originally separate. In this respect, the conditions in *E. stoutii* are likely plesiomorphic.

2.3.10.3. Homology

Although highly reduced, the superficial position and the apparent function of maintaining open efferent ducts from the gills point to a candidate homologue of the hagfish extrabranchial cartilages in the branchial arches of lampreys and the extrabranchial cartilages of gnathostomes. In lampreys, the elaborate branchial arches form the elastic pharyngeal basket that aids in ventilation (brb; Figure 2-4A; Luther 1938; Marinelli and Strenger 1954; Schaeffer and Thomson 1980; Mallatt 1984). In gnathostomes, the extrabranchial cartilages are small skeletal rods that support the external openings of the gill slits (brc, bre, brbrh, brp, brx; Figure 2-4G; Mallatt 1984). The conditions in hagfish resemble the latter, as the branchial muscle is not attached to the cartilages and as the cartilages do not form an interconnected web of skeletal rods.

2.3.11. Histology of Hagfish Cartilages and Keratinous Teeth

2.3.11.1. Cartilages: histological characteristics

Different types of cartilages in the hagfish skeleton were recognized as early as the classification based on colors and appearances by Müller (1834). Cole (1905) made crucial histological observations that continue to influence the classification of cartilage types in hagfish: hard and soft types in cartilage and pseudocartilages. Wright et al. (1984, 1998) and Robson et al. (2000) collectively described three types of cartilage, the classification adopted in this study (Figure 2-12). Type 1a cartilage (‘hard’ cartilage) is characterized by a large amount of eosinophilic extracellular matrix (Figure 2-12C). The polygonal chondrocytes are larger and denser toward the center of the cartilage, whereas the nuclei sit in smaller, elongate cells toward the outer surface. The mesenchymal perichondrium

is typically thin and is weakly attached to the cartilage when prepared for paraffin sections, likely due to dehydration. For its high content of extracellular matrix, Type 1a cartilages are harder and less elastic than other types, and occur in relatively inflexible portions of the skull that experience high mechanical stress or provide rigid structural support. These include the braincase, the longitudinal skeletal arches that suspend the lingual and dental apparatus via muscles, the lingual apparatus over which the dental apparatus slides, the tendon insertion of the retractor muscle to the dental apparatus, the proximal portion of the velar cartilage that experiences torque at the joint, and the ventral distal lingual cartilage.

In contrast to red- to pink-stained Type 1a cartilage, a Type 1b cartilage ('soft' cartilage) has a smaller amount of extracellular matrix and large spaces for chondrocytes (Figure 2-12D). This type stains blue, as the matrix is stained more by hematoxylin than by eosin, and as the chondrocytes are packed in higher density than in other cartilages. The perichondrium is thicker and more closely associated with the cartilage than in Type 1a. Type 1b cartilages are readily more elastic than Type 1a, and occur in portions of the skull that a) serve as sites of muscle insertion, b) require elastic recoil to torque or bending motions, or c) bridge two Type 1a skeletal rods to increase mechanical resistance of the skull to bending. So Type 1b cartilages have broader distribution in the cartilaginous skull than types 1a and 2. Most notably, it constitutes all of the skeletal rods that support the barbels, the cartilage that holds the tooth plates, and direct skeletal suspension of the lingual apparatus. It also makes up most of the velar skeleton and the cartilages closely associated with the nasohypophyseal complex (nasal skeleton and nasopharyngeal plate). Boundaries between types 1a and 1b cartilages are not always sharp, and both types may coexist in some parts of the skeleton. Notably, the parachordal cartilage between the otic capsules deviates from typical Type 1a cartilage in having densely packed chondrocytes and smaller proportions of the eosinophilic matrix (Figure 2-12F). The nasal capsule basket and the lateral basal plate of the dental apparatus consist of Type 1b cartilage with

proportions of the extracellular matrix intermediate between those typical to Type 1a and Type 1b cartilages.

Type 2 cartilages (Figure 2-12E, G) were termed pseudocartilage by Cole (1905) and described in detail by Wright et al. (1984). These cartilages have the collagenous perichondrium thicker than in Type 1 cartilages. The collagenous or collagen-like matrix continues into the cartilage and form septae between large lacunae occupied by hypertrophied chondrocytes. The thickest part of the matrix inside the cartilage typically has smaller chondrocytes actively depositing the eosinophilic matrix. The chondrocytes presumably mature into the hypertrophied cells separated by septa. Type 2 cartilages are flexible, and they are either antagonist for feeding muscles (posterior lingual cartilage; dorsal distal lingual cartilage) or perichondrial to Type 1a cartilage (anterior lingual cartilages). The orientations of the trabecular structure may be regular (posterior lingual cartilage) or irregular (anterolateral lingual cartilage), which Cole (1905) respectively designated as hard and soft types. But this difference does not parallel the hard and soft distinction in Type 1 cartilages, and no other significant histological difference is observed between the regular and irregular Type 2 cartilages. A more intriguing parallel is with tendons, which appear identical to the irregularly arranged Type 2 cartilage at the level of light microscopical observation of standard hematoxylin and eosin staining (Figure 2-12H). In the tendon of m. retractor dentalis major, the thick collagenous matrix extends between vacuoles of fibroblasts to form irregular trabeculae. The sizes of the vacuoles are slightly smaller than that in Type 2 cartilages, but otherwise tendon and Type 2 cartilages appear morphologically identical.

2.3.11.2. Taxonomic comparison

Histological characteristics and the distribution of the cartilages described here in the skull of *E. stoutii* are consistent with those described for *E. burgeri* (Ota and Kuratani 2010), and are almost identical to those of *M. glutinosa* (Cole 1905; Robson et al. 2000), except for some minor details (Figure 2-12I, J). These differences include (in *E. stoutii*): the nasal capsule basket composed primarily of

Type 1b; the parachordal composed of Type 1a and 1b intermediate; the presence of Type 1b in the anterior end of the nasopharyngeal plate; and the lack of extensive Type 1a distribution in the visceral plate.

Structural and histochemical similarities in cartilages exist between hagfish and lampreys, although they do not share common matrix proteins. These cartilages are resistant to CNBr dissolution, are stained by Verhoeff's reagent, and are rich in glycine and other non-polar amino acids (Wright and Youson 1983; Wright et al. 1984, 1988, 1998; Robson et al. 1997, 2000). Type 1a cartilage is similar to that in the annular cartilage and neurocranium of lampreys, which have thick extracellular matrix and lower densities of chondrocytes. Type 1b cartilages correspond to the branchial and pericardial cartilages of lampreys, which have a thin matrix separating the chondrocytes (Robson et al. 2000). This distribution of cartilage types and their structural properties is shared between hagfish and lampreys, and the correspondence is probably due to functional convergence.

2.3.11.3. Tooth plates: histological observations

Histological descriptions of the tooth plates and associated tissues (Figure 2-13) are provided here to supplement earlier accounts by Dawson (1963) and Krejsa et al. (1990). The tooth plate is a keratinous sheath with keratinohyaline granules and remnant nuclei (ks; Figure 2-13A, F). It caps the oral mucosa that consists of, from external to internal, the outer and epipokal epithelial layers (oel, epke), pokal cone (pkcn), inner epithelial layer (iel), and dental papilla within the pulp cavity (dp; Figure 2-13A). These layers represent one generation of mature tooth plate (the keratinous sheath and outer and epipokal epithelial layers) and up to two more generations of replacement tooth plates (the pokal cone, inner epithelial layer, and dental papilla). The tooth plates are occasionally shed. During routine tank cleaning under captivity, shed tooth plates were observed in the residual slime secreted by the animals. Sometimes they were seen in association with feces or aborted eggs, from October to December, but were rare from May to September (T.M. personal observation; no data from January to May). Fifteen shed tooth plates were recovered from the tank that held 50 individuals over two

months (October – November), although it is unknown how many more tooth plates escaped attention. These observations suggest that the tooth plates are replaced at least once a year but probably less than several times a year per individual in captivity. Alternatively, shedding of tooth plates may be accidental rather than periodic, because October and November coincided with intense feeding activities in the tank and because of the association with feces.

The keratinous sheath is embedded in the fold of the three- to four-cell thick outer epithelial layer. The epithelial cells in the fold are more elongate and spindle-shaped toward the basal lamina (Figure 2-13E). Those closer to the keratinous sheath have smaller, round nuclei, are richer in eosinophilic cytoplasm, and are partially keratinized at the boundary with the keratinous sheath. Outside the fold, the epithelial cells stretched along the curvature of the cusp continue to underlie the keratin toward the cusp in one- to two-cell thick layers (oel; Figure 2-13F). This outer layer is without the partially keratinized transition zone and loosely attached to the overlying keratin, and dehydration during formalin fixation or paraffin sectioning causes detachment of the layer from the keratin. All along the outer epithelial layer, no proliferation is observed near the boundary with the keratinous sheath. Therefore the tooth cusp, once exposed, does not grow, and is attached to the base only within the fold of the outer epithelium. Partial keratinization in the transition zone within the fold acts more as cement that roots the keratin and does not likely indicate growth of it as suggested by early authors (e.g., Behrends 1892).

Under the cusp, the epithelial cells poor in eosinophilic cytoplasmic contents are distributed between the outer epithelial layer and the underlying pokal cone in a four- to five-cell thick layer (epke; Figure 2-13B, F). These cells have larger nuclei in comparison to the outer epithelial cells. This epipokal layer delineates the pokal cone externally and has some extracellular fibrous connection with the outer epithelial layer. The cells are stretched into elongate shapes along the pokal cone, but none of these cells show differentiation into the underlying pokal or polygonal cells. Those lining the pokal cone contain neutral lipid granules (Dawson 1963). The epithelial pyramid caps the apex of the pokal cone.

In each of the pyramid epithelial cells, the nucleus is removed from the pokal cone by a long foot or process of cytoplasm.

The pokal cone consists of the collagenous outer layer and the inner cellular layer of the pokal and polygonal cells (Figure 2-13A-C). Toward the base of the pokal cone is a proliferation zone where the cells in the inner epithelium differentiate into the polygonal cells (Figure 2-13D). In a mature tooth plate, more than 95% of the cells in the pokal cone are polygonal cells. They have striated, highly eosinophilic cytoplasm and nuclei two or three times larger than those of the cells in the epipokal layer. The cells are denser toward the inner epithelium where they differentiate. The tower-like pokal cells are unique to the dental apparatus of hagfish (pkc; Figure 2-13B; Dawson 1963). Always at the outer edge of the pokal cone near the apex, the pokal cells have a broad base rich in phospholipids at the boundary with the epipokal epithelial layer, a long intervening foot, and a bulbous head of the cell with the nucleus. The last two characters contain a large number of neutral lipid granules (Dawson 1963). In a premature cusp, young pokal cells line the outer edge toward the apex of the pokal cone side by side. The young pokal cells have much shorter feet, and the cytoplasm is extremely rich in lipids (cytoplasm is entirely stained in dark purple by hematoxylin) that feed into deposition of phospholipids at the base. The mature pokal cells likely deposit the collagenous outer layer of the pokal cone. The collagenous outer layer accompanies keratinohyaline granules, which indicates partial keratinization.

Underneath the pokal cone, the inner epithelial cells tend to have larger nuclei and less eosinophilic cytoplasm than the outer epithelial cells (Figure 2-13C, D). The inner epithelium has two functions. The first is the proliferation zone at the base of the pokal cone where the presumptive tooth plate grows. Associated with capillaries and sensory neurons, a dense pack of the inner epithelial cells is incorporated into the pokal cone by producing the eosinophilic, collagenous matrix. The second function is to induce the dental papilla within the pulp cavity. The pulp cavity is an invagination of the inner epithelial layer, so it is lined with basal lamina. The cavity is constricted at the base, through which the

connective mesenchyme migrates and differentiates into epithelial cells with collagenous extracellular matrix within the pulp cavity (compare meso and dp in figure 2-13D). The upper portion of the population of pulp epithelial cells fills with extracellular collagen the grooves that separate clusters of the inner epithelial cells. This is a proliferation zone of the pulp cavity with capillaries and sensory neurons that eventually forms the next-generation pokal cone. The apex of the pulp proliferation zone is supported by processes of the inner epithelial cells, which will become the pyramidal epithelial cells upon replacement. Along the lining of the pulp cavity, about one in four to five inner epithelial cells is rich in lipids. A smaller proportion of these lipid-rich cells (less than 5%) have differentiated into cells with a bulbous head toward the basal lamina and a long foot away from the pulp cavity (pkca; Figure 2-13C). These are possible precursors of the pokal cell for the next generation tooth plate.

The outer epithelium continues into the non-odontogenic epithelial layer of the oral mucosa that wraps around and bounds together the dental apparatus. The space bounded by this epithelial layer is rich in connective mesenchyme.

2.3.11.4. Tooth plates: replacement and comparison

Histological observations suggest the following scenario of tooth plate replacement. When the keratinous sheath (functioning tooth plate) is shed, the outer and epipokal epithelial layers undergo apoptosis and the pokal cone is exposed. The collagenous outer layer of the pokal cone derived from the pokal cells becomes a new keratinous sheath; the polygonal cells differentiates into a new outer epithelial layer; the outer cells in the inner epithelial layer form a new epipokal epithelial layer; the lipid-rich inner cells in the inner epithelial layer become pokal cells in the new pokal cone and secrete a collagenous outer layer; the pulp epithelial cells associated with the new pyramidal epithelial cells differentiate into polygonal cells in a new pokal cone, whereas other pulp epithelial cells become a new inner epithelial layer, which invaginates to make a new pulp cavity.

In comparison with sketches and diagrams of the tooth plate histology in *M. glutinosa* (Dawson 1963), *E. stoutii* may be distinguished in several histological characters. The stellate tissue as described for *M. glutinosa* appears to be absent. The lack of the stellate tissue cannot be attributed to different stages of the tooth plate development because the tooth plates of *E. stoutii* described here include mature ones in which the stellate tissue is expected based on the series in *M. glutinosa*. The pokal cells of *E. stoutii* have a broad base but lacks terminal process, whereas these are absent and present, respectively, in *M. glutinosa* (Dawson 1963). Finally, the keratinohyaline granules are abundant in the pokal cone, which Dawson (1963) did not find in *M. glutinosa*.

2.3.11.5. Tooth plates: evolutionary implications and the origin of teeth

The keratinous tooth plate of hagfish has always been treated as a homologue of the keratinous teeth in lampreys based on the topology, anatomy, and functions (Beard 1888, 1889; Marinelli and Strenger 1954, 1956; Dawson 1963; Yalden 1985). Based on the positions of different tooth elements in lampreys, the lateral and medial tooth plates in hagfish correspond to the lingual tooth plates in lampreys, and the dorsal median tooth in hagfish corresponds to the supraoral teeth in lampreys. The mode of odontogenesis in lampreys is similar but simpler than that in hagfish. The exposed primary and subsurface secondary cusps are separated by a five- to eight-cell thick layer of the vacuolated stellate cells, and the secondary cusp is underlain by the inner epithelium, which becomes gently concave ventrally and attracts mesenchyme (Lethbridge and Potter 1981a, b).

Homology with gnathostome teeth and tooth-like elements in fossil jawless vertebrates has been more contentious. Krejsa et al. (1990) posited homology between the tooth plate of hagfish and the euconodont elements of conodonts (Figure 2-16 A-C) based on the similarity in arrangement, position, size, and overall shapes. This hypothesis has attracted extensive criticisms (Szaniawski and Bengtson 1993; Smith et al. 1996; Aldridge and Donoghue 1998). The critics ruled the criteria used to support the homology as superficial

resemblances, but more important to this argument is evidence against the putative element-to-element homology. Two histological observations of conodonts suggest that the basal body is not a replacement for the crown as expected from the homology with the hagfish tooth plate: the crown and basal body grew in synchrony; and the basal body is not similar to the crown in histology (Aldridge and Donoghue 1998). Additionally, the conodont crown consists of lamellar phosphatic layers (Donoghue 1998), whereas the pokal cells in hagfish do not deposit the collagenous outer layer in lamellar fashion. This does not rule out potential homology between the hagfish tooth plates and the conodont teeth, which is an attractive hypothesis because of functional similarity and because of the likely correspondence in the anatomical correlates of the tooth elements (Goudemand et al. 2011). Nevertheless, this homology requires several ad hoc explanations to resolve histological differences between the two elements (e.g., scenarios in which pokal-like cells derive odontogenic cells that deposit conodont hard tissue). Such assumptions would burden a phylogenetic analysis via definition of characters, and evidence at hand is not strong enough to tolerate unnecessary weight in the analysis. It is therefore best to rule out the homology as unresolved. Heterostracans and osteostracans both have oral plates that are possibly functionally analogous. Homology with conodont elements and heterostracan/osteostracan oral plates and functional correlations should be considered at the broader sense as the oral apparatus, and already discussed in *2.3.8.4. Homology*.

2.4. DISCUSSION

2.4.1. The Vertebrate Skull

2.4.1.1. Homology across vertebrates

Comparative analysis of hagfish skull morphology reveals conservative features of the vertebrate skull (Table 2-1; Figure 2-14). Notably, the skeletal support for the central nervous system and for the sensory epithelial sacs show perfect correspondence, indicating that the common ancestor of hagfish, lampreys, and gnathostomes likely had skeletal support for the nasal and otic

capsules and the rudimentary braincase level with or above the notochord. Although the pharyngolingual arches are difficult to interpret in the context of branchial arches, at least the extrabranchial skeletal support exists in hagfish as well. Therefore, the common ancestor also likely had skeletal elements that supported the pharyngeal arches.

To evaluate evolutionary conservation of these functionally similar chondrocranial elements along each of the three lineages, a simple test is to establish correspondence at the levels of anatomical organization higher than the trait in comparison. For example, the otic capsule houses the inner ear innervated by the two trunks of vestibulocochlear nerve, the primary function of which is detection of inclinations to maintain balance. Although the number of semicircular canals varies from one (hagfish) to three (gnathostomes), the anatomical correspondence is inescapable (Janvier 1996). Across vertebrates, the inner ear is induced at the otic placode. All cranial placodes are hypothesized to have originated from the precursor, called the panplacode, that surrounds the neural tube in the head (Schlosser 2005), and a similar structure has been observed in hagfish embryos (Kuratani and Ota 2008). Furthermore, once the placode induces sensory neurons and an epithelial sac, skeletal support is necessary for the sac to perform its sensory function in a soft-bodied animal. Therefore, there are good developmental and functional explanations for why such intricate anatomical correspondences are conserved at multiple levels across vertebrates. As such, the homology of the otic capsule presumes correspondence at higher levels of anatomical and developmental organization. The homologies of the nasal capsule and parachordal skeleton can be similarly established, although the epithelium of the nasohypophyseal complex in hagfish likely has a different tissue origin. These homologies suggest that the ancestor had the cartilages and associated structures, and also that a cascade of anatomical structures are conservative in each functional unit, namely the olfactory epithelium, the inner ear, the olfactory and vestibulocochlear nerves that innervate them, and the trigeminal and facial nerves that perforate the parachordal skeleton in all of these lineages, in addition to the chondrocranial elements.

2.4.1.2. Incomplete homology

On the other hand, the failure to identify complete homology does not mean that the structure was absent in the ancestor. The oral apparatus with tooth-like elements is almost certainly a conservative character across vertebrates. However, the homology of individual elements such as teeth cannot be established partly because of different modes of matrix deposition, and partly because of the inability to compare the cyclostome lingual apparatus and gnathostome jaw. Importantly, even if complete, element-to-element homology cannot be established with available anatomical evidence, the lack of support simply results from the limit of comparative morphological analysis: congruence can be tested only if correlates of the trait under comparison are congruent between those taxa. Admittedly, this is partly a circular argument, and its failure does not rule out the possible presence of homology. If synapomorphy is treated as homology, any functional, developmental, or anatomical correspondence may be posited as homology as long as there is enough reason to believe that such correspondence was evolutionarily conserved. The purpose of recognizing and comparing incomplete similarities nevertheless is to identify the novelty that led to the loss of congruence in traits and provide units of comparison to test phylogenetic scenarios. Therefore, a test of similarities is not always a test of phylogenetic relationship. A phylogenetic test depends on taxonomic distribution of the homologues and identification of congruence and incongruence among the putative incomplete and complete homologies (Chapter 4).

The larger number of similarities in hagfish with lampreys than with gnathostomes should not be taken as a support for the close relationships between the first two lineages. Features common between them could turn out to be plesiomorphies (Figure 2-14). To avoid this error, several possible solutions exist: comparison with intermediate fossil forms and comparison of similarities. Because the head of neither cephalochordates nor urochordates can be compared in the manner presented in Table 2-1, outgroup comparison is out of question.

2.4.1.3. Post-hyoid pharyngeal arches and fossils

The incongruence of the external branchial arches in lampreys and internal branchial arches in gnathostomes stimulated a lengthy discussion (reviewed by Janvier 2007). Two interpretations are possible to resolve the incongruence: either the branchial arches are homologous but the gill-associated structures are not (Jarvik 1980), or the branchial arches are not homologous between lampreys and gnathostomes (Schaeffer and Thomson 1980; Mallatt 1984; Janvier 1981a, 1996). There is no question that the branchial arches in both taxa arise from neural crest-derived chondrogenic cells, and the crest-derived cells surround the mesoderm on the lateral and medial sides (Hall and Hörstadius 1988; Langille and Hall 1988a, b; Kimmel et al. 2001, 2003; Meulemans and Bronner-Fraser 2002; McCauley and Bronner-Fraser 2003, 2006; Cerny et al. 2004a; Hall 2009). The incongruence can be reconciled if the crest-derived cells undergo chondrogenesis either on the lateral or medial side of the mesoderm (Cerny et al. 2004a), in which case the distinction of the internal and external branchial arches is crucial in designating homology.

Although the extrabranchial cartilages are likely conserved in hagfish, lampreys, and gnathostomes, the posterior migration of the branchial series in hagfish renders the pharyngolingual arches difficult to compare. On the other hand, at least the internal pharyngolingual arches form at the mesoendoderm interface in the head, as do the gnathostome branchial arches. Does this correspondence indicate homology? Given that the branchial series is closer to the rest of the head in fossil hagfish (Bardack and Richardson 1977; Bardack 1991, 1998), the posterior position of the branchial series in living hagfish is likely an apomorphy related to hypertrophy of the lingual apparatus. The enlarged lingual apparatus and posteriorly shifted branchial series assume newly derived lateral skeletal support of the pharynx. Therefore, the pharyngolingual arches probably represent novel elements independent from the gnathostome branchial arches, although the skeletogenic potential between the lateral wall of the pharynx and the mesoderm likely has broader phylogenetic distribution beyond gnathostomes.

Returning to the extrabranchial cartilages, osteological correlates in heterostracans, galeaspids, and osteostracans all indicate that the main skeletal support for the branchial cavities were lateral to the gill filaments as in hagfish and lampreys. Therefore, extrabranchial cartilages are likely the conserved feature throughout vertebrates, whereas the branchial cartilages on the medial side of the gills are so far only present in gnathostomes and neomorphs for that clade. This information from stem gnathostomes therefore aids greatly in determining the polarity of characters that was not apparent in the three-taxon comparison among the living vertebrate lineages.

2.4.1.4. Trabecula and comparison among homologues

If numbers of similarities do not necessarily indicate phylogenetic distance, and if plesiomorphic conditions are unknown, comparison can only be made within homology. An element equivalent to the gnathostome trabecula is variably present in hagfish and lampreys (Table 2-1; Figure 2-14). The trabecula-like element bridges the cartilage for the nasal capsule and parachordal cartilage, whereas the trabecula bridges the ethmoidal plate and parachordal cartilage and delineates the hypophyseal fenestra. In lampreys, a candidate counterpart of the gnathostome trabecula appears as a blastema of the mucocartilage, and it wraps around the nasal capsule from a more superficial position than the parachordal otic-trigeminal arch (Johnels 1948). So the trabecula homologue does not delineate the hypophyseal fenestra in both hagfish and lampreys. This comparison suggests that the trabecula-like element evolved in association with the nasal capsule, probably to provide skeletal support by bridging it from the parachordal skeleton.

The three-taxon comparison suggests derived features in each lineage. Delineation of the hypophyseal fenestra by the gnathostome trabecula is only possible with the nasal passage extending anterior to or below the parachordals and without the anterior extension of the parachordal cartilage all the way below the nasal capsule. Conversely, the anterior extension of the parachordal cartilage to the level of nasal capsule is probably a derived trait in lampreys, the

consequence of which would have been duplication of the function for the true trabecula to support the nasal capsule. This may explain why the element is transient in lamprey ammocoetes and disappears during metamorphosis without chondrification. So the true trabecula is probably secondarily reduced in lampreys. In hagfish, the parachordal skeleton extends anteriorly close to the level of the nasal capsule. The trabecula homologue (nasopharyngeal bar) still supports the nasal capsule above the parachordal skeleton in this taxon, because the nasohypophyseal complex extends further posteriorly above the level of the parachordal skeleton to join the pharynx. Therefore, the hypophyseal fenestra does not exist in hagfish.

2.4.2. The Cyclostome Skull

2.4.2.1. Upper lips

The presence and absence of jaws set apart the head anatomy of jawless and jawed vertebrates. Most of the incomparable chondrocranial elements between the jawless cyclostomes and gnathostomes are related to the origin of jaws (Table 2-1; Figure 2-14). Once the jaws originated, the gnathostome-specific elements are conserved along the lineage, and before the origin of jaws, many candidate homologues are identified between hagfish and lampreys. This distribution alone does not support cyclostome monophyly. More crucial to this argument is whether the hagfish-lamprey homology represents a symplesiomorphic state or a synapomorphic state. Under the recognition of incomplete similarity (e.g., chondrocranial elements comparable only at the level of mandibular or hyoid domains), it is also possible to speculate whether the cyclostome and gnathostome conditions are both independently derived from an unknown ancestral state or one is plesiomorphic with respect to the other.

Many skeletal elements unique to hagfish and lampreys occur in the upper lip. In hagfish, the premandibular domain — roughly marked by the innervation by the ophthalmic branch of the trigeminal nerve — extends anteriorly along with the nasal tube over the mouth; the mandibular domain — roughly marked by the innervation of the ‘maxillomandibular’ trunk of the trigeminal nerve — overlaps

the premandibular extension laterally (Holmgren 1919; Lindström 1949). Although the nasohypophseal canal does not extend forward, a similar pattern is observed in lamprey. This is most tangibly expressed during metamorphosis when the mucocartilage anlage formed within the mandibular region extends anteriorly and chondrifies (Figure 2-4D-F; Johnston 1905; Sewertzoff 1916; Tretjakoff 1926, 1927; Damas 1944; Johnels 1948; Lindström 1949; Horigome et al. 1999; Kuratani et al. 1997, 1999, 2001, 2004; Kuratani 2004, 2012). If the upper lip were truly unique to hagfish and lampreys, all the cartilaginous similarities identified in this region would support their sister-group relationship. However, the morphological pattern of the upper lip in the adult is similar in gnathostomes in that the upper jaw overlaps the premandibular domain laterally. Furthermore, the maxillary branch is lateral to the ophthalmic branch, except that the mouth forms more posteriorly. Consequently, the gnathostome upper lip has accordingly shifted posteriorly (Shigetani et al. 2002, 2005; Kuratani 2004b, 2005).

There is one way to determine if stem gnathostomes had the cyclostome-like upper lip or were more similar to gnathostomes (Figure 2-15). In osteichthyes, the maxillary branch of the trigeminal nerve superficial to the premandibular domain is entirely sensory, whereas the motor branch of the trigeminal nerve innervates muscles of the upper lip in hagfish and lampreys (Lindström 1949). Osteostracans, often posited as a sister group to gnathostomes, have impressions of muscular attachment on the roof of the oral region, nearby which is the foramen for one of branches of the ‘maxillomandibular’ trunk of the trigeminal nerve, undoubtedly transmitting motor neurons (Stensiö 1927, 1932; Wängsjö 1952; Janvier 1981b, 1985). The association of muscular attachment in the upper part of the oral region with the ‘maxillomandibular’ trunk of the trigeminal nerve indicates that stem gnathostomes had an upper lip similar to those of hagfish and lampreys. This also explains the similarity in overall morphology of the nasal and oral regions between hagfish and heterostracans and between lampreys and osteostracans (reviewed in Janvier 1996). These similarities highlight two ways of developing the upper lip, one by extending the premandibular region with the nasal tube forward of the mouth and by having the

mandibular domain overlap it (hagfish and heterostracans) and the other by extending the premandibular and mandibular domains in front of the nasohypophyseal canal around the enlarged or anteriorly shifted oral region (lampreys and osteostracans). Galeaspids may present an exception to this. This group is characterized by an enlarged nasohypophyseal aperture near the anterior end of the head (Halstead 1979; Halstead et al. 1979; Janvier 1984; Gai et al. 2011). The aperture and surrounding tissue were exclusively innervated by the ophthalmic branch of the trigeminal nerve, which was set apart from the orbit posterolaterally by the lateral wall (Gai et al. 2011). The anterior region of the head likely consisted mostly of the premandibular domain in galeaspids.

Chondrichthyes introduce some confusion in this argument. The chondriichthyan maxillary nerve does have a motor component, and the motor innervation by the maxillary nerve is particularly extensive in holocephalans (Cole 1896; Marion 1905; Song and Boord 1993; Mallatt 1996). Because of this pattern, Mallatt (1996) considered holocephalans as a model for primitive conditions for gnathostomes. However, the maxillary process of gnathostomes is not readily comparable to the cheek process of jawless vertebrates. The presence of the *Dlx*-free ectomesenchyme lateral to the premandibular domain indicates that the same gene expression domains (*Dlx* cascade for the mandibular mesoderm; *BMP2/4* and *FGF8* for oral epithelium) shifted posteriorly in gnathostomes (Kuratani et al. 2001; Shigetani et al. 2002, 2005; Kuratani 2004a, b, 2005, 2012). It may be argued that structural constraint (Wagner 1994) for functional upper lip muscles is conserved across vertebrates, but it does not form from the same progenitor. Regardless of similarity breaking between the gnathostome and cyclostome upper lips, the chondriichthyan condition probably represents independent evolution. Unlike placoderms, acanthodians, and osteichthyes, the jaw skeleton is incompletely connected to the neurocranium in elasmobranchs and requires muscular suspension of the anterior portion of the palatoquadrate. This is well within the innervation domain of the maxillary ramus of the trigeminal nerve and is far anterior to the domain of the mandibular ramus. Therefore, motor neurons can only extend within the maxillary branch to

innervate the muscles in this region. In support of this view, the maxillomandibular division of the trigeminal ganglion does not depend on the target contact, but on general directions of the migration of trigeminal neural crest cells (Scott and Atkinson 1999). Holocephalans show specialization toward suction feeding and durophagy (Mallatt 1996). However, holocephalans lack teleost-like cranial kinesis driven by free articulation of the anterior components of the upper jaw and by extension of the hypobranchial muscle from the ventral midline (innervated by the hypoglossal nerve). Instead, they utilize muscles in the upper labial area to create negative pressure within the oral cavity. Therefore, the motor innervation by the maxillary nerve is likely specific to chondrichthyes among gnathostomes, and not a plesiomorphy.

In summary, the cyclostome-like upper lip is likely a plesiomorphic condition in vertebrates, which gnathostomes lost. Even though only directly observed in hagfish and lampreys, the cartilages dependent on the presence of the cyclostome-like upper lip alone may not support cyclostome monophyly.

2.4.2.2. Velum

The velum is another structure shared by hagfish and lampreys but absent in gnathostomes. Although its unique appearance and function strongly suggest a common evolutionary origin, the adult velar morphology substantially differs between hagfish and lampreys. In hagfish, the velar skeleton extends in the fold on the dorsal side of the pharynx posteriorly and plays a central role in ventilation (Strahan 1958). The active role of the velum in ventilation is related to the posterior shift of the branchial series without significant constrictors and skeletal antagonists. In lampreys, the velar skeleton originally appears within the fold of the lateral wall of the pharynx and only actively drives feeding and respiring current during the larval stage (Dawson 1905a, b; Mallatt 1981). Through metamorphosis, the velar skeleton now sits on the ventral floor of the pharynx where the branchial duct passes below, and functions as a valve for the entrance into the branchial series (Dawson 1905a, b; Johnels 1948; Randall 1972). This shift is accompanied by muscles of the branchial basket that pumps water through

the gills, and by a change in feeding style from filtering to predatory or parasitic mode. These variations obscure an ancestral state of the velum. Cephalochordates and urochordates use cilia to generate the feeding current (Burighel and Cloney 1997; Ruppert 1997), so neither is useful in constraining the ancestral state. If the conditions in hagfish and lamprey ammocoetes are assumed to be more basal than the state in adult lampreys, the velar skeleton originates from the posterodorsal corner of the mandibular domain within the fold of the dorsolateral wall of the pharynx. So long as the velar skeleton is mobile, the skeletal element of the hyoid arch is topographically the closest to contact.

When looking for correlates of the velum in stem gnathostomes, it is not constructive to seek a structure exactly like those of hagfish or adult lampreys. This is because none of the extinct lineages of stem gnathostomes had specializations such as the posteriorly shifted branchial series or definitive evidence of lamprey-like parasitic or predatory mode of feeding that likely affected the morphology in the living models. If the velar morphology in ammocoetes is anything to compare with, the mandibular domain of the stem gnathostomes may have a prebranchial cavity in which no impressions of gill filaments or the base of the branchial arch is present (confirmed in heterostracans, osteostracans, and thelodonts; illustrated in Janvier 1996). Indeed, the velum has been reconstructed for the prebranchial cavity in osteostracans by various authors (e.g., Stensiö 1958, 1964; Janvier 1985, 1996). With the ridge that defines the prebranchial fossa interpreted as the base of epithelium, the reconstruction leads to a medially protruded, vertical epithelial fold into the pharynx just like the velum of ammocoetes. Galeaspids deviate from this pattern by having the tuber for skeletal support in the mandibular domain (reconstructed in Gai et al. 2011), which suggests that the skeletal rod supporting the prebranchial cavity was fixed. Heterostracans have an external opening to this cavity that was previously interpreted as a spiracle (Halstead 1971).

Admittedly, there is absolutely no direct evidence that the prebranchial cavity of these extinct jawless vertebrates housed a velum. Nor do they have a structure functionally analogous to the velum of living cyclostomes, such as the

impression of a muscle attachment, a joint with the hyoid arch, and neuroanatomical evidence that there was motor component to the innervation of this cavity. Still, the widespread occurrence of a prebranchial cavity across stem gnathostomes implies that the mandibular domain of vertebrates always had a non-respiratory visceral cavity specialized toward feeding or ventilation. It seems inconsistent to uphold the homology of the velar skeleton in living cyclostomes in spite of the divergent morphological variations, and simultaneously reject the presence of the velum in stem gnathostomes on the basis of the lack of correlates for the highly variable velum of living cyclostomes. Therefore, the most conservative position is to recognize the similarity of the velum among living cyclostomes, but refuse to use this similarity as a support of cyclostome monophyly, pending further investigation of the prebranchial cavity in stem gnathostomes.

The velum is so elusive that one earlier definition is as broad and simple as the separation between the prebranchial and branchial regions of the head (Ayers 1931). From the perspective of development of the endoderm, Ayers's definition may be informative and would expand the range of comparison to non-vertebrate chordates. But this view deviates from the comparative approach of anatomical correlation in this paper and has no bearing on the homology of the velar skeleton, which simply does not exist in cephalochordates and urochordates.

2.4.2.3. Lingual apparatus

A similar dilemma exists for the lingual apparatuses of hagfish and lampreys. As Yalden (1985) pointed out, an almost perfect anatomical correspondence between those of hagfish and lampreys clearly indicates that they are similar to each other. The question is whether the lingual apparatus is an exclusive homologue to these two lineages, or more widespread among basal vertebrates.

Heterostracans have long been reconstructed with a hagfish-like lingual apparatus (Stensiö 1932, 1958, 1964; Janvier 1974; Jarvik 1980). But the lack of wear on the tips of oral plates and the presence of denticles that formed anteriorly

directed barbs reject the hypothesis that the oral plates were used in macrophagy (White 1935; Purnell 2002). Although osteostracans also have oral plates, the feeding mechanics probably differed from those of the lingual apparatuses in hagfish and lampreys if the putative muscle with the impression on the roof of the oral cavity inserted to them (Wängsjö 1958; Janvier 1985, 1996, 2007). The presence of dermal skeleton around a small mouth is inconsistent with the hagfish- or lamprey-like lingual apparatus in arandaspids, non-naked anaspids, and thelodonts (Janvier 1996), although this does not entirely preclude the existence of its homologue.

The biomechanical analysis of euconodonts predicts the presence of the basal cartilage similar to the lingual apparatus and a set of protractors and retractors that functioned in a similar way in hagfish and lampreys (Goudemand et al. 2011; Figure 2-16 A-C). The presence of basal bodies for conodont teeth also suggests a skeletal support (Sansom et al. 1992), and the microwear on the teeth indicate that these elements were not fixed (Purnell and von Bitter 1992; Purnell 1995). Given the uncertain relationships of conodonts with respect to other vertebrate lineages, however, it is premature to assume the homology of the lingual apparatus in conodonts, which has never been preserved, and conclude that the lingual apparatus is plesiomorphic among stem gnathostomes. The lingual apparatus can be putatively considered a character that supports cyclostome monophyly, with the possible inclusion of conodonts.

An observation that could undermine the synapomorphic status of the lingual apparatus is that an uncannily similar oral apparatus develops in anuran tadopoles in which the oral region in front of jaws temporarily develops rasping keratinous teeth prior to the anterior extension of Meckel's cartilage and formation of the jaw joint (Huxley 1876; Figure 2-16D). This is not to posit evolutionary conservation of such oral patterning but to call attention to the likelihood of convergence. Kuratani (2004a) notes:

> *Be it a gnathostome or cyclostome, there may be as many as only two repertoires in the use of mesenchyme to develop a mobile oral*

> *apparatus with the morphological pattern of early pharyngula common to all vertebrates* [jaws or lingual apparatus]*; the only option for the tadpoles, which for some reason delay development of the adult oral apparatus* [jaws]*, may have been to converge onto the same plan independently and anciently deployed by jawless vertebrates.* (p. 415; translated by T.M.)

This is a convincing argument. If such convergence is possible between such distant lineages as cyclostomes and anurans, there should be little surprise that the much closer hagfish and lampreys have extremely similar lingual apparatususes; both likely had similar patterning of the cranial development (e.g., cyclostome upper lip) and were macrophagous, regardless of whether or not they are sister lineages to each other.

2.4.2.4. Cyclostome synapomorphies

Among the potentially homologous skeletal features identified in hagfish and lampreys but not in gnathostomes (Table 2-1; Figure 2-14), only the lingual apparatus has some degree of support as a potential synapomorphy of hagfish and lampreys. Even the lingual apparatus may not be unique to hagfish and lampreys, given the biomechanical prediction that a similar apparatus may exist in conodonts. Among all chondrocranial characters unique to hagfish, and potentially plesiomorphic with respect to hagfish and all other vertebrates, the lack of the lateral wall of the braincase could be a genuinely primitive feature. The lateral wall occurs both in lampreys and gnathostomes, and its absence in hagfish result in the loss of homology for the trigeminal fenestra and facial foramen (discussed in section *2.3.5.4*). Still, a secondary loss in hagfish or an independent acquisition in lampreys could also explain the character distribution, if hagfish and lampreys are sister groups to one another.

The chondrocranial characters neither support nor reject alternative topologies to resolve a polytomy at the base of the vertebrate tree. This is rather a frustrating result because the phylogenetic signals in skeletal characters are

equivocal, despite numerous similarities between these clades (Figure 2-17). Cyclostome paraphyly predicts that either hagfish or lampreys share derived traits with gnathostomes. However, a comparative analysis of the chondrocrania did not reveal significant apomorphies in the chondrocrania of either jawless vertebrates shared exclusively with those of gnathostomes. This indicates that the gnathostome skull is highly specialized; so gnathostomes make a poor comparative model in morphological studies of basal vertebrates.

The scheme of homology proposed here resembles that of Holmgren (1946) in several cartilaginous elements (Table 2-2) and only partly agrees with that of Hardisty (1982), who only listed the following chondrocranial characters shared exclusively between hagfish and lampreys: incomplete cranial roof, cranium with no occipital region, visceral skeleton attached to cranium, true trabeculae absent (likely present; *2.4.1.4*), branchial arches external, and muscular velum.

Holmgren (1946) was interested in the ground pattern of the vertebrate head rather than in phylogenetic relationships. He was accordingly quick to recognize similarities, several of which are upheld in this paper. However, this paper explicitly differs from Holmgren (1946) in two respects. First, when morphological correlates are not strictly comparable, homology is not extended onto gnathostomes (e.g., otic-trigeminal arch; dorsal longitudinal arch; lingual cartilages; Table 2-2). Second, disagreement over the trabecula-parachordal boundary and the identity of hagfish pharyngolingual arches with lamprey and gnathostome branchial arches resulted in identification of different homologues for those elements and for others around them. Hardisty (1982) explicitly argued that the similarities between hagfish and lampreys represent convergence, if not plesiomorphy, the view that perhaps contributed to rejection of many other similarities in the skull. This paper presents an equivocal view that the similarities alone do not support cyclostome monophyly. The difference is that many characters interpreted as convergence by Hardisty (1982) are hypothesized as plesiomorphies in this paper.

2.4.3. The Myxinoid Skull

2.4.3.1. Myxinoid synapomorphies

The description revealed a number of skeletal characters unique to hagfish. The major ones include: the skeleton for the nasal capsule is basket-like; the skeletal support for the nasal tube is a series of cartilaginous arches; cartilages support four pairs of barbels, derived from both premandibular and mandibular domains; the acrochordal commissure is below the nasopharyngeal passage; two longitudinal arches parallel the parachordal skeleton; the velar skeleton extends posteriorly within the fold of the pharynx; pharyngolingual arches support the lateral wall of the pharynx and suspend the lingual apparatus; the dental apparatus slides over the lingual apparatus, rather than being attached to it; and the posteriorly hypertrophied lingual apparatus has distal elements.

2.4.3.2. Taxonomic and intraspecific variations

Although published accounts of the hagfish skeleton are limited to three species (*Eptatretus stoutii*, *E. hexatrema*, and *Myxine glutinosa*), and although previous descriptions may present inaccurate information, a number of skeletal characters are likely to be taxonomically significant. The following appear to be significant at the generic level or above: 1) number of nasal arches (fixed at eleven in *Myxine*), 2) bilateral anterior terminal processes and posterior expansion of nasopharyngeal plate (lacking in *Myxine*), 3) lower expansion of visceral plate (absent in *Eptatretus*), shape of pharyngolingual fenestra (anteroposteriorly elongate in *Eptatretus*), 4) complete second internal pharyngolingual arch and contact with second external pharyngolingual arch (present in *E. stoutii*), 5) shape of medial velar skeleton (e.g., suprapharyngeal processes simpler in *E. stoutii*), and 6) numbers of cusps and fused cusps in tooth plates (total cusp n = 40 to 42). Morphological characters have not been widely used in hagfish systematics except for the numbers of gill pores and fused tooth cusps (Fernholm 1998). Along with the pioneering studies using nasal papillae and ventral aorta (Mok 2001; Mok and McMillan 2004), the characters identified in this paper add to the small data set of morphological characters for hagfish systematics.

On the other hand, potentially taxonomically useful characters are variable within species. For example, the number of nasal arches varies from eight to ten in *E. stoutii*. These interspecific and intraspecific variations highlight the promise of systematic study of the hagfish skeleton. Interspecific comparison of the hagfish skeletal morphology has barely been attempted beyond comparison between the three taxa used in this paper. In addition, only a few specimens tend to be used at a time, but the study of intraspecific variation requires multiple specimens to determine variability.

2.4.4. Early Evolution of Skeletal System: Cartilages, Tendons, and Teeth

2.4.4.1. Possible origins of cartilages and tendons

Histological similarity between the irregular Type 2 cartilages and the tendons for the dental retractors suggests some interesting evolutionary explanations (Figure 2-12 E-H). A simple hypothesis is that Type 2 cartilages arose as tendons. Alternatively, both cartilage and tendon represent differential specialization of the collagenous matrix in the musculoskeletal system. Under the latter scenario, Type 2 cartilages would represent the transitional stages in which the connective tissue with collagenous matrix is deployed for endoskeletal support (plesiomorphy) or in which the tendon-like connective tissue is derived from the cartilaginous endoskeleton (apomorphy). A shared evolutionary origin of cartilage and tendon has been inferred because both cartilages and their associated tendons develop from the same progenitor mesenchyme in vertebrates (Köntges and Lumsden 1996; Kardon 1998; Chai et al. 2000; Tozer and Duprez 2005; Schweitzer et al. 2010).

Type 2 cartilages have no counterpart in other vertebrate lineages, but are similar to invertebrate cartilages in gastropods and polychaetes (Person and Philpott 1967; Wright et al. 1998; Cole and Hall 2004a, b; Hall 2005). Cartilages in hemichordates and cephalochordates are acellular and dissimilar to vertebrate cartilages (Wright et al. 2001; Cole and Hall 2004a, b). These observations suggest that the collagenous trabecula with hypertrophied cells are the simplest elaboration of the collagen-matrix-rich cellular connective tissues to derive

skeletal or connective functions, and may have evolved independently of acellular cartilages within the Metazoa. At any rate, the histological similarity between Type 2 cartilage and tendon, coupled with the basal position of hagfish with other vertebrate lineages and the lack of cellular cartilaginous skeleton in non-vertebrate euchordates, suggests that Type 2 cartilage represents a transitional stage either from collagenous connective tissue to true cartilage or from cartilage to tendon. Given that tendon assumes skeletal support (unless tendons first originated in chordate myomeres; Summers and Koob 2002), the latter explanation may be evolutionarily more plausible. Perhaps related to this argument is the fact that Type 2 cartilages exist as tough perichondrial tissue associated with Type 1a cartilage in the anterior segments of the lingual skeleton of *E. stoutii* (Figure 2-12G).

Cartilages of hagfish and lampreys are unique in that collagen is not a singularly major matrix protein for them, whereas gnathostome cartilages mainly consist of fibrillar collagen (Wright and Youson 1983; Wright et al. 1983; Robson et al. 1997, 2000). Nevertheless, the genetic cascade that specifies deposition of fibrillar collagen in gnathostome cartilages, the *Sox-col2a1* cascade, is expressed in both hagfish and lamprey cartilages (Zhang and Cohn 2006; Zhang et al. 2006; Ohtani et al. 2008; Ota and Kuratani 2010). A curious observation is that, in hagfish, the *Sox-col2a1* cascade is expressed not only in cartilage, but also in the notochord and other non-cartilaginous connective tissues around cartilage (Ota and Kuratani 2010). The ancient origin of the involvement of this cascade in skeletonization is supported by the fact that cephalochordates and hemichorates also express this cascade for deposition of fibrillar collagen, although these cartilages are acellular (Cole and Hall 2004a, b; Rychel et al. 2006; Rychel and Swalla 2007; Kaneto and Wada 2011). The origin of vertebrate cartilage may lie in an acellular-to-cellular shift of expression of the matrix-building genetic cascade in which cellular connective tissues independently acquired expression of the cascade and deposited cartilaginous matrix. If this scenario is correct, fibrillar collagen specified by the *Sox-col2a1* cascade eventually took over as the main component of vertebrate cartilages (Figure 2-17). This scenario is consistent with

the hypothesis that type II collagen was deposited in the notochord first, and then in cartilages secondarily (Cole and Hall 2004a, b), and with the hypothesis of gradual replacement of the pharyngeal skeletom by neural-crest derived cellular cartilages in vertebrates (Rychel and Swalla 2007). Then hagfish and lamprey cartilage with distinct matrix proteins may represent just two variants derived from the transitional stage in which fibrillar collagen was still not a main matrix protein. In particular, the expression of the *Sox-col2a1* genetic cascade in non-cartilaginous tissues in hagfish (Ota and Kuratani 2010) is consistent with this scenario.

In summary, histological observations on the hagfish cartilage and tendon suggest the following evolutionary scenario (Figure 2-17): 1) basal chordates (e.g., cephalochordates) variably developed acellular cartilage; 2) expression of the *Sox-col2a1* cascade shifted to the cellular connective tissues at or near the origin of vertebrates, resulting in histologically identical matrix-based cellular tissues in the musculoskeletal system (Type 2 cartilages as skeletal support and tendons as connective tissue for muscles); 3) hard and soft types of Type 1 cartilages evolved from Type 2 cartilages independently along early vertebrate lineages; 4) in stem gnathostomes, collagen dominated as the matrix building protein as the *Sox-col2a1* cascade became specific to regulating deposition of the collagen matrix; and overall, 5) tendons and cartilages differentiated into histologically distinct tissues, and soft cartilages were lost along the gnathostome lineage as elastic recoiling of cartilage is no longer a significant factor in the biomechanics of the gnathostome skull (discussed in Chapter 3).

2.4.4.2. Possible conservation of odontogenic program

Differences in biochemical composition of teeth aside, an overall similarity between the proposed developmental process of hagfish tooth plates and that of gnathostome teeth is striking. This is seen particularly in the ability of the oral epithelium to induce condensation and differentiation of mesenchyme into odontogenic cells that deposit some form of matrix. In gnathostome odontogenesis, the condensing mesenchyme cells within a fold or under a

thickening of the oral epithelium differentiate into ameloblasts and odontobrasts. These subsequently deposit the outer enamel and inner dentine respectively, and form a pulp cavity in the dental papilla (Tucker and Sharpe 2007; Fraser et al. 2010; Richman and Handrigan 2012). The dentine formation by odontoblasts is analogous to the function of the pokal cells, and the dental papilla serves similar functions as the outer and inner epithelia. Interestingly, a replacement tooth forms outside the pulp cavity in gnathostomes, whereas the hagfish or lamprey counterpart is a stack of multiple-generation tooth plates. The similarity does not assume homology of the two elements, but at the very least hagfish deploy a process analogous to gnathostome odontogenesis to develop tooth-like feeding structures in the oral cavity.

This ability in hagfish has a profound implication on the origin of teeth. The oral mucosa that wraps around the dental apparatus is endodermal in hagfish and is not ingressed ectodermal tissue as in other vertebrates, because the gut is anteriorly blind at early stages of hagfish embryogenesis, and because the mouth only opens at stages later than the development of the oral mucosa (von Kupffer 1899; Stockard 1906; Gorbman 1983, 1997; Gorbman and Tamarin 1985; Wicht and Northcutt 1995). There is an ongoing debate whether the evolutionary origin of teeth lies in the endodermal pharyngeal scales (‘inside-out’) or in the ectodermal oral scales (‘outside-in’) (Soukup et al. 2008; Huysseune et al. 2009; Fraser et al. 2010; Rücklin et al. 2011; Blais et al. 2011; Rothova et al. 2012). Soukup et al. (2006) presented evidence that, at least in axolotols, the teeth have mixed endodermal/ectodermal origin. Therefore, the crucial evolutionary step is an acquisition of the odontogenic ectomesenchyme in contact with the oral or pharyngeal epithelium with induction potential, regardless of ectodermal or endodermal origin of the epithelium. The endodermal origin of the oral mucosa in hagfish supports the hypothesis of Soukup et al. (2008) that the cellular interaction that patterns teeth or tooth-like structures at the epithelium-mesenchyme interface functions regardless of source of the epithelium across vertebrates. This is an intriguing scenario, especially because there is evidence for enamel-like antigens and enamel-like matrix in hagfish tooth plates (Slavkin et al.

1983; Slavkin and Diekwisch 1996). As such, patterning of the oral cavity with teeth or homologues of teeth may be a deeply conserved trait of vertebrates.

However, anuran tadpoles provide a counter argument to this hopeful scenario (Figure 2-16). Although there is no detailed histological description of the keratinous teeth of anuran tadpoles to my knowledge, anurans develop true enamel teeth after reducing the larval-specific oral apparatus anteriorly. If the anuran keratinous teeth were developmentally and anatomically equivalent to those of hagfish and lampreys, it would be difficult to posit similarity among the keratinous teeth of cyclostomes, mineralized teeth of conodonts, and true enamel teeth of gnathostomes, despite congruences between cyclostome teeth and anuran tadopole teeth.

2.4.4.3 Lamprey mucocartilage

The lamprey mucocartilage is a fibroconnective tissue unique to the head of lamprey ammocoetes and juvenile lampreys (Hardisty 1981). This fibroconnective tissue eventually differentiates into various cartilaginous elements in the adult lamprey skull (Figure 2-4). The delayed development and tissue origin of the mucocartilage presents difficulty in the analysis of similarity. Damas (1944) attributed the origin of the mucocartilage to the neural crest cells. Grafting experiments and ablation experiments (Newth 1956; Langille and Hall 1988) did not support this claim. Of special note, ablation of the mesencephalic neural crest cells did not affect the formation of the mucocartilage, which raises the possibility that the mucocartilage consists of premandibular and mandibular mesodermal mesenchyme through stage 17 of Piavis (1961) examined by Langille and Hall (1988). If the mucocartilage is entirely mesodermal in origin, this could break down the putative homology that links the lateral tentacular cartilage, anterior and lower portions of the facial skeleton, and dental and lingual apparatus with various components of the lamprey mucocartilage.

On the other hand, the mucocartilage has not differentiated into a cartilaginous skeleton at Piavis's stage 17. Furthermore, only a small fraction of cells originally present in the mucocartilage dedifferentiates and persists to the

fully chondrified adult skull (Armstrong et al. 1985); migration of the unspecialized cells from surrounding connective tissues during metamorphosis degrades the extracellular matrix of the mucocartilage and induces chondrification (Armstrong et al. 1987). The mucocartilage in the hyoid and mandibular domains initially develop as if it is a serial homologue of the basket of the branchial arches, which derives from the neural crest (Johnels 1948; Langille and Hall 1988; Martin et al. 2009). Kuratani (2004a, b, 2012) also speculates that postoptic premandibular ectomesenchyme contributes to the mucocartilage and the skeleton derived from it based on the development of the cheek process in lamprey embryos. Finally, Yao et al. (2011) presented evidence that endothelin signaling regulates the lower part of the mucocartilage (lateral mouth plate). Endothelin signaling secreted by the ventral mesoderm acts upon the postmigratory neural-crest derived ectomesenchyme in vertebrate pharyngeal arches and patterns the ventral pharyngeal skeleton (Kurihara et al. 1994; Clouthier et al. 1998, 2000; Yanagisawa et al. 1998; Kempf et al. 1998; Kimmel et al. 2003; Nair et al. 2007), particularly Meckel's cartilage in gnathostomes (Miller et al. 2000; Kimmel et al. 2001; Sato et al. 2008). These observations strongly suggest the involvement of ectomesenchyme derived from neural crest in patterning of the mucocartilage and the adult cartilaginous skeleton. Coupled with the unique histology of the mucocartilage (Wright and Youson 1982, 1983) and subsequent chondrogenesis that replaces the element toward adult stage (Armstrong et al. 1987; Wright et al. 1988; McBurney and Wright 1996), it is best to consider the lamprey mucocartilage as an ontogenetic precursor of the adult cartilaginous skeleton and as a useful landmark for topographical comparison. However, its possible mesodermal origin is irrelevant in the assessment of similarity between hagfish and lamprey adult skulls.

2.5. SUMMARY

A detailed morphological description and comparative analysis of the hagfish skeleton reveals cartilaginous elements homologous at the level of vertebrates and

cyclostomes or unique to myxinoids, and characters taxonomically significant within myxinoids. Among these characters, the skeletal support for the epithelial sensory structures and the lower part of the brain are conserved in all of the three lineages compared. These include the nasal and otic capsules, parachordal skeleton, and a homologue of the gnathostome trabecula. Other elements are highly variable and often cannot be compared with gnathostomes because the origin of jaws coincided with extensive re-organization of head patterning. Consequently, morphological criteria for similarity are not applicable in adults even though homology may still exist. A comparative morphological approach is limited where the correspondence of morphological correlates breaks down. Nevertheless, many cartilages similar between hagfish and lampreys do not necessarily support a sister-group relationship between these two lineages. The fossil evidence indicates that these elements likely existed in stem gnathostomes, which would thereby render these similarities symplesiomorphies of basal vertebrates. The lingual apparatus — unique to hagfish and lampreys — offers some support for cyclostome monophyly. However, overall skeletal characters strongly support neither cyclostome monophyly nor cyclostome paraphyly.

This morphological study of hagfish skeletons provides an update after half a century hiatus of original description, and leads to novel interpretations in light of modern developmental, anatomical, and paleontological information. These observations provide a basis for subsequent comparative studies using hagfish. Histological observations on hagfish cartilages and tooth plates suggest evolutionary scenarios for cartilages, tendons, and teeth. The origins of cartilages and tendons were probably interconnected, with transitional stages at which similar histological characteristics exist in both cartilages and tendons. Tooth replacement in hagfish suggests that the gnathostome-like odontogenesis is another deeply conserved feature in vertebrate evolution and does not require ectoderm-derived epithelium.

2.6. LITERATURE CITED

Aldridge, R. J., and P. C. J. Donoghue. 1998. Conodonts: a sister group to hagfishes? Pages 15-31 in J. M. Jørgensen, J. P. Lonholt, R. E. Weber, and H. Malte, eds. The Biology of Hagfishes. Chapman, London.

Aldridge, R. J., M. A. Purnell, S. E. Gabbott, and J. N. Theron. 1995. The apparatus architecture and function of *Promissum pulchrum* Kovacs-Endrody (Conodonta, Upper Ordovician) and the prioniodontid plan. Philosophical Transactions of the Royal Society of London B 347:275-291.

Allis, E. P. 1903. On certain features of the cranial anatomy of *Bdellostoma dombeyi*. Anatomische Anzeiger 23:259-281, 321-339.

Allis, E. P. 1925. Is the ramus ophthalmicus profundus the ventral nerve of the premandibular segment? Journal of Anatomy 59:217-223.

Armstrong, L., G. M. Wright, and J. H. Youson. 1985. The development of cartilage during lamprey metamorphosis. Anatomical Record 211:12A.

Armstrong, L., G. M. Wright, and J. H. Youson. 1987. Transformation of mucocartilage to a definitive cartilage during metamorphosis in the sea lamprey, *Petromyzon marinus*. Journal of Morphology 194:1-21.

Ayers, H. 1931. Vertebrate cephalogenesis. V. The velum—its part in head building—the hyoid. The Velata. The origin of the vertebrate head skeleton B. Myxinoid characters inherited by the Teleostomi. Journal of Morphology and Physiology 52:309-371.

Ayers, H., and C. M. Jackson. 1901. Morphology of the Myxinoidei. I. Skeleton and musculature. Journal of Morphology 17:185-225.

Baker, C. V. H., and M. Bronner-Fraser. 2001. Vertebrate cranial placodes I. Embryonic induction. Developmental Biology 232:1–61.

Bardack, D. 1991. First fossil hagfish (Myxinoidea): a record from the Pennsylvanian of Illinois. Science 54:701-703.

Bardack, D. 1998. Relationships of living and fossil hagfishes. Pages 3-14 in J. M. Jørgensen, J. P. Lonholt, R. E. Weber, and H. Malte, eds. The Biology of Hagfishes. Chapman, London.

Bardack, D., and E. S. Richardson. 1977. New agnathous fishes from the Pennsylvanian of Illinois. Fieldiana: Geology 33:489-510.

Barreiro-Iglesias, A., M. P. Gómez-López, R. Anadón, and M. C. Rodicio. 2008. Early development of the cranial nerves in a primitive vertebrate, the sea lamprey, *Petromzon marinus* L. The Open Zoology Journal 1:37-43.

Bareiro-Iglesias, A., D. R. Romaus-Sanjurjo, P. Senra-Martínez, R. Anadón, and M. C. Rodicio. 2011. Doublecortin is expressed in trigeminal motorneurons that innervate the velar musculature of lampreys: considerations on the evolution and development of the trigeminal system. Evolution & Development 13:149-158.

Beard, J. 1888. The teeth of myxinoid fishes. Anatomische Anzeiger 3:169-172.

Beard, J. 1889. Morphological studies No.3. The nature of the teeth of marsipobranch fishes. Zoologische Jahrbücher 3:727-752.

de Beer, G. 1937. The Development of the Vertebrate Skull. Oxford University Press, London. 554 pp.

Behrends, G. 1892. Ueber Hornzähne. Nova Acta Academiae Caesareae Leopoldino-Carolinae 58:437-475.

Benouaiche, L., Y. Gitton, C. Vincent, G. Couly, and G. Levi. 2008. Sonic hedgehog signaling from foregut endoderm patterns the avian nasal capsule. Development 135:2221-2225.

Bjerring, H. C. 1970. Nervus tenuis, a hitherto unknown cranial nerve of the fourth metamere. Acta Zoologica 51:107–114.

Bjerring, H. C. 1972. The nervus rarus in coelacanthiform phylogeny. Zoologica Scripta 1:57–68.

Bjerring, H. C. 1977. A contribution to structural analysis of the head of craniate animals. Zoologica Scripta 6:127–83.

Bjerring, H. C. 1984. Major anatomical steps toward craniotedness: a heterodox view based largely on embryological data. Journal of Vertebrate Paleontology 4:17–29.

Blais, S. A., L. A. MacKenzie, and M. V. H. Wilson. 2011. Tooth-like scales in Early Devonian eugnathostomes and the 'outside-in' hypothesis for the origins of teeth in vertebrates. Journal of Vertebrate Paleontology 31:1189-1199.

Blieck, A. 1984. Les Hétérostracés Ptéraspidiformes, agnathes du Silurien-Dévonien du continent Nord-Atlantique et des blocs avoisinants: Révision systématique, phylogénie, biostratigraphie, biogéographie. Éditions du Centre National de la Recherche Scientifique 15:1-199.

Boorman, C. J., and S. M. Shimeld. 2002. Pitx homeobox genes in *Ciona* and amphioxus show left-right asymmetry is a conserved chordate character and define the ascidian adenohypophysis. Evolution & Development 4:354-365.

Brito, J., M.-A. Teillet, and N. M. Le Douarin. 2006. An early role for Sonic hedgehog from foregut endoderm in jaw development: ensuring neural crest cell survival. Proceedings of the National Academy of Sciences 103:11607-11612.

Burighel, P., and R. A. Cloney. 1997. Urochordata: Ascidiacea. Pages 221-347 in F. E. Harrison and E. E. Ruppert, eds. Microscopic Anatomy of Invertebrates. Volume 15: Hemichordata, Chaetognatha, and the Invertebrate Chordates. Wiley-Liss. Inc. New York.

Cerny, R., P. Lwigale, R. Ericsson, D. Meulemans, H.-H. Epperlein, and M. Bronner-Fraser. 2004b. Developmental origins and evolution of jaws: new interpretation of "maxillary" and "mandibular". Developmental Biology 276:225-236.

Cerny, R., M. Cattell, T. Sauka-Spengler, M. Bronner-Fraser, F. Yu, and D. Meulemans Medeiros. 2010. Evidence for the prepattern/cooption model of vertebrate jaw evolution. Proceedings of the National Academy of Sciences 107:17262-17267.

Cerny, R., D. Meulemans, J. Berger, M. Wilsch-Braüninger, T. Kurth, M. Bronner-Fraser, and H.-H. Epperlein. 2004a. Combined intrinsic and extrinsic influences pattern cranial neural crest migration and pharyngeal arch morphogenesis in axolotl. Developmental Biology 266:252–269.

Chai, Y., X. Jiang, Y. Ito, P. Bringas, J. Han, D. H. Rowitch, P. Soriano, A. P. McMahon, and H. M. Sucov. 2000. Fate of the mammalian cranial neural crest during tooth and mandibular morphogenesis. Development 127:1671-1679.

Chen, Y.-W., H.-W. Chang, and H.-K. Mok. 2006. Phylogenetic position of *Eptatretus chinensis* (Mycinidae: Myxiniformes) inferred by 16S rRNA gene sequence and morphology. Zoological Studies 44:111-118.

Clark, A. J., and A. P. Summers. 2012. Ontogenetic scaling of the morphology and biomechanics of the feeding apparatus in the Pacific hagfish *Eptatretus stoutii*. Journal of Fish Biology 80:86-99.

Clouthier, D. E., K. Hosoda, J. A. Richardson, S. C. Williams, H. Yanagisawa, T. Kuwaki, M. Kumada, R. E. Hammer, and M. Yanagisawa. 1998. Cranial and cardiac neural crest defects in endothelin-A receptor-deficient mice. Development 125:813-824.

Clouthier, D. E., S. C. Williams, H. Yanagisawa, M. Wieduwilt, J. A. Richardson, and M. Yanigisawa. 2000. Signaling pathways crucial for craniofacial development revealed by endothelin-A receptor-deficient mice. Developmental Biology 217:10-24.

Cole, A. G., and B. K. Hall. 2004a. The nature and significance of invertebrate cartilages revisited: distribution and histology of cartilage and cartilage-like tissues within the Metazoa. Zoology 107:261-273.

Cole, A. G., and B. K. Hall. 2004b. Cartilage is a metazoan tissue; integrating data from nonvertebrate sources. Acta Zoologica 85:69-80.

Cole, F. J. 1896. The cranial nerves of *Chimaera monstrosa*. Transactions of the Royal Society of Edinburgh 38:49-56.

Cole, F. J. 1905. A monograph on the general morphology of the myxinoid fishes, based on a study of *Myxine*. Part I. The anatomy of the skeleton. Transactions of the Royal Society of Edinburgh 41:749-791.

Cole, F. J. 1909. A monograph on the general morphology of the myxinoid fishes, based on a study of *Myxine*. Part III. Further observations on the skeleton. Transactions of the Royal Society of Edinburgh 46:669-681.

Couly, G., S. Creuzet, and N. M. Le Douarin. 1993. The triple origin of skull in higher vertebrates: a study in quail-chick chimeras. Development 117:409-429.

Couly, G., S. Creuzet, S. Bannaceur, C. Vincent, and N. M. Le Douarin. 2002. Interactions between *Hox*-negative cephalic neural crest cells and the foregut endoderm in patterning facial skeleton in the vertebrate head. Development 125:3445-3459.

Couly, G., A. Grapin-Botton, P. Coltey, B. Ruhin, and N. M. Le Douarin. 1998. Determination of the identity of the derivatives of the cephalic neural crest: incompatibility between *Hox* gene expression and lower jaw development. Development 125:3445-3459.

Croucher, S. J. and C. Tickle. 1989. Characterization of epithelial domains in the nasal passages of chick embryos: spatial and temporal mapping of a range of extracellular matrix and cell surface molecules during development of the nasal placode. Development 106:493-509.

Crump, J. G., M. E. Swartz, and C. B. Kimmel. 2004. An integrin-dependent role of pouch endoderm in hyoid cartilage development. PLoS Biology 2:1432-1445.

Damas, H. 1944. Recherches sur le dévelopment de *Lampetra fluviatilis* L. Contribution à l'étude de la cephalogénèse des vertébrés. Archives de Biologie Paris 55:1-289.

David, N. B., L. Saint-Etienne, M. Tsang, T. F. Schilling, and F. M. Rosa. 2002. Requirement for endoderm and FGF3 in ventral head skeleton formation. Development 129:4457–4468.

Dawson, J. 1905a. The breathing and feeding mechanism of the lampreys I. Biological Bulletin 9:1-21.

Dawson, J. 1905b. The breathing and feeding mechanism of the lampreys II. Biological Bulletin 9:91-111.

Dawson, J. A. 1963. The oral cavity, the 'jaws' and the horny teeth of *Myxine glutinosa*. Pages 231-255 in A. Brodal and R. Fänge, eds. The Biology of *Myxine*. Universtetsforlaget, Oslo.

Dean, B. 1899. On the embryology of *Bdellostoma stouti*. A general account of myxinoid development from the egg and segmentation to hatching. Pages 220-276 in Festschrift zum 70ten Geburststag Carl von Kupffer. Gustav Fischer Verlag, Jena.

Depew, M. J., and C. A. Simpson. 2006. 21st century neontology and the comparative development of the vertebrate skull. Developmental Dynamics 235:1256-1291.

Depew, M. J., T. Lufkin, and J. L. R. Rubenstein. 2001. Specification of jaw subdivisions by *Dlx* genes. Science 298:381-385.

Depew, M. J., C. A. Simpson, M. Morasso, and J. L. R. Rubenstein. 2005. Reassessing the *Dlx* code: the genetic regulation of branchial arch skeletal pattern and development. Journal of Anatomy 207:501-561.

Donoghue, P. J. C. 1998. Growth and patterning in the conodont skeleton. Philosophical Transactions of the Royal Society of London B 353:633-666.

Fernholm, B. 1998. Hagfish systematics. Pages 33-44 in J. M. Jørgensen, J. P. Lonholt, R. E. Weber, and H. Malte, eds. The Biology of Hagfishes. Chapman, London.

Forey, P. L. 1995. Agnathans recent and fossil, and the origin of jawed vertebrates. Reviews in Fish Biology and Fisheries 5:267-303.

Fraser, G. J., R. Cerny, V. Soukup, M. Bronner-Fraser, and J. T. Streelman. 2010. The odontode explositon: the origin of tooth-like structures in vertebrates. BioEssays 32:808-817.

Gai, Z., P. C. J. Donoghue, M. Zhu, P. Janvier, and M. Stampanoni. 2011. Fossil jawless fish from China foreshadows early jawed vertebrate anatomy. Nature 476:324-327.

Goette, A. 1901. Über die Kiemen der Fische. Zeitschrift für Wissenschaftliche Zoologie 69:533-577.

Goodrich, E. S. 1918. On the development of the segments of the head in *Scyllium*. Quarterly Journal of Microscopical Science 63:1–30.

Goodrich, E. S. 1930. Studies on the Structure and Development of Vertebrates. The Macmillan Company, London.

Gorbman, A. 1983. Early development of the hagfish pituitary gland: evidence for the endodermal origin of the adenohypophysis. American Zoologist 23:639-654.

Gorbman, A. 1997. Hagfish development. Zoological Science 14:375-390.

Gorbman, A., and A. Tamarin. 1985. Early development of oral, olfactory and adenohypophyseal structures of agnathans and its evolutionary implications. Pages 165-185 in E. E. Foreman, A. Gorbman, J. M. Dodd, and R. Olsson, eds. Evolutionary Biology of Primitive Fishes. NATO ASI Series A: Life Sciences. Volume 103. Plenum Press, New York.

Goudenmand, N., M. J. Orchard, S. Urdy, H. Bucher, and P. Tafforeau. 2011. Synchrotron-aided reconstruction of the conodont feeding apparatus and implications for the mouth of the first vertebrates. Proceedings of the National Academy of Sciences 108:8720-8724.

Graham, A., M. Okabe, and R. Quinlan. 2005. The role of the endoderm in the development and evolution of the pharyngeal arches. Journal of Anatomy 207:479-487.

Hall, B. K. 2005. Bones and Cartilage: Developmental and Evolutionary Skeletal Biology. Elsevier, San Diego.

Hall, B. K. 2009. The Neural Crest and Neural Crest Cells in Vertebrate Development and Evolution. Springer, New York.

Hall, B. K., and S. Hörstadius. 1988. The Neural Crest. Oxford University Press, New York.

Halstead, L. B. 1971. The presence of a spiracle in the Heterostraci (Agnatha). Zoological Journal of the Linnean Society 50:195-197.

Halstead, L. B. 1973a. Affinities of the Heterostraci (Agnatha). Biological Journal of the Linnean Society 5:339-349.

Halstead, L. B. 1973b. The heterostracan fishes. Biological Reviews 48:279-332.

Halstead, L. B. 1979. Internal anatomy of the polybranchiaspids (Agnatha, Galeaspida). Nature 282:833-836.

Halstead, L. B., Y. H. Liu, and K. P'an. 1979. Agnathans from the Devonian of China. Nature 282:831-833.

Halstead Tarlo, L. B. 1963. Aspidin: the precursor of bone. Nature 199:46-48.

Halstead Tarlo, L. B., and H. P. Whiting. 1965. A new interpretation of the internal anatomy of the Heterostraci (Agnatha). Nature 206:148-150.

Hamburger, V. 1961. Experimental analysis of the dual origin of the trigeminal ganglion in the chick embryo. Journal of Experimental Zoology 148:91–123.

Hansen, H. 1919. Anatomie und Entwicklung der Zyklostomenzähne unter Berücksichtigung ihrer phylogenetischen Stellung. Universitat Leipzig. 38 pp.

Hardisty, M. W. 1981. The skeleton. Pages 118-124 in M. W. Hardisty and I. C. Potter, eds. The Biology of Lampreys. Volume 3. Academic Press, New York.

Hardisty, M. W. 1982. Lampreys and hagfishes: analysis of cyclostome relationships. Pages 165-259 in M. W. Hardisty and I. C. Potter, eds. The Biology of Lampreys. Volume 4b. Academic Press, New York.

Haworth, K. E., C. Healy, P. Morgan, and P. T. Sharpe. 2004. Regionalisation of early head ectoderm is regulated by endoderm and prepatterns the orofacial epithelium. Development 131:4797–4806.

Haworth, K. E., J. M. Wilson, A. Grevellec, M. T. Cobourne, C. Healy, J. A. Helms, P. T. Sharpe, P.T, and A. S. Tucker. 2007. Sonic hedgehog in the pharyngeal endoderm controls arch pattern via regulation of Fgf8 in head ectoderm. Developmental Biology 303:244–258.

Hatschek, B. 1881. Studien über die Entwicklung des *Amphioxus*. Arbeiten aus den Zoologischen Instituten zu Wien 4:1-88.

Hillard, R. W., I. C. Potter, and D. J. Macey. 1985. The dentition and feeding mechanism in adult of the Southern Hemisphere lamprey *Geotria australis* Gray. Acta Zoologica 66:159-170.

Holmgren, N. 1919. Zur Anatomie des Gehirns von *Myxine*. Kungl Svenska Vetenskapsakademiens Handlingar 60:1-96.

Holmgren, N. 1940. Studies on the head of fishes. Part. I. Development of the skull in sharks and rays. Acta Zoologica 21:51-266.

Holmgren, N. 1943. Studies on the head of fishes. Part. IV. General morphology of the head in fish. Acta Zoologica 24:1-188.

Holmgren, N. 1946. On two embryos of *Myxine glutinosa*. Acta Zoologica 27:1-90.

Holmgren, N., and E. Stensiö. 1936. Kranium and Visceralskelett der Akranier, Cyclostomen und Fische. Pages 233-500 in L. Bolk, E. Göppert, E. Kallius, and W. Lubosch, eds. Handbuch der vergleichenden Anatomie der Wirbeltiere. Urban & Schwarzenberg, Berlin.

Horigome, N., M. Myojin, T. Ueki, S. Hirano, S. Aizawa, and S. Kuratani. 1999. Development of cephalic neural crest cells in embryos of *Lampetra japonica*, with special reference to the evolution of the jaw. Developmental Biology 207:287-308.

Huxley, T. H. 1876. On the nature of the craniofacial apparatus of *Petromyzon*. Journal of Anatomy and Physiology 10:412-429.

Huysseune, A., J.-Y. Sire, and P. E. Witten. 2009. Evolutionary and developmental origins of the vertebrate dentition. Journal of Anatomy 214:465-476.

Jansen, J. 1930. The brain of *Myxine glutinosa*. Journal of Comparative Neurology 49:359-507.

Janvier, P. 1974. The structure of the naso-hypophyseal complex, and the mouth in fossil and extant cyclostomes, with remarks on amphiaspiforms. Zoologica Scripta 3:193-200.

Janvier, P. 1975. Les yeux des Cyclostomes et le problem de l'origine des Myxinoïdes. Acta Zoologica 56:1-9.

Janvier, P. 1981a. The phylogeny of the Craniata, with particular reference to the significance of fossil 'agnathans'. Journal of Vertebrate Paleontology 1:121-159.

Janvier, P. 1981b. *Norselaspis glacialis* n.g., n.sp. et les relations phylogénétiques entre les Kiaeraspidiens (Osteostraci) du Dévonien inféerieur du Spitsberg. Palaeovertebrata 11:19-131.

Janvier, P. 1984. The relationships of the Osteostraci and Galeaspida. Journal of Vertebrate Paleontology 4:344-358.

Janvier, P. 1985. Les Céphalaspides du Spitsberg. Anatomie, phylogénie et systématique des Ostéostracés siluro-dévoniens. Révision des Ostéostracés de la Formation de Wood Bay (Dévonien inférieur du Spitsberg). Cahiers de Paléontologie, Centre national de la Recherche scientifique, Paris. 244 pp.

Janvier, P. 1993. Patterns of diversity in the skull of jawless fishes. Pages 131-188 in J. Hanken and B. K. Hall, eds. The Skull. Volume II. Patterns of Structural and Systematic Diversity. The University of Chicago Press, Chicago.

Janvier, P. 1996. Early Vertebrates. Oxford Monographs on Geology and Geophysics, 33. Clarendon Press, Oxford. 393 pp.

Janvier, P. 2007. Homologies and evolutionary transitions in early vertebrate history. Pages 57-121 in J. S. Anderson and H. D. Sues, eds. Major Transitions in Vertebrate Evolution. Indiana University Press, Bloomington.

Janvier, P. 2008. Early jawless vertebrates and cyclostome origins. Zoological Science 25:1045-1056.

Janvier, P. 2010. microRNAs revive old views about jawless vertebrate divergence and evolution. Proceedings of the National Academy of Sciences 107:19137-19138.

Janvier, P., and M. Arsenault. 2002. Calcification of early vertebrate cartilage. Nature 417:609.

Janvier, P., and M. Arsenault. 2007. The anatomy of *Euphanerops longaevus* Woodward, 1900, an anaspid-like jawless vertebrate from the upper devonian of Miguasha, Quebec, Canada. Geodiversitas 29:143-216.

Jarvik, E. 1980. Basic Structure and Evolution of Verebrates. 2 Volumes. Academic Press, London.

Jefferies, R. P. S. 1986. The Ancestry of the Vertebrates. 376 pp. British Museum (Natural History), London.

Johnels, A. G. 1948. On the development and morphology of the skeleton of the head of *Petromyzon*. Acta Zoologica 29:139-279.

Jones, D., A. R. Evans, K. K. W. Siu, E. J. Rayfield, and P. C. J. Donoghue. 2012. The sharpest tools in the box? Quantitative analysis of conodont element functional morphology. Proceedings of the Royal Society B 279:2849-2854.

Jørgensen, J. M. 1998. Structure of the hagfish inner ear. Pages 557-563 in J. M. Jørgensen, J. P. Lonholt, R. E. Weber, and H. Malte, eds. The Biology of Hagfishes. Chapman, London.

Jørgensen, J. M., J. P. Lonholt, R. E. Weber, and H. Malte (editors). 1998a. The Biology of Hagfishes. Chapman, London.

Jørgensen, J. M., M. Shichiri, and F. A. Geneser. 1998b. Morphology of the hagfish inner ear. Acta Zoologica 79:251-256.

Kaneto, S., and H. Wada. 2011. Regeneration of amphioxus oral cirri and its skeletal rods: implications from the origin of the vertebrate skeleton. Journal of Experimental Zoology B 316:409-417.

Kardon, G. 1998. Muscle and tendon morphogenesis in the avian hind limb. Development 125:4019-4032.

Kardong, K. V. 2006. Vertebrates: Comparative Anatomy, Function, Evolution. 4th edition. McGraw-Hill, Boston. 782 pp.

Kawasaki, R., and C. M. Rovainen. 1988. Feeding behavior by parasitic phase lampreys, *Ichthyomyzon unicuspis*. Brain, Behavior and Evolution 32:317-329.

Kempf, H., C. Linares, P. Corvol, and J. Gasc. 1998. Pharmacological inactivation of the endothelin type A receptor in the early chick embryo: a model of mispatterning of the branchial arch derivatives. Development 125:4931–4941.

Kimmel, C. B., and J. K. Everhart. 2008. The midline, oral ectoderm, and the arch-0 problem. Integrative and Comparative Biology 48:668-680.

Kimmel, C. B., C. T. Miller, and R. J. Keynes. 2001. Neural crest patterning and the evolution of the jaw. Journal of Anatomy 199:105-119.

Kimmel, C. B., B. Ullmann, M. Walker, C. T. Miller, and J. G. Crump. 2003. Endothelin 1-mediated regulation of pharyngeal bone development in zebrafish. Development 130:1339–1351.

Kingsbury, B. F. 1926. Branchiomerism and the theory of head segmentation. Journal of Morphology 42:82–109.

Koltzoff, N. K. 1901. Entwicklungsgeschichte des Kopfes von *Petromyzon planeri.* Bulletin de la Société das naturalists, Moscow 15:259-589.

Köntges, G., and A. Lumsden. 1996. Rhombencephalic neural crest segmentation is preserved throughout craniofacial ontogeny. Development 122:3229-3242.

Krejsa, R. J., P. Bringas, and H. C. Slavkin. 1990. A neontological interpretation of conodont elements based on agnathan cyclostome tooth structure, function, and development. Lethaia 23:359-378.

von Kuppfer, C. 1899. Zur Kopfentwicklung von *Bdellostoma*. Sitzungsberiche der Gesellschaft für Morhologie und Physiologie 15:21-35.

Kuratani, S. 2003. Evolutionary developmental biology and vertebrate head segmentation: a perspective from developmental constraint. Theory in Bioscience 122:230–251.

Kuratani, S. 2004a. [Evolutionary Morphology: Bauplan and Embryonic Development of Vertebrates]. The University of Tokyo Press, Tokyo. 611 pp. [In Japanese]

Kuratani, S. 2004b. Evolution of the vertebrate jaw: comparative embryology and molecular developmental biology reveal the factors behind evolutionary novelty. Journal of Anatomy 205:335-347.

Kuratani, S. 2005a. Craniofacial development and the evolution of the vertebrates: the old problems on a new background. Zoological Science 22:1-19.

Kuratani, S. 2005b. Developmental studies of the lamprey and hierarchical evolutionary steps towards the acquisition of the jaw. Journal of Anatomy 207:489-499.

Kuratani, S. 2008. Is the vertebrate head segmented?—evolutionary and developmental considerations. Integrative and Comparative Biology 48:647-657.

Kuratani, S. 2012. Evolution of the vertebrate jaw from developmental perspectives. Evolution & Development 14:76-92.

Kuratani, S., and K. G. Ota. 2008. Primitive versus derived traits in the developmental program of the vertebrate head: views from cyclostome developmental studies. Journal of Experimental Zoology B 310:294-314.

Kuratani, S., N. Horigome, and S. Hirano. 1999. Developmental morphology of the cephalic mesoderm and re-evaluation of segmental theories of the vertebrate head: evidence from embryos of an agnathan vertebrate, *Lampetra japonica*. Developmental Biology 210:381-400.

Kuratani, S., Y. Nobusada, N. Horigome, and Y. Shigetani. 2001. Embryology of the lamprey and evolution of the vertebrate jaw: insights from molecular and developmental perspectives. Philosophical Transactions of the Royal Society B 356:15-32.

Kuratani, S., T. Ueki, S. Aizawa, and S. Hirano. 1997. Peripheral development of cranial nerves in a cyclostome, *Lampetra japonica*: morphological distribution of nerve branches and the vertebrate body plan. Journal of Comparative Neurology 384:483–500.

Kuratani, S., N. Adachi, N. Wada, Y. Oisi, and F. Sugahara. 2012. Developmental and evolutionary significance of the mandibular arch and prechordal/premandibular cranium in vertebrates: revising the heterotopy scenario of gnathostome jaw evolution. Journal of Anatomy. Published online ahead of print. DOI: 10.1111/j.1469-7580.2012.01505.x

Kuratani, S., Y. Murakami, Y. Nobusada, R. Kusakabe, and S. Hirano. 2004. Developmental fate of the mandibular mesoderm in the lamprey, *Lethenteron japnicum*: comparative morphology and development of the gnathostome jaw with special reference to the nature of the trabecular cranii. Journal of Experimental Zoology B 302:458-468.

Kurihara, Y., H. Kurihara, H. Suzuki, T. Kodama, K. Maemura, R. Nagal, H. Oda, T. Kuwaki, W.-H. Cao, N. Kamada, K. Jishage, Y. Ouchi, S. Azuma, Y. Toyoda, T. Ishikawa, M. Kumada, and Y. Yazaki. 1994. Elevated blood pressure and craniofacial abnormalities in mice deficient in endothelin-1. Nature 368:703-710.

Langille, R. M., and B. K. Hall. 1988a. Role of the neural crest in development of the trabeculae and branchial arches in embryonic sea lamprey, *Petromyzon marinus* (L). Development 102:301-310.

Langille, R. M., and B. K. Hall. 1988b. Role of the neural crest in development of the cartilaginous cranial and visceral skeleton of the medaka, *Oryzias latipes* (Teleostei). Anatomy and Embryology 177:297-305.

Lethbridge, R. C., and I. C. Potter. 1981a. The skin. Pages 376-448 in M. W. Hardisty and I. C. Potter, eds. The Biology of Lampreys. Volume 3. Academic Press, New York.

Lethbridge, R. C., and I. C. Potter. 1981b. The development of teeth and associated feeding structures during the metamorphosis of the lamprey, *Geotria australis.* Acta Zoologica 62:201-214.

Linnaeus, C. 1758. Systema Naturae per Regna Tria Naturae. Regnum Animale. Laurentii Salvii, Stockholm.

Lindström, T. 1949. On the cranial nerves of the cyclostomes with special reference to n. trigeminus. Acta Zoologica 30:315-458.

Luther, A. 1938. Die Visceralmuskulatur der Acranier, Cyclostomen, und Fische. A. Acranier, Cyclostomen, Selachier, Holocephalen, Ganoiden und Dipnoer. Pages 468-542 in L. Bolk, E. Göppert, E. Kallius, and W.

Lubosch, eds. Handbuch der vergleichenden Anatomie der Wirbeltiere, volume 5. Urban & Schwarzenberg, Berlin.

Mallatt, J. 1981. The suspension feeding mechanism of the larval lamprey *Petromyzon marinus*. Journal of Zoology 194:103-142.

Mallatt, J. 1984. Early vertebrate evolution: pharyngeal structure and the origin of gnathostomes. Journal of Zoology 204:169-183.

Mallatt, J. 1996. Ventilation and the origin of jawed vertebrates: a new mouth. Zoological Journal of the Linnean Society 117:329-404.

Marinelli, W., and A. Strenger. 1954. Vergleichende Anatomie und Morphologie der Wirbeltiere. I Lieferung. *Petromyzon marinus* (L). 1-80.

Marinelli, W., and A. Strenger. 1956. Vergleichende Anatomie und Morphologie der Wirbeltiere. II Lieferung. *Myxine glutinosa* (L). 81-172.

Marion, G. E. Mandibular and pharyngeal muscles of *Acanthias* and *Raja*. American Naturalist 39:153-455.

Marshall, A. M. 1881. On the head cavities and associated nerves of elasmobranches. Quarterly Journal of Microscopical Science 21:72–97.

Martin, W. M., L. A. Bumm, and D. W. McCauley. 2009. Development of the viscerocranial skeleton during embryogenesis of the sea lamprey, *Petromyzon marinus.* Developmental Dynamics 238:3126-3138.

Martini, F. H. 1998. The ecology of hagfishes. Pages 57-77 in J. M. Jørgensen, J. P. Lonholt, R. E. Weber, and H. Malte, eds. The Biology of Hagfishes. Chapman, London.

McBurney, K. M., and G. M. Wright. 1996. Chondrogenesis of a non-collagen-based cartilage in the sea lamprey, *Petromyzon marinus*. Canadian Journal of Zoology 74:2118-2130.

McCauley, D. W., and M. Bronner-Fraser. 2003. Neural crest contributions to the lamprey head. Development 130:2317-2327.

McCauley, D. W., and M. Bronner-Fraser. 2006. Importance of SoxE in neural crest development and the evolution of the pharynx. Nature 441:750-752.

McMillan, C. B., and R. L. Wisner. 1984. Three new species of seven-gilled hagfishes (Mycinidae, *Eptatretus*) from the Pacific Ocean. Proceedings of the California Academy of Sciences 43:249-267.

McVean, A. 1991. The semicircular canals of the hagfish *Myxine glutinosa*. Journal of Zoology 224:213-222.

McVean, A. 1998. Physiology of the inner ear. Pages 564-573 in J. M. Jørgensen, J. P. Lonholt, R. E. Weber, and H. Malte, eds. The Biology of Hagfishes. Chapman, London.

Metscher, B. D. 2009. MicroCT for developmental biology: a versatile tool for high-contrast 3D imaging at histological resolutions. Developmental Dynamics 238:632-640.

Meulemans, D, and M. Bronner-Fraser. 2002. Amphioxus and lamprey AP-2 genes: implications for neural crest evolution and migration patterns. Development 129:4953-4962.

Miller, C. T., T. F. Schilling, K.-H. Lee, J. Parker, and C. B. Kimmel. 2000. *sucker* encodes a zebrafish Endothelin-1 required for ventral pharyngeal arch development. Development 127:3825-3828.

Mok, H.-K. 2001. Nasal-sinus papillae of hagfishes and their taxonomic implications. Zoological Studies 40:355-364.

Mok, H.-K., and C. B. McMillan. 2004. Bifurcating pattern of the ventral aorta and distribution of the branchial arteries of hagfishes (Myxiniformes), with notes on the taxonomic implications. Zoological Studies 43:737-748.

Moody, S. A., and M. B. Heaton. 1983a. Developmental relationships between trigeminal ganglia and trigeminal motoneurons in chick embryos. II. Ganglion axon ingrowth guides motoneuron migration. Journal of Comparative Neurology 213:344–349.

Moody, S. A., and M. B. Heaton. 1983b. Developmental relationships between trigeminal ganglia and trigeminal motoneurons in chick embryos. I. Ganglion development is necessary for motoneuron migration. Journal of Comparative Neurology 213:327–343.

Müller, J. 1834. Vergleichende anatomie der Myxinoiden, der Cyclostomen mit durchbohrtem Gaumen. Osteologie und Myologie. Abhandlungen der Königlichen Akademie der Wissenschaften zu Berlin 1834:65-340.

Müller, J. 1838. Vergleichende neurologie de Myxinoiden. Abhandlungen der Königlichen Akademie der Wissenschaften zu Berlin 1838:171-252.

Nair, S., W. Li, R. Cornell, and T. Schilling. 2007. Requirements for endothelin type-a receptors and endothelin-1 signaling in the facial ectoderm for the patterning of skeletogenic neural crest cells in zebrafish. Development 134:335–345.

Neumayer, L. 1938. Die entwicklung des kopskelettes von *Bdellostoma* St. L. Archivio Italiano di Anatomica e di Embriologia 40(suppl.):1-222.

Newth, D. R. 1956. On the neural crest of lamprey embryos. Journal of Embryology and Experimental Morphology 4:358-375.

Nishizawa, H., R. Kishida, T Kadota, and R. C. Goris. 1988. Somatotopic organization of the primary sensory trigeminal neurons in the hagfish, *Eptatretus burger*. Journal of Comparative Neurology 267:281-295.

Noden, D. M. 1992. Vertebrate craniofacial development: novel approaches and new dilemmas. Current Opinions in Genetics and Development 2:576-581.

Northcutt, R. G. 1990. Ontogeny and phylogeny: a re-evaluation of conceptual relationships and some applications. Brain, Behavior and Evolution 36:116–40.

Northcutt, R. G. 1993. A reassessment of Goodrich's model of cranial nerve phylogeny. Acta Anatomica 148:71–80.

Northcutt, R. G. 2008. Historical hypotheses regarding segmentation of the vertebrate head. Integrative and Comparative Biology 48:611-619.

Novacek, M. J. 1993. Patterns of diversity in the mammalian skull. Pages 438-545 343 in J. Hanken and B. K. Hall, eds. The Skull. Volume II. Patterns of Structural and Systematic Diversity. The University of Chicago Press, Chicago.

Ohtani, K., T. Yao, M. Kobayashi, R. Kusakabe, S. Kuratani, and H. Wada. 2008. Expression of Sox and fibrillar collagen genes in lamprey larval chondrogenesis with implications from the evolution of vertebrate cartilage. Journal of Experimental Zoology B 310:596-607.

Ota, K. G., and S. Kuratani. 2008. Developmental biology of hagfishes, with a report on newly obtained embryos of the Japanese inshore hagfish, *Eptatretus burger*. Zoological Science 25:999-1011.

Ota, K. G., and S. Kuratani. 2010. Expression pattern of two collagen type 2α1 genes in the Japanese inshore hagfish (*Eptatretus burger*) with special reference to the evolution of cartilaginous tissue. Journal of Experimental Zoology B 314:157-165.

Ota, K. G., S. Kuraku, and S. Kuratani. 2007. Hagfish embryology with reference to the evolution of the neural crest. Nature 446:672-675.

Ota, K. G., S. Fujimoto, Y. Oisi, and S. Kuratani. 2011. Identification of vertebra-like elements and their possible differentiation from sclerotomes in the hagfish. Nature Communications 2:373. 6 pp.

Parker, W. K. 1883a. On the skeleton of the marsipobranch fishes. Part I. The myxinoids (*Myxine* and *Bdellostoma*). Philosophical Transactions of the Royal Society of London 174:373-409.

Parker, W. K. 1883b. On the skeleton of the marsipobranch fishes. Part II. *Petromyzon*. Philosophical Transactions of the Royal Society of London 174:411-457.

Parsons, T. S. 1959. Studies on the comparative embryology of the reptilian noses. Bulletin of the Museum of Comparative Zoology 120:101-277.

Person, P., and D. E. Philpott. 1967. On the occurrence and biologic significance of cartilage tissues in invertebrates. Clinical Orthopedic Related Research 53:185-212.

Piavis, G. W. 1961. Embryological stages in the sea lamprey and the effect of temperature on development. Fishery Bulletin of Fish and Wildlife Service of the United States 61:111-143.

Platt, J. B. 1891. A contribution to the morphology of the vertebrate head, based on a study of *Acanthias vulgaris*. Journal of Morphology 5:79–112.

Purnell, M. A. 1994. Skeletal ontogeny and feeding mechanisms in conodonts. Lethaia 27:129-138.

Purnell, M. A. 1995. Microwear on conodont elements and macrophagy in the first vertebrates. Nature 374:798-800.

Purnell, M. A. 2002. Feeding in extinct jawless heterostracan fishes and testing scenarios of early vertebrate evolution. Proceedings of the Royal Society of London B 269:83-88.

Purnell, M. A., and P. H. von Bitter. 1992. Blade-shaped conodont elements functioned as cutting teeth. Nature 359:629-631.

Purnell, M. A., and P. C. J. Donoghue. 1997. Architecture and functional morphology of the skeletal apparatus of ozarkodinid conodonts. Philosophical Transactions of the Royal Society of London B 352:1545-1564.

Purnell, M. A., and P. C. J. Donoghue. 1998. Skeletal architecture, homologies and taphonomy of ozarkodinid conodonts. Palaeontology 41:57-102.

Randall, D. J. 1972. Respiration. Pages 287-306 in M. W. Hardisty and I. C. Potter, eds. The Biology of Lampreys. Volume 2. Academic Press, New York.

Retzius, G. 1881. Das Gehörogan der Fische un Amphibien. Samson & Wallin, Stockholm. 222 pp.

Richman, J. M., and G. R. Handrigan. 2012. Reptilian tooth development. Genesis 49:247-260.

Rieppel, O. 1993. Patterns of diversity in the reptilian skull. Pages 344-390 in J. Hanken and B. K. Hall, eds. The Skull. Volume II. Patterns of Structural and Systematic Diversity. The University of Chicago Press, Chicago.

Robson, P., G. M. Wright, and F. W. Keeley. 2000. Distinct non-collagen based cartilages comprising the endoskeleton of the Atlantic hagfish, *Myxine glutinosa*. Anatomia Embryologia 202:281-290.

Robson, P., G. M. Wright, J. H. Youson, and F. W. Keeley. 1997. A family of non-collagen-based cartilages in the skeleton of the sea lamprey, *Petromyzon marinus*. Comparative Biochemistry and Physiology B 118:71-78.

Romer, A. S. 1972. The vertebrate as a dual animal–somatic and visceral. Evolutionary Biology 6:121–56.

Romanoff, A. L. 1960. The Avian Embryo: Structural and Functional Development. The Macmillan Company, New York. 1305 pp.

Ronan, M. 1988. The sensory trigeminal tract of Pacific hagfish. Primary afferent projections and neurons of the tract nucleus. Brain, Behavior and Evolution 32:169-180.

Rothova, M., H. Thompson, H. Lickert, and A. S. Tucker. 2012. Lineage tracing of the endoderm during oral development. Developmental Dynamics 241:1183-1191.

Rovainen, C. M. 1996. Feeding and breathing in lampreys. Brain, Behavior and Evolution 48:297-305.

Rücklin, M., S. Giles, P. Janvier, and P. C. J. Donoghue. 2011. Teeth before jaws? Comparative analysis of the structure and development of the external and internal scales in the extinct jawless vertebrate *Loganella scotica*. Evolution & Development 13:523-532.

Ruhin, B., S. Creuzet, C. Vincent, L. Benouaiche, N. M. Le Douarin, and G. Couly. 2003. Patterning of the hyoid cartilage depends upon signals arising from the ventral foregut endoderm. Developmental Dynamics 228:239-246.

Ruppert, E. E. 1997. Cephalochordata (Acrania). Pages 349-504 in F. W. Harrison and E. E. Ruppert, eds. Microscopic Anatomy of Invertebrates. Volume

15: Hemichordata, Chaetognatha, and the Invertebrate Chordates. Wiley-Lis. New York.

Rychel, A. L., and B. J. Swalla. 2007. Development and evolution of chordate cartilage. Journal of Experimental Zoology B 308:325-335.

Rychel, A. L., S. E. Smith, H. T. Shimamoto, and B. J. Swalla. 2006. Evolution and development of the chordates: collagen and pharyngeal cartilage. Molecular Biology and Evolution 23:541-549.

Sansom, I. J., M. P. Smith, H. A. Armstrong, and M. M. Smith. 1992. Presence of the earliest vertebrate hard tissues in conodonts. Science 256:1308-1311.

Sato, T., Y. Kurihara, R. Asai, Y. Kawamura, K. Tonami, Y. Uchijima, E. Heude, M. Ekker, G. Levi, and H. Kurihara. 2008. An endothelin-1 switch specifies maxillomandibular identity. Proceedings of the National Academy of Sciences 105:18806–18811.

Schaefer, B., and K. S. Thomson. 1980. Reflections on agnathan-gnathostome relationships. Pages 19-33 in L. L. Jacobs, ed. Aspects of Vertebrate History: Essays in Honor of Edwin Harris Colbert. Museum of Northern Arizona Press, Flagstaff.

Schlosser, G. 2005. Evolutionary origins of vertebrate placodes: insights from developmental studies and from comparisons with other deuterostomes. Journal of Experimental Zoology B 304:347-399.

Schultze, H.-P. 1993. Patterns of diversity in the skulls of jawed fishes. Pages 189-254 in J. Hanken and B. K. Hall, eds. The Skull. Volume II. Patterns of Structural and Systematic Diversity. The University of Chicago Press, Chicago.

Schweitzer, R., E. Zelzer, and T. Volk. 2010. Connecting muscles to tendons: tendons and musculoskeletal development in flies and vertebrates. Development 137:2807-2817.

Scott, L., and M. E. Atkinson. 1999. Compartmentalisation of the developing trigeminal ganglion into maxillary and mandibular divisions does not depend on target contact. Journal of Anatomy 195:137-145.

Sewertzoff, A. N. 1916. Études sur l'évolution des Vertébrés inférieurs. I. Morphologie du squelette et de la musculature de la tête des Cyclostomes. Archives russes d'anatomie, d'histologie et d'embryologie 1:1-104.

Sewertzoff, A. N. 1917. Études sur l'évolution des Vertébrés inférieurs. II. Organisation des ancêtres des Vertébrés actuels. Archives russes d'anatomie, d'histologie et d'embryologie 1:425-572.

Shigetani, Y., F. Sugahara, and S. Kuratani. 2005. A new evolutionary scenario for the vertebrate jaw. BioEssays 27:331-338.

Shigetani, Y., S. Howard, S. Guidato, K. Furushima, T. Abe, and N. Itasaki. 2008. Wise promotes coalescence of cells of neural crest and placode origins in the trigeminal region during head development. Developmental Biology 319:346-358.

Shigetani, Y., F. Sugahara, Y. Kawakami, Y. Murakami, S. Hirano, and S. Kuratani. 2002. Heterotopic shift of epithelial-mesenchymal interactions in vertebrate jaw evolution. Science 296:1316-1319.

Slavkin, H. C., and T. Diekwisch. 1996. Evolution in tooth developmental biology: of morphology and molecules. The Anatomical Record 245:131-150.

Slavkin, H. C., E. Graham, M. Zeichner-David, and W. Hildemann. 1983. Enamel-like antigens in hagfish: possible evolutionary significance. Evolution 37:404-412.

Smith, M. M., I. J. Sansom, and M. P. Smith. 1996. 'Teeth' before armour: the earliest vertebrate mineralized tissues. Modern Geology 20:303-320.

Song, J., and R. L. Boord. 1993. Motor components of the trigeminal nerve and organization of the mandibular arch muscles in vertebrates: phylogenetically conservative patterns and their ontogenetic basis. Acta Anatomica 148:139-149.

Soukup, V., H.-H. Epperlein, I. Horácek, and R. Cerny. 2008. Dual epithelial origin of vertebrate oral teeth. Nature 455:795-799.

Stark, M. R., J. Sechrist, M. Bronner-Fraser, and C. Marcelle. 1997. Neural tube-ectoderm interactions are required for trigeminal placode formation. Development 124:4287–4295.

Stensiö, E. A. 1927. The Devonian and Downtonian vertebrates of Spitsbergen. Part I. Family Cephalaspidae. Skrifter om Svalbard og Nordishavet 12:1-391.

Stensiö, E. A. 1932. The Cephalaspids of Great Britain. Trustees of the British Museum, London. 220 pp.

Stensiö, E. A. 1958. Les Cyclostomes fossles ou Ostracodermes. Pages 173-425 in P. P. Grassé, ed. Traité de Zoologie. Volume 13. Masson et Cie, Paris.

Stensiö, E. A. 1964. Les Cyclostomes fossils ou Ostracodermes. Pages 96-383 in J. Piveteau, ed. Traité de Paléontologie, Volume 4. Masson et Cie, Paris.

Stensiö, E. A.1968. The cyclostomes with special reference to the diphyletic origin of the Petromyzontida and the Myxinoidea. Pages 13-71 in T. Ørvig, ed. Current Problems in Lower Vertebrate Phylogeny. Almqvist and Wiksell, Stockholm.

Stockard, C. R. 1906. The development of the mouth and gills in *Bdellostoma stouti*. American Journal of Anatomy 5:481-517.

Strahan, R. 1958. The velum and the respiratory current of *Myxine*. Acta Zoologica 39:227-240.

Summers, A. P., and T. J. Koob. 2002. The evolution of tendon — morphology and material properties. Comparative Biochemistry and Physiology Part A 133:1159-1170.

Szaniawski, H., and S. Bengtson. 1993. Origin of euconodont elements. Journal of Paleontology 67:640-654.

Tozer, S. and D. Duprez. 2005. Tendon and ligament: development, repair and disease. Birth Defects Research. Part C. Embryo Today 75: 226-236.

Tretjakoff, D. 1926. Das skelett und die Muskulatur im Kopfe des Flüssneunauges. Zeitschrift für Wissenschaftliche Zoologie 128:267-304.

Trueb, L. 1993. Patterns of cranial diversity among the Lissamphibia. Pages 255-343 in J. Hanken and B. K. Hall, eds. The Skull. Volume II. Patterns of Structural and Systematic Diversity. The University of Chicago Press, Chicago.

Tucker, A., and P. Sharpe. 2007. The cutting-edge of mammalian development; how the embryo makes teeth. Nature Reviews Genetics 5:499-508.

Wada, N., T. Nohno, and S. Kuratani. 2011. Dual origins of the prechordal cranium in the chicken embryo. Developmental Biology 356:529-540.

Wagner, G. P. 1994. Homology and the mechanisms of development. Pages 273-299 in B. K. Hall, ed. Homology: The Hierarchical Basis of Comparative Biology. Academic Press, San Diego.

Wängsjö, G. 1952. The Downtonian and Devonian vertebrates of Spitsbergen. 9. Morphologic and systematic studies of the Spitzbergen cephalaspids. Results of Th. Vogt's Expedition 1928 and the English-Norwegian-Swedish Expedition in 1939. Norsk Polarinstitutt Skrifter 97:1-611.

Welsch, U., A. Chiba, and Y. Honma. 1998. The notochord. Pages 145-159 in J. M. Jørgensen, J. P. Lonholt, R. E. Weber, and H. Malte, eds. The Biology of Hagfishes. Chapman, London.

White, E. H. 1935. The ostracoderm *Pteraspis* Kner and the relationships of the agnathous vertebrates. Philosophical Transactions of the Royal Society of London B 225:381-457.

Wicht, H., and R. Nieuwenhuys. 1998. Hagfishes (Myxinoidea). Pages 497-549 in R. Nieuwenhuys, H. J. ten Donkelaar, and C. Nicholson, eds. The Central Nervous System of Vertebrates. Volume 1. Springer, Berlin.

Wicht, H., and R. G. Northcutt. 1995. Ontogeny of the head of the Pacific hagfish (*Eptatretus stouti*, Myxinoidea): development of the lateral line system. Philosophical Transactions of the Royal Society of London B 349:119-134.

van Wijhe, J. W. 1882. Über die Mesodermsegmente und die Entwicklung der Nerven des Selachierkopfes. Verhandelingen der Koninklijke Akademie van Wetenschappen 22:1–50.

Willey, A. 1894. *Amphioxus* and the Ancestry of the Vertebrates. Columbia University Biological Series II. Macmillan, London.

Wisner, R. L., and C. B. McMillan. 1995. Review of new world hagfishes of the genus *Myxine* (Agnatha, Myxinidae) with descriptions of nine new species. Fishery Bulletin 93:530-550.

Worthington, J. 1906. The descriptive anatomy of the brain and cranial nerves of *Bdellostoma dombeyi*. Quarterly Journal of Microscopical Science 49:137-181.

Wright, G.M., and J. H. Youson. 1982. Ultrastructure of mucocartilage in the larval anadromous sea lamprey, *Petromyzon marinus* L. American Journal of Anatomy 165:39–51.

Wright, G. M., and J. H. Youson. 1983. Ultrastructure of cartilage from young adult sea lamprey, *Petromyzon marinus* L: a new type of vertebrate cartilage. American Journal of Anatomy 167:59–70.

Wright, G. M., F. W. Keeley, and M. E. DeMont. 1998. Hagfish cartilage. Pages 160-170 in J. M. Jørgensen, J. P. Lonholt, R. E. Weber, and H. Malte, eds. The Biology of Hagfishes. Chapman, London.

Wright, G. M., F. W. Keeley, and P. Robson. 2001. The unusual cartilaginous tissues of jawless craniates, cephalochordates and inveretbrates. Cell and Tissue Research 304:165-174.

Wright, G. M., F. W. Keeley, J. H. Youson, and D. L. Babineau. 1984. Cartilage in the Atlantic hagfish, *Myxine glutinosa*. American Journal of Anatomy 169:407-424.

Wright, G. M., L. A. Armstrong, A. M. Jacques, and J. H. Youson. 1988. Trabecular, nasal, branchial, and pericardial cartilages in the sea lamprey, *Petromyzon marinus*: fine structure and immunohistochemical detection of elastin. American Journal of Anatomy 182:1–15.

Yalden, D. W. 1985. Feeding mechanisms as evidence for cyclostome monophyly. Zoological Journal of the Linnean Society 84:291-300.

Yanagisawa, H., M. Yanagisawa, R. P. Kapur, J. A. Richardson, S. C. Williams, D. E. Clouthier, D. de Wit, N. Emoto, and R. E. Hammer. 1998. Dual genetic pathways of endothelin-mediated intercellular signaling revealed by targeted disruption of endothelin converting enzyme-1 gene. Development 125:825-836.

Yao, T., K. Ohtani, S. Kuratani, and H. Wada. 2011. Development of lamprey mucocartilage and its dorsal-ventral patterning by endothelin signaling, with insight into vertebrate jaw evolution. Journal of Experimental Zoology (Molecular and Developmental Evolution) 316:339-346.

Zhang, G., and M. J. Cohn. 2006. Hagfish and lancelet fibrillar collagens reveal that type II collagen-based cartilage evolved in stem vertebrates. Proceedings of the National Academy of Sciences 103:16829-16833.

Zhang, G., M. M. Miyamoto, and M. J. Cohn. 2006. Lamprey type II collagen and *Sox9* reveal an ancient origin of the vertebrate collagenous skeleton. Proceedings of the National Academy of Science 103:3180-3185.

Zusi, R. L. 1993. Patterns of diversity in the avian skull. Pages 391-437 343 in J. Hanken and B. K. Hall, eds. The Skull. Volume II. Patterns of Structural and Systematic Diversity. The University of Chicago Press, Chicago.

2.7. TABLES

Table 2-1. Summary of potential homology in the vertebrate chondrocrania. The skull elements of hagfish and lampreys are listed accordingly with potential homologues between them and with gnathostomes. Each element in the columns for lampreys and gnathostomes is followed by notations for anatomical criteria of similarity that showed congruence with the corresponding element of hagfish. Upper-case notations show congruence, whereas lower-case notations indicate either partial incongruence or uncertain information. Question marks (?) indicate uncertain similarity. Only specific, element-to-element similarities are listed (this is designated as 'complete' homology, but this terminology does not necessarily mean that all the criteria are congruent). Incomplete similarity and potential homology in extinct jawless vertebrates are noted at the far right column. The criteria of similarity are not independent from each other. The more criteria are scored, the stronger the support is for conservation of the anatomical organization of that element relative to surrounding tissues. See main text for detailed discussion of the criteria.

Notations for criteria of similarity: C= congruence in relationships with other cartilages; E= ectomesenchyme (also noted for hagfish); F= congruence in functions; IC= congruence in tissues that form likely site of induction or delineate cartilage; M= mesoderm (also noted for hagfish); N= congruence in nerve innervation in associated structures; PCh= position with respect to notochord (prechordal or parachordal); PM= position with respect to associated mesodermal structures (external or internal; muscle attachment); PN= position with respect to major nerve branch or sensory organ; PV= position with respect to major vessels (e.g., internal carotid artery, branchial arteries); S= general morphology (e.g., capsule as opposed to rod).

Domains	Hagfish	Lampreys	Gnathostomes	Notes
Premandibular				
	Nasal capsule basket[1, E]	Nasal capsule[1, 2, C, E, F, IC, N, PN]	Nasal capsule[2, C, E, F, IC, N, PN]	Osteological correlates in stem gnathostomes[3]
	Nasopharyngeal bar[E]	Dorsolateral blastema[C, e, f, IC, PCh, PN, S]	Trabecula[C, E, f, IC, PCh, PN, s]	Dorsolateral blastema disappears before chondrification
	Nasal arches[E]	No evidence	Not comparable; ?Ethmoidal plate[c, E, N]	Osteological correlate in heterostracans[4]
	Subnasal cartilage[E]	?Posterior tectal cartilage[c, E, IC, N, PN]	Not comparable[5]	Osteological correlate in heterostracans[4]
	Palatal commissure[E]	Commissure of subocular arches[C, E, F, PN, S]	Not comparable	These elements may belong to the mandibular domain
	Not comparable	Anterior tectal cartilage[E]	Not comparable[5]	
	Not comparable	No evidence	Trabecular commissure	
Mandibular				
	Lateral tentacular cartilage (labial ramus)[E]	Anterior lateral plate[c, E, IC, N, pm, PN]	Not comparable[5]	
	Oral tentacular cartilage; perioral tentacular process?	Annular cartilage; stylet cartilage[C, E, F, IC, pm]	Not comparable[5]	Similar cartilage in anaspids[7]
	Cornual process[E]	Posterior dorsal plate[C, E, F, N, PM, PN, S]	Not comparable[5]	
	Palatal arch[E]	Base of posterodorsal plate[C, E, F, IC, pm, PN, S]	Not comparable[5]	
	Dorsal longitudinal arch[E]	Subocular arch[C, E, F, IC, pm, PN, S]	Not comparable[6]	

	Ventral longitudinal arch[E]	No evidence	Not comparable[6]	
	Lateral velar cartilage[E]	Lateral velar cartilage[C, E, IC, F, N, PM, PN, S]	Not comparable[6]	
	Medial velar cartilage[E]	?Medial velar plate[C, E, IC, F, PN, S]	Not comparable[6]	Uncertainty in PM; may be internal arch skeleton as in gnathostome jaws[8]
	Dental apparatus[E]	Supralingual cartilage[C, E, F, N, PM, S]	Not comparable[5, 6]	
	Tooth plates[e]	Lingual teeth[C, E, F, N, PM, S]	?Teeth[E, F, S]	Conodonts may have equivalent structures[9]; IC incongruent[10]
	Median dorsal tooth[e]	Supraoral teeth[C, E, F, N, PM, S]	Not comparable	IC incongruent[9]
	No evidence	Medioventral cartilage[E]	Not comparable[5]	
	Not comparable	Not comparable	Palatoquadrate, Meckel's cartilage[6]	
Hyoid and post-hyoid				
	Visceral plate[E]	Styliform cartilage[C, E, F, IC, PM, PN, S]	Not comparable[6]	
	Velar process[E]	Cornual plate[C, E, F, PM, PN]	Not comparable[6]	
	No evidence	Extrahyal[E]	Not comparable[6]	
	External pharyngolingual arch[E]	?Branchial arch[E, ic, pm, PV, s]	No evidence[11]	
	Internal pharyngolingual arch[E]	No evidence	Branchial arches[C, E, IC, PM, PV, S]	
	Extrabranchial cartilage[E]	Branchial arch[E, F, IC, N, PM, PN, PV]	Extrabranchial cartilage[E, F, IC, N, PM, PN, PV, S]	

	Extrapharyngocutaneous cartilage[E]	Not comparable	Not comparable	Serial homologue of extrabranchial cartilage
	No evidence	Pericardial cartilage	No evidence	
	Not comparable	Not comparable	Hyomandibula[6]	
Ventral midline pharyngeal (post-mandibular)				
	Anterior lingual cartilages[12, E]	Apical cartilage[C, E, F, N, PM, PN, S]	Not comparable[5, 6]	Conodonts may have had equivalent cartilage[8]
	Middle lingual cartilage[E]	Copular cartilage[C, E, F, N, PM, PN, S]	Not comparable[5, 6]	
	Posterior lingual cartilage[E]	Piston cartilage[C, E, F, N, PM, PN, S]	Not comparable[5, 6]	
	Distal lingual cartilages[e]	Distal lingual cartilage[C, E, F, N, PM, PN, S]	Not comparable[5, 6]	
Parachordal				
	Nasopharyngeal plate[M]	Acrochordal commissure[13, 14, C, f, ic, M, PCh, PN, PV]	Acrochordal cartilage; dorsum sellae[13, C, f, ic, M, PCh, PN, PV]	Parasphenoid in gnathostome braincase
	Otic-trigeminal arch[M]	Otic-trigeminal arch[C, F, IC, M, PCh, PN, S]	Parachordal cartilage[C, F, IC, M, PCh, PN, S]	Sphenoids and prootic in gnathostome braincase
	Otic capsule[M]	Otic capsule [C, F, IC, M, N, PCh, PN, S]	Otic capsule [C, F, IC, M, N, PCh, PN, S]	Prootic and opisthotic in gnathostome braincase
	Parachordal cartilage[M]	Parachordal cartilage[C, F, IC, M, PCh, PN, S]	Parachordal cartilage[C, F, IC, M, PCh, PN, S]	Basisphenoid in gnathostome braincase

Footnotes:

1, unpaired;

2, similarity in overall morphology (capsule as opposed to basket);

3, impressions of olfactory bulbs indicate the presence of nasal capsule in various stem gnathostomes [the nasal capsule was likely unpaired in osteostracans as in hagfish and lampreys, and was paired in galeaspids, heterostracans, and thelodonts (Janvier 1996; Gai et al. 2011)];

4, prenasal sinus in heterostracans is topographically similar, and grooves on the floor of the sinus suggest the presence of paired barbels (Stensiö 1958, 1964; Janvier 1974);

5, gnathostomes do not have structures equivalent to the upper lip [this region within the mandibular arch cannot be compared, because important criteria of similarity (C, N, PN, and PM) cannot be extended across gnathostomes and jawless vertebrates];

6, homology obscured by innovation of jaws [important criteria of similarity (C, N, PN, and PM) cannot be extended across gnathostomes and jawless vertebrates];

7, the anaspid-like vertebrate *Euphanerops* has a cartilage that topographically corresponds to the annular cartilage of lampreys (Janvier and Arsenault 2007);

8, if the medial velar skeleton represents an internal arch skeleton medial to the mesoderm, this is a potential incomplete homologue of jaws;

9, functional analyses (e.g., Goudemand et al. 2011) assume cyclostome-like feeding structures such as basal cartilage (see main text for discussion);

10, the hagfish tooth plates are unique for its development within the endodermal epithelium (IC is applicable to lampreys and gnathostomes, but not to hagfish);

11, if the external pharyngolingual arches in hagfish are lateral with respect to the mesoderm, or truly external, it is possible that the external pharyngolingual arches have no homologue, or represent incomplete serial homologues of the internal pharyngolingual arches (if this hypothesis were to be demonstrated, the homology would follow that of the internal pharyngolingual arch);

12, the anterior segment in the hagfish lingual apparatus has three (a pair of lateral elements and a single medial element) whereas that in the lamprey lingual apparatus has a single midline;

13, traditionally regarded as trabecula; and

14, a nasohypophyseal canal or nasal cavity passes below or anterior to the acrochordal cartilage, whereas the hagfish nasopharyngeal duct extends above the nasopharyngeal plate.

Table 2-2. The scheme of homology in the vertebrate skull by Holmgren (1946). The elements are in the order of the original list. Shaded rows indicate Holmgren's assessment supported by the present analysis (including homology and absence of homology; Table 2-1). Question mark (?) indicates unknown, whereas em dash (—) indicates absence.

Hagfish	Lampreys	Gnathostomes
Parachordals[1]	Parachordals	Posterior parachordals
—?	Lamina basiotica	Lamina basiotica
Otic-trigeminal arch[2]	Otic-trigeminal arch[2]	Trabecula and polar cartilage
Nasopharyngeal plate	—?	Cartilage in polar fenestra
Palatal commissure[4]	—?	—
Trabecular commissure*	Acrochordal commissure[3]	Trabecular commissure
Interfenestral strut[5]	Pedicle process	Basitrabecular process
Nasal capsule	Nasal capsule	Primary nasal capsule
—	—	Secondary nasal capsule
Dorsal longitudinal arch	Base of extrahyal and subocular arch	Antorbital process and lamina orbitonasalis
First internal pharyngolingual arch[6]	—	First branchial arch
Dorsal rim of first pharyngolingual fenestra[7]	—	Hyoid arch
Palatoquadrate (embryo)	?	Palatoquadrate
Tooth plates[8]	?	Mandibular complex
?	Cornual plate	—
Medial basal plate of dental apparatus[9]	—	Mandibular symphyseal cartilage
?	Medial ventral plate	?
Lateral tentacular skeleton[10]	Anterior lateral plate	?
Second external pharyngolingual arch[11]	Second external branchial arch	Second lower extrabranchial
First external pharyngolingual arch[12]	First external branchial arch	Frst lower extra-branchial
Visceral plate[13]	Extrahyal	Extrahyal
Ventral longitudinal arch[14]	Styliform cartilage	—
Anteromedial lingual cartilage[15]	Apical cartilage[16]	Copulae of hyobranchial skeleton (?)
Anterolateral lingual cartilage[17]	Suprapical cartilage[18]	
Middle lingual cartilage[19]	Copular cartilage[20]	

Posterior lingual cartilage[21]	Piston cartilage[22]	
Velar skeleton	Velar skeleton	—
Subnasal cartilage	Posterior tectal plate[23]	Prelabial cartilage
?	Anterior tectal plate[24]	Prenasal cartilage
Cornual process	Posterior lateral plate	Pedicle cartilage
?	Annular cartilage	Prmaxillary cartilage
?	Stylet cartilage	—
—	—	Labial cartilages

Original terminology by Holmgren (1946): [1]termed posterior parachordals; [2]trabecle, but this element is now demonstrated to be a part of parachordal skeleton; [3]trabecular commissure; [4]ethmoid commissure; [5]preauditory transverse bridge; [6]first internal branchial arch; hyoid arch; [7]hyoid arch in embryo; [8]toothplate cartilage; [9]postsymphysial plate of the tooth plate; [10]labial cartilage; [11]second external branchial arch; [12]first external branchial arch; [13]extrahyal; [14]extra-mandibular; [15]medial frontal basal plate; [16]medial lingual; [17]lateral frontal basal plate; [18]lateral lingual; [19]medium basal plate; [20]connecting piece of apicales; [21]unpaired caudal basal plate; [22]unpaired lingual cartilage; [23]posterior dorsal plate; and [24]anterior tectal plate.

*Mesenchymal tissue that does not chondrify; lateral parts of this population chondrify into the lower longitudinal bar of the nasal capsule basket.

2.8. FIGURES

Figure 2-1. The chondrocranium of the northeastern Pacific hagfish *Eptatretus stoutii* in (A) left lateral view without distal lingual and branchial cartilages; and in (B) dorsal view with posterior lingual, distal lingual, and branchial cartilage and dental apparatus removed for clarity. (C) The cranial nerves of *E. stoutii* with the semi-transparent chondrocranium based on original observation and the description of the cranial nerves of the Atlantic hagfish *Myxine glutinosa* by Lindström (1949). Only the major branches are represented. The innervation of the vagus nerve is omitted.

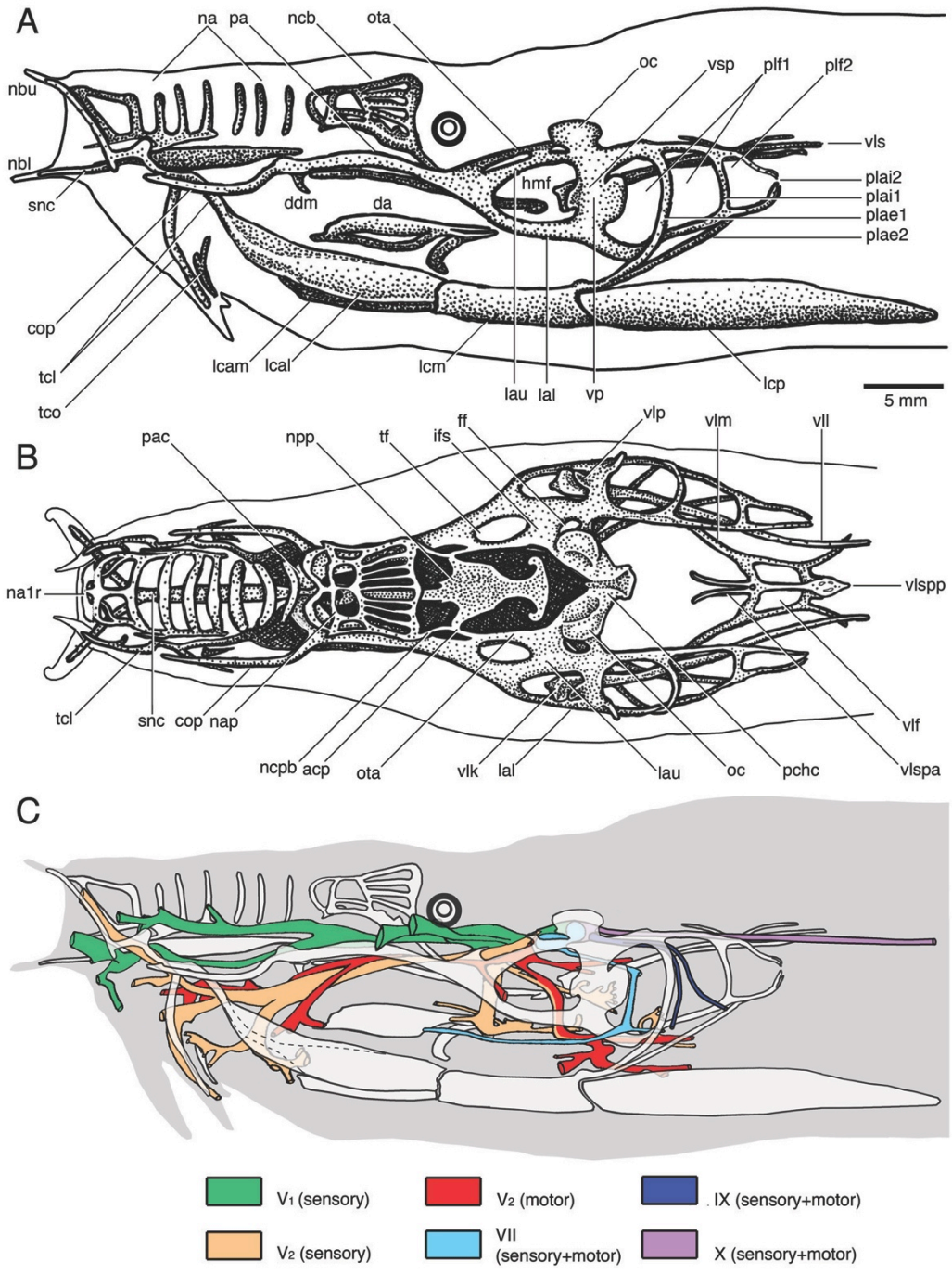
A
na
pa
ncb
ota
oc
vsp
plf1
plf2
nbu
nbl
snc
ddm
da
hmf
vls
plai2
plai1
plae1
plae2
cop
tcl
tco
lcam
lcal
lcm
lau
lal
vp
lcp
5 mm
B
pac
npp
tf
ifs
ff
vlp
vlm
vll
na1r
vlspp
tcl
snc
cop
nap
ncpb
acp
ota
vlk
lal
lau
oc
pchc
vlf
vlspa
C
V1 (sensory)
V2 (motor)
IX (sensory+motor)
V2 (sensory)
VII (sensory+motor)
X (sensory+motor)

Figure 2-1.

Figure 2-2. Comparison of previous reconstructions of the hagfish chondrocrania. (A-D) The chondrocranium of *E. hexatrema* as reconstructed by Müller (1834) in (A) left lateral and (B) dorsal views; and the chondrocranium of the same taxon as reconstructed by Parker (1883a) in (C) left lateral and (D) dorsal views. (E) The chondrocranium of *M. glutinosa* in lateral view as reconstructed by and modified after Holmgren (1946). Holmgren's reconstruction is more accurate than that by Cole (1905, 1909; Figure 2-12I, J) who omitted the outgrowth of the ventral longitudinal arch (discussed in main text). (F-G) The chondrocranium of *E. stoutii* reconstructed from μCT scan in (F) left lateral view and (G) dorsal view, showing the *in situ* nasal skeleton (provided by W. Liu and B. Halgrìmsson, May 2012). Specimens A-E not to scale.

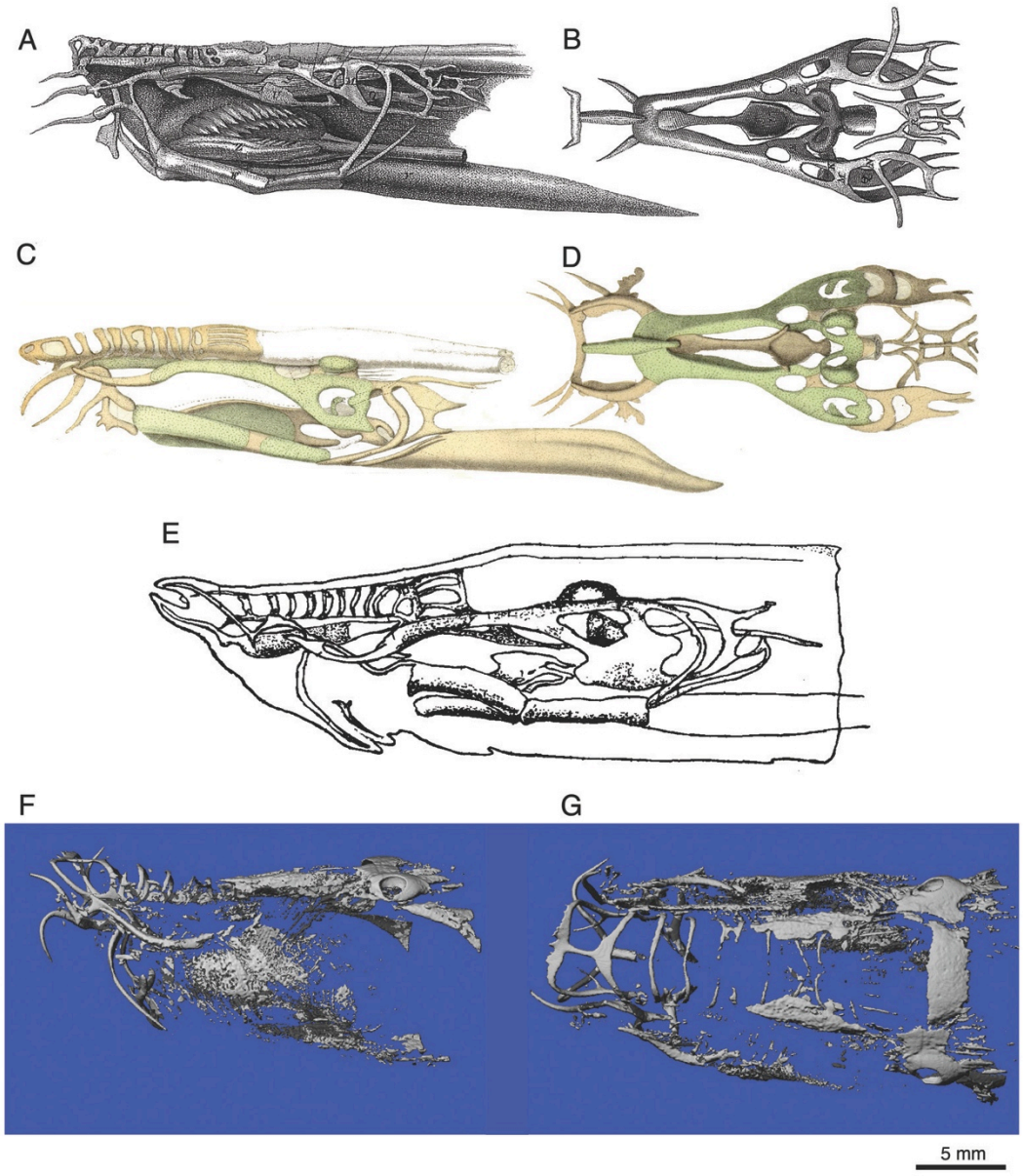

Figure 2-2.

Figure 2-3. Development of the chondrocrania of *E. stoutii* (A, C-F) and the Atlantic hagfish *M. glutinosa* (B), both color-coded according to anatomical domains (defined in the lower right corner). (A) The chondrocranium of an embryo of *E. stoutii* at Neumayer's stage I in left lateral (A_1) and dorsal (A_2) views. (B) The chondrocranium of an embryo of *M. glutinosa* between Neumayer's stages I and II in left lateral (B_1), dorsal (B_2), and ventral (B_3) views. In dorsal and ventral views, the dental and lingual apparatus, nasal skeleton, and lateral tentacular skeletons are omitted for clarity. Holmgren (1946) included the notochord and mesenchyme that he interpreted as primordial cartilages. These are included here, marked by asterisk (*). (C) The chondrocranium of an embryo of *E. stoutii* at Neumayer's stage II in left lateral (C_1), dorsal (C_2), and ventral (C_3) views. (D) The chondrocranium of an embryo of *E. stoutii* at Neumayer's stage III in left lateral (D_1), dorsal (D_2), and ventral (D_3) views. (E) The chondrocranium of an embryo of *E. stoutii* at Neumayer's stage IV in left lateral view. (F) The chondrocranium of an adult of *E. stoutii* in left leteral view. Neumayer (1938) only included chondrifications in his illustrations, whereas Holmgren (1946) also described mesenchyme that he believed would chondrify. Unless marked by asterisk (*), all elements in this figure represent chondrifications or keratizations. Specimens not to scale. Color codes not to be confused with those in other figures. A and C-E are redrawn and reinterpreted after Neumayer (1938); B after Holmgren (1946). Specimens not to scale.

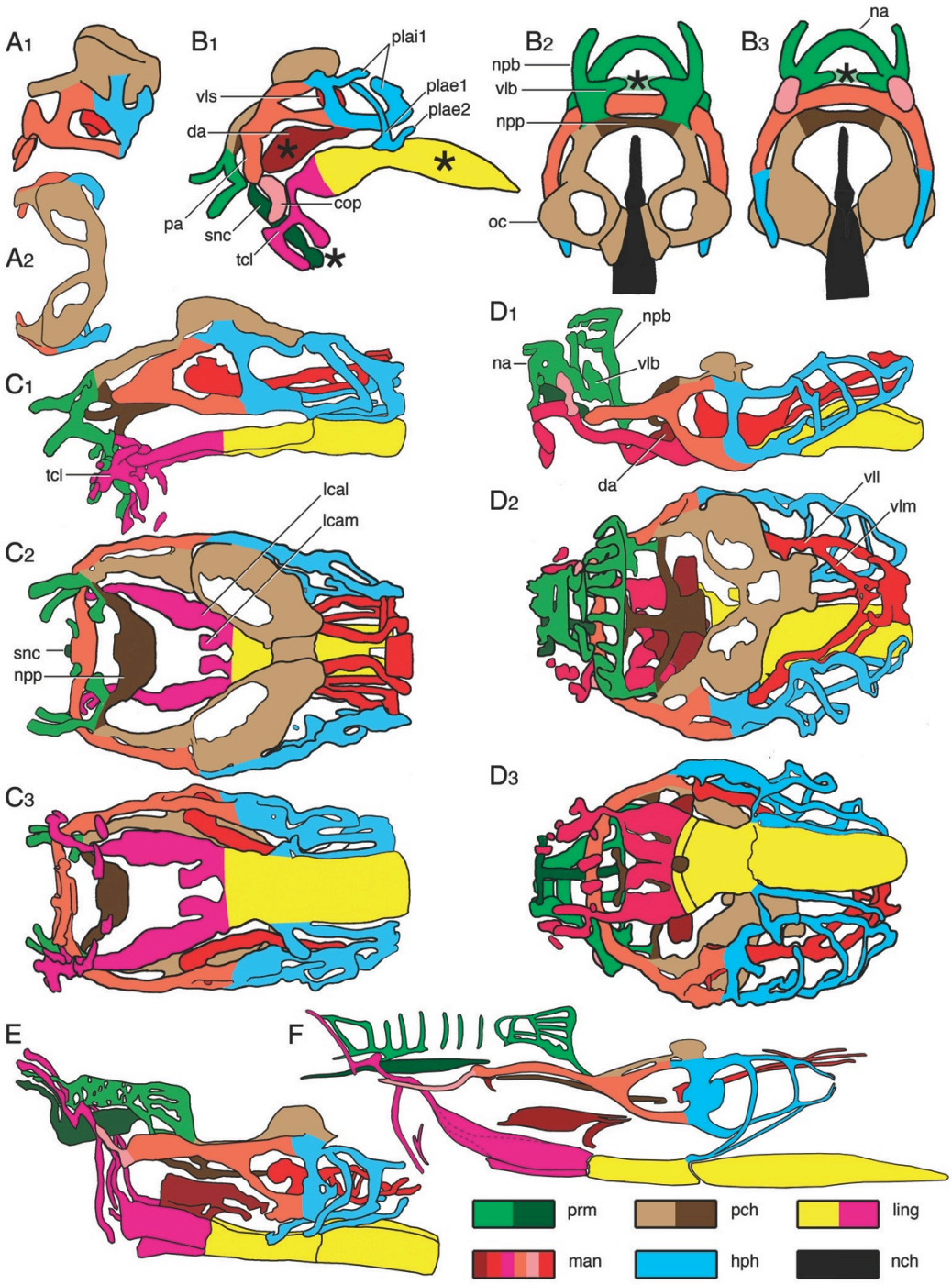
A1
A2
B1
plai1
vls
plae1
plae2
da
pa
snc
cop
tcl
B2
npb
vlb
npp
oc
B3
na
C1
tcl
C2
lcal
lcam
snc
npp
C3
D1
npb
na
vlb
da
D2
vll
vlm
D3
E
F
prm
pch
ling
man
hph
nch

Figure 2-3.

Figure 2-4. Comparison of the chondrocrania of representative vertebrates, the lampreys *Lampetra fluvialis* (A-C) and *Petromyzon marinus* (D-F), and the catshark *Scyliorhinus canicula* (G, H). The adult chondrocranium of the lamprey *Lampetra fluvialis* in (A) left lateral view with the nasal capsule (nc) (redrawn and modified after Marinelli and Strenger 1954). (B) The lingual apparatus of adult *Lampetra fluvialis* drawn based on Marinelli and Strenger (1954) and Johnel's (1948) illustration of the same apparatus of *P. marinus.* (C) The skeleton of the velum in dorsal view, redrawn and modified after Marinelli and Strenger (1954). (D-F) The development of the chondrocranium of *P. marinus* in left lateral view at (D) larval stage, stage 8 metamorphosis (E), and stage 11 metamorphosis (F), redrawn and modified after Johnels (1948). An asterisk (*) indicates un-chondrified anlagen of the adult chondrocranium in the mucocartilage. The notochord is omitted in (F) for clarity. Note that the cranial nerves are closely associated with elements of the chondrocrania and therefore make suitable landmarks for the assessment of morphological similarity with the chondrocrania of other vertebrates. (G, H) The chondrocranium of *S. canicula* in (G) left lateral and (H) dorsal views, with hypothetical branchial series that shows successive stages of differentiation of the branchial elements to show ontogenetic transformation of the pharyngeal skeleton (from posterior to anterior), redrawn and modified after de Beer (1937). The boundary between the premandibular and mandibular domains follows Kuratani et al. (2004, 2012). The legend of color codes for D-H is at the bottom of the figure. Specimens not to scale.

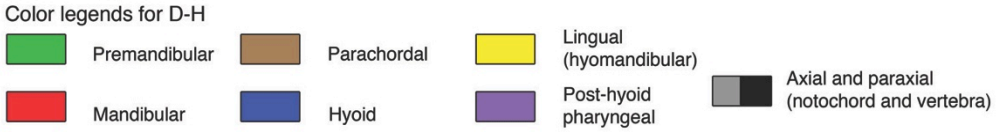

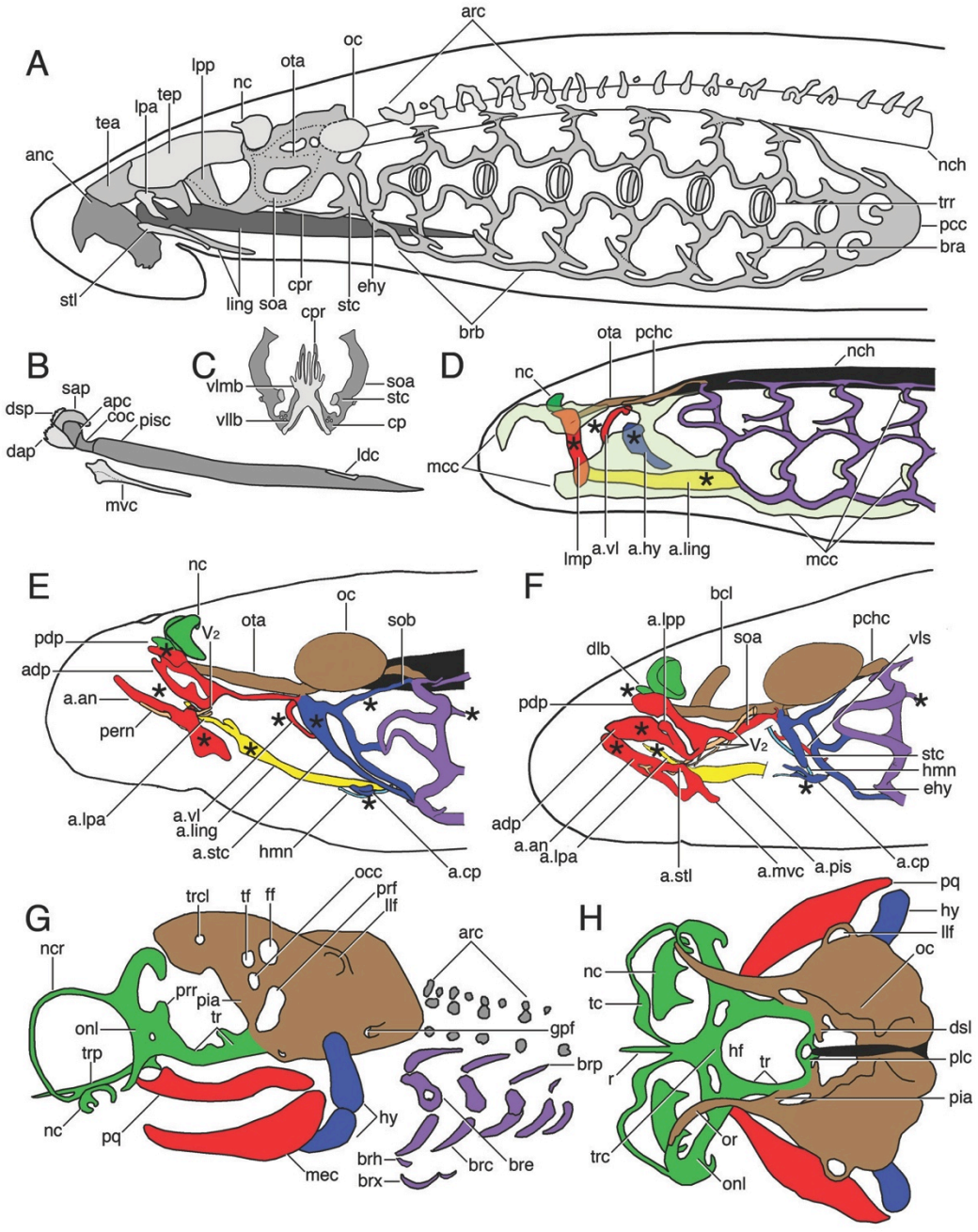
A
arc
oc
lpp
nc
ota
tep
lpa
tea
anc
nch
trr
pcc
bra
stl
ling
soa
cpr
ehy
stc
brb
B
sap
dsp
apc
coc
pisc
dap
ldc
mvc
C
vlmb
soa
stc
vllb
cp
D
ota
pchc
nch
nc
mcc
lmp
a.vl
a.hy
a.ling
mcc
E
nc
oc
V2
ota
sob
pdp
adp
a.an
pern
a.lpa
a.vl
a.ling
a.stc
hmn
a.cp
F
bcl
a.lpp
pchc
dlb
soa
vls
pdp
V2
stc
hmn
ehy
adp
a.an
a.lpa
a.stl
a.mvc
a.pis
a.cp
G
occ
prf
trcl
tf
ff
llf
arc
ncr
prr
pia
tr
onl
gpf
trp
brp
hy
nc
pq
brh
brc
bre
mec
brx
H
pq
hy
llf
oc
nc
tc
dsl
hf
tr
plc
r
pia
or
trc
onl

Figure 2-4.

Figure 2-5. The nasal morphology of *E. stoutii*. (A) Reconstruction of the nasohypophyseal complex (nhc), oral cavity, and pharynx in the head of *E. stoutii* with a semitransparent chondrocranium. The nasohypophyseal complex consists of three subdivisions from anterior to posterior: the non-olfactory nasal tube (nt), the olfactory nasal capsule (nc), and the nasopharyngeal duct (npd) with the adenohypophysis exposed along the roof. The nasopharyngeal duct and oral cavity (orc) join into the pharynx medial to the proximal portion of the velar skeleton (vls). (B-D) Transverse histological sections of the head of *E. stoutii* stained with eosin and hematoxylin (positions of slices B and C indicated in A), showing (B) the sensory nasal papillae and (C) the nasal capsule, with (D) a close-up of the olfactory epithelium and longitudinal bars of the nasal capsule of area D in C. (E) The nasal skeleton of *E. stoutii* in dorsal view, based on specimens with ten nasal arches.

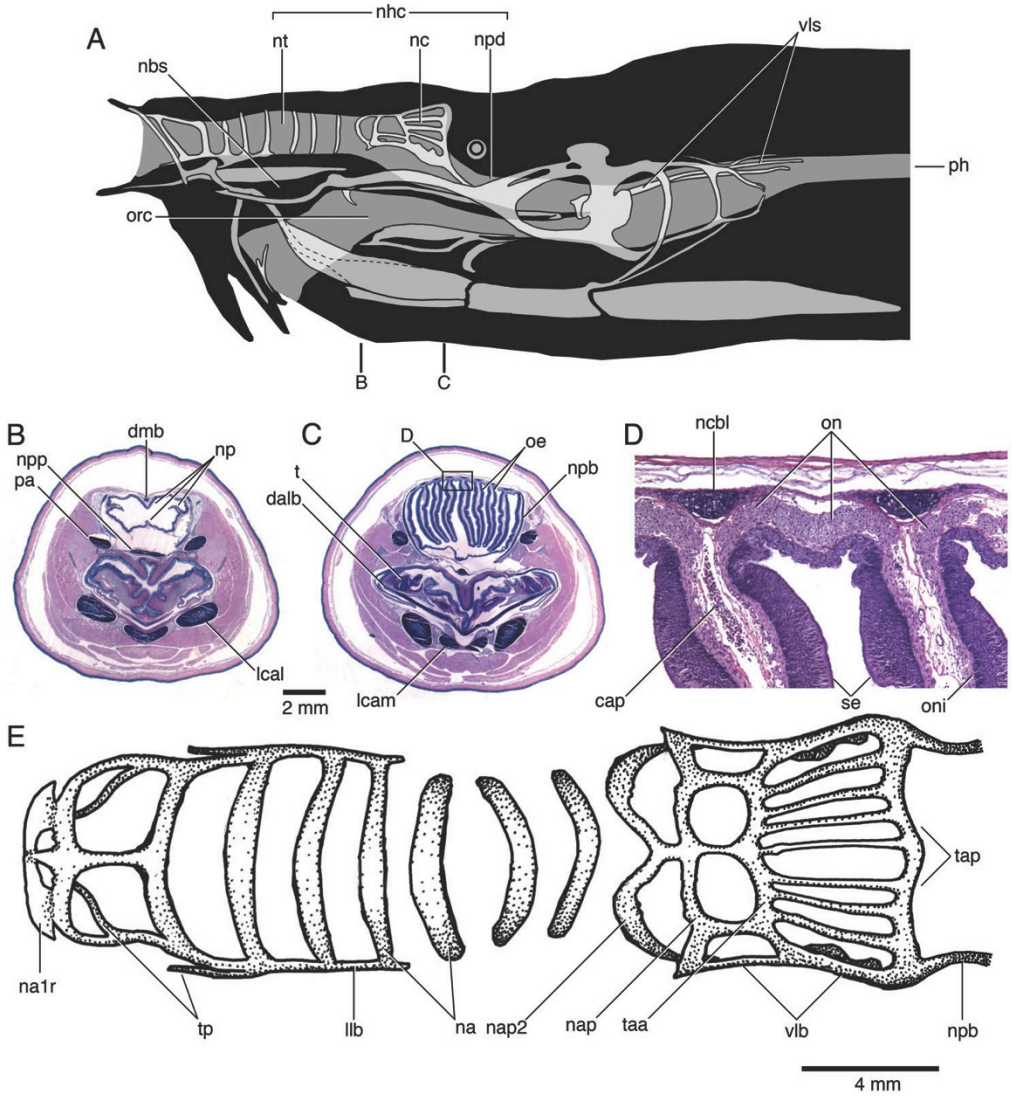
A
nhc
nt
nc
npd
vls
nbs
ph
orc
B
C
B
dmb
np
npp
pa
lcal
2 mm
C
D
oe
t
dalb
npb
lcam
D
ncbl
on
cap
se
oni
E
tap
na1r
tp
llb
na
nap2
nap
taa
vlb
npb
4 mm

Figure 2-5.

Figure 2-6. The morphology of the tentacular skeleton of *E. stoutii* in (A) dorsal and (B) left lateral views. The cornual process is omitted for clarity in both A and B. The perichondrium of the anterolateral lingual cartilage is removed to reveal the proximal portion of the labial ramus of the lateral tentacular cartilage; for an illustration including the perichondrium, see Figure 2-10B. (C) A transverse histological section of the head of *E. stoutii* anterior to the lingual apparatus and at the palatal commissure, showing the perichondrium around the proximal portion of the labial ramus and the proximal section of the subnasal cartilage.

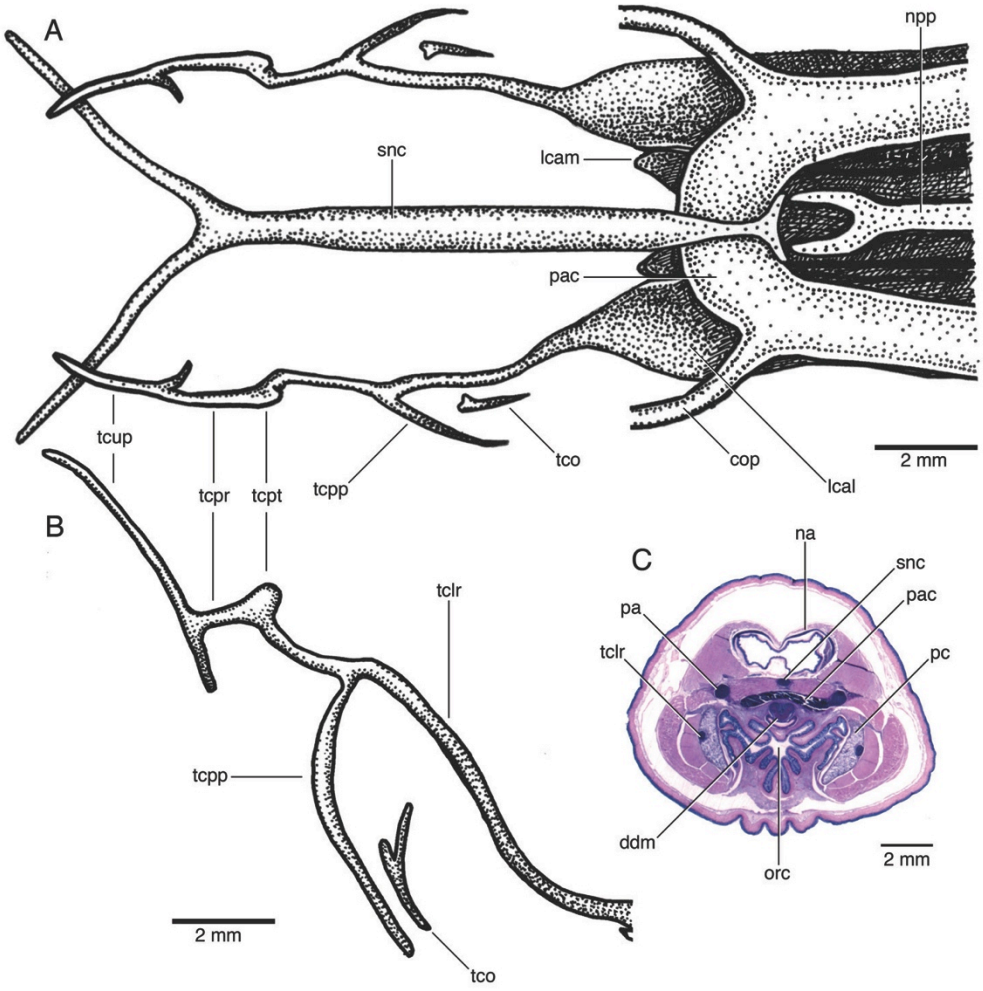
A
npp
snc
lcam
pac
tcup
tcpr
tcpt
tcpp
tco
cop
lcal
2 mm
B
tclr
tcpp
2 mm
tco
C
na
snc
pac
pa
tclr
pc
ddm
orc
2 mm

Figure 2-6.

Figure 2-7. The morphology of the facial and parachordal skeletons of *E. stoutii* in dorsal view. The roots of the cranial nerves and paths of major branches are included in color on the left side of the chondrocranium. Color codes for the nerves follow Figure 2-1C. The ellipse shows a relative location and size of the root.

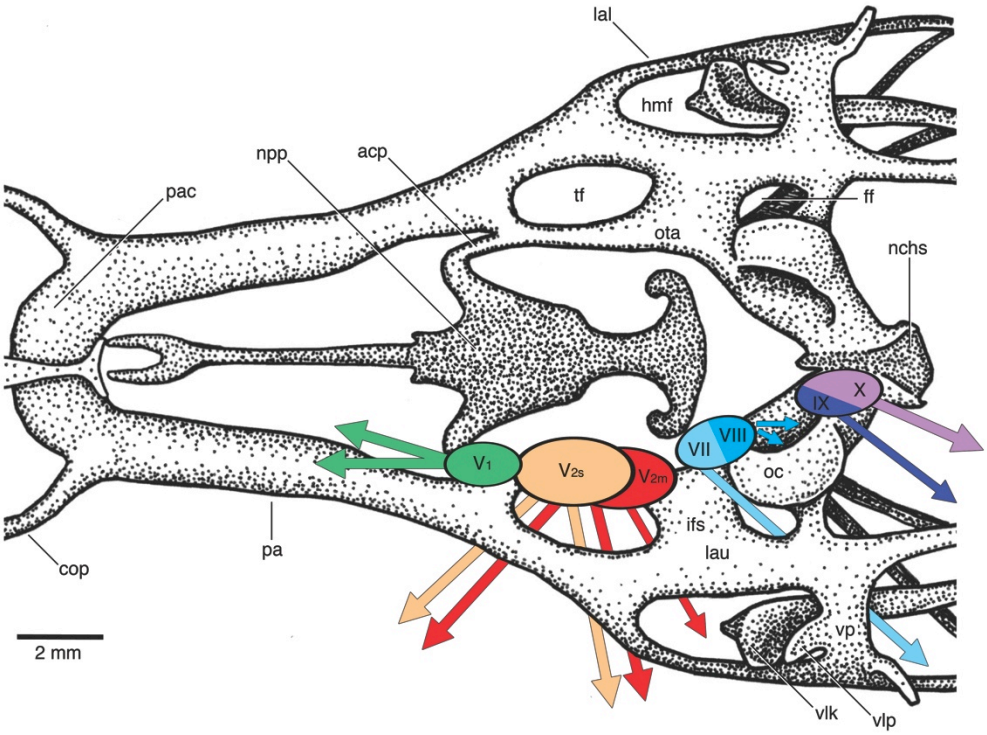
lal
hmf
npp
acp
pac
tf
ff
ota
nchs
X
IX
VIII
VII
V1
V2s
V2m
oc
ifs
lau
pa
cop
vp
vlk
vlp
2 mm

Figure 2-7.

Figure 2-8. The morphology of the velar skeleton of *E. stoutii* in (A) dorsal and (B) lateral views. The facial skeleton and the pharyngolingual arches (plae1,2; plai 1,2) are removed on the left side to show the entire length of the velar skeleton (vls), whereas its bilateral counterpart is illustrated with the overlapping elements. (C-F) Transverse histological sections of the head of *E. stoutii* showing the velar skeleton and other musculoskeletal features behind the otic capsule. The cardinal heart forms between the velar knob and the visceral plate (D). Positions of the slices are indicated in (A).

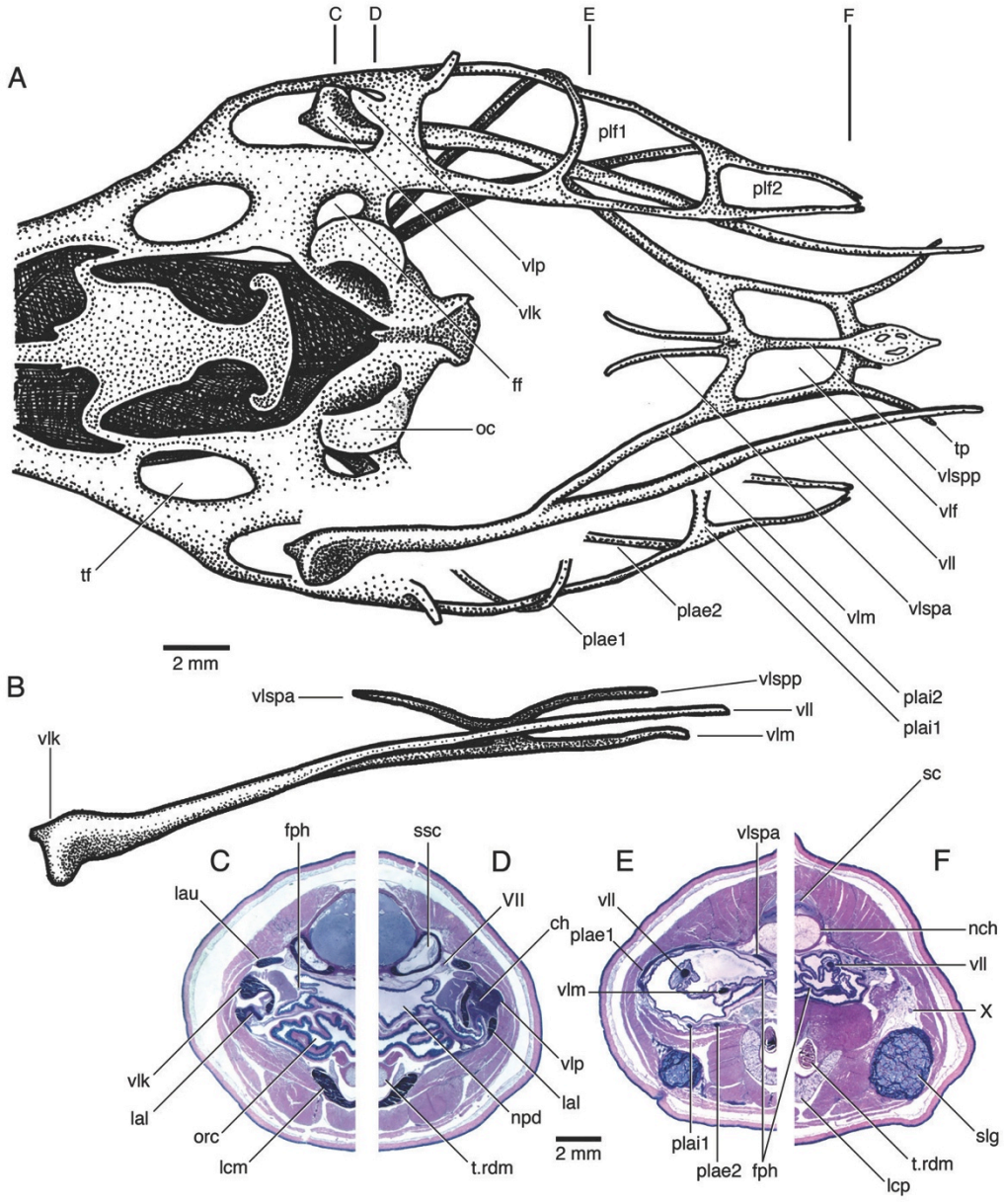
A
C
D
E
F
plf1
plf2
vlp
vlk
ff
oc
tf
tp
vlspp
vlf
vll
vlm
vlspa
plae2
plae1
2 mm
B
vlspa
vlspp
vll
vlm
vlk
plai2
plai1
C
D
E
F
fph
ssc
lau
VII
ch
vlk
lal
orc
lcm
vlp
lal
npd
t.rdm
2 mm
vlspa
vll
plae1
vlm
plai1
plae2
fph
sc
nch
vll
X
slg
t.rdm
lcp

Figure 2-8.

Figure 2-9. The morphology of the dental apparatus of *E. stoutii*. (A) The dental apparatus in dorsal view, with the left side reconstructed bearing two tooth plates; (B) the medial tooth plate and (C) the lateral tooth plate in dorsal view. (D) The isolated dental apparatus in dorsal view, and a medial (E) and lateral (F) tooth plate in ventral view.

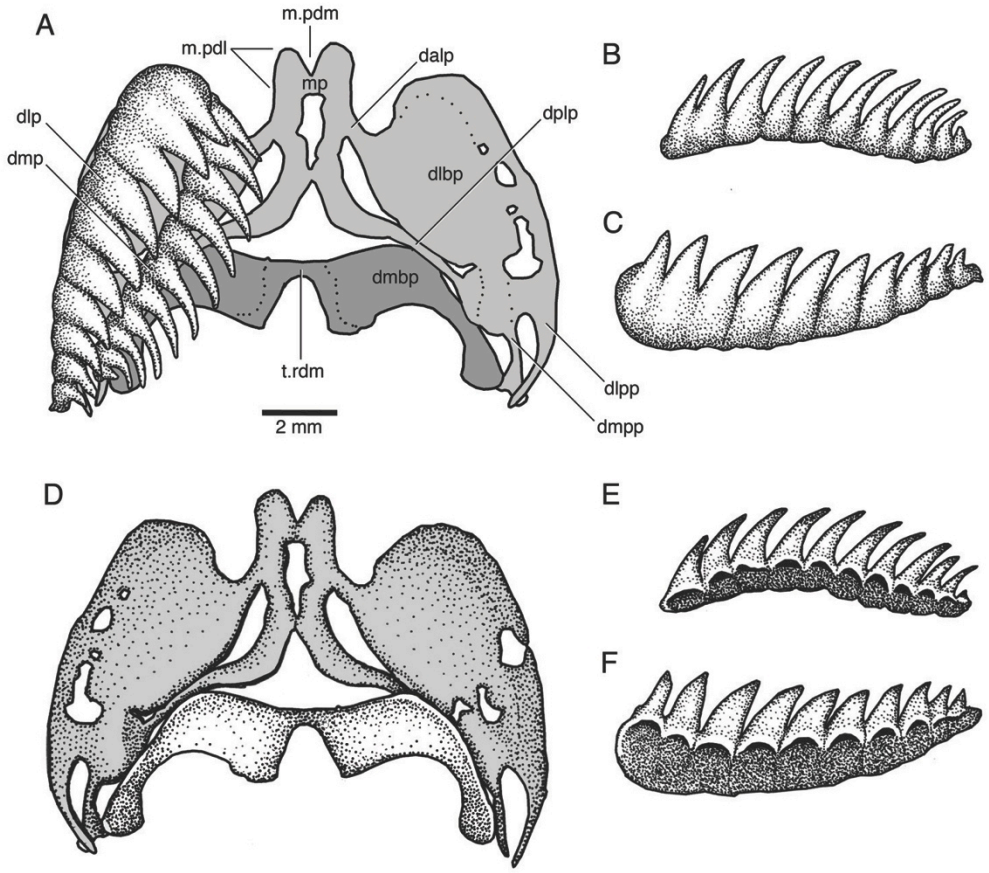
A
m.pdm
m.pdl
dalp
mp
dplp
dlp
dmp
dlbp
dmbp
t.rdm
2 mm
dlpp
dmpp
B
C
D
E
F

Figure 2-9.

Figure 2-10. The morphology of the lingual apparatus of *E. stoutii*. (A) The anterolateral, anteromedial, and middle lingual cartilages with the distal portions of the pharyngolingual arches in dorsal view. The right side of the apparatus is reconstructed with the anterolateral lingual cartilage nearly vertical anteriorly, a resting position in which the dental apparatus is retracted deep within the oral cavity. In contrast, the left side is illustrated in position during protraction of the dental apparatus when the plane of the anterolateral cartilage is oblique dorsolaterally. (B) The lateral tentacular cartilage, anterolateral, anteromedial, and middle lingual cartilages, and the dental apparatus in left lateral view, showing the perichondrium of the anterolateral lingual cartilage and the lateral tentacular cartilage (indicated by hatched lines). (C) Transverse histological section of the head of *E. stoutii* (position of the slice indicated in A) showing the anterior extension of the perichondrium of the posterior tentacular cartilage. The dental apparatus is anchored to this ridge (pcpl), and the tendon for m. retractor dentalis major (t.rdm) passes between the right and left ridges. (D) The posterior lingual cartilage (lcp) in lateral view, showing positions of the slices for G-J. (E, F) Transverse histological sections of the head of *E. stoutii* showing distal lingual cartilages, far posterior to the main lingual apparatus shown in this figure: (E) upper distal lingual cartilage (histologically identical to perichondrium, tendon, and ligament) and (F) lower distal lingual cartilage. (G-J) Transverse histological sections of the head of *E. stoutii* showing the change in the cross-section morphology of the cartilage longitudinally. Scales are uniform in G-J.

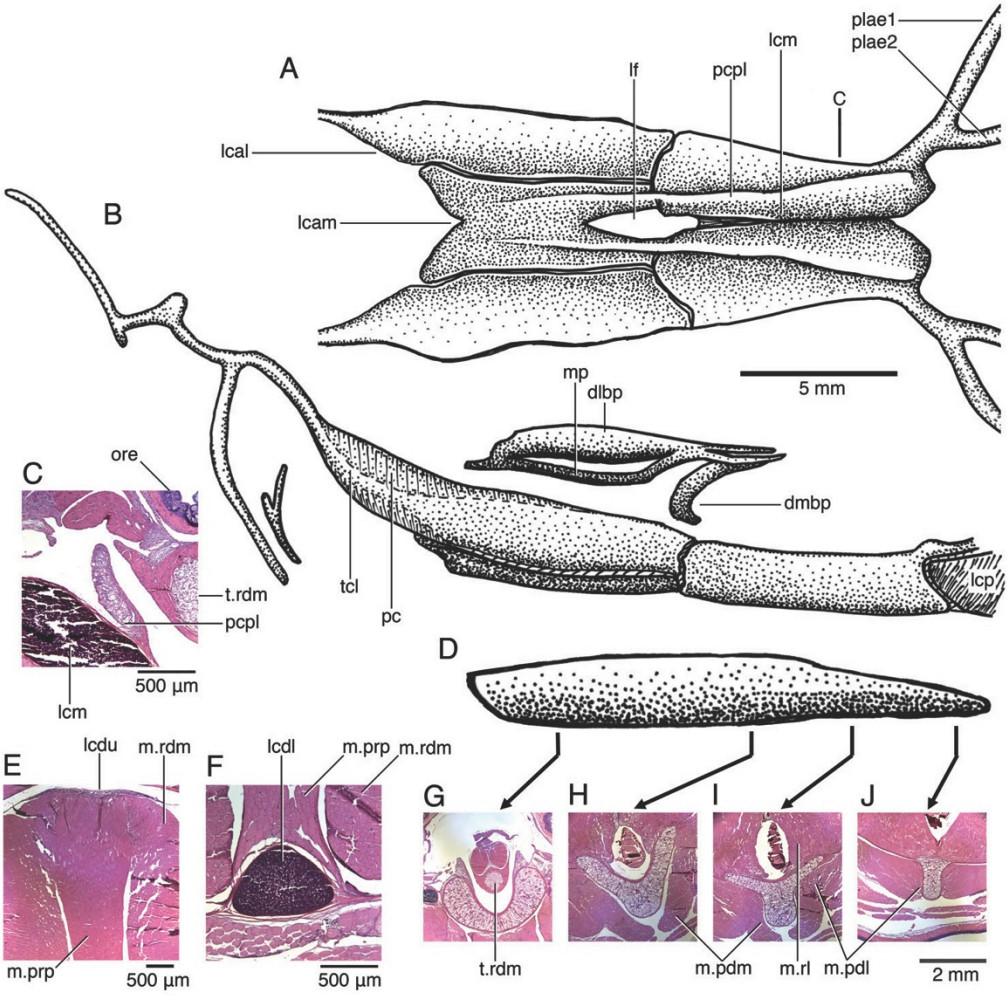
A
plae1
plae2
lcm
lf
pcpl
C
lcal
lcam
B
5 mm
mp
dlbp
dmbp
lcp
tcl
pc
C
ore
t.rdm
pcpl
500 µm
lcm
D
E
lcdu
m.rdm
m.prp
500 µm
F
lcdl
m.prp
m.rdm
500 µm
G
H
I
J
t.rdm
m.pdm
m.rl
m.pdl
2 mm

Figure 2-10.

Figure 2-11. The morphology of the extrabranchial cartilages of *E. stoutii*. (A) The extrabranchial cartilage (brxh) in left lateral view . (B) The extra-pharyngocutaneous cartilage in left lateral view, showing position and morphology of the cartilage on the pharyngocutaneous duct (phcd). (C) Transverse histological section of the branchial region of *E. stoutii*, showing the extrabranchial cartilage that supports the efferent branchial duct (brde). A and B redrawn after Ayers and Jackson (1901).

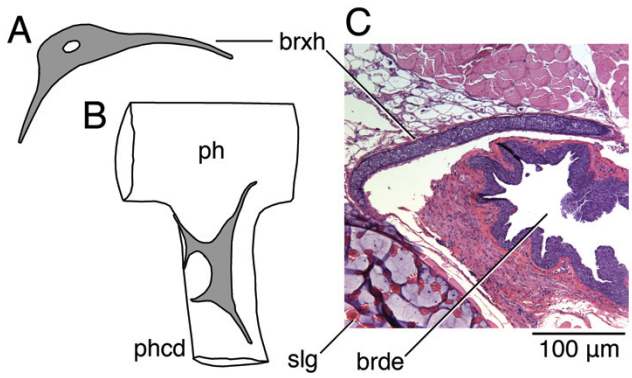

Figure 2-11.

Figure 2-12. Histology of the cartilages in *E. stoutii*. (A, B) The chondrocranium of *E. stoutii* in (A) left lateral and (B) dorsal views, color-coded according to the type of cartilage (red=Type 1a; blue=Type 1b; pink=intermediate of types 1a and 1b; green=type 2, pseudocartilage). Stippled area indicates where multiple types of cartilage co-exist. (C-H) Transverse histological sections of the major types of cartilage in *E. stoutii*: (C) Type 1a, hard cartilage; (D) Type 1b, soft cartilage; (E) Type 2, pseudocartilage, regular trabeculae; (F) Type 1a-1b intermediate; (G) perichondrium around Type 1b cartilage, showing histological characteristics of irregular Type 2 pseudocartilages; and (H) tendon for m. retractor dentalis major (m.rdm), showing nearly identical histological characteristics with Type 2 pseudocartilages. (I, J) Histology of the chondrocranium of *M. glutinosa* for comparison (modified after Cole 1905). The color codes are as in A and B. Description of each type of cartilages and pseudocartilages in main text. Location of the slices are labeled in A and B.

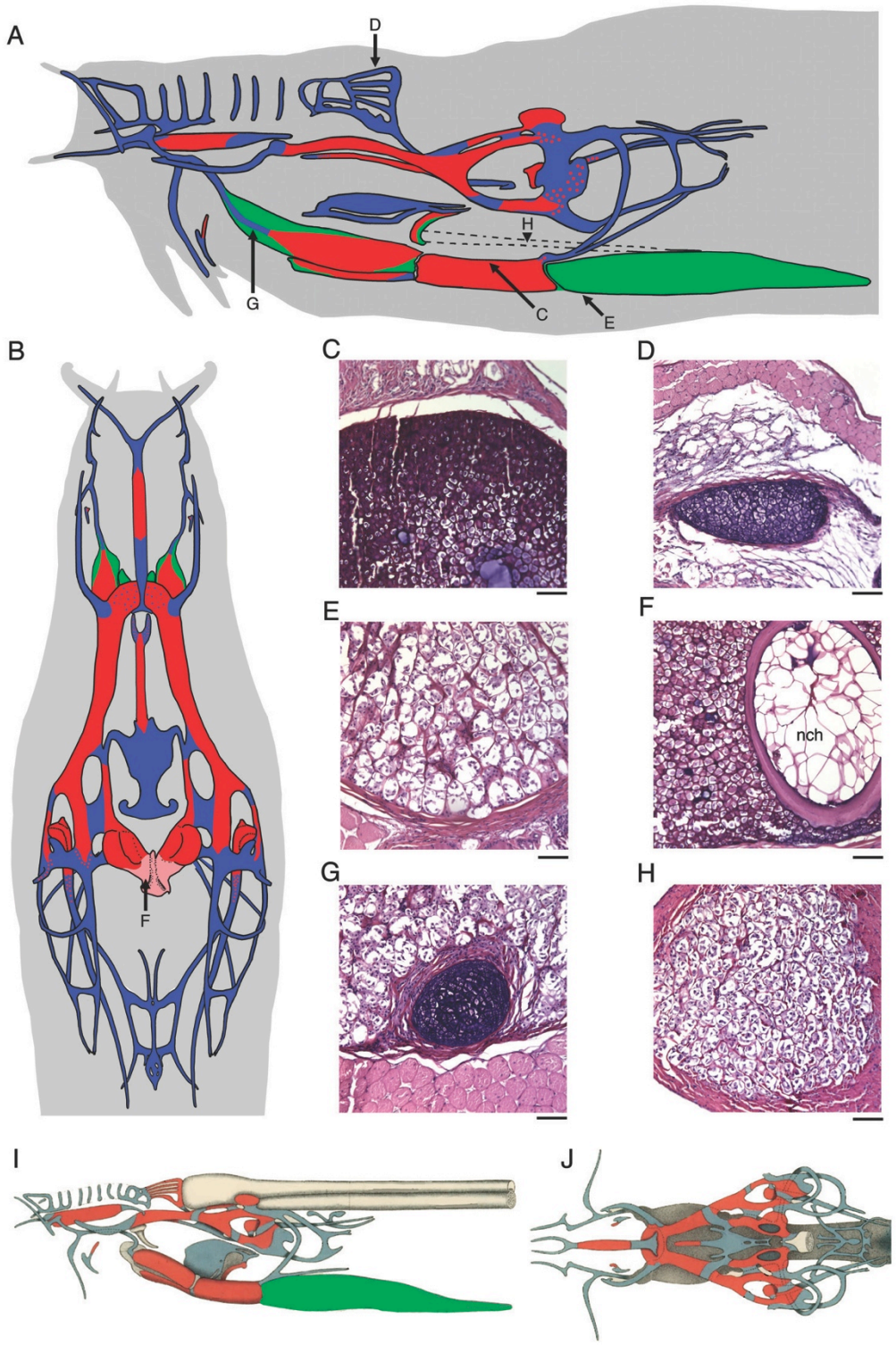

Figure 2-12.

Figure 2-13. Histology of the teeth of *E. stoutii* in a clockwise direction. (A-F) Transverse sections through the oral cavity of *E. stoutii*, showing: (A) the overall morphology of a tooth and its underlying periodontal tissues with labels indicating approximate location of each panel in the figure; (B) upper part of the pokal cone (pkcn) and epipokal epithelial layer (epke), with an active pokal cell (pkc, indicated by an arrow). The section is not close enough to the apex to show the pyramidal tissue; (C) interface between the inner epithelial layer and the upper part of the mesenchymal dental papilla (dp), with possible precursors of pokal cells (pkca, indicated by arrows); (D) interface between the inner epithelial layer and the lower part of the papilla with a proliferation zone (pz) of the pokal cone (pkcn) and documenting rapid differentiation of the epsinophilic mesenchyme into the papilla; (E) a fold of the outer epithelium with a transition zone that anchors the keratinous sheath (ks), and this is morphologically easily distinguished from the neighboring epipokal epithelial layer (epke); (F) keratinous sheath (ks) and the underlying epithelial layers.

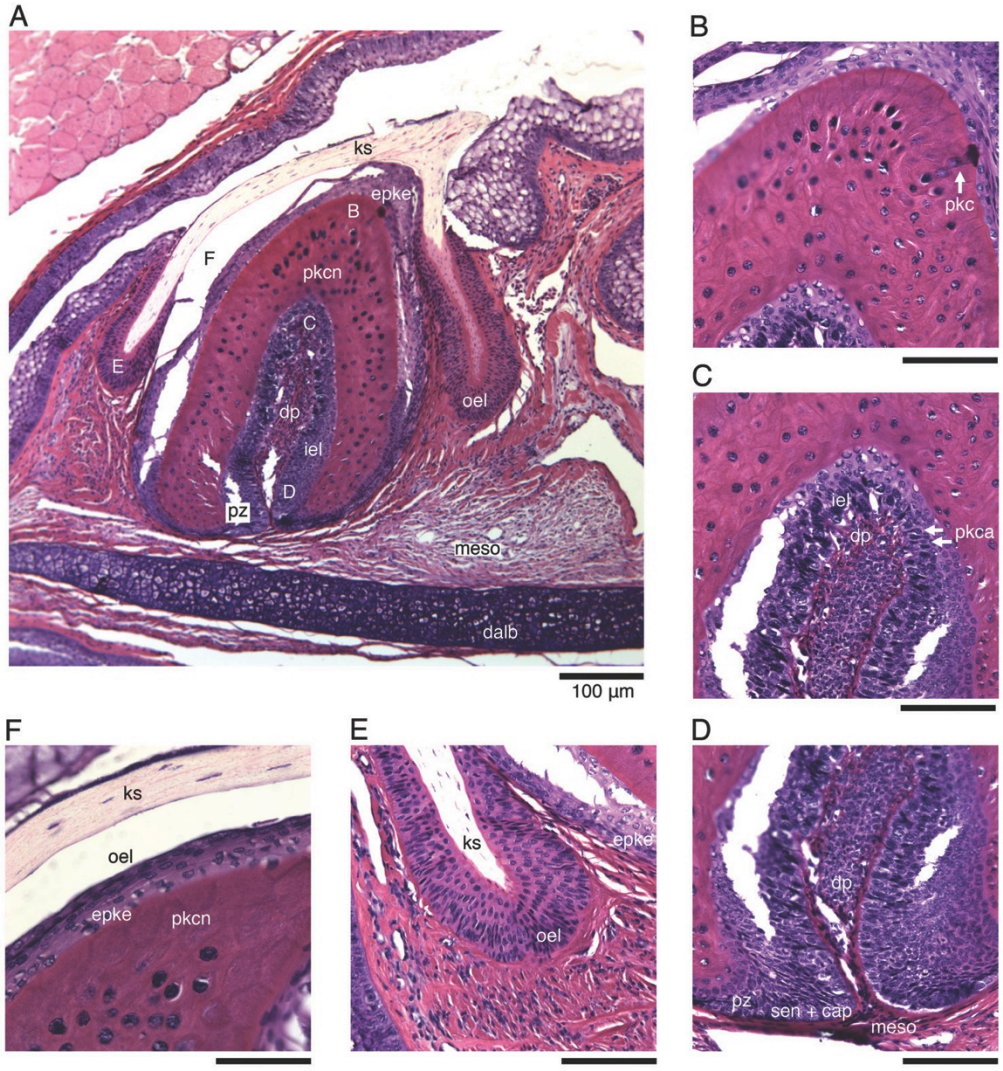
A
ks
epke
B
F
pkcn
C
E
oel
dp
iel
D
pz
meso
dalb
100 µm
B
pkc
C
iel
dp
pkca
F
ks
oel
epke
pkcn
E
ks
epke
oel
D
dp
pz
sen + cap
meso

Figure 2-13.

Figure 2-14. Homology of the vertebrate chondrocrania based on Table 2-1. Each homologue is color-coded but is not to be confused with the color codes in other figures. (A) Hagfish (*E. stoutii*) with (A_1) the chondrocranium in lateral view, (A_2) left half of the velar skeleton in dorsal view, (A_3) distal lingual cartilages in left lateral view, and (A_4) extrabranchial cartilage in left lateral view. (B) Lamprey with (B_1) the chondrocranium in lateral view, (B_2) lingual apparatus in lateral view, and (B_3) velar skeleton in dorsal view. (C) Gnathostome (*S. canicula*) with the chondrocranium in (C_1) lateral and (C_2) dorsal views. B redrawn and modified after Marinelli and Strenger (1954) and Johnels (1948); C redrawn and modified after de Beer (1937). Specimens not to scale. This is not comprehensive representation of the homologues. For details, see Table 2-1 and main text.

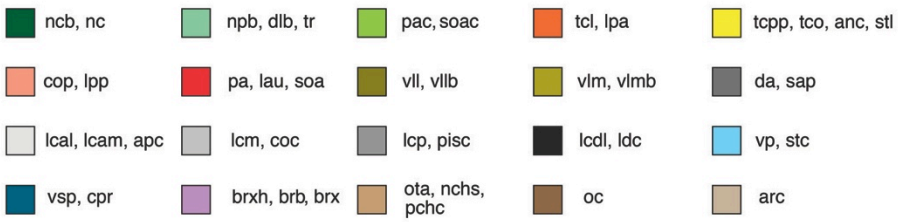

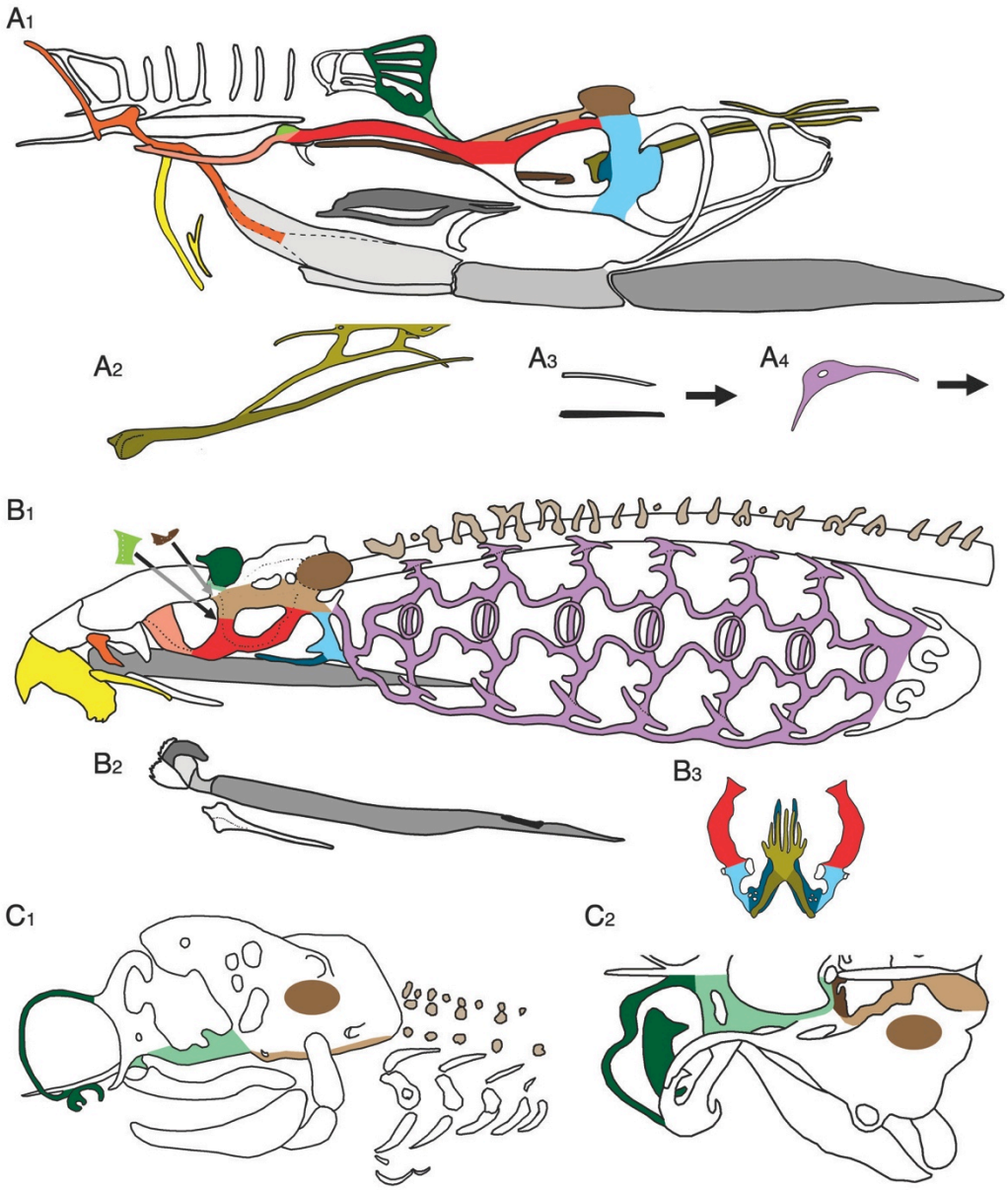

Figure 2-14.

Figure 2-15. The evidence for the cyclostome-like upper lip in stem gnathostomes. (A) The dorsal head shield of the osteostracan *Norselaspis* in ventral view. (B) The holotype of the osteostracan *Hirella* with oral plates preserved, in ventral view. (C) A silhouette of an osteostracan based on *Supercilliaspis* in left lateral view, showing the area for (D) the sagittal section of a generalized osteostracan with the oral plates and reconstructed muscle. Osteostracans show the muscle scar and foramina for the maxillomandibular trunk of the trigeminal nerve (V, VII) that must have innervated the muscle. The motor component in this region indicates that the mandibular domain of the osteostracan extended anteriorly with the mesodermally derived connective tissues and motor branches. See main text for details. A, B, and D either based on or modified after Janvier (2007).

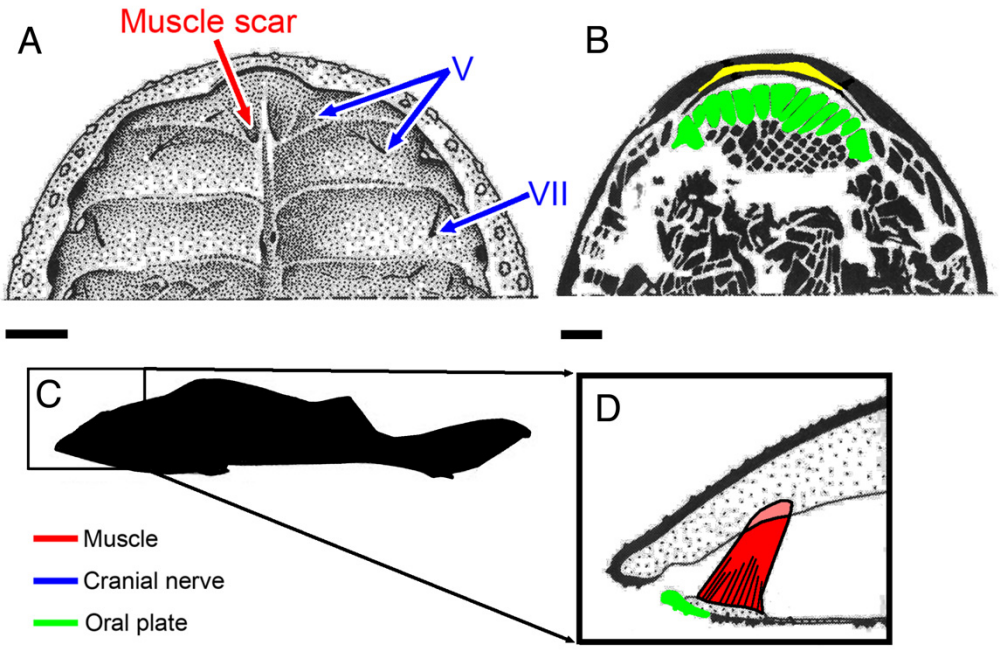

Figure 2-15.

Figure 2-16. Cyclostome-like feeding structures in vertebrates. (A-C) Conodont feeding mechanics as reconstructed by Goudemand et al. (2011): (A) *Ellisonia* in left lateral view; (B) *Hibbardella* in left lateral view; and (C) *Novispathodus* in left lateral view. (D) Sagittal section of the head of a tadpole of the anuran *Rana temporaria*, showing the feeding structure with keratinous teeth (tk, orange) in front of the anlagen for the jaw skeleton (mec). Cartilages are shaded in yellow; branchial structure in pink; gut in blue; dorsal nerve cord in dark blue (colour codes differ from those of A-C by Goudemand et al. 2011). A-C modified after Goudemande et al. (2011); B redrawn after Huxley (1876). Specimens not to scale.

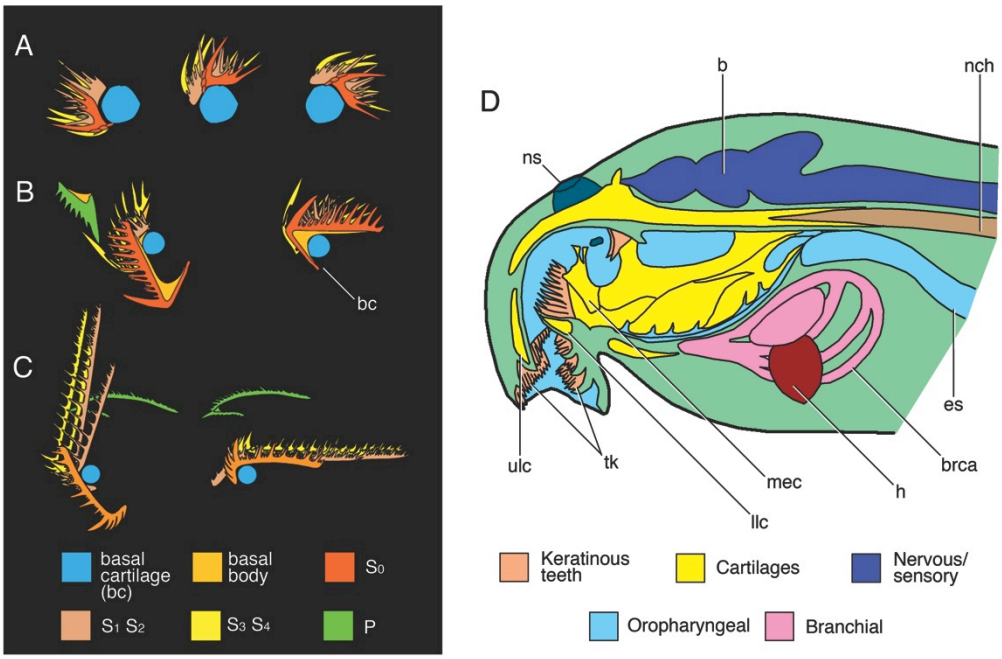
A
B
C
bc
basal cartilage (bc)
basal body
S0
S1 S2
S3 S4
P
D
b
nch
ns
es
ulc
tk
mec
h
brca
llc
Keratinous teeth
Cartilages
Nervous/ sensory
Oropharyngeal
Branchial

Figure 2-16.

Figure 2-17. Evolutionary scenario for the vertebrate chondrocrania in the context of deuterostome evolution. Characters related to the vertebrate chondrocranium are mapped onto the tree at each major node, except for those that vary among jawless vertebrates (listed and numbered on the right hand side). Question mark (?) indicates uncertain timing of origin. Blue line represents relationships according to paraphyly of cyclostomes, whereas red line depicts tree topology according to monophyly of cyclostomes. The interrelationships of jawless vertebrate lineages are based on the consensus summarized by Janvier (2007, 2008, 2010). Sketches for anaspids to osteostracans were redrawn after Forey (1995).

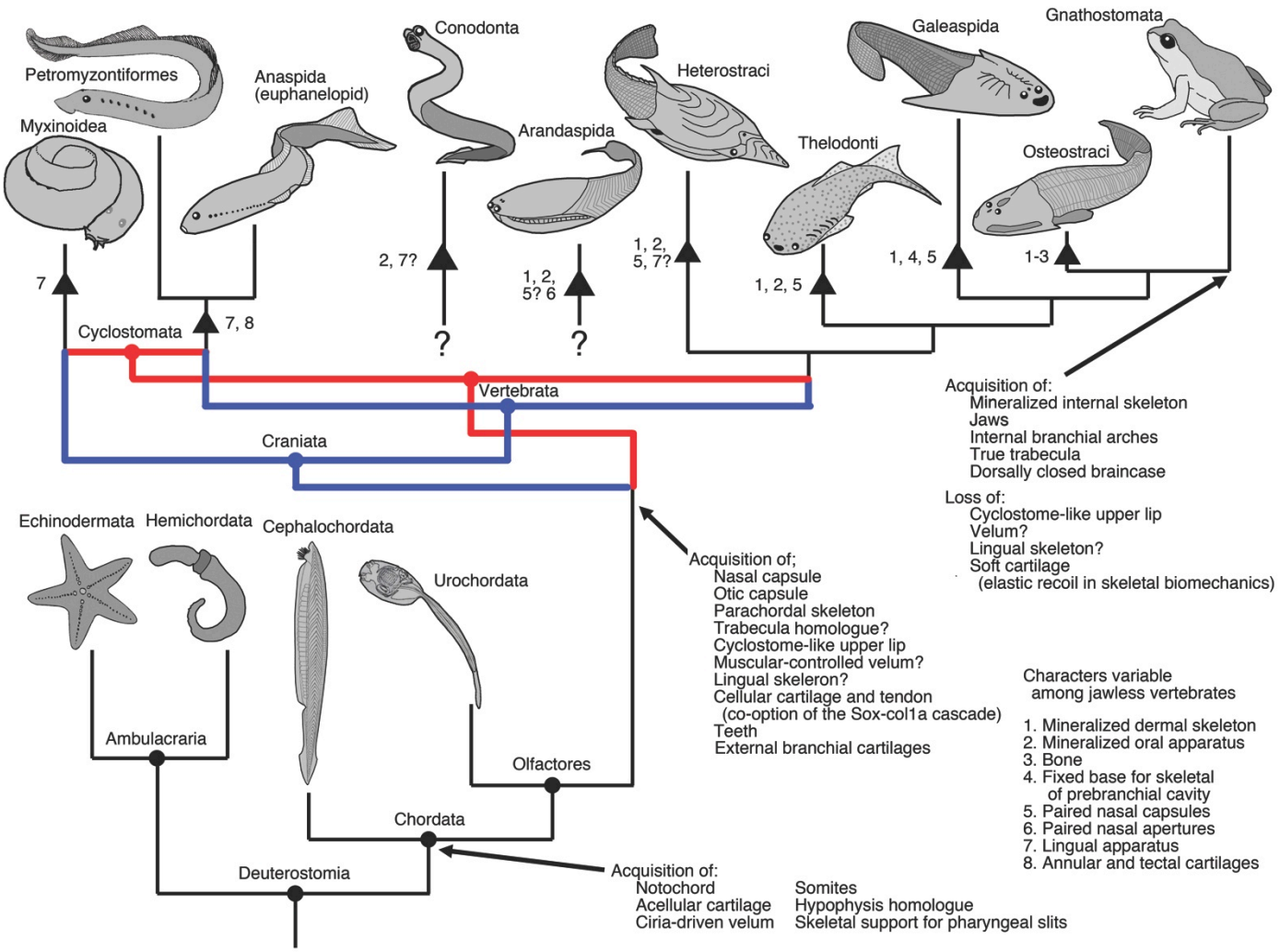
Petromyzontiformes
Myxinoidea
Anaspida
(euphanelopid)
Conodonta
Arandaspida
Heterostraci
Galeaspida
Thelodonti
Gnathostomata
Osteostraci
7
7, 8
Cyclostomata
2, 7?
?
1, 2,
5? 6
?
1, 2,
5, 7?
1, 2, 5
1, 4, 5
1-3
Vertebrata
Craniata
Acquisition of:
Mineralized internal skeleton
Jaws
Internal branchial arches
True trabecula
Dorsally closed braincase
Loss of:
Cyclostome-like upper lip
Velum?
Lingual skeleton?
Soft cartilage
(elastic recoil in skeletal biomechanics)
Echinodermata
Hemichordata
Cephalochordata
Urochordata
Acquisition of;
Nasal capsule
Otic capsule
Parachordal skeleton
Trabecula homologue?
Cyclostome-like upper lip
Muscular-controlled velum?
Lingual skeleron?
Cellular cartilage and tendon
(co-option of the Sox-col1a cascade)
Teeth
External branchial cartilages
Characters variable
among jawless vertebrates
1. Mineralized dermal skeleton
2. Mineralized oral apparatus
3. Bone
4. Fixed base for skeletal
of prebranchial cavity
5. Paired nasal capsules
6. Paired nasal apertures
7. Lingual apparatus
8. Annular and tectal cartilages
Ambulacraria
Olfactores
Chordata
Deuterostomia
Acquisition of:
Notochord
Acellular cartilage
Ciria-driven velum
Somites
Hypophysis homologue
Skeletal support for pharyngeal slits

Chapter 3 – The Cranial Musculature of the Northeastern Pacific Hagfish *Eptatretus stoutii* and Early Evolution of the Vertebrate Head

What have we here — a man or a fish? — dead or alive?
A fish: he smells like a fish; a very ancient and fish-like smell;
a kind of a not-of-the-newest Poor-John. A strange fish!
Were I in England now, as once I was, and had but this fish painted,
not a holiday-fool there but would give a piece of silver.

William Shakespeare (1610), The Tempest

3.1. INTRODUCTION

More than 250 years since the taxonomic description by Linnaeus (1758), the evolutionary relations between hagfish and 'true' vertebrates still remains contentious. Because of the phylogenetic uncertainty, hagfish have always been central to debates about vertebrate origins (Chapter 1; Janvier 1996, 2008 for brief reviews). Molecular and developmental evidence has recently weighed in on the issue, but it does not resolve the paradoxical morphology of hagfish, which shows a mosaic of primitive and unique characters. As with the chondrocranium (Chapter 2), it is extremely challenging to distinguish plesiomorphies and autapomorphies, partly because of long-branch length for living vertebrate lineages, and partly because of confusion between novel structures and potential homologues. Developmental evidence based on long-awaited hagfish embryos suggests that hagfish have neural crest development comparable to that in other vertebrates and axial skeletal elements that represent potential homologues of vertebrae (Ota et al. 2007, 2011). Even these similarities do not necessarily indicate that hagfish and lampreys are sister groups within vertebrates, because it is equally parsimonious to assume that these characters are symplesiomorphies or synapomorphies of vertebrates.

Solutions to this uncertainty may lie in the classic morphological approach that spawned research interest in the curious characters of hagfish (Müller 1834;

Parker 1893a; Ayers and Jackson 1901; Cole 1905, 1907, 1909; Marinelli and Strenger 1956). Indeed, enduring problems identified in these early works provide the main questions for recent molecular and developmental research on hagfish. The description of neural crest development in hagfish (Ota et al. 2007) directly tested an observation made 50 years prior that the hagfish neural crest may develop as an outpocket of the dorsal neural tube (Conel 1942). The identification of a potential vertebrate homologue (Ota et al. 2011) was built on classic anatomical descriptions of the element more than a century ago (Parker 1893a; Ayers and Jackson 1901). Two purposes of updating the classical morphological approach are 1) to facilitate comparison of characters across vertebrates and 2) to test the phylogenetic utility of these characters. Ideally, the most informative test would focus on a set of characters that tests the strength of an alternative phylogenetic hypothesis to the one favoured by traditional morphological characters.

The muscular system of hagfish is a promising area in this regard. Although morphological data tend to support cyclostome paraphyly (i.e. hagfish are the sister-group to vertebrates), similar configurations of the feeding musculature between hagfish and lampreys have been used as evidence for cyclostome monophyly (i.e. hagfish and lampreys form a clade; Yalden 1985; Kuratani and Ota 2008). If homologies could be established, the lack of typical vertebrate characteristics in hagfish could represent secondary loss rather than plesiomorphy. On the other hand, Mallatt (1994, 1996) identified a number of homologues in the oral and pharyngeal structures across chordates to support his scenario for the origin of the jaw as a step-wise sophistication of these structures toward enhanced ventilation. Although Ventilation Hypothesis by Mallatt (1996, 2008) does not propose novel phylogenetic relationships, the hypothetical origin of the jaw as a closing apparatus for enhanced ventilation depends on a large number of oropharyngeal homologues between cephalochordates, hagfish, lampreys, stem gnathostomes, and living gnathostomes. Consequently, the Ventilation Hypothesis predicts a series of gradual transitions. The hypothetical pre-gnathostome conditions closely follow those in lamprey ammocoetes, whereas the hypothetical vertebrate ancestor is assumed to resemble

cephalochordates (Mallatt 1996, 2008). This stepwise scenario contradicts developmental evidence that gene expression domains for the oropharyngeal structures drastically shifted their positions (Kuratani et al. 2001, 2004, 2005, 2012; Shigetani et al. 2002, 2005; Kuratani 2004a, b, 2005, 2012). This alternative view (the Heterotopic Theory) rejects the muscular and nervous homologues proposed by Mallatt (1996) and earlier authors he cited. Therefore, a test of the scheme of Mallatt (1984, 1996, 2008) is simultaneously a test of proposed evolutionary scenario for the origin of the jaw.

Particularly due to the half-century long hiatus in primary literature on the classical anatomy of hagfish, a detailed morphological description of the cranial musculature of hagfish is an urgent need. In this paper, the cranial muscles of hagfish are re-described. This updated morphological description forms a basis for assessment of similarity across vertebrates to evaluate the schemes by Yalden (1985) and Mallatt (1996). This analysis eventually tests the bearing of cranial musculature on the phylogenetic relations of vertebrates and on evolutionary scenarios for the origins of vertebrates and gnathostomes.

3.2. MATERIALS AND METHODS

More than a hundred adult specimens of northeastern Pacific hagfish (*Eptatretus stoutii*) were trapped from approximately 80 m deep in Barkley Sound, British Columbia, Canada (latitude: N 48° 84’ 96.37”; longitude: W 125° 13’ 18.01”) and held in running seawater aquaria at the Bamfield Marin Sciences Centre, Bamfield, British Columbia from May 2010 to November 2011. Among these adults, a total of 16 euthanized individuals of varying sizes (body lengths between 250 and 450 mm) were dissected to study the musculature. One additional specimen (body length of approx. 320 mm) underwent paraffin sectioning. Two to four of every fifty 7.5 μm sections were retained and stained with eosin and hematoxylin. Histological sections and functional analysis supplemented the gross morphology of the muscles. Functions were determined by observation of behaviours in captivity, manual

excitation of the nerves in freshly euthanized specimens with metal tweezers charged with static electricity, and manipulation of muscles along the orientation of fibres during dissection. An analysis of similarity is based on comparison of the muscular morphology of hagfish (Figures 3-1 and 3-4 through 3-10) with those of lampreys and gnathostomes (Figures 3-2 through 3-4).

The previous terminology of muscles by Cole (1907) and Marinelli and Strenger (1956) was extensively revised for several reasons. The terminology of Cole (1907) is intuitive in the context of functions (e.g., m. copulo-copularis) or of general position in the head (m. nasalis), but his terminology assumes similarity with the generalized gnathostome head, including terms such as m. quadrato-palatinus and m. palato-ethmoidalis. Hagfish do not have any skull elements that are equivalent to the palatine, quadrate, or ethmoid. Nor is it clear whether or not any part of the pharyngolingual skeleton derives from the hyoid arch. Functions are sometimes misleading in identification of muscles, partly because they may have multiple different functions and partly because many muscles overlap in directions of motion. The same problem persists in the terminology of Marinelli and Strenger (1956) to a lesser extent. For example, their term “basilis” is used in reference to the lingual skeleton, but this is confusing with the usage of basilar in mammals. In light of the revised description of cartilages (Chapter 2), a new terminology for muscles is needed that reflects both conventional usage in literature and accurate anatomical positions without excessive assumption of function or homology. The traditional terminology is used for some of muscles if it is either currently in use in literature (e.g.,. m. parietalis) or still suitable for general description of the muscles (e.g.,. m. nasalis). Two exceptions are the terms lingual and dental. Neither the lingual nor the dental apparatus in hagfish are exact homologues of the functionally corresponding parts in gnathostomes (Chapter 2). These two terms are used in reference to function, partly because they are widely used in the hagfish literature, partly because they do accurately refer to function, and partly because there is simply no better way to describe them. Gnathostome tongue muscles are usually referred to with “glossus” rather than with “lingualis,” and this justifies the use of lingualis. Other muscles were

renamed based on more generic terms to describe positions within the head (e.g., palatal instead of palatine) and supplemented with major functions in special cases (e.g.,. m. retractor lingualis medialis). When two regions are used to describe a muscle (e.g., m. palatolingualis superficialis), the site of origin precedes the site of insertion as a general rule. The ventral somatic m. obliquus might potentially be confused with several extraocular muscles in other vertebrates (e.g., m. obliquus anterior). But, the traditional usage of m. obliquus is retained, because m. obliquus has been used consistently in literature, and because hagfish have no extraocular muscles.

3.3. DESCRIPTION

The description proceeds from superficial muscles to deep muscles and then from anterior to posterior within major anatomical and functional groups ordered in the following manner: 1) somatic muscles that extend into the head; 2) superficial facial muscles over the nasal tube; 3) muscles that suspend the lingual apparatus; 4) deep muscles in the subnasal, preoral, and facial regions; 5) muscles of the velar skeleton; 6) muscles of the lingual apparatus; and 7) branchial muscles. These groups, although convenient, are not always distinct from each other and many muscles overlap in function or anatomical region (e.g., m. nasolingualis, which may be classified to both 3 and 4). For these muscles, the order of description among other muscles is arbitrary.

The integument is anchored to the orbit by two bands of ligaments. The posterior band originates from the posteroventral margin of the orbit and inserts into the posterior margin of the integumentary eyespot. The anterior band originates from the anterior corner of the orbit and inserts to the anterior margin of the integumentary eyespot. The fascia membrane along the dorsal midline anchors the integument to m. parietalis. The perinasal ligaments tightly attach the integument around the nasohypophyseal aperture and the facial region anterior to the mouth.

3.3.1. Somatic Muscles

3.3.1.1. M. obliquus (m.ob; Figures 3-1A, 3-5, 3-8 C-E)

Origin: fascia over the lateral surface of m. parietalis (above the level of the slime pores).

Insertion: fascia of the bilateral counterpart; integument (ventrally).

Nerve innervation: spinal nerve.

Functions: suspension of ventral part of body from m. parietalis; anchoring the ventral part of the integument.

Notes: M. obliquus is a somatic muscle that occurs all along the postcranial body and extends anteriorly into the cranial region. This sheet of ventral superficial muscle connects the right and left m. parietalis ventrally. As the name suggests, the muscle fibres are oriented anteroventrally. The segments meet with their bilateral counterparts in an interdigitated fashion along the ventral midline and extends anteriorly as far as the first external pharyngolingual arch. Anterior to this point, m. obliquus inserts into the integument lateroventrally. In both the cranial and postcranial regions, the level of origin for this muscle is above the row of slime glands. The cranial portion of m. obliquus expands in surface area in lateral view and overlaps the facial segment of m. parietalis (Figure 3-5A).

M. obliquus is tightly attached to the integument in the postcranial region, but the attachment is relatively looser in the cranial region to the extent that tweezers can separate the integument and the muscle. It does not spread anteriorly beyond the anterior border of m. parietalis. M. obliquus is thinner than m. parietalis and is segmented, but not in the same myotomal fashion as in m. parietalis. M. obliquus has no attachment with any of the facial muscles except for m. rectus and m. retractor lingualis at the midline via weak fascia.

3.3.1.2. M. parietalis (m.pa; Figures 3-1A, 3-5, 3-8 B-E, 3-10A)

Origin: neighbouring segments within this muscle and spinal membrane (all segments); bilateral counterpart (all but facial segments); membrane of notochord; perioptic membrane (facial, first, and second segments); membrane over m. palatolingualis superficialis (facial segment); lateral surface of dorsal longitudinal arch of facial skeleton (second and third segments); lateral surface of otic capsule (fourth segment); membranes for brain and spinal chord above skull (first to sixth segments).

Insertion: neighbouring segments of the same muscle (all segments); membrane over lateral side of the dental protractors (facial to fourth segments); dorsal surface of the slime glands (segments after the fourth).

Nerve innervation: spinal nerve.

Function: undulation or bending of body axis.

Notes: M. parietalis is a somatic muscle that migrates anteriorly into the cranial region to form the lateral superficial muscle of the head. The facial segment is the most anterior and thinnest of m. parietalis, restricted ventrally, and overlapped laterally by m. obliquus. All remaining segments of m. parietalis are numbered along the dorsal midline from the head to the tail. In dorsal view, the first and second segments of m. parietalis split into a bilateral pair between the eyes, departing from the sagittal plane. The first segment extends onto the nasal capsule basket, but is separated dorsally from the facial segment by the eye. The second segment is the first complete segment of m. parietalis. It wraps around the eye posterodorsally, spreads ventrally to insert into m. obliquus and the integument, and connects the facial segment with the rest of m. parietalis posteriorly.

The segments posterior to the second segment reach the top of the head to meet with their counterparts behind the eye. The third segment is strongly attached to the lateral surface of the facial skeleton; in effect, this segment laterally and dorsally overlaps the trigeminal and facial nerves as they extend out from the spinal membrane laterally and pass through the

fenestrae ventrally. The fourth segment is attached to the lateral surface of the otic capsule. The second to sixth segments are attached to the lateral surface of the spinal membrane. In lateral view, the segments posterior to the facial and first segments have gentle sinuous outlines as in all other euchordates. A series of slime glands develops along the body in a segmented fashion, starting in the fourth segment. M. parietalis inserts onto the slime glands ventrally. Each segment is innervated by independent spinal nerves in the dorsal part near the midline. M. parietalis of a hagfish lacks the horizontal myoseptum that marks the division of the epaxial and hypaxial muscles in gnathostomes. A band of ligaments for m. parietalis originates to the integument within the midline membrane above the fourth and fifth segments.

3.3.1.3. M. rectus (m.re; Figures 3-5A, E-G, 3-6A, 3-8E)

Origin: ventromedial surfaces of slime glands.

Insertion: ventral surface of perichondrium of the middle lingual cartilage, medial to the first external pharyngolingual arch.

Nerve innervation: spinal nerve.

Function: posterior retraction of the lingual apparatus as the dental apparatus is protracted and everted; ejection of slime.

Notes: M. rectus is the third, and smallest somatic muscle in the cranial region. For most of the body length, the longitudinal bundle of the muscle is set deeper than the more superficial slime glands and m. obliquus. Anteriorly beyond the first slime gland, the muscle becomes narrow and devoid of myomeres and passes between m. protractor dentalis lateralis and m. protractor dentalis medialis. Contraction of m. rectus in the somatic region squeezes out slime stored in the glands.

3.3.2. Superficial Facial Muscles

3.3.2.1. M. tentacularis posterior (m.tp; Figures 3-1A, 3-5 A-D, 3-6A, B, 3-7 B-D)

Origin: perioptic membrane (anterior to the eye).

Insertion: perichondria of the upper nasohypophyseal process of the lateral tentacular cartilage, the lateral tip of the oral tentacular cartilage, and the lateral side of the perioral tentacular cartilage; and the integument around these barbels.

Nerve innervation: trigeminal nerve, anterior branch (V_{2a}).

Functions: dorsal extension of upper nasohypophyseal barbel; anterior extension of perioral and oral barbels; suspension of lateral lingual muscles in facial region (m. palatolingualis superficialis; m. palatolingualis profundus).

Notes: M. tentacularis posterior is the most superficial of the muscles that originate in the head of hagfish. The muscle originates in front of the eye and extends anteriorly lateral to the nasal capsule basket in a longitudinal bundle, from the ventral edge of which m. palatolingualis superficialis and m. palatolingualis profundus originate. In particular, m. palatolingualis produndus forms a vertically continuous muscular sheet with m. tentacularis posterior, and distinction between the two muscles is difficult to see at the level of gross dissection but can be identified in a thin myoseptum between closely packed bundles of myofibres in histological section. The muscle fibres of m. tentacularis posterior are oriented vertically to obliquely in the dorsal part and longitudinally in the ventral part, fulfilling two functions of this muscle. The bundle of the muscle spreads into a sheet over the cornual process and inserts to the cartilages of the perioral and upper nasohypophyseal barbels and the integument around the barbels. For most of its length, m. tentacularis posterior covers m. subnasalis superficialis laterally, but the attachment between the two muscles via fascia is restricted to the part posterior to the cornual process.

3.3.2.2. M. nasalis (m.na; Figures 3-1A, 3-5 A-D, 3-6A, 3-7 B-D, 3-10A)

Origin: perioptic membrane; membrane over the lower longitudinal bar and anterior transverse arch of nasal capsule basket and the last two nasal arches.

Insertion: dorsolateral and lateral surface of the membrane over the nasal tube, as anterior as the second nasal arch; two tendons to the paranasal tuber and the paranasal rod.

Nerve innervation: trigeminal nerve, anterior branch (V_{2a}).

Functions: suspension of the lateral tentacular cartilage; anterior extension of the perioral barbel; maintenance of an open passage in the anterior region of nasal tube; anteroposterior contraction of the nasal tube during "sneezing"; anchoring m. tentacularis posterior.

Notes: M. nasalis is a simple longitudinal muscle along the nasal tube. M. nasalis broadly inserts over the nasal membrane and extends as far anteriorly as the second nasal arch. The ventral surface of m. nasalis is tightly attached to the underlying m. subnasalis superficialis via ligaments and myoseptum. In the region of closest proximity between the lateral tentacular cartilage and the nasal tube, m. nasalis extends two tendons, one each to the paranasal rod and the paranasal tuber. The first tendon originates at the level of the second nasal arch, whereas the second tendon inserts at the level of the fourth nasal arch. The connections between the nasal tube and the nasohypophyseal tentacular cartilage also include a bundle of ligaments that inserts onto the first annular arch, but this is not a part of m. nasalis. These connections with the nasal tube elevate the cartilage above the subnasal bar and m. subnasalis superficialis, both of which pass anteriorly beneath these connections.

3.3.3. Suspension of Lingual Apparatus

3.3.3.1. M. palatolingualis superficialis (m.pls; Figure 3-1A, 3-5 C-E, 3-6A, 3-8C, 3-10A, B)

Origin: fascia over the lateroventral surface of m. tentacularis posterior, over the lateral surface of m. palatolingualis profundus, and at the ventral edges of m. craniolingualis; perioptic membrane.

Insertion: fascia at the dorsal edge of the most posterior portion of m. cornual lingualis; perichondria between the anteromedial and anterolateral lingual

cartilages on the ventral side, ventral surface of the middle lingual cartilage close to the midline, and the lateral surface of the first external pharyngolingual arch near the junction with the middle lingual cartilage.

Nerve innervation: facial nerve (VII).

Functions: suspension of the lingual apparatus; anterior protraction of the lingual apparatus as the dental apparatus is retracted posteriorly; antagonist to m. craniolingualis, m. palatolingualis profundus, and m. retractor lingualis.

Notes: M. palatolingualis superficialis is the superficial layer of the muscular lateral wall of the buccal cavity that hangs the lingual apparatus. Among all the muscles involved in suspension of the lingual apparatus, this muscle has the most extensive attachment with the lingual cartilages and also is unique in that the suspension is against a group of facial muscles rather than against cartilages or the somatic body wall. Consequently, m. palatolingualis superficialis has complex relationships with the surrounding muscles. The fibres of m. palatolingualis superficialis are mostly longitudinally oblique in an anterodorsal direction, and the vertically oriented fibres are restricted to the anterodorsal portion. As such, the contraction of this muscle results in anterodorsal protraction of the lingual apparatus, a motion necessary to accompany retraction of the dental apparatus during feeding.

3.3.3.2. M. craniolingualis (m.cl; Figures 3-5E, 3-6A, 3-8B, D, 3-10A)

Origin: perichondria of the lateral surface of the dorsal longitudinal arch posterior to the interfenestral strut, and dorsal margin of the first pharyngolingual fenestra as posterior as the base of the first external pharyngolingual arch; fascia over the lateral surface of m. palatolingualis profundus (lateral to ventral longitudinal arch) and over the medial surface of m. parietalis (sixth segment).

Insertion: membranes at the dorsal edge of m. palatolingualis superficialis and the laterodorsal edge of m. protractor dentalis lateralis.

Nerve innervation: facial nerve, hyomandibular branch (VII).

Function: suspension of the lingual apparatus; posterior retraction of the lingual apparatus as the mouth opens and as the dental apparatus is protracted anteriorly; and antagonist for m. protractor dentalis lateralis, m. cornual lingualis, m. palatolingualis superficialis.

Notes: M. craniolingualis is at the same superficial level with m. palatolingualis superficialis, which makes it the most superficial cranial muscle in the post-hyoid part of the head, but it functions to pull the lingual apparatus in a posterior direction in opposition to that of m. palatolingualis superficialis. The muscle has a broad attachment along the dorsal longitudinal elements of the facial and pharyngolingual skeletons and overlaps broadly over the lateral surface of the head. The muscle inserts onto other muscles rather than cartilages, and the targets of the insertion are both protractors, indicating an important function of m. craniolingualis as an antagonist for the muscles that cause anterior sliding of the lingual apparatus. M. craniolingualis is unique among cranial muscles in having the site of origin at the medial surface of m. parietalis. In *M. glutinosa*, m. craniolingualis appears to attach neither to the dorsal longitudinal arch nor to the dorsal rim of the first pharyngolingual fenestra (Cole 1907; Marinelli and Strenger 1956), and this difference in attachment is possibly a taxonomically informative character.

3.3.3.3. M. cornual lingualis (m.coi; Figures 3-1A, B, 3-5C, 3-6A, B, 3-10A, B)

Origin: perichondrium of the lateral surface of the posterior, transverse portion of the cornual process.

Insertion: ventral surface of the perichondria for the anterior portions of the anteromedial and anterolateral lingual cartilages.

Nerve innervation: trigeminal nerve, anterior branch (V_{2a}).

Functions: suspension of the anterior and middle lingual cartilages from the cornual process; anterior protraction of the lingual apparatus as the dental apparatus is retracted; antagonist for m. palatolingualis profundus and m. craniolingualis.

Notes: M. cornual lingualis is robust enough to bulge laterally when the laterally overlapping m. parietalis and m. obliquus are removed. The site of origin for this muscle is in the transverse portion of the cornual process, just posterior to that of m. cornual labialis. The muscle extends posterodorsally to overlap the anterior portion of the lingual apparatus, sends a tongue of muscle beneath the apparatus, and inserts to the perichondrium at the ventral surface of the anteromedial and anterolateral lingual cartilages, medial to m. palatolingualis superficialis and on the opposite side of the cartilage from the site of insertion of m. palatolingualis profundus. M. cornual lingualis is at the same parasagittal plane with, and therefore is a direct antagonist of, the latter muscle.

3.3.3.4. M. palatolingualis profundus (m.plp; Figures 3-1B, 3-5 C-E, 3-6B, 3-8B, C, D, 3-10A, B)

Origin: fascia along the ventral edge of m. tentacularis posterior and the dorsolateral surface of m. palatocoronarius; perioptic membrane; perichondrium over the lateroventral surface of the palatal arch and ventral longitudinal arch.

Insertion: perichondrium of the ventral surfaces of the posterior half of the anterolateral lingual cartilage and of the anterior half of the middle lingual cartilages along the lateral edges.

Nerve innervation: trigeminal nerve, anterior branch (V_{2a}).

Functions: suspension of the lingual apparatus; posterior retraction of the lingual apparatus as the mouth opens and as the dental apparatus is protracted; antagonist for m. cornual lingualis and m. palatolingualis superficialis.

Notes: M. palatolingualis superficialis et profundus form a muscular lateral wall of the buccal cavity that suspends the lingual apparatus. Among all the muscles involved in suspension of the lingual apparatus, these two muscles have the most extensive attachment with the lingual cartilages and also are unique in that they suspend the apparatus against a group of facial muscles rather than against cartilages, with an exception of the palatal arch. Consequently, m.

palatolingualis superficialis et profundus both have complex relationships with the surrounding muscles. M. tentacularis posterior has the longest contact anteroposteriorly among the muscles to which m. palatolingualis profundus attaches, and this coincides with the thickest portion of both m. palatolingualis superficialis et profundus. The fibres of m. palatolingualis superficialis et profundus are mostly longitudinally oblique in an anteroventral direction; the vertically oriented fibres are in the anterodorsal portion of m. palatolingualis superficialis and in the anteroventral portion of m. palatoligualis profundus. As such, the contraction of these muscles results in posterodorsal retraction of the lingual apparatus, a motion necessary to accompany protraction of the dental apparatus during feeding. The anterior branch of the maxillomandibular trigeminal nerve extends between m. palatolingualis profundus and m. palatocoronarius.

3.3.3.5. M. otic lingualis (m.ol; Figures 3-1B, 3-6B, 3-8B, 3-10A, B)

Origin: perichondrium of the posterior surface of the otic capsule.

Insertion: perichondrium of the distal portion of the first external pharyngolingual arch.

Nerve innervation: facial nerve (VII).

Function: suspension of the first external pharyngeal arch and the lingual apparatus; antagonist for m. constrictor pharyngis pars anterior.

Notes: M. otic lingualis is vertically the tallest of the muscles that suspend the lingual apparatus. The muscle originates from the back of the otic capsule, passes medially with respect to the dorsal rim of the first pharyngolingual fenestra and through that fenestra to the lateral side to insert onto the first external pharyngolingual arch. In this region, the muscle laterally overlaps the facial nerve. In the area of insertion, m. otic lingualis is tightly associated with m. palatolingualis superficialis and m. retractor dentalis lateralis by fascia where the margins coincide with each other. On the opposite side of the arch, m.

constrictor pharyngis pars anterior inserts onto the posterior surface as an antagonist for m. otic lingualis.

3.3.3.6. M. constrictor pharyngis (m.cp; Figures 3-1B, 3-5F, 3-6A, 3-8B, E, 3-10A, B)

Origin: membrane over the ventral surface of m. parietalis lateral to the notochord.

Insertion: perichondrium of the posterior surface of the first external pharyngolingual arch (pars anterior); perichondrium of the dorsal edge of the posterior lingual cartilage and fascia over the laterodorsal corner of m. retractor lingualis (pars posterior).

Nerve innervation: glossopharyngeal nerve (IX) for pars anterior; vagus nerve (X) for pars posterior.

Functions: suspension of the lingual apparatus (pars anterior and pars posterior); antagonist for m. otic lingualis (pars anterior); circulation of the coelomic cavity (pars posterior).

Notes: M. constrictor pharyngis is a longitudinally extensive muscular sheet external to the digestive tract and internal to the somatic body wall, and at the same parasagittal plane as m. otic lingualis. The site of origin is consistently at the ventral surface of m. parietalis along the notochord. In lateral view, the anterior margin of m. constrictor pharyngis wraps around the transversely widest portion of the pharynx from behind and extends anteriorly under and just lateral to the bulge of the pharynx to insert onto the posterior surface of the first external pharyngolingual arch. This is the domain of m. constrictor pharyngis pars anterior. Pars anterior is distinct from pars posterior in the glossopharyngeal innervation and in being more robust than pars posterior. The site of insertion for pars anterior makes this muscle an antagonist of m. otic lingualis, the contraction of which would pull the first external pharyngeal arch anteriorly as well as dorsally. The motion of m. constrictor pharyngis pars anterior is in the opposite direction. Posterior to that point, the site of insertion for m. constrictor pharyngis pars posterior is along the dorsal

edge of the posterior lingual cartilage and the lateral surface of the retractor of that cartilage.

M. constrictor pharyngis pars posterior develops within the mucosa on the inner side of the somatic lateral body wall. The mucosa contains the muscle, dorsal arteries, anterior cardinal veins, and vagus nerve. Circulation within the tissue is at least partly open because red blood cells are scattered outside the vessels. Within this tissue, the thin sheet of m. constrictor pharyngis pars posterior is divided into five or more anteroventrally-oriented bundles between the eighth and fourteenth slime glands. In this posterior-most region, the volume of the muscle is too small to suspend the lingual apparatus from the somatic body wall by itself. Instead, contraction of the muscle likely controls the pressure in the cavity between the mesodermally derived lateral body wall and digestive tract through which the major vessels pass.

3.3.4. Preoral, Subnasal, and Deep Muscles

3.3.4.1. M. cornual labialis (m.coa; Figures 3-1A, B, 3-6A, B, 3-7C, D, 3-10A)

Origin: perichondrium of the lateral surface of the cornual process (anterior, longitudinal portion).

Insertion: fascia over the lateral surface of m. lingual tentacularis pars labialis; labial integument.

Nerve innervation: trigeminal nerve, anterior branch (V_{2a}).

Functions: suspension of the labial integument; opening passage of the dental apparatus transversely; opening the mouth transversely; and extension of oral barbel.

Note: M. cornual lingualis originates as the anterior of the two muscles that originate from the cornual process. Rather than suspending the lingual apparatus as its posterior neighbour, the muscle is responsible for the passage of the dental apparatus through the mouth. The mouth of hagfish is a longitudinal slit covered bilaterally by the folded oral barbels. M. cornual labialis inserts onto

m. lingual tentacularis and the labial integument from laterally so that its contraction opens the slit transversely and unfolds the oral barbels laterally.

3.3.4.2. M. lingual tentacularis (m.lt; Figures 3-1C, 3-6C, 3-7, 3-10 A-C)

Origin: ventral surface of the perichondrium covering the anterior segment of the lingual cartilage between the anteromedial and anterolateral plates, posteromedial to the origin of m. nasolingualis.

Insertion: perichondrium covering the proximal portion of the oral tentacular cartilage (pars oralis); posterior and dorsal surfaces of perichondrium of the perioral tentacular process and labial ramus of the lateral tentacular cartilage at the base of the process (pars perioralis); perichondrium covering the paranasal rod and upper nasohypophyseal process (pars lateralis); and membrane covering the lateroventral surface of m. nasolingualis and the perichondrium covering the ventral surface of the terminal process of the subnasal cartilage (pars medialis).

Nerve innervation: trigeminal nerve, anterior branch (V_{2a}).

Functions: anterior extension of the oral and perioral barbels (pars oralis and perioralis); anterior flexion of the upper nasohypophyseal barbel (pars lateralis); lateral extension of the lower nasohypophyseal barbel (pars medialis); antagonist for posterior retraction of the lingual apparatus.

Notes: M. lingual tentacularis is one of the smallest muscles that originate from the lingual cartilages, and yet it connects to all cartilages that support the barbels. As such, the muscle has complex topographical relationships with the surrounding musculoskeletal elements. M. lingual tentacularis pars oralis passes below m. nasolingualis and inserts to the medial surface of the oral tentacular cartilage. Here, the muscle sandwiches the cartilage with m. tentacularis posterior from the lateral side. The muscle not only contracts on its own, but also can unfold the oral barbel laterally by contraction of m. cornual labialis that inserts onto the lateral surface of pars oralis.

M. lingual tentacularis lateraris pars perioralis lies just medial to pars oralis and continues anterodorsally, wrapping onto the base of the perioral tentacular process, inserting onto the lateral and dorsal surfaces of the labial ramus and the posterior and dorsal surfaces of the perioral tentacular process of the lateral tentacular cartilage. Here, the muscle also sends a tendon below the labial ramus to insert onto the medial surface of the tip of the cornual process; in effect, it anchors this part of the lateral tentacular cartilage close to the cornual process.

M. lingual tentacularis pars medialis extends dorsomedially and inserts onto the ventral surface of the terminal process of the subnasal cartilage, more distally along the process than the insertion of m. nasolingualis. The insertion to the subnasal cartilage compensates the insertion to the upper nasohypophyseal process by m. lingual tentacularis pars lateralis. The insertion onto the upper nasohypophyseal process is restricted to the ventral projection, which acts as a handle to flex the barbel anteriorly. The dual insertions of pars lateralis and medialis keep the upper and lower nasohypophyseal barbels in proximity. As the contraction of this muscle relaxes the tension of the integument around the mouth, the tooth plates can be protracted through the opened mouth.

3.3.4.3. M. nasolingualis (m.nl; Figures 3-1C, 3-6C, D, 3-7, 3-10 A-C)

Origin: perichondrium covering the ventral surface of the most distal portion and terminal process of the subnasal cartilage; membranes covering the ventral surface of m. subnasalis superficialis and the medial surface of m. lingual tentacularis; and the ventral surface of the perichondrium covering the labial ramus of the lateral tentacular cartilage.

Insertion: lateral surface of the perichondrium covering the proximal portion of the lateral tentacular cartilage and the most anterior portion of the anterolateral lingual cartilage.

Nerve innervation: trigeminal nerve, anterior branch (V_{2a}).

Functions: anterodorsal protraction of the lingual apparatus; closure of the passage for the dental apparatus.

Notes: M. nasolingualis is the most anterior of the muscles that attach to the lingual apparatus. The site of insertion is mostly the lateral surface of the vertically tall perichondrium along the proximal portion of the lateral tentacular cartilage, and it does not broadly overlap the anterolateral lingual cartilage. However, the proximal portion of the lateral tentacular cartilage is still functionally a part of the lingual apparatus, and contraction of m. nasolingualis causes the lingual apparatus to slide anteriorly and fold medially as the dental apparatus is retracted. The right and left counterparts meet at the midline and form a transverse muscular sheet between the terminal processes of the subnasal cartilage.

3.3.4.4. M. subnasalis superficialis (m.sns; Figures 3-1B, 3-5C, 3-6C, 3-7, 3-10A, C)

Origin: perichondrium over the dorsal surface of the palatal arch.

Insertion: perichondrium on the posterior surface of the terminal process and the lateral surface of the anterior half of the subnasal cartilage.

Nerve innervation: trigeminal nerve, anterior branch (V_{2a}).

Functions: lateral flexion of the lower nasohypophyseal barbel; suspension of the subnasal bar; floor for nasal tube; anteroposterior contraction of the nasal tube during “sneezing”; antagonist for m. nasolingualis.

Notes: M. subnasalis superficialis forms the floor for the nasal tube between the subnasal cartilage and the cornual process, and the lower half of the lateral wall of the tube above the palatal arch. M. subnasalis superficialis is between the overlapping m. nasalis and the underlying m. subnasalis profundus and more robust than both. Bridging between the subnasal cartilage and the palatal arch, m. subnasalis superficialis passes over the cornual process with no attachment. The lower edge of m. subnasalis superficialis parallels the anterior branch of the ‘maxillomandibular’ trigeminal nerve.

3.3.4.5. M. subnasalis profundus (m.snp; Figures 3-1B, C, 3-6C, D, 3-7, 3-10A, C)

Origin: perichondrium over the lateral surface of the posterior one third of the subnasal cartilage.

Insertion: perichondrium over the medial surface of the cornual process.

Nerve innervation: trigeminal nerve, anterior branch (V_{2a}).

Functions: antagonist for m. cornual lingualis, m. cornual labialis, and m. nasolingualis.

Notes: M. subnasalis profunds connects the cornual process and the subnasal cartilage underneath m. subnasalis superficialis. Its site of origin on the subnasal cartilage is posterior to the insertion of m. subnasalis superficialis. M. subnasalis profundus broadly inserts onto the medial surface of the corual process from the base to the tip. The dorsal surface of m. subnasalis profundus is associated with the overlying m. subnasalis superficialis via fascia. The ventral surface is attached to the roof of the mouth.

Although m. subnasalis profundus is not directly involved in major motions of the cranial muscular system, its insertion onto the cornual process makes it a sole muscular antagonist for two muscles crucial in feeding, m. cornual lingualis and m. cornual labialis. The cornual process is solid only at the base, and the tip of the process has a ligamentous connection with the flexible lateral tentacular cartilage beside m. subnasalis profundus. Without this muscle, the cornual process projects anterolaterally, not anteriorly as in life position. Contraction of the muscle counteracts the lateral pull of the process by these superficial muscles. Furthermore, m. nasolingualis pulls the anterior portion of the subnasal cartilage ventrally. M. subnasalis superficialis et profundus both antagonize this movement.

3.3.4.6. M. palatocoronarius (m.pc; Figures 3-1C, 3-5C, 3-6C, 3-8C, 3-10A, B)

Origin: ventral surface of the perichondrium of the palatal arch anterior to the eye.

Insertion: dorsal edge of the perichondrium over the proximal portion of the lateral tentacular cartilage.

Nerve innervation: trigeminal nerve, anterior branch (V_{2a}).

Function: opening passage for the dental apparatus through the mouth; posterior retraction of the lingual apparatus as the dental apparatus is protracted; suspension of the lateral tentacular cartilage; antagonist for m. lingual tentacularis and m. nasolingualis.

Notes: M. palatocoronarius is a thick, robust muscle connecting the lateral tentacular cartilage to the facial skeleton. The muscle passes dorsal to m. palatolabialis and medial to m. palatolingualis profundus, and these muscles are associated via fascia. The bundle of the motor and sensory neurons of the anterior branch of the maxillomandibular trigeminal nerve extend at the interface of these muscles, and the motor branch eventually extends within m. palatocoronarius anterior to the point of insertion of m. palatolabialis onto the labial tendon. Cole (1907) described two heads for this muscle, but in *E. stoutii* the muscle only has a single head.

3.3.4.7. M. palatolabialis (m.pal; Figures 3-1C, 3-5D, 3-6C, D, 3-8C, 3-10A)

Origin: ventral surface of the perichondrium of the ventral longitudinal arch (facial skeleton).

Insertion: via tendon to the dorsal oral mucosa anterior to the dental pouch.

Nerve innervation: trigeminal nerve, posterior branch (V_{2p}).

Functions: antagonist for protraction of the predental oral mucosa as the dental apparatus is everted; posterior retraction of the dorsal oral mucosa as the dental apparatus slides backward.

Notes: M. palatolabialis is one of the deepest facial muscles. Its site of origin is posterior to that of the overlying m. palatocoronarius. The muscle parallels the anterior branch of the maxillomandibular trigeminal nerve and passes to the ventromedial side of m. palatocoronarius as it inserts onto the labial tendon below the anterior end of the nasal capsule. The tendon extends further anteriorly over the dental pouch to the roof of the oral mucosa in front of the dental apparatus. As the everted dental apparatus is retracted,

contraction of m. palatolabialis tucks the everted oral mucosa back into the oral cavity. The labial tendon does not have typical histological characteristics of other tendons in hagfish such as an aggregate of fibroblasts depositing matrix in trabecular fashion. Instead, it is similar to the dermis of the oral mucosa in having numerous elongate nuclei in the dense collagenous extracellular matrix. Probably the labial tendon is an extension of the oral dermis, but it is functionally equivalent to a tendon. The labial tendon is also associated with vessels extending from the hypophyseal sinus on the medial side of the tendon.

3.3.5. Velar Muscles

3.3.5.1. M. craniovelar anterior dorsalis (m.vad; Figures 3-1B, C, 3-5D, 3-6B, 3-8 A-C)

Origin: ventral surface of the perichondrium of the acrochordal process; lateral surface of the perichondrium in the lower portion of the nasopharyngeal bar of the nasal capsule basket; and ventral surface of the perichondrium of the palatal arch anterior to a point below the eye.

Insertion: perichondrium of the dorsomedial hook of velar knob.

Nerve innervation: trigeminal nerve, velar branch (V_{2v}).

Function: dorsal recovery of the ventrally flexed lateral velar cartilage; lateral expansion of the velar skeleton; driving the incurrent of the pharynx; antagonist for m. spinovelaris; pumping of the cardinal heart.

Notes: M. craniovelar anterior dorsalis is one of the three extensor muscles of the velar skeleton. The muscle originates as anteriorly as the eye under the palatal arch and the acrochordal process, and passes over m. craniovelar anterior ventralis and m. craniovelar posterior to the small dorsomedial hook on the medial side of the velar knob. The site of insertion for m. craniovelar anterior dorsalis is dorsomedial with respect to that of m. craniovelar anterior ventralis and anterior with respect to m. spinovelaris. The velar knob forms a mobile tooth-in-socket joint with the velar process of the visceral plate and is the

centre of rotation for the velar skeleton. Together with other velar muscles, m. craniovelar anterior dorsalis restores the horizontal position of the ventrally flexed lateral velar cartilage. M. craniovelar anterior dorsalis is tightly associated with m. craniovelar anterior ventralis for its entire length. In contrast to the condition in *E. stoutii*, both m. craniovelar anterior dorsalis et ventralis in *M. glutinosa* extend anteromedially and insert onto the lateral margin of the nasopharyngeal plate (Cole 1907; Marinelli and Strenger 1956; Strahan 1958).

A large blood sinus sits between the velar knob and visceral plate. The sinus is large enough to occupy the entire area of the hyomandibular fenestra in lateral view and is frequently referred to as the cardinal heart. The sinus itself lacks a muscular wall expected for a true heart to contract on its own, but the motion of the velar skeleton secondarily pumps this 'heart'. Therefore, all the velar muscles have secondary functions of pumping the cardinal heart.

3.3.5.2. M. craniovelar anterior ventralis (m.vav; Figures 3-1B, C, 3-5D, 3-6B, 3-8 A-C)

Origin: ventral surface of the perichondrium of the palatal arch.

Insertion: anterior surface of the velar knob.

Nerve innervation: trigeminal nerve, velar branch (V_{2v}).

Function: dorsal recovery of the ventrally flexed lateral velar cartilage; lateral expansion of the velar skeleton; driving the incurrent of the pharynx; antagonist for m. craniovelar posterior; compensating for torque of velar skeleton by m. craniovelar anterior dorsalis and m. spinovelaris; pumping of the cardinal heart.

Notes: M. craniovelar anterior ventralis is another extensor of the velar skeleton and similar in size and shape to m. craniovelar anterior dorsalis. However, the site of origin for this muscle is slightly more anterior and more lateral with respect to that of m. craniovelar anterior dorsalis. These two muscles parallel the anterior portion of m. craniovelar posterior to the medial side. The

insertion is into the same perichondrial tissue as the insertion of m. craniovelar anterior dorsalis. Functionally, m. craniovelar anterior ventralis is similar to m. craniovelar anterior dorsalis, but has an additional function of correcting the medial-ward torque of the velar skeleton by the contraction of m. craniovelar anterior dorsalis and m. spinovelaris. Both of these muscles attach to the medial side of the velar knob, whereas the orientation of m. craniovelar anterior ventralis is nearly parasagittal. Without the parasagittal contraction of this muscle, the torque could disjoint the tooth-and-socket contact between the velar and facial skeletons.

3.3.5.3. M. spinovelaris (m.vs; Figures 3-1B, C, 3-5E, 3-6B, 3-8A, B, D, E)

Origin: lateral surface of the most anterior region of the notochord below the site of insertion of m. craniopharyngis and posterior to that of m. otic lingualis.

Insertion: posteromedial surface of the dorsomedial process of the velar knob.

Nerve innervation: trigeminal nerve, velar branch (V_{2v}).

Functions: dorsal and medial recoveries of the ventrally flexed lateral velar cartilage; posteromedial retraction of the velar knob to compensate for forward sliding of the knob by m. craniovelar anterior dorsalis et ventralis; antagonist for posterolateral torque of the velar knob by contraction of m. craniovelar posterior; driving the incurrent to the pharynx; pumping of the cardinal heart.

Notes: M. spinovelaris is the last extensor of the velar skeleton. The muscle is similar in shape and size to other extensors, but differs in its anterolateral orientation and the site of origin above the pharynx. It extends along the dorsal edge of the velar knob and passes medially underneath the otic capsule before it attaches to the notochord. In addition to its main function of dorsal recovery of the lateral velar cartilage, m. spinoveralis antagonizes the lateral displacement of the velar knob that accompanies contraction of m. craniovelar posterior. The distal point of the insertion for the latter muscle causes the distal portion of the velar skeleton to bend anteriorly, and the elastic consequence of this is the posterolateral motion of the velar knob that

potentially results in displacement of the knob. M. spinoventralis compensates for that by pulling the knob posteromedially. M. spinovelaris also antagonizes contraction of m. craniovelar anterior dorsalis et ventralis to prevent forward slinding of the velar knob.

3.3.5.4. M. craniovelar posterior (m.vp; Figures 3-1B, C, 3-5E, 3-6B, 3-8A, B, D, E)

Origin: posterior surface of the perichondrium at the base of the acrochordal process; ventral surface of the perichondrium along the lateral edge of the nasopharyngeal plate posterior to the acrochordal process.

Insertion: medial surface of the perichondrium of the lateral velar cartilage, proximal to the base of the medial velar cartilage.

Nerve innervation: trigeminal nerve, velar branch (V_{2v}).

Function: anteromedial and ventral flexion of the lateral velar cartilage; ventral unrolling of the velar scroll (dorsal fold of the pharyngeal epithelium); pumping of the cardinal heart.

Notes: M. craniovelar posterior is entirely responsible for ventral flexion of the velar skeleton during ventilation. Medial to other velar muscles, m. craniovelar posterior originates from the lateral edge of the nasopharyngeal plate. Unlike all other velar muscles that insert to the velar knob, m. craniovelar posterior inserts more distally, onto the medial surface of the lateral velar cartilage just proximal to the base of the medial velar cartilage. The internal velar skeleton is anchored to the spinal membrane above the pharynx such that during slow, full contraction of m. craniovelar posterior, the right and left lateral velar cartilages bend anteroventrally and medially and approach each other (Strahan 1958).

3.3.6. Protractors and Retractors of Lingual Apparatus

3.3.6.1. M. protractor dentalis lateralis (m.pdl; Figures 3-5 D-F, 3-6A, 3-8 C-E, 3-10A, D)

Origin: lateral surface of the perichondrium of the posterior lingual cartilage.

Insertion: anterolateral margin of the dental apparatus.

Nerve innervation: trigeminal nerve, posterior branch (V_{2p}).

Function: protraction, eversion, and lateral unfolding of the dental apparatus.

Notes: M. protractor dentalis lateralis is the larger, and therefore stronger, protractor for the dental apparatus. The muscle originates from the lateral surface of the posterior lingual cartilage below the site of insertion for m. retractor lingualis. Its site of origin occupies the lateral surface of the posterior lingual cartilage for the posterior half of the cartilage. In ventral view, the origin of m. protractor dentalis lateralis is visible along the ventral margin of the cartilage until that of m. protractor dentalis medialis separates it dorsally from the ventral margin. The site of origin for m. protractor dentalis lateralis extends anterodorsally above that for m. protractor dentalis medialis, eventually reaching the tallest point of the posterior lingual cartilage. The transverse width of m. protractor dentalis lateralis is slightly narrower than that of m. retractor lingualis.

The muscle extends anteriorly below the middle and anterior segments of the lingual apparatus in parallel with m. protractor dentalis medialis and splits into two heads. These heads wrap around the anterior margin of the anteromedial lingual cartilage and insert onto the anterolateral margin of the dental apparatus. As such, contraction of this muscle results in forward movement, eversion, and lateral unfolding of the dental apparatus. M. protractor dentalis lateralis is always slightly more dorsal than m. protractor dentalis medialis from the origin to the insertion.

3.3.6.2. M. protractor dentalis medialis (m.pdm; Figures 3-5 D, E, 3-6A, B, 3-8 C-E, 3-10A, D)

Origin: lateral surface of the perichondrium of the posterior lingual cartilage ventral to the origin of m. protractor dentalis lateralis.

Insertion: ventral surface of the dental apparatus along the midline.

Nerve innervation: trigeminal nerve, posterior branch (V_{2p}).

Function: protraction and eversion of the dental apparatus.

Notes: M. protractor dentalis medialis is the smaller, bilaterally paired protractor that sits on the ventral midline of the head. Its site of origin on the posterior lingual cartilage is substantially smaller than that of m. protractor dentalis lateralis just above. This attachment sets apart m. protractor dentalis lateralis from the ventral margin of the cartilage, and anteriorly beyond this point, the lower half of the lateral surface of the cartilage is free of muscle attachment. The muscle extends along the midline below the middle and anterior lingual cartilages in parallel with m. protractor dentalis lateralis. In contrast to m. protractor dentalis lateralis that splits into two heads, however, the right and left bundles of m. protractor dentalis medialis join to form a single midline band. The muscle passes between the right and left bundles of m. protractor dentalis lateralis as it wraps around the anterior margin of the lingual apparatus and inserts onto the ventral surface of the dental apparatus along the midline.

As in the case of m. protractor dentalis lateralis, contraction of m. protractor dentalis medialis protracts and everts the dental apparatus through the mouth. However, the muscle cannot unfold the dental apparatus as does m. protractor dentalis lateralis.

3.3.6.3. M. retractor dentalis lateralis (m.rdl; Figures 3-1B, C, 3-5E, 3-6C, D, 3-10A, B, D)

Origin: lateral margin of the perichondrium of the middle lingual cartilage along the posterior one third; perichondrium of the distal-most portion of the first external pharyngolingual arch.

Insertion: lateral surface of the mucosa of the dental apparatus.

Nerve innervation: trigeminal nerve, posterior branch (V_{2p}).

Function: retraction of the dental apparatus posteriorly; unfolding of the dental apparatus in resting position.

Notes: M. retractor dentalis lateralis consists of a thin band of muscle fibres and anchors the dental apparatus posteroventrally on the middle lingual cartilage. Around the site of origin, this muscle is tightly associated with (but lying medial to) m. craniolingualis and m. palatolingualis superficialis, both lying lateral to this muscle. Anteriorly along the lateral margin of the middle lingual cartilage, the site of origin for m. retractor dentalis lateralis is replaced by that of m. palatolingualis profundus. From here, m. retractor dentalis lateralis extends anteriorly beneath the dental apparatus and inserts onto the apparatus via two bands of mucosa, one that arises from the lateral margin of the anterior portion of the dental apparatus, and the other that arises from the ventral surface where the apparatus is widest transversely. The dental apparatus is folded medially as it is retracted from the mouth. M. lingual dentalis retracts the apparatus to the resting position on the middle lingual cartilage and unfolds the apparatus laterally.

3.3.6.4. M. retractor lingualis (m.rl; Figures 3-1B, 3-5F, G, 3-6A, 3-9A, B, 3-10A, B, D)

Origin: mucosa of the distal lingual complex; ligamentous membrane along the dorsal midline; bilateral counterpart along the dorsal and ventral midlines.

Insertion: dorsal margin of the perichondrium of the posterior lingual cartilage; perichondrium of the second external pharyngolingual arch.

Nerve innervation: trigeminal nerve, posterior branch (V_{2p}).

Function: posterior retraction of the lingual apparatus as the dental apparatus is everted (antagonist for m. protractor dentalis lateralis and medialis); contraction of the distal lingual complex (antagonist for m. retractor dentalis major).

Notes: Except for the somitic muscles, m. retractor lingualis is the largest muscle in the head of a hagfish. The muscle is anchored posteriorly to the anterior mucosal wall of the branchial region and laterally to the notochord via the mucosa of m. constrictor pharyngis. This massive, tubular muscle encloses m.

retractor dentalis major within its body. M. retractor lingualis has an anteroposteriorly long site of insertion along the dorsal margin of the posterior lingual cartilage above, where it overlaps the site of origin for m. protractor dentalis lateralis and overarches the deep trough of the posterior lingual cartilage that accommodates the tendon of m. retractor dentalis. The insertion of this muscle almost reaches the junction of the first and second external pharyngolingual arches and the anterior end of the posterior lingual cartilage.

M. retractor lingualis is innervated by the posterior branch of the trigeminal nerve. The branch emerges from the medial side of the ventral longitudinal arch of the facial skeleton and passes posteroventrally below the visceral plate and the lower first internal pharyngolingual arch and along the second external pharyngolingual arch. Beyond the point of innervation for m. retractor lingualis, the nerve continues posteriorly within the tube of m. retractor lingualis on the dorsal side of m. retractor dentalis major all the way back to the posterior end of the tube. Here, the nerve innervates m. retractor dentalis major.

The fibres of m. retractor lingualis are oriented longitudinally where they insert onto the posterior lingual cartilage, and vertically where they enclose m. retractor dentalis major. Contraction of m. retractor lingualis pulls the lingual apparatus posteriorly to antagonize the anterior motion of the apparatus by contraction of the dental protractors. This simultaneously causes contraction of the distal lingual complex and raises the internal pressure within. Relaxation of the muscle provides extra space and lower pressure necessary for contraction of m. retractor dentalis major to pull the dental apparatus back into the oral cavity.

3.3.6.5. M. retractor dentalis major (m.rdm; Figures 3-1C, 3-5F, G, 3-6B, 3-8D, E, 3-9, 3-10D)

Origin: dorsal surface of the perichondrium of the anterior portion of the lower distal lingual cartilage; membrane over the lateral surface of m. perpendicularis near the dorsal edge; ventral surface of the perichondrium of the distal portion of the upper distal lingual cartilage.

Insertion: perichondrium of the medial basal plate (via tendon).

Nerve innervation: trigeminal nerve, posterior branch (V_{2p}).

Function: retraction of dental apparatus.

Notes: M. retractor dentalis major is the powerful muscle almost solely responsible for retraction of the dental apparatus. The muscle is anchored at the distal lingual complex where m. perpendicularis connects the upper and lower distal lingual cartilages. The muscle fibres of m. retractor dentalis major are substantially shorter anteroposteriorly than m. retractor lingualis and the protractors of the dental apparatus, which indicates slow but powerful retraction of the dental apparatus after capture of a food item. The muscle sits within the midline trough of the posterior lingual cartilage under the roof formed by m. retractor lingualis and becomes a thick tendon. The tendon passes through the trough and inserts to the middle plate of the dental apparatus.

Because m. retractor dentalis is enveloped within m. retractor lingualis, and because the muscular body of the former closely fits the space within the latter, contraction of m. retractor dentalis is only possible following the contraction of m. retractor lingualis at the time of protraction and eversion of the dental apparatus.

3.3.6.6. M. perpendicularis (m.prp; Figures 3-5G, 3-9C)

Origin: perichondrium of the upper distal lingual cartilage.

Insertion: perichondrium of the lower distal lingual cartilage.

Nerve innervation: trigeminal nerve, posterior branch (V_{2p}).

Functions: antagonist for contraction of m. retractor dentalis major.

Notes: M. perpendicularis is a thick median sheet of muscle that connects the two distal lingual cartilages. This is the only unpaired muscle in the hagfish head. Contraction of this muscle antagonizes sliding of the upper and lower distal lingual cartilages against each other and stabilizes the anchoring attachment of m. retractor dentalis major.

3.3.7. Branchial Muscles

3.3.7.1. M. constrictor branchialis, cardialis, et hepatis (m.cbr; Figure 3-9A)

Origin: mesentery.

Insertion: membrane over the dorsal surface of m. rectus; ventrolateral surface of the gill pouch (branchialis); left anterolateral surface of the systemic heart (cardialis); lateral surface of the liver (hapatis).

Nerve innervation: vagus nerve (X).

Functions: suspension of gill pouches, heart, and liver.

Note: M. constrictor branchialis develops within the mucosa of the mesentery along with m. constrictor cardialis and hepatis at the same parasagittal level with m. constrictor pharyngis. As in the posterior part of m. constrictor pharyngis, m. constrictor branchialis is a complex of weak muscular bundles that are not powerful enough to facilitate spontaneous motions of the inserted tissue. It merely suspends the gill pouches in the coelomic cavity. Each head of m. constrictor branchialis develops between the gill pouches, indicating that they each represent a remnant of pharyngeal pouches between the pharyngeal slits. Although the branchial heads may be absent in some of the gills between individuals, no trend emerges after dissections of ten individuals, and the variation appears to be random. As such, m. constrictor branchialis does not actively participate in ventilation through the gill pouches. M. constrictor cardialis is only present on the left side and is deeper than its superficial counterparts. M. constrictor hepatis wraps around the lateral side of the anterior portion of the liver. Except for one prebranchial head that inserts to

m. retractor lingualis anteriorly, all heads of these muscles connect to m. rectus.

3.3.8. Histology of muscle fibres

This description follows classic accounts of hagfish muscular histology in recognizing red, white, and intermediate fibres (Cole 1907; Korneliussen 1972, 1973; Korneliussen and Nicolaysen 1973; Flood 1998). In histological sections stained with eosin and hematoxylin, these fibres can be distinguished by diameters, vascularization, and lipid contents (Figure 3-11). Red fibres (rf; Figure 3-11A, B) have diameters less than three quarters those of white fibres, and have a high concentration of fat vacuoles, and are associated with capillaries. White fibres (wf; Figure 3-11 A, C, D) are thicker than red fibres, and are poor in lipid contents and vascularization. Intermediate fibres (if; Figure 3-11A) fall between these two types of fibres. The somatic muscles (m. parietalis, m. obliquus, and m. rectus) contain fibres of all three types, although the white fibres occupy 80 to 90% of the area in cross section (Figure 3-11A).. The white fibres are dominant in almost all cranial muscles, and red fibres are absent in the protractors and retractors of the lingual apparatus. Although the distinction between white and intermediate fibres is not obvious in sections prepared for this study, at least m. retractor dentalis major and m. retractor lingualis consist of the white fibres only (Figure 3-11C). On the other hand, the velar muscles (m. craniovelar anterior dorsalis et ventralis, m. craniovelar posterior, and m. spinovelaris) consist exclusively of red fibres (Figure 3-11B). Red fibres in the velar muscles are distinct in having significantly smaller diameters (a quarter that of the red fibres in m. parietalis) and large numbers of fat vacuoles and mitochondria (Korneliussen and Nicolaysen 1973). The dorsal fold of the pharynx within which the velar muscles extend is an open blood sinus, which functionally explains the large volume of red fibres. Physiologically, white fibres are interpreted as fast muscle fibres susceptible to fatigue, whereas red fibres are slow and fatigue-resistant (Flood 1998; Sänger and Stoiber 2001).

The occurrence of the fibres is consistent with the function of these muscles. The slow, fatigue-resistant red fibres continuously drive ventilation by the velar muscles, and the fast white fibres are solely responsible for quick, forceful sagittal retraction of the dental apparatus by m. retractor dentalis major. The dominance of the white fibres in the somatic muscles explains the fact that hagfish are neither active nor pelagic swimmers. Instead, hagfish behaviours employ short bursts of the strong axial bending or undulation in burrowing bilateral undulation, coiling in resting positions, making a knot during feeding or as escape behaviour, and swimming toward already detected food sources (Worthington 1905; Adam 1960; Strahan 1963; Martini 1998). The dominance of white fibres in other cranial muscles indicates that these muscles — mostly involved in suspension of the lingual apparatus or other cranial cartilages — also contract in short bursts rather than continuously.

3.3.9. Development of the cranial muscles

In adult hagfish, the somatic muscles (m. parietalis, m. obliquus, and m. rectus) extend anteriorly and overlap the head. However, this is a secondary migration during ontogeny and the somatic muscles do not develop within the head. In the description of *E. stoutii* embryos by Dean (1899), the somites are clearly restricted behind the otic capsule up to embryonic stages past the development of 13-14 gill slits (Figure 3-12). The anterior migration of somatic muscles initiates some time between this stage and the late embryonic stage in which the embryo extends more than 180° of the longitude of the egg around the yolk (Dean 1899). A similar anterior migration of the somatic muscles occurs in lampreys, although the timing is delayed until after hatching (Damas 1944; Kuratani et al. 1999; Kusakabe et al. 2004, 2011; Kusakabe and Kuratani 2005). In both hagfish and lampreys, the main somatic muscle (m. parietalis in the former) extends above and below the eye in lateral view, and the infraoptic part of the muscle never extends beyond the level just posterior to the mouth.

The only description of the development of true cranial musculature in hagfish (Holmgren 1946) is based on an embryo of *M. glutinosa* (Figure 3-12). Following the order of description, a pair of superficial and deep muscle anlagen exists lateral with respect to the nasal tube. The deep muscle between the nasal tube and the future position of the cornual process represents m. subnasalis profundus, whereas the one superficial with respect to the anlage is likely an anlage of m. cornual labialis and possibly includes that of m. cornual lingualis. Holmgren (1946) did not recognize any other facial muscles innervated by the motor component of the trigeminal nerve. The delayed development of the muscles probably reflects positions of these muscles and correlation with the tissues to which the muscles attach. The muscles not differentiated at this early stage must exist as a pool of myogenic mesenchyme, and two functional explanations for that condition are: 1) that the myogenic mesenchyme has not reached a position where it differentiates into muscle; and 2) that the surrounding tissues have not differentiated enough to induce myogenesis. Indeed, the muscle rudiments that are already distinct at this stage are apart from the expected position of the cranial paraxial and lateral mesoderm (Dean 1899; Stockard 1906; Neumayer 1938; Holmgren 1946; Wicht and Northcutt 1995). Therefore, they are likely to represent early migration and differentiation of the myogenic mesenchyme from either the paraxial or lateral mesoderm.

In the same embryo, a sheet of a muscular anlage develops on the lateral side of the pharynx below the geniculate ganglion (facial nerve), and the ventral part is more robust than the dorsal part (Holmgren 1946). In adult, m. craniolingualis innervated by the hyomandibular nerve sits in that position. Taking the cephalic flexure of the embryo into account, however, the long axis of this anlagen is anatomically closer to anteroposterior than dorsoventral, and the position directly below the geniculate ganglion corresponds with the buccal region. Given the same parasagittal position in the adult, the anlage represents both m. palatolingualis superficialis and m. craniolingualis. A plate of muscle anlage behind it topographically corresponds to the anterior portion of m. constrictor pharyngis innervated by the glossopharyngeal nerve (Holmgren 1946).

There is a pair of superficial and deep muscle anlagen in the dorsal fold of the pharynx (Holmgren 1946). The superficial anlage is undoubtedly m. craniovelar posterior, whereas the deep one is likely a mixture of the velar muscles involved in recovery stroke of the velum and attached to the velar knob from either the medial or anterior side (m. craniovelar anterior dorsalis et ventralis; m. spinovelaris). Importantly, the dorsal fold (presumptive velar scroll) at this stage is just medial to the trigeminal ganglion and clearly within the mandibular domain, and the position of these muscle anlagen is medial with respect to the paraxial mesoderm of the head.

Rudiments of the protractors of the dental apparatus (m. protractor dentalis lateralis and medialis) develop right below the anlage for m. palatolingualis superficialis and m. craniolingualis (Holmgren 1946). Muscles of the distal lingual complex form above the anlage of the posterior lingual cartilage right behind the anlagen of the protractors and below the anlagen of m. constrictor pharyngis (Holmgren 1946). Both rudiments of m. retractor dentalis major and m. retractor lingualis are paired and separated by the mesenchymal precursors of the upper and lower distal lingual cartilages. Between the upper and lower elements develops the anlage of m. perpendicularis (Holmgren 1946). The anlage of m. retractor dentalis major is associated with the tendon extending over the proximal portion of the anlage of the dental apparatus; another set of tendons that bilaterally develop on the lingual skeleton also persist into adults as the anchoring connective tissue between the ventral side of the dental pouch and the middle lingual cartilage (Holmgren 1946). The protractors and retractors are all innervated by the motor component of the trigeminal nerve. These conditions are essentially identical to those in lampreys (Damas 1944).

The muscle anlagen of the lingual apparatus are all innervated by the motor component of the trigeminal nerve, even though the muscle rudiments right above them are variably innervated by the facial, glossopharyngeal, or vagus nerve. This indicates that the protractors and retractors form at the floor of the pharynx presumably after the posterior migration along the ventral midline, and do not come from a ventromedial extension of the post-mandibular pharyngeal mesoderm. In

gnathostomes, hypoglossal muscles sit in the anatomically equivalent region. The anlagen of these gnathostome-specific muscles migrate from the somatic body wall below the pharynx along the midline anteriorly as part of hypobranchial muscles (Edgeworth 1902, 1911, 1923, 1926a, b, 1928, 1935; Miyake et al. 1992; Diogo and Abdala 2010). As such, the hypoglossal nerve, a serial homologue of the spinal nerve, innervates the hypoglossal muscles in gnathostomes. The significance of this is discussed in context of the origin of the jaw (3.4.3.2. Mandibular Siege Hypothesis).

3.4. DISCUSSION

3.4.1. Biomechanics of the Cranial Muscles

3.4.1.1. Muscle antagonism and elastic recoil of cartilages

The cranial musculature of hagfish has a remarkably large number of components and, given the number, a remarkably low diversity of muscular functions. This is largely because of the condition specific to jawless vertebrates where muscles antagonize each other in the absence of hard skeletons. In total, eight muscles participate in suspension of the lingual apparatus against the main part of the chondrocranium (Figure 3-13), as well as two protractors and two retractors (m. protractor dentalis lateralis and medialis, m. retractor dentalis lateralis, and m. retractor lingualis), m. constrictor pharyngis, and the somatic m. rectus anchored to the lingual apparatus. Many of these muscles form pairs of antagonists at the same parasagittal level (Figure 3-13), from superficial to deep: m. palatolingualis superficialis and m. craniolingualis; m. cornual lingualis and m. palatolingualis profundus; m. palatocoronarius and m. nasolingualis; m. retractor dentalis lateralis, m. otic lingualis, and m. constrictor pharyngis; and possibly m. lingual tentacularis and m. rectus. Except for the last two pairs, muscles within each pair are innervated by the neighbouring motor branches (Figures 3-1, 3-15). Simultaneous contraction of these pairs stabilizes the lingual apparatus, and these muscles as a whole can antagonize the anteroposterior sliding motion generated by contraction of the dental protractors and retractors. This complex system of antagonizing muscles is essential for the lingual apparatus independent of the main chondrocranium, because

otherwise sliding of the lingual apparatus would prevent opening the mouth or everting the dental apparatus through the opening. Likewise, stiffening of the origin of m. retractor dentalis major by contraction of m. retractor lingualis and m. perpendicularis represents an antagonistic action to stabilize the feeding apparatus, and this stiffening allows forceful retraction of the dental apparatus (Clark et al. 2010).

Another functional feature of the hagfish musculoskeletal system is the role of elastic recoil. Coupled with the distribution of Type 1b soft cartilages (Chapter 2), the muscles are arranged in positions that take advantage of elastic recoiling of the cartilages that they attach to. Examples include the velum (dorsal recovery of the velar skeleton; Strahan 1958), barbels (resting position versus erection observed by Clark and Summers 2007; m. lingual tentacularis, m. subnasalis superficialis, and m. tentacularis posterior), cornual process (antagonism between m. subnasalis profundus and m. cornual lingualis and labialis), nasopharyngeal plate and nasopharyngeal bar (suspension of the nasohypophyseal complex), external pharyngolingual arches (suspension of the lingual apparatus; m. palatolingualis superficialis, m. craniolingualis, m. otic lingualis, and m. constrictor pharyngis), and external branchial cartilage (efferent branchial duct; m. constrictor branchialis). The elastic recoil compensates for the lack of a mobile joint in the skull of hagfish. The cartilages either fuse to each other or attach via perichondral tissues, and no contact in the skull forms a ball-and-socket joint. The proximal velar knob and the visceral plate have a tooth-in-socket contact via the velar process and with a blood sinus (cardinal heart) between the elements, but neither element forms a plane of contact over which the other could slide (Chapter 2).

3.4.1.2. Functional constraints against mineralized internal skeleton

The muscle antagonism and elastic recoil of the skeleton in hagfish stands in stark contrast to the lever system of a hard skeleton powered by adductors and abductors in gnathostomes. Scenarios for early vertebrate evolution unanimously posit mineralization of the internal skeletons as a key innovation preceding or

facilitating the origin of jaws (Løvtrup 1977; Gans and Northcutt 1983; Northcutt and Gans 1983; Maisey 1986, 1988; Gans 1993; Janvier 1993, 1996, 2007; Mallatt 1996, 2008; Donoghue 2002; Donoghue and Sansom 2002; Kuratani 2004a; Donoghue et al. 2006). It is curious, then, that mineralized or calcified feeding structures did exist in jawless vertebrates, most notably as the teeth of conodonts (Donoghue 1998) and as the perioral cartilage of anaspids (Janvier and Arsenault 2002, 2007). As reviewed in Chapter 2, there is evidence for a non-mineralized cartilaginous internal skeleton in anaspids, arandaspids, conodonts, galeaspids, heterostracans, osteostracans, and thelodonts, all of which had mineralized an external skeleton as scales or shields (also reviewed by Janvier 1993, 1996, 2007; Donoghue 2002; Donoghue and Sansom 2002; Donoghue et al. 2006). Hagfish and lampreys both lack mineralization altogether, although they both have keratinous teeth. The early origin and wide distribution of mineralization in vertebrates implies constraints against mineralization of the internal skeleton in jawless vertebrates.

Constraints against mineralization were likely functional. The biomechanics of the hagfish musculoskeletal system offers a simple thought experiment: replacement of cartilages with bones or mineralized cartilages. This would result in instantaneous malfunction due to the loss of elastic recoil and the lack of a mobile joint in the skull. The same is true for lampreys. Lamprey adults ventilate by elastic distortion and recovery of the branchial basket (Dawson 1905a, b; Luther 1938; Marinelli and Strenger 1954; Randall 1972; Kawasaki 1979, 1984) and require retraction of the perioral cartilages to expose the suprapical teeth (Hilliard et al. 1985; Kawasaki and Rovainen 1988; Rovainen 1996). At the larval stage, the ammocoete use elastic recoil in recovery of the velar skeleton as in hagfish (Dawson 1905a, b; Rovainen and Schieber 1975; Mallatt 1981), and cranial musculature is attached to the flexible mucocartilage (Sewertzoff 1916; Tretjakoff 1926; Damas 1944; Hardisty and Rovainen 1982). Requirement of skeletal elasticity in these functions explains why the phylogenetic distribution of soft cartilages is limited to hagfish and lampreys among living vertebrates. It is also reasonable to hypothesize that ventilation through gills required elastic recoil of cartilages in extinct jawless

vertebrate lineages such as arandaspids, galeaspids, heterostracans, osteostracans, and pituriaspids because these fish had inflexible, mineralized external skeletons over the branchial region either as a shield or as a series of branchial plates. As such, the musculoskeletal system in the heads of jawless vertebrates is highly specialized toward muscle antagonism and skeletal elasticity, and the origin of a hard internal skeleton probably accompanied extensive remodelling of the musculoskeletal system and did not occur simply as mineralization of cartilages.

3.4.1.3. Possible origin of synovial joints

Although the 'agnathan' skeletal elasticity and the gnathostome hard skeleton consisting of jointed levers are functionally not interchangeable, the muscle antagonism in hagfish and lampreys is functionally analogous to adductors and abductors of the gnathostome jaw except for two important differences. First, a lever motion at the joint requires proximodistal polarization of muscle attachment sites. The *Dlx* expression module in the mandibular domain indicates that the development of the jaw is coupled with the proximodistal polarization (Depew et al. 2001, 2005; Depew and Simpson 2006). Second, paired abductors and adductors contract alternately, not simultaneously as antagonizing muscles do. Still, paired antagonizing muscles in jawless vertebrates need not correspond to an abductor-adductor functional pair in gnathostomes.

The transitions in motor patterns must couple with formation of mobile joints to derive a functioning lever system of a hard internal skeleton. Evolutionary origin of a mobile skeletal joint has rarely been discussed in the context of early evolution of internal skeleton in vertebrates except for the cap-and-hinge model (Depew and Simpson 2006), but diarthrosis is a prerequisite for a mobile, hard internal skeleton. In the context of the origin of gnathostomes, the mandibular joint is an obvious key innovation to form a jaw. Depew and Simpson (2006) hypothesized an evolutionary scenario that gene expression domains in the mandibular arch of gnathostomes specify the position of the mandibular joint. However, the acquisition of the jaw cannot simply be described as positional specification for the joint. Non-gnathostome

chordates do not have a synovial joint, whereas a mandibular joint develops as a synovial joint in all gnathostomes with a mobile jaw. Therefore, a synovial joint itself is likely a gnathostome synapomorphy and a key innovation that facilitated the origin of the jaw.

Development of a synovial joint initiates with the formation and growth of an interzone between two endochondral elements in a continuous prechondrogenic mesenchyme population (exception: the temporal bone undergoes intramembranous ossification in the mammalian temporomandibular joint), which includes presumptive synovial cells (Whillis 1940; Craig et al. 1987; Archer et al. 1994, 2003; Hall and Miyake 2000; Hayes et al. 2001; Pitsillides and Ashhurst 2008). The growth accompanies expansion of the synovial membrane and an increase in the number of synovial folds (Tsuyama et al. 1995). Cavitation of the synovial capsule follows, with the development of a condyle and hyaline-like articular cartilage that lacks perichondrium (Whillis 1940; Archer et al. 1994, 2003; Hayes et al. 2001; Pitsillides and Ashhurst 2008). Morphogenesis and separation of articular cartilage and condyle require expression of the hedgehog signalling pathways (Spater et al. 2006; Koyama et al. 2007a, b; Shibukawa et al. 2007; Purcell et al. 2009), whereas the maintenance of an interzone in a synovial joint requires that of the BMP signalling pathways (Storm and Kingsley 1996; Brunet et al. 1998; Francis-West et al. 1999; Gong et al. 1999; Tsumaki et al. 2002). Particularly, the Indian hedgehog (*Ihh*) signalling regulates chondrogenesis and endochondral ossification (St. Jacques et al. 1999; Dy et al. 2010). Lampreys have the proposed orthologue of the gnathostome *Ihh* (Kano et al. 2010). Although the existence of an *Ihh* orthologue remains unknown in hagfish, the negative feedback loop of *Ihh* eventually links to the expression of *Col2a1* responsible for the deposition of extracellular matrix via regulation of PTH-related protein targeted to *Sox9* (direct transcriptional regulator of *Col2a1*), and expression of *Col2a1* is confirmed in both lamprey and hagfish cartilages as well as in other vertebrate models (Zhang et al. 2006, 2009; Ohtani et al. 2008; Ota and Kuratani 2010). The gene expression modules required for the formation of a synovial joint therefore already exist in jawless vertebrates.

Morphologically the closest model in the hagfish head to a gnathostome synovial joint is the proximal portion of the velar skeleton. Here, the hyaline-like Type 1a cartilage with little perichondrium has a tooth and socket contact with the velar process of the facial skeleton, and the cardinal heart forms a pad between the two cartilages (Figure 3-14). The movement at this contact due to downward flexion of the velar skeleton exerts pressure on the cardinal heart and potentially aids in cranial circulation. Simultaneously, the ligamentous wall of the cardinal heart links the two cartilages via perichondrium (Figure 3-14B, C). The morphology closely resembles a synovial joint, with blood as a functional analogue of synovial fluid. The similarity is further reinforced by two facts: that synovial fluid derives from blood plasma and that synovial connective tissue is highly vascularized (Tortora and Derrickson 2008). This morphological similarity does not necessarily mean that the proximal velar contact is a presumptive jaw joint. The velar skeleton belongs to the mandibular domain, whereas the visceral plate presumably belongs to the hyoid domain (Chapter 2). Nevertheless, the proximal velar contact in hagfish suggests a possibility that a precursor of the mandibular joint co-opted a flexible tooth-and-socket contact of hard, hyaline-like cartilages with a blood sinus as an intermediate cushion and connective tissue and with blood as lubricant. No cartilaginous contacts other than the proximal velar contact show this morphology in living jawless vertebrates. In support of this hypothesis, *Bapx1* expression specifies the jaw joint in gnathostomes, and its orthologue is expressed along the boundary between the lower lip and velum in lampreys (Kuraku et al. 2010). Morphological correspondence is difficult to establish between the mandibular skeleton and velar skeleton due to extensive remodelling of the mandibular domain during early vertebrate evolution (Kuratani 2004a, b, 2005, 2012; Barreiro-Iglesias et al. 2011). It remains unknown whether stem gnathostomes had a velum similar to those in lampreys and hagfish (Chapter 2). Despite these challenges, potential co-option of the proximal velar contact between hard cartilages within the mandibular domain merits further investigation.

3.4.2. Homology of Vertebrate Cranial Muscles

Muscle homology is an elusive concept. When evolutionary conservation of a particular muscle is hypothesized, the argument typically concerns three different types of similarities: 1) functional similarity in which a particular muscular function is conserved across taxa (Table 3-1); 2) developmental similarity in which muscles arise from the same progenitor between taxa (Table 3-2); and 3) morphological similarity in which the positions of muscles are comparable so that relationships with surrounding tissues (nerves, cartilages, vascular and connective tissues, and others) are conserved (Table 3-3; Figure 3-15). Consensus among these similarities rigorously tests for muscles congruent in all or almost all of criteria for similarity between hagfish, lampreys, and gnathostomes (Table 3-4; Figure 3-16). Importantly, only developmental similarity among the three categories describes tissue identity of muscles at the cellular level. The functional and morphological similarities do not guarantee that the muscles in question derive from the homologous progenitor population, because neomorph, migration, and remodelling all could functionally and/or topographically alter the configuration of muscles (the most recent and comprehensive historical review in Diogo and Abdala 2010). Unfortunately, developmental identity is the hardest of these similarities to establish because it requires sophisticated cell labeling techniques including marker gene expression, and because it poses a question of arbitral decisions. The most tangible example is misalignments between fate maps of mesoderm in quail-chick chimeric embryos at different developmental stages (Noden 1978a, 1983a, b, 1986a, b, 1988; McClearn and Noden 1988; Couly and Le Douarin 1988; Couly et al. 1992, 1993; Noden et al. 1999; Borue and Noden 2004; Noden and Trainor 2005; Evans and Noden 2006; Noden and Francis-West 2006). In other examples, somatic myofibers during primary myogenesis arise in different positions within myotomes and migrate during secondary myogenesis differently between mouse and chick (reviewed by Bryson-Richardson and Currie 2008), and overall configurations of the cranial muscles are subject to ontogenetic modification (e.g., zebrafish: Schilling and Kimmel 1997; Diogo et al. 2008). Because the position of progenitors for specific muscles can shift

during embryogenesis relative to each other, the choice of sampling stage impacts the assessment. At this point, it is extremely challenging to completely resolve progenitor cell lineages and test the developmental identities of individual muscles; neither is biological significance of such approach clear in the context of evolutionary comparison, if plasticity exists, or if tissue interaction at later stages has stronger effects on patterning of muscles.

On the other hand, muscular function and configuration are readily observable phenotypes. Problematically, these phenotypes may be partly independent of the developmental origins of muscles, if developmentally non-identical muscles conserve function or configuration. Evolutionary conservation of the phenotypes indicates adaptive significance at some level and extrinsic or intrinsic selection, thereby carrying developmental burden (Riedl 1978; Kuratani 2004a) or structural constraint (Wagner 1994). If a homology is evolutionary continuity of information in the broadest sense (Van Valen 1982), then functional or morphological identities of muscles are statements of possible homology and may be tested phylogenetically. This stance leads to an unorthodox argument that homology of tissues may be independent of homology of properties of morphological topology or morphological field because both could be subject to selection. Philosophical implications of this argument are beyond the scope of this paper and are not discussed further. However, all types of similarities are considered in this paper, and the breaking of homologous relationships may point to an evolutionary novelty (Müller and Wagner 1991; Wagner 1994) or to a change in properties of a morphological field. The difficulty of establishing muscular homology across all vertebrate clades conversely suggests that this is potentially a rich source of phylogenetically meaningful variations. If cranial musculature of vertebrates were so conservative that homology is obvious, there would have been no meaningful phylotypic variations, and that would have provided no merit to a comparative approach in the first place.

3.4.2.1. Phenotypic criteria

There are partly overlapping phenotypic criteria for each type of similarity. Functions are evaluated based on behaviours and kinematics. Developmental similarity may be established by myogenic precursors and position amongst other mesodermal derivatives at the onset of differentiation of individual muscles. Patterning of the mesoderm by signals from the surrounding tissues and by gene expression domains within it provide a basis for the importance of the position of myogenic precursors at stages immediately preceding the onset of individual muscle differentiation. Antagonizing signals from the *Retinoic Acid*, *FGF*, and *BMP* pathways from the peri-mesodermal tissues such as the neural tube and pharyngeal arches establish anteroposterior and lateromedial coordinates and specify precursors of the extraocular, jaw, branchiomeric, and cardial muscles (Tajbakhsh et al. 1997; Hacker and Guthrie 1998; Mootoosamy and Dietrich 2002; Tzahor et al. 2003; Bothe and Dietrich 2006; von Scheven et al. 2006; Bothe et al. 2007, 2011; Tzahor 2009). In concordance with the signalling landscape, topographically restricted gene expressions in the myogenic mesoderm (e.g., myogenic regulatory factors; comprehensive review by Sambasivian et al. 2011) specify fates of muscles into head versus trunk, prechordal/paraxial versus visceral, and mandibular versus other pharyngeal arches in a wide variety of vertebrates from lampreys to mice and chicks (Hatta et al. 1990; Holland et al. 1993; Weintraub et al. 1993; Hacker and Guthrie 1998; Gage et al. 1999; Mootoosamy and Dietrich 2002; Alvares et al. 2003; Kusakabe et al. 2004, 2011; Kusakabe and Kuratani 2005; Bothe and Dietrich 2006; Bothe et al. 2007; Sambasivan and Tajbakhsh 2007; Knight et al. 2008; Hinits et al. 2009; Sambasivan et al. 2009; Adachi et al. 2012). In addition, this is as early a developmental stage as could be reconstructed for all of hagfish, lampreys, and gnathostomes with available data.

Morphological similarity draws upon many phenotypic criteria: nerve innervation, vascular irrigation, attachment to cartilages, associated connective tissues such as tendons and fascia, and functional and topographical correspondence with surrounding muscles. Amongst these associated tissues, neural crest cells give

rise to Schwann cells and sensory neurons of the cranial nerves, visceral cartilages and sensory capsules, and connective tissues; the paths of the cranial nerves follow migration of the crest cells (Noden 1978a, b for chick-quail chimeric embryo; reviewed in Hall 2009). Not only are there spatial and temporal correlations between differentiation of neural crest-derived ectomesenchyme and cranial myogenesis (Noden 1983a; McClearn and Noden 1988; Noden and Trainor 2005; Noden and Francis-West 2006), various myogenetic defects in genetic perturbation and ablation experiments provide evidence that neural crest-derived ectomesenchyme regulate migration, patterning, and differentiation of individual cranial muscles (Rinon et al. 2007; Grenier et al. 2009; Minoux et al. 2009; Heude et al. 2010). Because each cranial nerve follows the origins and paths of a population of neural crest cells, the innervation pattern is a particularly useful guide for an analysis of muscle configurations (Figure 3-15). Apart from induction by the neural crest-derived cells, topographically close myogenic precursors may be specified from muscle configurations in adults. Loss of function of the *Ret* signalling pathway caused myogenetic defects affecting just opercular muscles in zebrafish, but *Ret* expression was not lost after ablation of the cranial neural crest (Knight et al. 2011). The pharyngeal endoderm may also be responsible for some of the cranial muscles that originate in the adjacent area (von Scheven et al. 2006; Knight et al. 2008). These latter examples provide a developmental basis for using topographical relationships amongst muscles, and with the pharynx, as phenotypic criteria.

The following comparison of musculature treats the visceral muscles of ammocoetes (Figure 3-3) as distinct from those of adult lampreys (Figure 3-2). There is disagreement in the early literature over whether ammocoete muscles are precursors of adult muscles (Tretjakoff 1929) or those present in adults derive from mucocartilage (Kaensche 1890; Bujor 1891; Schneider 1879). The visceral muscles of adult lampreys differentiate from blastema as those in ammocoetes degenerate during metamorphosis (Damas 1935; Balabai 1946; Johnels 1948; Hardisty and Rovainen 1982). Therefore, it is best to treat these muscles as distinct traits except for several branchial muscles that persist into the adult.

3.4.2.2. Somatic muscles

Although muscles derived from myotomes vary in patterns of differentiation into individual muscles, they are overall congruent developmentally, functionally, and morphologically across vertebrates (Tables 3-1, 2, 3). At the level of myomeres, the congruence even extends to cephalochordates. In both hagfish and lampreys, dorsal somatic muscles extend anteriorly into the cranial region and have supraoptic and suboptic components. Gnathostomes are characterized by epaxial and hypaxial musculature separated by myosepta and the presence of cucullaris; the lamprey myomeres are already patterned dorsoventrally by expression of the orthologues of the genes that specify the hypobranchial, cucullaris, and fin muscle progenitors in gnathostomes (Kusakabe et al. 2004, 2011; Kusakabe and Kuratani 2005). It remains unknown whether the myomeres are similarly patterned dorsoventrally in hagfish, but m. obliquus and m. rectus morphologically correspond to m. hypobranchialis and the ventral portion of m. parietalis in lampreys (Figure 3-2A). Hagfish do not have the prebranchial differentiation of the dorsal somatic muscle, which would correspond to m. cornealis and m. probranchialis in lamprey adults (m.con and m.spo; Figure 3-2A). The absence is probably functional rather than phylogenetic, because the eyes are reduced and because the branchial series is displaced posteriorly in hagfish. The pharyngeal ventral somatic muscles are closely associated with the pharynx in gnathostomes, but are separated by the branchial series and by the lingual apparatus in hagfish and lampreys. This difference indicates two evolutionary changes that are crucial to the gnathostome body plan, namely reduction of the lingual apparatus and internalization of the branchial skeleton, where the latter is probably related to the origin of the hard internal skeleton.

3.4.2.3. Absence of extraocular muscles

Hagfish have neither extraocular muscles nor motor neurons that would have innervated them (oculomotor, trochlear, and abducens nerves; cranial nerves III, IV, and VI). The extraocular muscles are highly conserved among vertebrates from

lampreys to humans except for one change in the site of origin for m. obliquus superior (m. obliquus posterior) in lampreys (Figure 3-2F; Neal 1918; Fritzsch et al. 1990). Extinct placoderms had a pattern similar to lampreys (Young 2008), and even conodonts may have had extraocular muscles (Gabbott et al. 1995). Hagfish either did not have extraocular muscles ancestrally or lost them altogether. However, degeneration of extraocular muscles is rare even amongst vertebrates with degenerated eyes. All extraocular muscles may be present in the fossorial moles, some blind troglodyte salamanders, and troglodyte blatulas (Eigenmann 1909). The muscles may be underdeveloped but present in vertebrates with poor or no vision, such as the fossorial naked mole rat, the blind typhlopid snake *Typhlopus*, the troglodyte blind cavefish *Phreaichthys*, blind catfish *Troglogranis* and *Satan*, and the amblyopsid fish *Troglichthys* (Eigenmann 1909; Langecker and Longley 1993; Berti et al. 2001; McMullen et al. 2010). In the last case, motor innervation by the cranial nerves is absent. Nonetheless, extraocular muscles are absent in the fossorial amphisbaenians, some troglodyte salamanders, and some troglodyte amblyopsid fish (Eigenmann 1909; Foureaux et al. 2010).

Although hagfish may have secondarily lost extraocular muscles, this hypothesis requires several *ad hoc* explanations, because there is no evidence that hagfish had bona fide vertebrate eyes ancestrally. The indisputable fossil hagfish *Myxinikela* and the putative fossil hagfish *Gilppichthys* (Bardack and Richardson 1977; Bardack 1991) from the Westphalian, Pennsylvanian (300 MYA) both had small eyes. With due reservation for the nature of fossil evidence, there is no trace of extraocular muscles (Bardack 1998). The eyes being closer together near the dorsal midline plus the absence of a cartilaginous braincase wall in hagfish leaves a doubt if there could have been any room for attachment of extraocular muscles. If hagfish secondarily lost extraocular muscles, the event preceded the fossil taxa.

The rudimentary eyes of hagfish are often interpreted as degenerative in the context of a deep-sea habitat. However, some hagfish live in shallow depths less than 100 m from the surface (even occasionally appearing in the intertidal zone; Fernholm 1998; Cavalcanti and Gallo 2008), including the Pensylvanian fossil forms (Badack

1998). Other deep-sea fish tend to increase visual acuity rather than reduce it, and exceptions to this trend (and troglodytes) tend to have well-developed electrosensory or mechanosensory system; but hagfish have neither well-developed visual nor electrosensory systems (Bullock et al. 1983), and their lateral line system is as rudimentary as the eyes (Kishida et al. 1987; Wicht and Northcutt 1995; Braun and Northcutt 1997). Although hagfish have sensitive mechano- and chemoreception with the barbels and olfactory epithelium (Georgieva et al. 1973; Theisen 1973; Holmberg and Lundin 1973; Andres and Düring 1993), it is puzzling that highly predatorial hagfish (Martini 1998; Zintzen et al. 2011) have degenerate sensory systems that are well-developed in other predatorial deep sea species and have developed the sensory barbels and acute olfaction instead, if they had highly sophisticated vertebrate eyes equipped with fully developed extraocular muscles in the first place. It is reasonable to hypothesize instead that the hagfish eye and lateral line systems reflect their basal phylogenetic position, and that the barbels and olfactory apparatus complement the rudimentary eyes and lateral lines. Consistent with this hypothesis, hagfish eyes are comparable in function to the vertebrate pineal organ rather than to a visual, image-forming eye. Their similarity to the eyes of ammocoetes hints at the possibility that the eyes of lampreys may have independently evolved (Lamb et al. 2007).

That said, developmental fate of the prechordal mesoderm in hagfish should be closely observed. Precursors of most of the extraocular muscles arise in this region in response to signalling from the neural tube (von Scheven et al. 2006), and express *Pitx2* that regulate myogenic regulatory factors (Sambasivan et al. 2009; Kusakabe et al. 2011). As the development of reduced extraocular muscles in fossorial or troglodyte vertebrates indicate (Langecker and Longley 1993; McMullen et al. 2010), the presumptive precursors in hagfish could undergo vestigial myogenesis prior to degeneration or develop into tissues other than extraocular muscles. The former case would support secondary loss.

3.4.2.4. Muscles in the upper lip

In both hagfish and lampreys, numerous muscles occur in the upper lip. However, surprisingly little homology can be established based on similarity criteria between the two taxa (Figure 3-16; Table 3-4). None of the homology proposed by Mallatt (1996) is supported (m. subnasalis profundus with m. levator labialis in gnathostomes and m. buccalis anterior in ammocoetes; m. lingual tetacularis with m. labialis posterior in holocephalans, m. elevator labialis ventralis in ammocoetes, and peri-buccal muscles in cephalochordates; and m. palatolingualis superficialis et profundus and m. cornual lingualis with m levator anguli oris posterior in holocephalans, m. levator labii superioris in elasmobranchs, and m. constrictor buccalis in ammocoetes). These muscles may be similar to each other in function, but developmental and morphological characteristics are incongruent (Tables 3-1, 3-2, 3-3). Even the potential homologues in this region (Table 3-4) only show partial congruence. Their attachment sites, functions, and general morphology are not identical. M. basilariglossus of lampreys (m.bag; Figure 3-2B) has clear morphological and functional resemblances to the group of facial muscles that suspend the lingual apparatus in hagfish (m. palatolingualis profundus, m. cornual lingualis; m.plp, m.coi; Figure 3-1B), but it cannot be resolved based on morphological information alone whether one or both of the hagfish counterparts represent homologues. Similarly, topographical correspondence identifies m. lingual tentacularis and m. nasolingualis (m.lt, m.nl; Figure 3-1C) as possible homologues to m. spinocopularis and m. tectospinosus respectively (m.spc, m.tsa, m.tsp; Figure 3-2A, C, D). However, functions and attachment sites are modified. M. spinocopularis of lampreys is involved in the movement of the funnel, whereas m. lingual tentacularis of hagfish extends the barbels. M. tectospinosus anterior et posterior of lampreys extend the funnel and move the stylet cartilage, and do not suspend the lingual apparatus as m. nasolingualis of hagfish does. The latter two homologies are provisional.

These numerous incongruences imply differences in body plans. As discussed in Chapter 2, the distinguishing feature of cyclostome anatomy is the extent of the

nasohypophyseal complex. In hagfish, the nasal tube extends far beyond the mouth anteriorly. In lampreys, the oral hood is well developed, whereas the nasohypophyseal aperture opens anterodorsally. The similarity of cartilages breaks down in this region (Chapter 2). Muscles in the same position with respect to some anatomical landmark such as the mouth or nasohypophyseal aperture, or those that perform similar functions, may not have a congruent attachment site or innervation pattern, and vice versa. This is not to say that each of the muscles that do not have homologous counterparts between the two taxa (Table 3-4) is a neomorph. Rather, the inability to establish homology in this region indicates changes in developmental patterning of the cheek process, as the upper lip as a whole is comparable between hagfish and lampreys.

The two prominent functions of the upper lip muscles in hagfish are the suspension, protraction, and retraction of the lingual apparatus and control of the skeletons of the barbels via elevation of the upper lip. In contrast, the upper lip muscles of lampreys (both ammocoetes and adults) either control the oral hood or suspend the perioral cartilages from the tectal cartilages (Table 3-1). The suspension of the lingual apparatus in this region is minor in lampreys, and involves only m. basilariglossus (m.bag; Figure 3-2B). The cyclostome upper lip is developmentally not comparable to the maxillary process of gnathostomes, because the latter forms from the more posterior region of the mandibular domain (Shigetani et al. 2002, 2005; Kuratani 2012). Therefore, the muscles in the upper lips of holocephalans and elasmobranchs (Song and Boord 1993; Mallatt 1996) are not homologous with those in hagfish and lampreys. The implication is that the maxillary branch of the trigeminal nerve in gnathostomes may not be a homologue of the anterior branch of the trigeminal nerve in cyclostomes either (Lindström 1949).

Osteostracans have paired muscle scars on the roof of the oral cavity near the anterior margin and close to the midline, and the muscles were innervated by the anterior branch of the trigeminal ‘maxillomandibular’ nerve (Figure 2-15; Stensiö 1927, 1932; Wängsjö 1952; Janvier 1981, 1985). Reconstruction of the muscles suggests that they inserted onto the oral plates or near them (Janvier 1996, 2007).

The dorsomedial orientation of the muscle and the topology of the muscle attachment are strikingly similar to m. nasolingualis in hagfish, if the oral plates and the anterior edge of the lingual apparatus are both interpreted as the posterior margin of the mouth. The innervation of the osteostracan feeding muscle was near the terminal end of the anterior branch (Stensiö 1927, 1932; Wängsjö 1952; Janvier 1981a, 1985), which is also the case in m. nasolingualis in hagfish. Given the medial position of the origin, no muscles in adult or larval lampreys mimic these conditions. Without information about other soft tissue structures, it would be premature to assume homology, and osteostracans are generally considered more similar to lampreys than to hagfish, particularly based on the morphology of the nasohypophyseal complex (Stensiö 1927, 1932, 1958, 1964, 1968; Janvier 1981b, 1996, 2007). This uncanny similarity implies that the soft tissue anatomy in the oral region has a complex history among early vertebrates.

3.4.2.5. Velar muscles

The difficulty with identifying similarity in the velar muscles between hagfish and lampreys is that the orientation and length of the velar skeleton varies not only between hagfish and lampreys, but also between the ammocoetes and adults of lampreys (see Chapter 2). The flexor of the velar skeleton (m. craniovelar posterior; m.vp; Figure 3-8) is functionally similar to m. depressor veli in lamprey adults (m.dev; Figure 3-2G). The nerve innervation is by the mandibular branch for lampreys, whereas the velar branch innervates m. craniovelar posterior in hagfish (Figure 3-15D, G). The proximal portion of the velar skeleton in lamprey adults is close to the posteroventral corner of the expected mandibular domain, which typically receives innervation by the mandibular ramus, but the velar branch is also in proximity (Kuratani et al. 1997). The proposed homology between m. craniovelar posterior and m. depressor veli is therefore provisional.

The extensors of the velar skeleton (m. craniovelar anterior dorsalis et ventralis, m. spinovelaris) cannot be homologized to specific muscles in lampreys. The nerve innervation is the same as in the velar extensor in lampreys (Figure 3-15),

but the attachment sites and general morphology (including orientation) are not perfectly congruent. Therefore, these muscles can be compared at the level of the group of the velar extensors, but not to the level of individual muscles.

3.4.2.6. Muscles of the lingual apparatus

The similarity of the lingual apparatus between hagfish and lampreys is striking, but the homology is not perfect as Yalden (1985) implied (Figure 3-16; Tables 3-1, 3, 4). The attachment sites and functions differ between the two taxa associated with different feeding strategies in hagfish and lampreys. The protractors of the dental apparatus wrap around the anterior edge of the lingual apparatus and insert onto the free, mobile dental apparatus in hagfish. In lampreys, the corresponding muscles are retractors (Figure 3-2). They insert onto the annular and stylet cartilages and pull the funnel to expose the apical tooth plates (Hilliard et al. 1985; Kawasaki and Rovainen 1988; Rovainen 1996). These muscles are nonetheless topographical counterparts of each other. Both m. protractor dentalis lateralis in hagfish (m.pdl; Figure 3-6A) and m. copuloglossus rectus in lampreys (m.cgr; Figure 3-2B) originate more posteriorly on the lateral surface of the posterior element of the lingual apparatus than their counterparts on the medial side. These muscles are innervated by the most distal motor branch of the trigeminal nerve (Figure 3-15; Lindström 1949). In lampreys, m. copuloglossus obliquus protracts the apical tooth plates when the funnel is retracted (m.cgo; Figure 3-2C). No muscle in hagfish corresponds to it.

The lateral retractor of the dental apparatus in hagfish (m. retractor dentalis lateralis; m.rdl; Figure 3-1C) originates from the contact between the lingual apparatus and the first external pharyngolingual arch, the latter of which likely belongs to the hyoid domain (Chapter 2). The lamprey counterpart originates from the styliform cartilage of the hyoid domain (m.sta; Figure 3-2D). The major midline retractor in hagfish (m. retractor dentalis major; m.rdm; Figure 3-9) attaches to the distal lingual cartilages and their associated connective tissues, with the branchial series displaced posteriorly. In lampreys, the retractor (m. cardioapicalis; m.cap;

Figure 3-2H) extends between the branchial pouches along the midline all the way back to the pericardial cartilage. M. retractor lingualis and m. perpendicularis in hagfish (Figure 3-9) stabilize the distal lingual apparatus for the retraction of m. retractor dentalis major. There is no muscle in lampreys that corresponds to m. perpendicularis. Like m. retractor lingualis in hagfish, m. constrictor cornualis superficialis and m. constrictor glossus internus (m.ccs, m.cgi; Figure 3-2B, E) together wrap around m. cardioapicalis and constrict the lingual apparatus. Therefore, these muscles topographically and functionally correspond to m. retractor lingualis in hagfish. However, the position is substantially more proximal in lampreys, and the muscles are attached to the cartilage of the hyoid domain. Topographically (ventral portion of mandibular domain) and functionally (transverse constriction), these muscles may correspond to the intermandibular muscle in gnathostomes (m.imd, ima; Figure 3-4). However, the absence of the lingual apparatus precludes further analysis.

Again, different feeding strategies between hagfish and lamprey adults provide a functional explanation. Hagfish grasp food by protracting and everting the dental apparatus, and rely on forceful retraction of the dental apparatus for tearing apart and ingesting the food (Clark and Summers 2007; Clark et al. 2010). Posterior displacement of the branchial series accommodates the hypertrophied retractor system (Figure 3-9). The progressively posterior position of the branchial series from fossil to living hagfish (Bardack 1991, 1998; Janvier 1996) documents this transition. A posterior migration of the presumptive branchial series also occurs during embryogenesis of hagfish (Dean 1899; von Kupffer 1900; Stockard 1906; Holmgren 1946). Consequently, the retractor is outside the branchial region. The distal lingual cartilages provide attachments for the retractor, and the circular and perpendicular muscles aid in contraction of the retractor. On the other hand, lampreys retract the funnel and expose the apical teeth, but the dental apparatus does not slide over the lingual apparatus as freely as that of hagfish because lampreys remain attached to prey while feeding (Hilliard et al. 1985; Kawasaki and Rovainen 1988; Rovainen 1996).

It is difficult to determine whether hagfish or lampreys are closer to an ancestral vertebrate condition. The biomechanics of conodont teeth (Goudemand et al. 2011) suggests that the feeding apparatus powered by protractors and retractors existed in jawless vertebrates other than hagfish and lampreys. However, it remains unknown whether the condont system was more similar to hagfish or lampreys because of the uncertainty about the presence of external gill slits in conodonts (Turner et al. 2010). Conodonts also have paired posterior teeth either vertically oriented and occluded lateromedially (Purnell and von Bitter 1992; Purnell 1995; Purnell and Donoghue 1997; Donoghue and Purnell 1999) or lateromedially oriented and occluded obliquely toward the midline (Goudemand et al. 2011). Either way, there would have been no space for either hagfish-like or lamprey-like retractor system, unless the retractor was attached to the bases of the posterior teeth. In addition, no muscles known in hagfish or lampreys could remotely produce the motion of the posterior teeth reconstructed either by Purnell (1995) or by Goudemand et al. (2011), unless the branchial constrictors were highly modified and reorganized. The same is true for M elements, the anterior lateral teeth (Donoghue and Purnell 1999; Goudemand et al. 2011). The protractor-retractor systems with basal cartilages and distal attachment known for hagfish and lampreys could not extend onto the lateral component. Given the small body size, the feeding strategy of conodonts probably differed significantly from those of hagfish and lampreys, and it would not be surprising if conodonts deviated from hagfish and lampreys in morphology of the lingual apparatus. The implications are that the lingual apparatus with protractors and retractors likely represent a plesiomorphic condition to vertebrates, and that the apparatus experienced independent specialization along each lineage.

3.4.2.7. Absence of jaw muscle homologues

Almost none of the gnathostome jaw muscles is morphologically readily comparable to muscles of hagfish and lampreys described so far, because neither hagfish nor lampreys have unequivocal homologues of the gnathostome mandibular

skeleton and the mandibular branch of the gnathostome trigeminal nerve. Only m. intermandibularis is similar to the constrictors of the lingual apparatus topographically and functionally (Table 3-4), but this similarity may be due to convergence. The gnathostome *Dlx* code is essential in the development of masticatory muscles (Heude et al. 2010). Morphologically and developmentally, the gnathostome jaw muscles represent neomorphs dependent on the *Dlx* code expressed in the cranial neural crest cells only in that clade.

3.4.2.8. Muscles in the hyoid domain

Hagfish have three prominent muscles innervated by the facial nerve: the superficial m. palatolingualis superficialis and m. craniolingualis, and the deep m. otic lingualis (Figure 3-15B, C). The muscles innervated by the facial nerve in lampreys are part of the branchial motor system (Figure 3-15 H-K). In hagfish, however, the muscles in the hyoid domain suspend the lingual apparatus. M. palatolingualis superficialis and m. craniolingualis (m.pls, m.cl; Figure 3-6A) extend anteriorly to overlap muscles innervated by the trigeminal nerve. The position of m. craniolingualis is similar to the one occupied by m. cornuoglossus in lampreys (m.cgl; Figure 3-2B), and the attachment sites are also comparable. However, m. cornuoglossus is innervated by the mandibular branch of the trigeminal nerve (Figure 3-15I). Either the muscles or motor innervation changed, but this cannot be determined based on the morphology of hagfish and lampreys alone.

3.4.2.9. Branchial muscles

M. constrictor pharyngis (m.cp; Figure 3-1B) connects the chondrocranium and branchial series in hagfish. The anterior portion of this muscle receives innervation by the glossopharyngeal nerve, whereas the rest is innervated by the vagus nerve. Because the branchial series is closely associated with the rest of the head in other vertebrates, m. constrictor pharyngis is unique to hagfish and has no homologue in other vertebrates. Motor neurons of the branchiomeric nerves extend into the post-trematic branch (Johnston 1905; Goodrich 1930; Sperry and Boord

1993). The glossopharyngeal innervation of m. constrictor pharyngis indicates that the most anterior gill in hagfish corresponds to the second or more posterior branchial arch in lampreys and gnathostomes.

M. constrictor branchialis in hagfish is simple compared to that of the powerful branchial motor systems in lampreys and gnathostomes (Figures 3-2, 3, 4). The muscle is too weak to contribute to constant active ventilation. The paths of the muscle over and between the branchial pouches are similar to the external constrictors and interbranchial constrictors in other vertebrates. However, it cannot be homologized to individual muscles.

3.4.2.10. Phylogenetic implications

As is the case for cartilages (Chapter 2), hagfish share more potentially homologous muscles with lampreys than with any other chordates (Figure 3-16; Table 3-4). Unfortunately, several muscles potentially shared between hagfish and lampreys occur in both the upper lip and lingual apparatus. The former is not comparable to the maxillary process of gnathostomes, and the latter does not exist in gnathostomes or cephalochordates. This means that the homologies are phylogenetically uninformative. If all outgroups to cyclostomes have neither the cyclostome upper lip nor lingual apparatus, muscles associated with these structures cannot exist either. Cladistically, proper coding of these characters is not absence ("0") but inapplicable ("-") or missing ("?"). Neither an inapplicable or missing state computationally gives support for any relationship whatsoever, because the characters can be scored only for hagfish and lampreys, both of which have the muscles. The only solution to incorporate these muscles into a phylogenetic analysis as informative characters is to find a homologue of the cyclostome upper lip or the lingual apparatus in non-cyclostome taxa. Because morphological similarity breaks down, however, comparative morphology cannot identify such homologues.

Nevertheless, an oral apparatus functionally and morphologically similar to the cyclostome lingual apparatus likely existed in conodonts (Goudemand et al. 2011). The feeding muscle functionally and topologically similar to m. nasolingualis

in hagfish existed in osteostracans. Coupled with minor differences in the morphology of the lingual apparatus between hagfish and lampreys that correspond to their different feeding strategies, the similarities between hagfish and lampreys could very well reflect plesiomorphic conditions in vertebrates rather than explicitly support Cyclostomata as the monophyletic clade of hagfish and lampreys. Although reduced in lampreys, the branchial constrictors are also a broadly conserved feature across vertebrates.

The conservation of somatic muscles is reassuring (Table 3-4). Cephalochordate myomeres are an obvious candidate for a homologue with myomeres in vertebrates, and the cephalochordate pterygial muscles correspond to the hypobranchial musculature of vertebrates based on the ventral position and association with the gut and innervation by the visceral motor neurons of the spinal nerve (Goodrich 1930; Jefferies 1986; Fritzsch and Northcutt 1993). Therefore, this pattern may have been conserved not just across vertebrates, but across chordates.

Few muscles in lamprey ammocoetes are similar to those of hagfish (Figure 2-3; Table 2-4). This incongruence is partly because the ammocoete chondrocranium is not developed well enough to allow comparison of attachment sites, and partly because the filter-feeding specialization of ammocoetes resulted in a configuration of muscles not comparable to that in hagfish. The large number of homologues between hagfish and lamprey adults is equally compatible with the hypothesis that ammocoetes represent a neomorphic larval stage inserted into the life history of lampreys, and with the hypothesis that hagfish secondarily lost the larval stage. If this is viewed as near absence of the probable vertebrate symplesiomorphies in ammocoetes, however, it is more consistent with the former hypothesis. In that case, similarities in feeding style and overall morphology between ammocoetes and cephalochordates are likely convergent.

3.4.3. A New Hypothesis for Early Vertebrate Evolution

3.4.3.1. Traditional and new hypotheses on early vertebrate evolution

Hagfish provide crucial insights into two long-standing problems in vertebrate zoology: the origin of vertebrates and the origin of gnathostomes. Traditionally, comparative morphological approaches interpreted the vertebrate head mesoderm as segmented as it is in somites (Figure 3-17B; Goethe 1790, 1820; Oken 1807; Balfour 1878; Gaupp 1898; Johnston 1905; van Wijhe 1915; Goodrich 1909, 1918, 1930; de Beer 1937; Bjerring 1977, 1984; Jollie 1977; Jarvik 1980; Jefferies 1986). This notion is now discredited by a body of developmental evidence, but has heavily influenced evolutionary scenarios for vertebrate origins (reviews and critiques in Gregory 1936, 1946; Romer 1972; Gee 1996; Northcutt 1993, 2008; Thomson 1993; Kuratani 2004a, 2008a; Adachi and Kuratani 2012; Adachi et al. 2012). Likewise, the jaw has long been interpreted as a modification of the mandibular arch. Discussion centered over how to derive the jaw skeleton from a typical pharyngeal arch skeleton (Goodrich 1909, 1930; de Beer 1937; Bjerring 1977; Jollie 1977; Jarvik 1980; Jefferies 1986), or, more recently, how the mandibular arch acquired genetic patterning that allowed specialization of the jaw skeleton (Depew et al. 2001, 2005; Shigetani et al. 2002, 2005; Cerny et al. 2004a, b, 2010; Kuratani 2004a, b, 2005, 2012; Kuratani et al. 2004, 2012; Depew and Simpson 2006).

Among evolutionary models for vertebrate and gnathostome origins, the New Head Hypothesis identified the neural crest as the key vertebrate novelty (Gans and Northcutt 1983; Northcutt and Gans 1983), an idea that most subsequent studies have followed. However, predictions of this model and its subsequent versions (Gans 1993; Northcutt 2005) have little support. The neural tube is comparable across chordates even to the anterior domain (Lacalli et al. 1994; Lacalli 1996, 2001, 2008a, b; Schilling and Knight 2001; Reichert and Simeone 2001; Wicht and Lacalli 2005; Imai et al. 2009; Stolfi and Levine 2011; Wagner and Levine 2012), which rejects a central element of the New Head Hypothesis that the vertebrate forehead is a neomorph (Kuratani 2004a).

Ventilation Hypothesis of Mallatt (1996, 2008) is not supported by the comparative morphological analysis presented here (Chapter 2 and this chapter), and is contradicted by genetic and developmental evidence for heterotopy of oral patterning gene expression (Shigetani et al. 2002, 2005; Kuratani 2012). On the other hand, the genetic and developmental evidence for heterotopy in oral patterning gene expression has not provided a complete picture of early vertebrate evolution. A beautiful union of the developmental approach and fossil evidence provided a convincing scenario in which diplorhiny preceded the origin of the jaw (Janvier 1996, 2007; Shigetani et al. 2002, 2005; Kuratani 2004a, b, 2005; Kuratani and Ota 2008; Gai et al. 2011). This is tied to the origin of true trabecula (Couly et al. 1992, 1993; Kuratani et al. 2012). The patterning and specification of body musculature also links the cucullaris and the origin of the neck (Kusakabe et al. 2004, 2011; Kusakabe and Kuratani 2005; Kuratani 2008b). With a vertebrate-like neural crest origin (Ota et al. 2007) and with possible vertebral homologues (skeletal support for the caudal fin; Ota et al. 2011), the body plan of hagfish is now interpreted as a subset of the vertebrate body plan (Kuratani 2004a; Kuratani and Ota 2008). These are impressive accomplishments, but the shifts in developmental patterning have not been incorporated into a comprehensive model of early vertebrate evolution.

In these highly innovative studies, the jaw is still regarded as derived from the mandibular arch. Comparison across gnathostomes certainly reinforces that assumption. The jaw and branchial arches are obvious serial homologues in these animals, because the mandibular arch takes on the basic morphology of the posterior pharyngeal arches (Goodrich 1909, 1930; de Beer 1937; Bjerring 1977; Jarvik 1980; Jefferies 1986; Kuratani 2004a). However, my detailed examination of hagfish cranial morphology, and my comparisons with lampreys and gnathostomes, suggests an alternative to this long-standing assumption in vertebrate zoology. Namely, the jaw may have evolved as a result of: 1) a limitation of the differentiation and specialization of the mandibular domain; and 2) anterior transfer of identity as a pharyngeal arch onto the defaulted mandibular domain. The new model of early vertebrate evolution proposed here incorporates earlier findings, but it rejects two

traditional assumptions: the head is, segmented and the jaw is a specialized mandibular arch.

3.4.3.2. Mandibular Siege Hypothesis

The Mandibular Siege Hypothesis associates the origin of vertebrates with the neural crest, and the origin of the jaw with delineation of the mandibular domain. As such, the emphasis is on evolutionary changes that facilitated, accompanied, or constrained the two morphogenetic events (Figures 3-17, 3-18; Table 3-5). This hypothesis interprets early vertebrate evolution as a mosaic of modifications to head patterning leading toward a mandibular arch serially homologous to the branchiomeric pharyngeal arches. The mandibular domain shows a variety of specializations across early vertebrates, and also an increasing trend of delimitation by premandibular, mandibular, hyoid, and somatic domains. This hypothesis differs from previous models in proposing that the mandibular domain did not originally evolve as a serial homologue of the pharyngeal arches. Instead, the mandibular domain arose in the beginning as a highly specialized and differentiated domain specific to the anterior oropharyngeal region and as a bridge between the preoral premandibular domain and the postoral, branchiomeric head. The origin of the jaw required delimitation of the mandibular domain first, or, in other words, defaulting the mandibular domain into a serial homologue of the branchiomeric pharyngeal arches. This hypothesis therefore predicts that the default pharyngeal-arch state of the mandibular domain in vertebrates is derived, not ancestral. The neural crest and its ectomesenchyme are central to this Mandibular Siege Hypothesis, but also important are tissues and regions involved in signaling that patterns surrounding tissues. Examples include notochord, neural tube, gut endoderm, somites and placodes (updated review in Gilbert 2010).

3.4.3.3. Vertebrate origins

Neural crest derivatives and downstream tissue interactions accounts for the majority of vertebrate synapomorphies (Gans and Northcutt 1983; Northcutt and

Gans 1983; Hall 2009; Table 3-5). The developmental and evolutionary origin of the neural crest are fascinating topics extensively discussed elsewhere (e.g., Hall and Gillis 2012). Whatever evolutionary antecedent for the vertebrate neural crest may exist in non-vertebrate chordates, the origin of the neural crest can be equated to acquisition of the migratory capability of the dorsal neural plate border and the formation of substantial ectomesenchyme populations, both observed in vertebrates only (Hall 2009). This paper accepts that position, and restricts the neural crest to vertebrates. This paper restricts the usage of ectodermal placodes to vertebrates for similar reasons (Schlosser 2005, 2008). The main interest here is in the set of conditions that allowed such a remarkable proliferation and diverse differentiation of neural crest-derived ectomesenchyme in the ancestral vertebrate head.

The Mandibular Siege Hypothesis postulates an ancestral vertebrate as a motile, somitomeric and branchiomeric chordate akin to the somitovisceral animal postulated by Romer (1972), except that this hypothetical ancestor a) lacked segmentation of mesoderm above the mouth and b) truncated the anterior and preoral end of the notochord. This hypothetical ancestor can be derived from either cephalochordates or urochordates. The cephalochordate model requires an anterior truncation of the notochord and loss of segmentation in the mesoderm around the anterior end of the truncated notochord. On the other hand, the urochordate model posits that the notochord and mesoderm extended anteriorly without segmentation at these anterior extremes. Having said that, the presence of Rohon-Beard cells in the dorsal border of the neural plate of cephalochordates and in the neural tube of several vertebrates suggests that cephalochordates may the better model (Fritzsch and Northcutt 2003; Holland and Holland 2001). That domain in cephalochordates expresses *Snail* and likely is an antecedent of the neural crest (Holland and Holland 2001; Hall and Gillis 2012). A cephalochordate derivation is also convenient in that regional differentiation is minimal amongst chordates. If cephalization is a derived state for chordates, the first notochord and somites would have developed without regional axial differentiation, which would extend the notochord and somitomeres to the anterior end of the animal. Conversely, it is equally possible to derive both

cephalochordates and urochordates from this hypothetical ancestor. An addition of segmentation to the anterior mesoderm and anterior terminal growth of the notochord to the hypothetical ancestor would lead to cephalochordate body plan, whereas a loss of the mesoderm and notochord in the anterior region would lead to urochordate body plan. So, an animal like this could have been a pan-chordate ancestor.

At any rate, in the hypothetical vertebrate ancestor, the head had the anteriorly non-terminal notochord and unsegmented mesoderm, which would be intermediate in degree of reduction of the respective structures between cephalochordates and urochordates. The notochord only extends the full length and reaches the anterior end of the head during ontogeny in cephalochordates (Hatchek 1881), so the truncation could result from cessation of the growth. The vertebrate head mesoderm has gene expression patterns that are distinct from the somitomeric trunk mesoderm (Bothe and Dietrich 2006; Bothe et al. 2007); thus this distinct molecular profile may have specified the unsegmented anterior mesoderm ancestrally. The anterior truncation of the notochord and the loss of segmentation in the head would have accommodated functionally correlated size increases in sensory and feeding structures and cerebral ganglion in the head. The near absence of mesodermal tissue in the head region of ascidian tadpole larvae may be interpreted as a feature permitting an enlarged filter-feeding pharyngeal basket and sensory vesicle. The sensory and feeding structures in cephalochordates and urochordates are highly asymmetrical, perhaps because there is no space for pairs of such structures (Miyashita and Palmer in review). If true, the hypothetical vertebrate ancestor at the adult stage was probably 1) larger than living cephalochordates or ascidian tadpole larvae, 2) equipped with bilaterally symmetrical sensory and feeding structures and relatively large cerebral ganglion, and 3) highly active as a pelagic swimmer and filter feeder.

Without such an ancestral stage, the neural crest would have had little potential to differentiate and would therefore have experienced little selection. The non-terminal anterior notochord and the unsegmented head mesoderm are prerequisite not only to size increase of the organs, but also to the formation of the

ectomesenchyme that patterns the vertebrate head. In the presence of somites in the vertebrate trunk, most neural crest cells take intrasomitic pathways (Tosney 1978; Erickson and Goins 1995; Hall 2009), and the molecular landscape created by expression of signaling pathways such as *Eph* imposes the segmented pattern (Keynes and Stern 1984; Pasquale 2008; Kulesa et al. 2010). In the head, however, neural crest cells migrate over the mesoderm to form peripheral ganglia for cranial nerves and cause de-epithelialization at the interface to form a large population of ectomesenchyme (Figure 3-17A; Tosney 1982; Noden 1984; Hall 2009). Given that vertebrate synapomorphies facilitated by the neural crest (Table 3-5; Gans and Northcutt 1983; Northcutt and Gans 1983) occur mostly in the head, differentiation potentials of neural-crest derived cells could only have been exposed to selection in the absence of head somitomerism in the hypothetical ancestor.

Because extensive migration and labiality for tissue interaction underlie the differentiation potential of neural crest cells, a simple loss of segmentation in the head mesoderm would enable, but not directly facilitate, delamination, migration, and differentiation of the cells into tissues specific to the head. The vertebrate neural crest was likely preceded by neurogenic placode-like ectodermal specifications and the gut endoderm was likely pre-patterned by the stomodeum and branchiomerism, and possibly by rhombomeres (Figure 3-17A). Dealing with these structures one at a time, interactions between neurogenic ectodermal placodes and neural crest cells induce peripheral ganglia and sensory capsules or sensory epithelia (Schlosser 2005), and each of the placodes (olfactory-adenohypophyseal, profundal, lens, trigeminal, otic, lateral line, and epibranchial) is a bona fide vertebrate synapomorphy. It cannot be determined whether placodes or neural crest preceded the other. Different transcription requirements strongly suggest that placodes and the neural crest evolved independently (Schlosser 2008). Molecular evidence has recovered probable homologues of vertebrate placodes in urochordates (Wada et al. 1998; Manni et al. 2004, 2005; Bassham and Postlethwait 2005; Mazet and Shimeld 2005; Mazet et al. 2005; Kourakis and Smith 2007). Although these authors regarded the urochordate counterparts as placodes, the putative urochordate placodes lack the ability for

dynamic tissue interaction and the potential for diverse differentiation, which vertebrate placodes achieve through interaction with neural crest cells. In other words, in vertebrates placodes as presently recognized cannot exist without neural crest cells, and vice versa. Placode homologues and neural crest homologues likely co-existed along the main stem of chordates (Schlosser 2008), but placodes and the neural crest as vertebrate synapomorphies must have appeared simultaneously, when the neural crest homologue in the hypothetical ancestor underwent delamination and established developmental crosstalk with placode homologue or pan-placode (Schlosser 2005). In that context, whether placodes or the neural crest appeared first may be a futile debate.

Once neural crest cells developed as ectomesenchyme, the gut endoderm and rhombomeres determined distribution of cranial neural crest cells (Figure 3-17A). Between these two structures, at least the stomodeum with pharyngeal slits (all derived from gut endoderm) is a plesiomorphic condition in chordates and it almost certainly existed in the vertebrate ancestor (Chapter 4). Diverticula of the archenteron include the oropharyngeal cavity, pharyngeal slits, and the nasohypophyseal complex in hagfish (Chapter 2). Not only do pharyngeal slits set apart pharyngeal arches, the gut endoderm has the potential to induce differentiation of the ectomesenchyme in ways specific to the pharyngeal domains, and signals from the gut endoderm determine positional identities of the ectomesenchyme with respect to diverticula of the endoderm (Hunt et al. 1995; Couly et al. 1998, 2002). The ectomesenchyme that migrates into individual arches differentiate independently from each other and accordingly to the positional identities for and within the arch.

There are no somites that impose segmented pattern on the migration of neural crest cells in the vertebrate head. Instead, rhombomeres in the hindbrain constrain the migration of the cells (Figure 3-17A). In all vertebrates including lampreys, neural crest cells only migrate from the second, fourth, sixth, and seventh rhombomeres (Moody and Heaton 1983a, b, c; Lumsden and Keynes 1989; Guthrie and Lumsden 1991, 1992; Lumsden et al. 1991; Horigome et al. 1999), and the metameric pattern of the rhombomeres is associated with gene expressions specific

to certain segments including FGF and *Eph* signaling and *Hox* cluster, which also appears to be conserved across vertebrates (Schneider-Maunoury et al. 1993, 1997; Carpenter et al. 1993; Marin and Charnay 2000; Küry et al. 2000; Prin et al. 2005). Amongst these genes, genes closer to the 3' end of the *Hox* cluster are serially and collinearly expressed — one additional *Hox* per two rhombomeres — except for: 1) *Hoxb1*, which is specific to the fourth rhombomere; and 2) the first two rhombomeres, which are free of *Hox* expression (Sundin and Eichele 1990; Hunt and Krumlauf 1991; Hunt et al. 1991a, b, c; Krumlauf 1993; Schilling and Knight 2001; Trainor and Krumlauf 2001). The neural crest cells take on the *Hox* code of the rhombomere from which they migrate, and carry it to the pharyngeal domains that they fill. As a result, the premandibular and mandibular domains are *Hox*-free, hyoid domain and subsequent pharyngeal arches express *Hoxa2*, post-hyoid pharyngeal arches expresses *Hoxa3*, and the post-glossopharyngeal ones express *Hoxa4* (Hunt and Krumlauf 1991; Hunt et al. 1991a, b, c; Krumlauf 1993; Pasqualetti et al. 2000; Schilling and Knight 2001; Graham and Smith 2001; Trainor and Krumlauf 2001; Trainor et al. 2002; Oury et al. 2006). This cranial *Hox* code is conserved in both the hindbrains and pharyngeal domains of lampreys (Murakami et al. 2002, 2004, 2005; Takio et al. 2004, 2007). Therefore, this *Hox*-free 'default' condition of the mandibular domain is consistent with the Mandibular Siege Hypothesis, which posits that the domain does not develop originally as a pharyngeal arch but simply fills in the space between the premandibular and hyoid domains.

The cranial *Hox* code helps explain why the neural crest cells that migrate from different rhombomeres do not mix at the boundary (Köntges and Lumsden 1996). Clearly, rhombomeres are essential in regional differentiation of neural crest cell populations and, coupled with branchiomerism, explain the distribution of ectodermal placodes (and, in turn, branchiomeric nerves) correlated with particular rhombomeres. Urochordates have a pattern of gene expressions similar to the tripartite vertebrate brain, the most posterior domain being a likely homologue of the vertebrate hindbrain (Wada et al. 1998). The formation of the peripheral ganglia requires a boundary cap of the neural crest cells over the rhombomeres from which

the crest cells migrate (Altman and Bayer 1982; Kuratani 1991; Niederländer and Lumsden 1996). Then, rhombomeres probably preceded the evolutionary origin of the neural crest.

The characters discussed so far transform the hypothetical vertebrate ancestor into a hypothetical first vertebrate upon appearance of the neural crest. Crucially, the newly derived ectomesenchyme covering the face and filling in the visceral part of the head is patterned anteroposteriorly into distinct domains, and these domains are delineated by the gut endoderm (ps; Figure 3-17A). The preoral-nasobuccal region corresponds to the premandibular domain. The first pharyngeal lateral diverticulum or its external slit (which never opens in hagfish and lampreys) sets apart the hyoid domain posterior to it, and the second lateral diverticulum or the first branchial opening separates the hyoid domain anteriorly and the glossopharyngeal domain posteriorly, and so on. Each domain is filled by a distinct population of ectomesenchyme characterized by *Hox* code from the hindbrain. This way, the premandibular domain is confined to the nasobuccal shelf and the snout anterior to that by the mouth and between the eyes, and this region originally has no mesoderm component. The hyoid and post-hyoid domains are each a distinct pharyngeal arch. The mandibular arch, however, falls into neither of the categories. This is the *Hox*-free domain that occupied the large space between the confined premandibular and hyoid domains, or between the mouth and the first lateral pharyngeal diverticulum. The lip was neither a preoral shelf nor a pharyngeal arch.

As the mouth opens on the ventral midline, there was no lateral diverticulum of the gut endoderm that could form a sharp anterior boundary for the mandibular domain. The mandibular domain was only confined by the premandibular domain anteromedial to it and the first lateral pharyngeal diverticulum posterior to it. So the mandibular ectomesenchyme could spread in association with the gut endoderm anteriorly and posteriorly in the first vertebrate. It then overlapped the premandibular domain to form: 1) an upper lip extending within the dorsal fold of the pharynx posteriorly to form a velum; and 2) a lingual apparatus extending below the pharynx longitudinally. All of this corresponds to the body plan described so far for hagfish

and lampreys and was likely present in other jawless vertebrates (Figure 3-17 C-E). It also makes sense that the trigeminal crest cells that migrate to the premandibular and mandibular domains are *Hox*-free. This implies that this population of crest cells 1) is not committed to a specific branchial *Hox* code and is only limited by physical barriers (e.g., eyes, placodes, and facial crest cells that migrate to the hyoid domain), and 2) simply spreads over space not already filled in by other populations of the ectomesenchyme.

3.4.3.4. Early vertebrate evolution and the origin of the jaw

The origin of the jaw remains as an unresolved problem. Recent molecular evidence highlights *Dlx* code as a key innovation facilitating gnathostome body plan. Gnathostomes are characterized by a dorsoventrally patterned, cascading expression of the *Dlx* pathway, which is essential in the formation of the jaw and jaw muscles (Depew et al. 2001, 2005; Heude et al. 2010; Figure 3-17A). The region of the mandibular domain that expresses the *Dlx* pathway, and genes specifying the oral ectoderm, both shift posteriorly within the domain from lampreys to gnathostomes (Shigetani et al. 2002, 2005; Kuratani 2012). These findings suggest that the establishment of the *Dlx* code and heterotopy of *Dlx* expression domain led to the origin of the jaw. However, a causal relationship behind these events is unknown. The duplication of *Dlx* and its downstream genes long preceded the origin of the jaw, before the split of the lamprey and gnathostome lineages, and cannot explain the origin of the *Dlx* code (Kuraku et al. 2010). Dorsoventrally patterned expression of downstream genes of the *Dlx* pathway already exists in lampreys, with *dHand* expressed ventrally and *Edn* expressed orally (Cerny et al. 2010; Kuraku et al. 2010). The oral expression of *Edn-2* and *Edn-3* is lost in gnathostomes, and the expression of *Bapx* is restricted to the jaw joint in gnathostomes (Kuraku et al. 2010). Overall, the molecular mechanism behind the establishment of the gnathostome *Dlx* code is unknown, except that the ventrally expressed genes may have been co-opted in jaw formation (Cerny et al. 2010).

There are two ways to probe for the origins of the *Dlx* code and jaw. First, a genomic and functional analysis of *Dlx* and its pathway genes may reveal factors facilitating the gnathostome-specific expression patterns and cascade structure. However, there is no guarantee that such an approach could ever fully explain the origin of the jaw. Because extinct stem gnathostomes cannot be used for comparison, no rigorous test exists for causality between the *Dlx* code and the origin of the jaw. Related to that point, contrasting the cyclostome and gnathostome *Dlx* pathways could spiral into an endless search for the master control of master controls for each pathway — an attempt to reduce such a crucial phenotype as jaws into a single genetic factor far upstream from the mandibular morphogenesis. Little does this reductionist practice enlighten us about the complex patterns of early vertebrate evolution documented by fossils, as long as this problem is approached solely from a molecular perspective.

An alternative approach to complement the hitherto successful molecular genetic approach would be to identify phenotypic changes that may have contributed to the cyclostome- and gnathostome-specific *Dlx* expression patterns and affected the origin of the jaw. The Mandibular Siege Hypothesis does just this. It interprets early vertebrate evolution as a mosaic of innovations for spatial regulation of the mandibular domain, and the origin of the jaw as the point at which the mandibular domain became a pharyngeal arch as a result of these innovations.

In the previous section, the mandibular domain at the origin of vertebrates is reconstructed as the domain between the preorally confined premandibular domain, and the hyoid domain set between the first and second lateral pharyngeal diverticula (Figure 3-17A). As such, the mandibular domain shows a high degree of differentiation along the pharynx in jawless vertebrates (Figure 3-17C, E). With such a highly differentiated state, the mandibular domain may be inhibited from developing a jaw-like pharyngeal arch skeleton. Developmentally, the substantial ectomesenchyme required for a jaw skeleton may restrict such a highly differentiated domain from extensive remodeling. Evolutionarily, the highly differentiated mandibular domain must be compensated to produce such a novelty as a jaw. From

classical comparative morphology to molecular genetics, it is unanimously accepted that the jaw skeleton is a serial homologue of the dorsoventrally patterned branchial arches, and that the origin of the jaw can be explained morphologically as a forward bending of the pharyngeal arch skeleton and formation of the joint at the hinge (Goodrich 1909, 1930; de Beer 1937; Bjerring 1977; Jarvik 1980; Jefferies 1986; Janvier 1996; Mallatt 1996; Depew et al. 2001, 2005; Kuratani et al. 2001, 2012; Shigetani et al. 2002, 2005; Kuratani 2004a, b, 2005, 2012). Then, the origin of the jaw must default the highly differentiated mandibular domain into a serial homologue of a pharyngeal arch. In other words, the mandibular domain must be confined to the region lateral to the oral cavity. If true, any phenotypic and genomic change that spatially limits the mandibular domain to the mandibular arch would be a key innovation that potentially allows the making of a pharyngeal arch in the mandibular domain. The coincidental occurrence of all of these innovations in one lineage of jawless vertebrates resulted in the origin of the jaw. Undoubtedly, key innovations include co-option of the *Dlx* code (Depew et al. 2001) and heterotopy of genes for the mandibular ectomesenchyme and oral epithelium (Shigetani et al. 2002). But these events need not causally explain the origin of the jaw. At the onset of expression of these genes, a gnathostome embryo does not necessarily show cyclostome-like morphology. Rather, the cyclostome upper lip and the gnathostome jaw diverge from a similar pharyngula state, as illustrated by Kuratani (2012). Therefore, neither the *Dlx* code nor heterotopy alone could pattern a jawless vertebrate into a gnathostome. In other words, neither the *Dlx* code nor heterotopy could produce phenotypes significant enough for selection, if the embryo is constrained to develop into an adult with a highly differentiated mandibular domain including upper lip, velum, and lingual apparatus. A comparative morphological approach can recover phenotypes that potentially reduce such a constraint, in this case a spatial confinement of the mandibular domain. Such phenotypes may allow co-option of the *Dlx* code and heterotopy to produce conditions that permitted significant selection. These key phenotypic innovations include: 1) diplorhiny; 2) a trabecula; 3) an adenohypophysis; 4) a spiracle; 5) internalization of the branchial

skeleton; 6) mineralization of the internal skeleton and synovial joint; 7) epaxial-hypaxial differentiation and paired fins: 8) hypoglossal muscles and true hypobranchial muscles; 9) a dorsal head shield and cucullaris; and 10) a maxillary process and trigeminal nerve conforming to the branchial nerve pattern. Many of the innovations have been discussed extensively in the literature, most notably by Janvier (Janvier 1981a, b, 1993, 1996, 2007) and Kuratani and associates (Kuratani et al. 1997, 2001, 2004, 2012; Shigetani et al. 2002, 2005; Kuratani 2004a, b, 2005, 2010, 2011, 2012; Kusakabe et al. 2004, 2011; Kusakabe and Kuratani 2005; Kuratani and Ota 2008; Sambasivan et al. 2011). Their insights are re-interpreted in this chapter for each of the innovations in the context of 1) fossil evidence and 2) confinement of the mandibular domain (Figure 3-18).

3.4.3.4.1 Diplorhiny, trabecula and adenohypophysis—Pre-gnathostome vertebrate conditions include a single nasohypophyseal placode, the gnathostome homologues of which are paired olfactory placodes (olp) and a single hypophyseal placode (Rathke's pouch,; rap; Figure 3-17A). Because the single nasohypophyseal placode blocks the preoptic ectomesenchyme from migrating ventrally to meet the lip — which consists of the postoptic premandibular and mandibular ectomesenchyme —, the midline split of the nasohypophyseal placode into paired olfactory placodes (diplorhiny) is required for: 1) ventral migration of the preoptic premandibular ectomesenchyme; 2) confluence of the preoptic and postoptic premandibular ectomesenchyme, resulting in the anterior delineation of Rathke's pouch; and 3) formation of trabecula in this region (Kuratani et al. 2001, 2004, 2012; Shigetani et al. 2002, 2005; Kuratani 2004a, b, 2005, 2012; Kuratani and Ota 2008). In turn, the postoptic premandibular ectomesenchyme forming the trabecula: 1) provides skeletal support for the nasal capsules; 2) separates the nasal cavity and hypophysis; and 3) limits the mandibular ectomesenchyme ventrally from overlapping laterally. Stem gnathostomes (Figure 3-18) show diverse nasohypophyseal morphology (Janvier 1974, 1981a, b, 1993, 1996, 2007; Janvier and Blieck 1979; Gai et al. 2011). The nasal capsules were paired in heterostracans and galeaspids, and the hypophyseal

duct opened toward the oral cavity (or into the confluence of the nasal passage and oral cavity) in galeaspids (Gai et al. 2011). The nasopharyngeal duct opens into the pharynx in hagfish and heterostracans, but the adenohypophysis sits on top of the duct in these animals. As such, only galeaspids could possibly have developed the trabecula, although the presence of trabecula has not been confirmed. As the nasal aperture is single in all known jawless vertebrates except for arandaspids (Gagnier 1993; Janvier 1996), the interorbital and nasal septa did not exist in these animals. Arandaspids have a T-shaped plate between the eyes, and this plate is presumed to have split the nasal apeature into a bilateral pair. Unfortunately, the internal anatomy of arandaspids is poorly known, and the nasohypophyseal structure still needs to be described. The paired nasal apertures in gnathostomes possibly develop in response to the complete separation of the unpaired adenohypophysis from the nasal cavity, and a shift in the site of the invagination for the nasal passage from Rathke's pouch to the paired olfactory placodes. In that sense, heterostracans, galeaspids, and possibly arandaspids foreshadow the gnathostome condition.

3.4.3.4.2 Spiracle—The spiracle (spr; Figure 3-4B) may have been both a developmental and a functional innovation that freed the mandibular domain from forming the velum. It is likely correlated with internalization of the branchial skeleton. A spiracle is an external opening of the first lateral pharyngeal diverticulum, or mandibular-hyoid pouch. Because the pouch sets apart the hyoid and mandibular domains, its dorsolateral extension precludes the mandibular domain from extending along the dorsal side of the pharynx posteriorly to become a velum. Simultaneously, the spiracle maintains an inhalant passage for ventilation. In hagfish, the large nasopharyngeal duct maintains an open passage, and the velum drives the current (Strahan 1958). In lamprey ammocoetes, the incurrent from the mouth is driven by the power-stroke of the velum, whereas adults have the velum as a valve for the main branchial duct and respire via external branchial openings by muscular deformation of the pharyngeal basket (Randall 1972; Rovainen 1996). The impressions of the branchial skeleton lateral to the gill chambers in various stem gnathostomes

(anaspids, galeaspids, heterostracans, osteostracans, and thelodonts; Janvier 1993, 1996; Figure 3-18) suggest that they conformed to either hagfish or lamprey-like ventilations. The nasal passage was likely an inhalant duct for arandaspids, galeaspids, heterostracans, and thelodonts. The nasohypophyseal complex is a blind sac in anaspids and osteostracans, leaving the mouth and external branchial openings as the only available entrance for incurrent ventilation. Euphanelopid anaspids likely used deformation of pharyngeal basket for ventilation as do lamprey adults (Janvier 1996). The mineralized roof of the branchial chambers in galeaspids, heterostracans, and osteostracans, and a common external branchial opening in heterostracans, are incompatible with pharyngeal basket deformation as a ventilation mechanism in these animals. Most jawless vertebrates lack a spiracle. Heterostracans and pituriaspids both have an adorbital opening (Stensiö 1958, 1964; Janvier 1974; Blieck 1984; Young 1991), and the one in heterostracans has been interpreted as a spiracle (Halstead 1971). Whether this is a true spiracle or not remains uncertain, but the consensus is that the opening had an inhalant function similar to the gnathostome spiracle (Janvier 1996).

3.4.3.4.3 Branchial skeleton and synovial joint—The branchial arches internal to the gill lamellae are so far restricted to gnathostomes, which likely reflects a shift from soft to hard skeletons, because a hard external branchial skeleton with little potential for elastic deformation and recoil is hardly effective as a pumping device. In living gnathostomes, flexibility of the hard branchial skeleton is maintained by connective tissues of the dorsoventrally separate elements of the arch. This system assumes dorsoventral patterning, and likely arose with the establishment of the *Dlx* code (Figure 3-17A). The jaw skeleton, then, may be viewed as an anterior transfer of the dorsoventral patterning mechanism to the default mandibular domain. A hard internal skeleton with a jaw requires a synovial joint. A possible evolutionary precursor for a synovial joint in the velar skeleton of hagfish is the proximal velar contact (Figure 3-14). Developmentally, the internalization of branchial arches reflects a shift of skeletogenic potential from the lateral to the medial side of the ectomesenchyme

filling in a pharyngeal arch (Kimmel et al. 2001, 2003; McCauley and Bronner-Fraser 2003, 2006; Cerny et al. 2004a, b; Janvier 2007; reviewed in Chapter 2). This set of character changes associated with the soft-to-hard shift of the internal skeleton is perfectly correlated with the origin of the jaw.

The internal branchial arches allow migration of the hypobranchial and hypoglossal muscles unique to gnathostomes that would either inhibit or limit a lingual apparatus in the mandibular domain. In gnathostomes, the hypobranchial muscles extend between the pharynx and ventral constrictors and penetrate the floor of the pharynx as hypoglossal muscles (m.cob, m.coh, m.com; Figure 3-4C; Edgeworth 1902, 1911, 1923, 1926a, b, 1928, 1935; Miyake et al. 1992; Diogo and Abdala 2010). The somatic muscles in the hypobranchial region of cyclostomes cannot occupy that position because the lingual apparatus and branchial series separate them ventrally from the pharynx. Because branchial morphology is highly modified in hagfish, lampreys form a better comparative model here for the general condition in jawless vertebrates (Figure 3-2). The branchial arches external to the gill lamellae in jawless vertebrates meet at the ventral midline to form a basket in lampreys and also in other jawless vertebrates, because bases for the branchial arches are identified only on the dorsal side of the skull, and because otherwise the arches cannot provide structural support for the branchial chambers. Under this condition, the pharyngeal basket separates the somatic muscles ventrally, whereas the mandibular domain can extend within the basket under the pharynx. Instead, the gill arches internal to the branchial chambers lack the ventral sagittal confluence, because the hard internal skeleton is no longer capable of dramatic elastic deformation and recoil. The lack of ventral-midline skeletonization allows the migration of somatic muscles from posterior to anterior positions along the floor of the pharynx and branchial series. The ventral constrictors of the branchial arches may partially overlap this. In effect, the mandibular domain along the floor of the pharynx is restricted anteriorly. Hagfish have no complete branchial arch skeleton. However, the pharyngolingual arches are developmentally comparable to the external branchial arches (Chapter 2), and they form a basket around the pharynx and velum, separating

the somatic muscles externally from these inner structures. Therefore, hagfish morphology can also be interpreted in this context.

Defects in the hypoglossal muscles in the mutant mice *Dlx5/6*$^{-/-}$ and *EdnRA*$^{-/-}$ (Heude et al. 2010) indicate that the muscles are downstream of the gnathostome-specific *Dlx* code. Therefore, the origin of the hypoglossal muscles was likely linked with the establishment of the *Dlx* code, as well as the internalization of the branchial arches. No jawless vertebrates are known to have the internal branchial arches, so the hypoglossal muscles are candidates for the final key innovation facilitating the origin of the gnathostome jaw.

3.4.3.4.4. Migration of somatic muscles—The origin of the gnathostome hypobranchial muscles has been linked to epaxial-hypaxial differentiation. Dorsoventrally patterned gene expression involved in epaxial-hypaxial differentiation of myotomes in gnathostomes also exists in lampreys, and specifies regions of the somatic musculature that correspond to specific hypaxial muscles in gnathostomes — such as the cucullaris, hypobranchials, and pectoral muscles (m.hyb; Figure 3-2A, 3-3A; Kusakabe et al. 2004, 2011; Kusakabe and Kuratani 2005; Kuratani 2008b). Hagfish lack epaxial-hypaxial differentiation of myotomes, but two somatic muscles (m. obliquus and m. rectus) are restricted to the ventral side of the body. These observations indicate that dorsoventral patterning of the somatic musculature already existed in jawless vertebrates, and co-option of this patterning might have facilitated epaxial-hypaxial differentiation. In relation to this, paired fins just behind the branchial series occur in anaspids and osteostracans (Wilson et al. 2007; Figure 3-18). Osteostracans even have an impression for the attachment of fin muscles (Janvier 1985, 1996). Therefore, somatic muscles were likely already differentiated in this region among those lineages of stem gnathostomes, hinting at the potential for the hypobranchial muscles to migrate along the floor of the pharynx in these animals. Thelodonts deviate from other stem gnathostomes in that their paired fins develop above the branchial series (Wilson et al. 2007; Figure 3-18). The position indicates that muscles attached to the fins in thelodonts are comparable to

the cucullaris of gnathostomes. The morphology of heterocercal tails may be correlated with epaxial-hypaxial differentiation (Kuratani 2004a; Janvier 2007). However, this is not discussed further here because the tail morphology is not directly related to the head morphology.

Somatic muscles extend onto the face in hagfish and lampreys (Figures 3-1, 2, 3), whereas the comparable muscles in gnathostomes lie behind the otic capsule (Figure 3-4). The lack of a somatic-muscle cover in the mandibular region allows large, bulbous jaw adductors to be housed within the mandibular domain. The presence of an inflexible head shield in arandaspids, galeaspids, heterostracans, and osteostracans (Figure 3-18) suggests that the somatic musculature did not cover the facial region in these animals. This is because the rigid skull eliminates any functional advantage to having somatic musculature extend into that region. Therefore, the somatic musculature was likely restricted along the axial skeleton within the shield. The presence of paired fins above the branchial series in thelodonts (Wilson et al. 2007) also indicates that the muscles, which would otherwise extend anteriorly to cover the face in lampreys, were likely associated with fins.

3.4.3.4.5. Branchiomeric nerves—The trigeminal nerve of gnathostomes has been treated as a branchiomeric nerve (Johnston 1905; Goodrich 1930; de Beer 1937; Jarvik 1980; Northcutt 1993; Kuratani 2004a; Figure 3-17A). As the trigeminal nerve consists of two ganglia, only the posterior one (maxillomandibular nerve) that innervates the mandibular domain is considered. The trigeminal placode is distinct in its composition as an aggregate of small placodes, and does not appear to be a serial homologue of the epibranchial placodes that induce the branchiomeric nerves (Schlosser 2005). The maxillomandibular nerve lacks a special visceral sensory column to innervate taste buds in the branchiomeric nerves (Kuratani 2004a). Furthermore, motor neurons extend along all major branches of the maxillomandibular nerve in hagfish and lampreys (Figure 3-1D), whereas motor neurons are restricted to the post-trematic branch in each of the branchiomeric nerves (Lindström 1949). These distinctions are consistent with the Mandibular Siege

Hypothesis, which does not treat the mandibular domain in jawless vertebrates as a serial homologue of branchial arches. In gnathostomes, the motor neurons are largely restricted to the mandibular branch. The posterior, distal branch of the maxillomandibular nerve, thereby partly mimicks the condition of the branchiomeric nerves in which motor neurons occur in the post-trematic branch (Song and Boord 1993). The exception to this is chondrichthyans. As already discussed (Chapter 2), however, this is likely an independently derived character for chondrichthyans, and motor neurons in the maxillary process of chondrichthyans branch out proximally (Song and Boord 1993). The restriction of motor neurons to the mandibular branch and possibly to the proximal maxillary branch is consistent with the Heterotopic Theory, which predicts that the maxillary process originates from the posterior region of the mandibular domain in gnathostomes (Shigetani et al. 2002, 2005; Kuratani 2004a, b, 2005, 2012; Kuratani et al. 2004, 2012). This gnathostome pattern has not been identified in jawless vertebrates. As discussed, osteostracans likely had the upper lips that were similar to those of hagfish and lampreys, and do not conform to the gnathostome pattern.

3.4.3.5. Hypothetical gnathostome ancestor

The key innovations that spatially confined the mandibular domain and allowed the making of a pharyngeal arch in that domain occur in jawless vertebrate lineages in a mosaic manner (Figures 3-17, 3-18). Different jawless vertebrates variably foreshadow the gnathostome condition, which implies that none of these key innovations by itself led directly to the origin of the jaw. The jaw became inducible when the mandibular domain was spatially restricted into a default state that exhibited several qualities in this hypothetical gnathostome ancestor. First, the upper lip was freed from support of the snout; the velum was freed from ventilation; and the lingual apparatus was freed from longitudinal protraction and retraction. Instead, the animal had: 1) a trabecula and paired nasal capsules in the snout; 2) a spiracle and hard internal branchial arches for ventilation; and 3) hypobranchial and hypoglossal muscles for feeding. Second, the *Dlx* code for pharyngeal arches was established by

this time, and the *Dlx* expression domain to induce the maxillary process shifted more posteriorly than the presumptive cyclostome upper lip. This left a *Dlx* free region at the anterodorsal portion of the mandibular domain along the trabecula, because that portion of the mandibular domain no longer overlapped the premandibular domain. Third, the synovial joint existed either in a fully developed state, or in an intermediate state between the hagfish proximal velar contact and the gnathostome synovial joint, where a blood sinus functioned as a pad. The mandibular domain in this default, serially homologous state had high potential to differentiate a large population of ectomesenchyme over the face between the premandibular and hyoid domains, because the domain was no longer constrained to develop the upper lip, the velum, or the lingual apparatus as in stem gnathostome lineages. Crucially, each key innovation functionally compensated for the structure it replaced by restricting the mandibular region in that location (e.g., spiracle versus velum; hypoglossal muscles versus lingual apparatus).

This hypothetical ancestor is a model for convenience. It is a theoretical construct from which gnathostomes can be induced. Realistically, the mandibular default stage did not likely exist as reconstructed. A reasonable scenario is that no ancestor lacked the upper lip, velum, and lingual apparatus altogether without developing some intermediate, jaw-like structure. Functional compensations and complementation probably bridged between evolutionary stages. So there must have been intermediate stages in which the gnathostome conditions existed in mosaic, just as the key innovations variably and independently evolved among jawless vertebrate lineages. However, there is not enough information on which character preceded others along the gnathostome lineage, and the best theoretical approach to reconstruct the origin of the jaw is to postulate an idealized hypothetical ancestor. Regardless of whether or not such a hypothetical ancestor existed, the comparative analysis presented here recovered enough morphological and developmental evidence that all of the key innovations occurred at or before the origin of gnathostomes.

3.6. SUMMARY

A detailed anatomical description of the cranial musculature of the hagfish *Eptatretus stoutii*, combined with a comparative morphological analysis of other basal vertebrate lineages, yields a much more complete picture of muscle form and function in hagfish, and highlights an important functional contrast of the musculoskeletal system between jawless vertebrates and gnathostomes. In hagfish and other jawless vertebrates such as lampreys, muscle antagonism and elastic recoil of the cartilaginous skeleton dictate the configurations and functions of muscles, whereas gnathostomes use a lever-and-hinge system with abductors and adductors. Hagfish have a large number of muscles that suspend the lingual apparatus and hypertrophied muscles associated with it. Lampreys have fewer muscles that suspend the apparatus, and the protractors and retractors of the dental apparatus are relatively smaller and weaker. Instead, they have a large number of muscles that elevate the lip and funnel. These differences reflect feeding strategies unique to each lineage. A synovial joint is potentially the single most important morphological character that sets apart the hagfish-like cartilaginous musculoskeletal system and the gnathostome-like mineralized musculoskeletal system. The proximal velar contact of hagfish is a possible precursor for a synovial joint, with a tooth-and-socket contact between hard Type1a cartilages and with a blood sinus as a fluid-filled pad in between.

Muscle homology is an elusive concept. Similarities may be determined based on functions, developmental origins, and association with other tissues. These similarities depend partly on each other, but selection and constraints on each property may be independent. Therefore, all similarities are potentially subjects for comparison, and concordance between them is interpreted as evidence for potential homology. Based on this approach, hagfish and lampreys share many potentially homologous muscles. The similarity is striking in the lingual apparatus. Many of these potential homologues cannot be identified in gnathostomes. However, these muscles occur in regions only comparable amongst jawless vertebrates. Therefore,

the breaking of similarity in gnathostomes does not necessarily support a sister group relationship between hagfish and lampreys.

Finally, a synthesis of morphological and developmental evidence leads to a new hypothesis for the origins of vertebrates and gnathostomes. Contrary to the common notion in vertebrate zoology that the jaw is a highly differentiated branchial skeleton, the mandibular domain in jawless vertebrates is not an obvious serial homologue of the branchial arches. Rather, an analysis of vertebrate origins based on neural crest patterning suggests that the mandibular domain is highly specialized in early vertebrates. The domain bridges the premandibular domain (anterior to the mouth) and the hyoid domain (the first branchial arch), and extends longitudinally along the pharynx and laterally onto the premandibular domain to form structures unique to jawless vertebrates. Although the *Dlx* code and the heterotopy of *Dlx* expression are both prerequisites for the origin of the jaw, the molecular evidence alone cannot reveal a causal relationship leading to this gnathostome novelty. The new hypothesis interprets early vertebrate evolution in the context of the making of a pharyngeal arch in the mandibular domain. In other words, the jaw could only be induced after the mandibular domain attained a serially homologous state to the branchial arches. A number of morphological characters are identified as key innovations that spatially limit the mandibular domain to the space between the premandibular and hyoid domains. These key innovations evolved variably and independently along early vertebrate lineages, showing a pattern of mosaic evolution. The jaw eventually arose when all the key innovations occurred in one lineage, which eventually led to gnathostomes.

3.6. LITERATURE CITED

Adachi, N., and S. Kuratani. 2012. Development of head and trunk mesoderm in the dogfish, *Scyliorhinus torazame*: I. Embryology and morphology of the head cavities and related structures. Evolution & Development 14:234-256.

Adachi, N., M. Takechi, T. Hirai, and S. Kuratani. 2012. Development of the head and trunk mesoderm in the dogfish, *Scyliorhinus torazame*: II. Comparison of

gene expression between the head mesoderm and somites with reference to the origin of the vertebrate head. Evolution & Development 14:257-276.

Adam, H. 1960. Different types of body movement in the hagfish, *Myxine glutinosa*. Nature 188:595-596.

Altman, J., and S. A. Bayer. 1982. Development of the cranial nerve ganglia and related nuclei in the rat. Advances in Anatomy, Embryology, and Cell Biology 74:1-90.

Alvares, L. E., F. R. Schubert, C. Thorpe, R. C. Mootoosamy, L. Cheng, G. Parkyn, A. Lumsden, and S. Dietrich. 2003. Intrinsic, Hox-dependent cues determine the fate of skeletal muscle precursors. Developmental Cell 5:379-390.

Anderson, P. S. L. 2008. Cranial muscle homology across modern gnathostomes. Biological Journal of the Linnean Society 94:195-216.

Andres, K. H., and M. von Düring. 1993. Cutaneous and subcutaneous sensory receptors of the hagfish *Myxine glutinosa* with special respect to the trigeminal system. Cell and Tissue Research 274:353-366.

Archer, C. W., G. P. Dowthwaite, and P. Francis-West. 2003. Development of synovial joints. Birth Defects Research Part C 69:144-155.

Archer, C, W., H. Morrison, and A. A. Pitsillides 1994. Cellular aspects of the development of diarthrodial joints and articular cartilage. Journal of Anatomy 184:447–456.

Ayers, H., and C. M. Jackson. 1901. Morphology of the Myxinoidei. I. Skeleton and musculature. Journal of Morphology 17:185-225.

Balabai, P. P. 1946. Metamorphosis of the visceral apparatus of the lamprey. Doklady, Academy of Sciences U.S.S.R. 53:765-768.

Balfour, F. M. 1878. The development of the elasmobranchial fishes. Journal of Anatomy and Physiology 11:405-706.

Bardack, D. 1991. First fossil hagfish (Myxinoidea): a record from the Pennsylvanian of Illinois. Science 54:701-703.

Bardack, D. 1998. Relationships of living and fossil hagfishes. Pages 3-14 in J. M. Jørgensen, J. P. Lonholt, R. E. Weber, and H. Malte, eds. The Biology of Hagfishes. Chapman, London.

Bardack, D., and E. S. Richardson. 1977. New agnathous fishes from the Pennsylvanian of Illinois. Fieldiana: Geology 33:489-510.

Bareiro-Iglesias, A., D. R. Romaus-Sanjurjo, P. Senra-Martínez, R. Anadón, and M. C. Rodicio. 2011. Doublecortin is expressed in trigeminal motorneurons that innervate the velar musculature of lampreys: considerations on the evolution and development of the trigeminal system. Evolution & Development 13:149-158.

Bassham, S., and J. H. Postlethwait. 2005. The evolutionary history of placodes: a molecular genetic investigation of the larvacean urochordate *Oikopleura dioica*. Development 132:4259-4272.

Berti, R., J. P. Durand, S. Becchi, R. Brizzi, N. Kller, and G. Ruffat. 2001. Eye degeneration in the blind cave-dwelling fish *Phreatichthys andruzzii*. Canadian Journal of Zoology 79:1278-1285.

Bjerring, H. C. 1977. A contribution to structural analysis of the head of craniate animals. Zoologica Scripta 6:127–83.

Bjerring, H. C. 1984. Major anatomical steps toward craniotedness: a heterodox view based largely on embryological data. Journal of Vertebrate Paleontology 4:17–29.

Blieck, A. 1984. Les Hétérostracés Ptéraspidiformes, agnathes du Silurien-Dévonien du continent Nord-Atlantique et des blocs avoisinants: Révision systématique, phylogénie, biostratigraphie, biogéographie. Éditions du Centre National de la Recherche Scientifique 15:1-199.

Boorman, C. J., and S. M. Shimeld. 2002a. Pitx homeobox gene in *Ciona* and amphioxus shows left-right asymmetry is a conserved chordate character and define the ascidian adenohypophysis. Evolution & Development 4:354-365.

Boorman, C. J., and S. M. Shimeld. 2002b. The evolution of left-right asymmetry in chordates. BioEssays 24:1004-1011.

Borue, X., and D. M. Noden. 2004. Normal and aberrant craniofacial myogenesis by grafted trunk somitic and segmental plate mesoderm. Development 131:3967-3980.

Bothe, I., and S. Dietrich. 2006. The molecular setup of the avian head mesoderm and its implication for craniofacial myogenesis. Developmental Dynamics 235:2845-2860.

Bothe, I., G. Tenin, A. Oseni, and S. Dietrich. 2011. Dynamic control of head mesoderm patterning. Development 138:2807-2821.

Bothe, I., M. U. Ahmed, F. L. Winterbottom, G. von Scheven, and S. Dietrich. 2007. Extrinsic versus intrinsic cues in avian paraxial mesoderm patterning and differentiation. Developmental Dynamics 236:2397-2409.

Braun, C. B., and R. G. Northcutt. 1997. The lateral line system of hagfishes (Craniata: Myxinoidea). Acta Zoologica 78:247-268.

Brunet, L. J., J. A. McMahon, A. P. McMahon, and R. M. Harland. 1998. Noggin, cartilage morphogenesis, and joint formation in the mammalian skeleton. Science 280:1455–1457.

Bryson-Richardson, R. J., and P. D. Currie. 2008. The genetics of vertebrate myogenesis. Nature Reviews Genetics 9:632-646.

Bujnor, M. P. 1891. Contribution a l'étude de la métamorphose de l'ammocète branchialis de *Petromyzon planeri*. Revue de Biologie 3:478-486.

Bullock, T. H., A. Bodznick, and R. G. Northcutt. 1983. The phylogenetic distribution of electroreception: evidence for convergent evolution of a primitive vertebrate sense modality. Brain Research Reviews 6:25-46.

Carpenter, E. M., J. M. Goddard, O. Chisaka, N. R. Manley, and M. R. Capecchi. 1993. Loss of *Hox-A1* (*Hox-1, 6*) function results in the reorganization of the murine hindbrain. Development 118:1063-1075.

Cavalcanti, M. J., and V. Gallo. 2008. Panbiogeographical analysis of distribution patterns in hagfishes (Craniata: Myxinidae). Journal of Biogeography 35:1258-1268.

Cavey, M. J., and R. A. Cloney. 1974. Fine structure and differentiation of ascidian muscle. II. Morphometrics and differentiation of the caudal muscle cells of *Distaplia occidentalis* tadpoles. Journal of Morphology 144:23-70.

Cerny, R., P. Lwigale, R. Ericsson, D. Meulemans, H.-H. Epperlein, and M. Bronner-Fraser. 2004b. Developmental origins and evolution of jaws: new interpretation of "maxillary" and "mandibular". Developmental Biology 276:225-236.

Cerny, R., M. Cattell, T. Sauka-Spengler, M. Bronner-Fraser, F. Yu, and D. Meulemans Medeiros. 2010. Evidence for the prepattern/cooption model of vertebrate jaw evolution. Proceedings of the National Academy of Sciences 107:17262-17267.

Cerny, R., D. Meulemans, J. Berger, M. Wilsch-Braüninger, T. Kurth, M. Bronner-Fraser, and H.-H. Epperlein. 2004a. Combined intrinsic and extrinsic influences pattern cranial neural crest migration and pharyngeal arch morphogenesis in axolotl. Developmental Biology 266:252–269.

Chen, J.-Y., D.-Y. Huang, and C.-W. Li. 1999. An Early Cambrian craniate-like chordate. Nature 377:720-722.

Clark, A. J., and A. P. Summers. 2007. Morphology and kinematics of feeding in hagfish: possible functional advantages of jaws. The Journal of Experimental Biology 210:3897-3909.

Clark, A. J., E. J. Maravilla, and A. P. Summers. A soft origin for a forceful bite: motor patterns of the feeding musculature in Atlantic hagfish, *Myxine glutinosa*. Zoology 113:259-268.

Cole, F. J. 1905. A monograph on the general morphology of the myxinoid fishes, based on a study of *Myxine*. Part I. The anatomy of the skeleton. Transactions of the Royal Society of Edinburgh 41:749-791.

Cole, F. J. 1907. A monograph on the general morphology of the myxinoid fishes, based on a study of *Myxine*. Part II. The anatomy of the muscles. Transactions of the Royal Society of Edinburgh 45:683-757.

Cole, F. J. 1909. A monograph on the general morphology of the myxinoid fishes, based on a study of *Myxine*. Part III. Further observations on the skeleton. Transactions of the Royal Society of Edinburgh 46:669-681.

Conel, J. L. 1942. The origin of the neural crest. The Journal of Comparative Neurology 75:191-215.

Couly, G., and N. M. Le Douarin. 1988. The fate map of the cephalic neural primordium ad the presomitic to the 3-somite stage in the avian embryo. Development 103:101-113.

Couly, G. F., P. M. Coltey, and D. M. Le Douarin. 1992. The developmental fate of the cephalic mesoderm in qual-chick chimeras. Development 114:1-15.

Couly, G., S. Creuzet, and N. M. Le Douarin. 1993. The triple origin of skull in higher vertebrates: a study in quail-chick chimeras. Development 117:409-429.

Couly, G., S. Creuzet, S. Bannaceur, C. Vincent, and N. M. Le Douarin. 2002. Interactions between *Hox*-negative cephalic neural crest cells and the foregut endoderm in patterning facial skeleton in the vertebrate head. Development 125:3445-3459.

Couly, G., A. Grapin-Botton, P. Coltey, B. Ruhin, and N. M. Le Douarin. 1998. Determination of the identity of the derivatives of the cephalic neural crest: incompatibility between *Hox* gene expression and lower jaw development. Development 125:3445-3459.

Craig, F. M., G. Bentley, and C. W. Archer. 1987. The spatial and temporal pattern of collagens I and II and keratan sulphate in the developing chick metatarsophalangeal joint. Development 99:383–391.

Damas, H. 1935. Contribution à l'étude de la metamorphose de la tête de la lamproie. Archives de Biologie Paris 46:171-227.

Damas, H. 1944. Recherches sur le dévelopment de *Lampetra fluviatilis* L. Contribution à l'étude de la cephalogénèse des vertébrés. Archives de Biologie Paris 55:1-289.

Dawson, J. 1905a. The breathing and feeding mechanism of the lampreys I. Biological Bulletin 9:1-21.

Dawson, J. 1905b. The breathing and feeding mechanism of the lampreys II. Biological Bulletin 9:91-111.

Dean, B. 1899. On the embryology of *Bdellostoma stouti*. A general account of myxinoid development from the egg and segmentation to hatching. Pages 220-276 in Festschrift zum 70ten Geburststag Carl von Kupffer. Gustav Fischer Verlag, Jena.

Depew, M. J., and C. A. Simpson. 2006. 21st century neontology and the comparative development of the vertebrate skull. Developmental Dynamics 235:1256-1291.

Depew, M. J., T. Lufkin, and J. L. R. Rubenstein. 2001. Specification of jaw subdividions by *Dlx* genes. Science 298:381-385.

Depew, M. J., C. A. Simpson, M. Morasso, and J. L. R. Rubenstein. 2005. Reassessing the *Dlx* code: the genetic regulation of branchial arch skeletal pattern and development. Journal of Anatomy 207:501-561.

Diogo, R., and V. Abdala. 2010. Muscles of Vertebrates: Comparative Anatomy, Evolution, Homologies and Development. CRC Press, Boca Raton. 482 pp.

Diogo, R., Y. Hinits, and S. M. Hughes. 2008. Development of mandibular, hyoide and hypobranchial muscles in the zebrafish: homologies and evolution of these muscles within bony fishes and tetrapods. BMC Developmental Biology 8:24. 22 pp.

Donoghue, P. J. C. 1998. Growth and patterning in the conodont skeleton. Philosophical Transactions of the Royal Society of London B 353:633-666.

Donoghue, P. J. C. 2002. Evolution of development of the vertebrate dermal and oral skeletons: unraveling concepts, regulatory theories, and homologies. Paleobiology 28:474-507.

Donoghue, P. J. C., and M. A. Purnell. 1999. Mammal-like occlusion in conodonts. Paleobiology 25:58-74.

Donoghue, P. J. C., and I. J. Sansom. 2002. Origin and early evolution of vertebrate skeletonization. Microscopy Research and Technique 59:352-372.

Donoghue, P. J. C., I. J. Sansom. And J. P. Downs. 2006. Early evolution of vertebrate skeletal tissues and cellular interactions, and the canalization of skeletal development. Journal of Experimental Zoology B 306:278-294.

Dy, P., P. Smits, A. Silvester, A. Penzo-Méndez, B. Dumitriu, Y. Han, C. A. de la Motte, D. M. Kingsley, and V. Lefebvre. 2010. Synovial joint morphogenesis requires the chondrogenic action of *Sox5* and *Sox6* in growth plate and articular cartilage. Developmental Biology 341:346-359.

Edgeworth, F. H. 1902. The development of the head muscles in *Scyllium canicula*. Journal of Anatomy and Physiology 37:73-88.

Edgeworth, F. H. 1911. On the morphology of the cranial muscles in some vertebrates. Quarterly Journal of Microscopical Science 56:167-316.

Edgeworth, F. H. 1923. On the development of the hypobranchial, branchial, and laryngeal muscles of *Ceratodus*, with a note on the development of the quadrate and epihyal. Quarterly Journal of Microscopical Science 67:325-368.

Edgeworth, F. H. 1926a. On the hyomandibula of Selachii, Teleostomi and *Ceratodus*. Journal of Anatomy and Physiology 60:173-193.

Edgeworth, F. H. 1926b. On the development of the cranial muscles in *Protopterus* and *Lepidosiren*. Transactions of the Royal Society of Edinburgh 54:719-734.

Edgeworth, F. H. 1928. The development of some of the cranial muscles of ganoid fishes. Philosophical Transactions of the Royal Society of London B 217:39-89.

Edgeworth, F. H. 1935. The Cranial Muscles of Vertebrates. Cambridge University Press, Cambridge.

Eigenmann, C. H. 1909. Cave Vertebrates of America, a Study in Degenerative Evolution. Carnegie Institute of Washington, Washington, D. C. 241 pp.

Erickson, C. A., and T. L. Goins. 1995. Avian neural crest cells can migrate in the dorsolateral path only if they are specified as melanocytes. Development 121:915–924.

Evans. D. J. R., and D. M. Noden. 2006. Spatial relations between avian craniofacial neural crest and paraxial mesoderm cells. Developmental Dynamics 235:13101325.

Fernholm, B. 1998. Hagfish systematics. Pages 33-44 in J. M. Jørgensen, J. P. Lonholt, R. E. Weber, and H. Malte, eds. The Biology of Hagfishes. Chapman, London.

Flood, P. R. 1998. The skeletal muscle fibre types of *Myxine glutinosa*. Pages 173-202 in J. M. Jørgensen, J. P. Lonholt, R. E. Weber, and H. Malte, eds. The Biology of Hagfishes. Chapman, London.

Foureaux, G., M. I. Egami, C. Jared, M. M. Antoniazzi, R. C. Gutierre, and R. L. Smith. 2010. Rudimentary eyes of squamate fossorial reptiles (Amphisbaenia and Serpentes). The Anatomical Record 193:351-357.

Francis-West, P. H., J. Parish, K. Lee, and C. W. Archer. 1999. BMP/GDF-signaling interactions during synovial joint development. Cell Tissue Research 296:111–119.

Fritzsch, B., and R. G. Northcutt. 1993. Cranial and spinal nerve organization in amphioxus and lampreys: evidence for an ancestral craniate pattern. Acta Anatomica 148:96-109.

Fritzsch, B., R. Sonntag, R. Duboc, Y Ohta, and S. Grillner. 1990. Organization of the six motor nuclei innervating the ocular muscles in lamprey. Journal of Comparative Neurology 294:491-506.

Gage, P. J., H. Suh, and S. A. Camper. 1999. Dosage requirement of Pitx2 for development of multiple organs. Development 126:4643-4651.

Gagnier, P. Y. 1993. *Sacabambaspis janvieri*, Vertévré ordovicien de Bolivie. 1. Analyse morphologique. Annales de Paléontologie 79:19-69.

Gai, Z., P. C. J. Donoghue, M. Zhu, P. Janvier, and M. Stampanoni. 2011. Fossil jawless fish from China foreshadows early jawed vertebrate anatomy. Nature 476:324-327.

Gans, C. 1993. Evolutionary origin of the vertebrate skull. Pages 1-35 in J. Hanken and B. K. Hall, eds. The Skull. Volume 2. Patterns of Structural and Systematic Diversity. The University of Chicago Press. Chicago.

Gans, C., and R. G. Northcutt. 1983. Neural crest and the origin of vertebrates: a new head. Science 220:268-274.

Gaupp, E. 1898. Die Metamerie des Schädels. Ergebnisse der Anatomie und Entwicklungsgeschite 7:793-885.

Gee, H. 1996. Before the Backbone. Chapman & Hall, London. 346 pp.

Georgieva, V., R. A. Patzner, and H. Adam. 1979. Transmissions- und rasterelektronen-mikroskopische Untersuchung an den Sinnersknospen der Tentakeln von *Myxine glutinosa* L. (Cyclostomata). Zoologica Scripta 8:61-67.

Gilbert, S. F. 2010. Developmental Biology (9th edition). Sinaeur Associates, Sunderland. 711 pp.

Goethe, J. W. 1790. Das Schädelgrüt aus sechs Wirbelknochen aufgebaut. Zur Naturwissenschaft überhaupt, besonders zur Morphologie. II 2. (cited in Gaupp 1899; Kuratani 2004a)

Goethe, J. W. 1820. Zur Naturwissenschaften überhaupt, besonders zur Morphologie. (cited in de Beer 1937; Kuratani 2004a)

Gong, Y., D. Krakow, J. Marcelino, D. Wilkin, D. Chitayat, R. Babul-Hirji, L. Hudgins, C. W. Cremers, F. P. M. Cremers, H. G. Brunner, K. Reinker, D. L. Rimoln, D. H. Cohn, F. R. Goodman, W. Reardon, M. Patton, C. A. Francomano, and M. L. Warman. 1999. Heterozygous mutations in the gene encoding noggin affect human joint morphogenesis. Nature Genetics 21:302-304.

Goodrich, E. S. 1909. A Treatise on Zoology. Part IV. Vertebrata Craniata. Adam and Charles Black, London. 518 pp.

Goodrich, E. S. 1917. "Proboscis pores" in craniate vertebrates, a suggestion concerning the premandibular somites and hypophysis. Quarterly Journal of Microscopical Science 62:539-553.

Goodrich, E. S. 1918. On the development of the segments of the head in *Scyllium*. Quarternary Journal of Microscopical Science 63:1-30.

Goodrich, E. S. 1930. Studies on the Structure and Development of Vertebrates. The Macmillan Company, London.

Goudenmand, N., M. J. Orchard, S. Urdy, H. Bucher, and P. Tafforeau. 2011. Synchrotron-aided reconstruction of the conodont feeding apparatus and implications for the mouth of the first vertebrates. Proceedings of the National Academy of Sciences 108:8720-8724.

Graham, A., and A. Smith. 2001. Patterning the pharyngeal arches. BioEssays 23:54-61.

Gregory, W. K. 1936. Transformation of organic designs: a review of the origin and deployment of the earlier vertebrates. Biological Reviews 11:311-344.

Gregory, W. K. 1946. The roles of motile larvae and fixed adults in the origin of the vertebrates. The Quarterly Review of Biology 21:348-364.

Grenier, J., M.-A. Teillet, R. Grifone, R. G. Kelly, and D. Duprez. 2009. Relationship between neural crest cells and cranial mesoderm during head muscle development. PLoS ONE 4:e4381. 15 pp.

Guthrie, S., and A. Lumsden. 1991. Formation and regeneration of rhombomere boundaries in the developing chick hindbrain. Development 112:221-229.

Guthrie, S., and A. Lumsden. 1992. Motor neuron pathfinding following rhombomere reversals in the chick embryo hindbrain. Development 114:663-673.

Hacker, A., and S. Guthrie. 1998. A distinct developmental programme for the cranial paraxial mesoderm in the chick embryo. Development 125:3461-3472.

Hall, B. K. 2009. The Neural Crest and Neural Crest Cells in Vertebrate Development and Evolution. Springer, New York.

Hall, B. K., and J. A. Gillis. 2012. Incremental evolution of the neural crest, neural crest cells and neural crest-derived skeletal tissues. Journal of Anatomy. Published online ahead of print. DOI: 10.1111/j.1469-7580.2012.01495.x

Hall, B. K., and T. Miyake. 2000. All for one and one for all: condensations and the initiation of skeletal development. BioEssays 22:134–147.

Hardisty, M. W., and C. M. Rovainen. 1982. Morphological and functional aspects of the muscular system. Pages 137-231 in M. W. Hardisty and I. C. Potter, eds. The Biology of Lampreys. Volume 4a. Academic Press, New York.

Hatta, K., T. F. Schilling, R. A. BreMiller, and C. B. Kimmel. 1990. Specification of jaw muscle identity in zebrafish: correlation with *engrailed*-homeoprotein expression. Science 250:802-805.

Hatschek, B. 1881. Studien über die Entwicklung des *Amphioxus*. Arbeiten aus den Zoologischen Instituten zu Wien 4:1-88.

Hayes, A. J., S. MacPherson, H. Morrison, G. Dowthwaite, and C. W. Archer. 2001. The development of articular cartilage: evidence for an appositional growth mechanism. Anatomia Embryologia 203:469-479.

Heude, É., K. Bouhali, Y. Kurihara, H. Kurihara, G. Couly, P. Janvier, and G. Levi. 2010. Jaw muscularization requires *Dlx* expression by cranial neural crest cells. Proceedings of the National Academy of Sciences 107:11441-11446.

Hillard, R. W., I. C. Potter, and D. J. Macey. 1985. The dentition and feeding mechanism in adult of the Southern Hemisphere lamprey *Geotria australis* Gray. Acta Zoologica 66:159-170.

Hinits, Y., D. P. S. Osborn, and S. M. Hughes. 2009. Differential requirements for myogenic regulatory factors distinguish medial and lateral somitic, cranial and fin muscle fibre populations. Development 136:403-414.

Holland, L. Z., and N. D. Holland. 2001. Evolution of neural crest and placodes: amphioxus as a model for the ancestral vertebrate? Journal of Anatomy 199:85-98.

Holland, N. D., and J. Chen. 2001. Origin and early evolution of the vertebrates: new insights from advances in molecular biology, anatomy, and palaeontology. BioEssays 23:142-151.

Holland, N. D., L. Z. Holland, Y. Honma, and T. Fujii. 1993. *Engrailed* expression during development of a lamprey, *Lampetra japonica*: a possible clue to homologies between agnathan and gnathostome muscles of the mandibular arch. Development, Growth & Differentiation 35:153-160.

Holmberg, K., and V. Lundin. 1973. The olfactory system in the hagfish *Myxine glutinosa*. Acta Zoologica 54:285-295.

Holmgren, N. 1946. On two embryos of *Myxine glutinosa*. Acta Zoologica 27:1-90.

Horigome, N., M. Myojin, T. Ueki, S. Hirano, S. Aizawa, and S. Kuratani. 1999. Development of cephalic neural crest cells in embryos of *Lampetra japonica*, with special reference to the evolution of the jaw. Developmental Biology 207:287-308.

Hunt, P., and R. Krumlauf. 1991. Deciphering the *Hox* code: clues to patterning branchial regions of the head. Cell 66:1075-1078.

Hunt, P., D. Wilkinson, and R. Krumlauf. 1991a. Patterning the vertebrate head: murine *hox 2* genes mark distinct subpopulations of premigratory and migrating cranial neural crest. Development 112:43-50.

Hunt, P., P. Ferretti, R. Krumlauf, and P. Thorogood. 1995. Restoration of normal Hox code and branchial arch morphogenesis after extensive deletion of hindbrain neural crest. Developmental Biology 168:584-597.

Hunt, P., J. Whiting, I. Muchamore, H. Marshall, and R. Krumlauf. 1991b. Homeobox genes and models for patternin the hindbrain and branchial arches. Development Suppl. 1:187-196.

Hunt, P., M. Gulisano, M. Cook, M.-H. Sham, A. Faiella, D. Wilkinson, E. Boncinelli, and R. Krumlauf. 1991c. A distinct *Hox* code for the branchial region of the vertebrate head. Nature 353:861-864.

Imai, K. S., A. Stolfi, M. Levine, and Y. Satou. 2009. Gene regulatory networks underlying the compartmentalization of the *Ciona* central nervous system. Development 136:285-293.

Janvier, P. 1974. The structure of the naso-hypophyseal complex, and the mouth in fossil and extant cyclostomes, with remarks on amphiaspiforms. Zoologica Scripta 3:193-200.

Janvier, P. 1981a. *Norselaspis glacialis* n.g., n.sp. et les relations phylogénétiques entre les Kiaeraspidiens (Osteostraci) du Dévonien infeérieur du Spitsberg. Palaeovertebrata 11:19-131.

Janvier, P. 1981b. The phylogeny of the Craniata, with particular reference to the significance of fossil 'agnathans'. Journal of Vertebrate Paleontology 1:121-159.

Janvier, P. 1985. Les Céphalaspides du Spitsberg. Anatomie, phylogénie et systématique des Ostéostracés siluro-dévoniens. Révision des Ostéostracés de la Formation de Wood Bay (Dévonien inférieur du Spitsberg). Cahiers de Paléontologie, Centre national de la Recherche scientifique, Paris. 244 pp.

Janvier, P. 1993. Patterns of diversity in the skull of jawless fishes. Pages 131-188 in J. Hanken and B. K. Hall, eds. The Skull. Volume II. Patterns of Structural and Systematic Diversity. The University of Chicago Press, Chicago.

Janvier, P. 1996. Early Vertebrates. Oxford Monographs on Geology and Geophysics, 33. Clarendon Press, Oxford. 393 pp.

Janvier, P. 2007. Homologies and evolutionary transitions in early vertebrate history. Pages 57-121 in J. S. Anderson and H. D. Sues, eds. Major Transitions in Vertebrate Evolution. Indiana University Press, Bloomington.

Janvier, P. 2008. Early jawless vertebrates and cyclostome origins. Zoological Science 25:1045-1056.

Janvier, P., and M. Arsenault. 2002. Calcification of early vertebrate cartilage. Nature 417:609.

Janvier, P., and M. Arsenault. 2007. The anatomy of *Euphanerops longaevus* Woodward, 1900, an anaspid-like jawless vertebrate from the Upper Devonian of Miguasha, Quebec, Canada. Geodiversitas 29:143-216.

Janvier, P., and A. Blieck. 1979. New data on the internal anatomy of the Heterostraci (Agnatha), with general remarks on the phylogeny of the Craniata. Zoological Scripta 8:287-296.

Jarvik, E. 1980. Basic Structure and Evolution of Verebrates. 2 Volumes. Academic Press, London.

Jefferies, R. P. S. 1986. The Ancestry of the Vertebrates. 376 pp. British Museum (Natural History), London.

Johnels, A. G. 1948. On the development and morphology of the skeleton of the head of *Petromyzon*. Acta Zoologica 29:139-279.

Johnston, J. B. 1905. The morphology of the vertebrate head from the viewpoint of the functional divisions of the nervous system. Journal of Comparative Neurology and Psychology 15:175-273.

Jollie, M. T. 1977. Segmentation of the vertebrate head. American Zoologist 17:323-333.

Kaensche, C. C. 1890. Beiträge zur Kenntnis der Metamorphose des Ammocoetes branchialis in *Petromyzon*. Zoologische Beiträge 2:219-250.

Kano, S., J.-H. Xiao, J. Osório, M. Ekker, Y. Hadzhiev, F. Müller, D. Casane, G. Magdelenat, and S. Rétaux. 2010. Two lamprey hedgehog genes share non-coding regulatory sequences and expression patterns with gnathostome hedgehogs. PLoS One 5:e13332. 12 pp.

Kawasaki, R. 1979. Breathing rhythm-generation in the adult lamprey, *Entosphcnus japonica*. Japanese Journal of Physiology 29:327-338.

Kawasaki, R. 1984. Breathing rhythm-generation mechanism in the adult lamprey (*Lampetra japonica*). Japanese Journal of Physiology 34:319-335.

Kawasaki, R., and C. M. Rovainen. 1988. Feeding behavior by parasitic phase lampreys, *Ichthyomyzon unicuspis*. Brain, Behavior and Evolution 32:317-329.

Keynes, R. J., and C. D. Stern. 1984. Segmentation in the vertebrate nervous system. Nature 310:786-789.

Kimmel, C. B., C. T. Miller, and R. J. Keynes. 2001. Neural crest patterning and the evolution of the jaw. Journal of Anatomy 199:105-119.

Kimmel, C. B., B. Ullmann, M. Walker, C. T. Miller, and J. G. Crump. 2003. Endothelin 1-mediated regulation of pharyngeal bone development in zebrafish. Development 130:1339–1351.

Kishida, R., R. C. Goris, H. Nishizawa, H. Koyama, T. Kadota, and F. Amemiya. 1987. Primary neurons of the lateral line nerves and their central projections in hagfishes. Journal of Comparative Neurology 264:303-310.

Knight, R. D., K. Mebus, and H. H. Roehl. 2008. Mandibular arch muscle identity is regulated by a conserved molecular process during vertebrate development. Journal of Experimental Zoology B 310:355-369.

Knight, R. D., K. Mebus, A. d'Angelo, K. Yokoya, T. Heanue, Tübingen 2000 Screen Consortium, and H. Roehl. 2011. Ret signaling integrates a craniofacial muscle module during development. Development 138:2015-2024.

Köntges, G., and A. Lumsden. 1996. Rhombencephalic neural crest segmentation is preserved throughout craniofacial ontogeny. Development 122:3229-3242.

Korneliussen, H. 1972. Identification of muscle fibre types in 'semithin' sections stained with p-phenylene-diamine. Histochemie 32:95-98.

Korneliussen, H. 1973. Ultrastructure of motor nerve terminals on different types of muscle fibres in the Atlantic hagfish (*Myxine glutinosa*, L.). Occurrence of round and elongate profiles of synaptic vesicles and dense-core vesicles. Zeitschrift für Zellforschung 143:273-290.

Korneliussen, H., and K. Nicolaysen. 1973. Ultrastructure of four types of striated muscle fibres in the Atlantic hagfish (*Myxine glutinosa*, L.). Zeitschrift für Zellforschung 143:273-290.

Kourakis, M. J., and W. C. Smith. 2007. A conserved role for FGF signaling in chordate otic/atrial placode formation. Devleopmental Biology 312:245-257.

Koyama, E., T. Ochiai, R. B. Rountree, D. M. Kingsley, M. Enomoto-Iwamoto, M. Iwamoto, and M. Pacifici. 2007a. Synovial joint formation during mouse limb skeletogenesis. Roles of Indian hedgehog signaling. Annals of the New York Academy of Science 1116:100-112.

Koyama, E., B. Young, M. Nagayama, Y. Shibukawa, M. Enomoto-Iwamoto, M. Iwamoto, Y. Maeda, B. Lanske, B. Song, R. Serra, and M. Pacifici. 2007b. Conditional Kif3a ablation causes abnormal hedgehog signaling topography, growth plate dysfunction, and excessive bone and cartilage formation during mouse skeletogenesis. Development 134:2159-2169.

Krumlauf, R. 1993. *Hox* genes and pattern formation in the branchial region of the vertebrate head. Trends in Genetics 9:106-112.

Kulesa, P. M., C. M. Bailey, J. C. Kasemeier-Kulesa, and R. McLennan. 2010. Cranial neural crest migration: new rules for an old road. Developmental Biology 344:543-554.

von Kupffer, C. 1900. Studien zur vergleichenden Entwicklungsgeschichte des Kopfes der Kranioten. 4 heft: Zur Kopfentwicklung von *Bdellostoma*. Verlag von J. F. Lehmann, Muchen. 86 pp.

Kuraku, S., Y. Takio, F. Sugahara, M. Takechi, and S. Kuratani. 2010. Evolution of oropharyngeal patterning mechanisms involving *Dlx* and *endothelins* in vertebrates. Developmental Biology 341:315-323.

Kuratani, S. C. 1991. Alternate expression of the HNK-1 epitope in rhombomeres of the chick embryo. Developmental Biology 144:215-219.

Kuratani, S. 2004a. [Evolutionary Morphology: Bauplan and Embryonic Development of Vertebrates]. The University of Tokyo Press, Tokyo. 611 pp. [In Japanese]

Kuratani, S. 2004b. Evolution of the vertebrate jaw: comparative embryology and molecular developmental biology reveal the factors behind evolutionary novelty. Journal of Anatomy 205:335-347.

Kuratani, S. 2005a. Craniofacial development and the evolution of the vertebrates: the old problems on a new background. Zoological Science 22:1-19.

Kuratani, S. 2005b. Developmental studies of the lamprey and hierarchical evolutionary steps towards the acquisition of the jaw. Journal of Anatomy 207:489-499.

Kuratani, S. 2008a. Is the vertebrate head segmented?—evolutionary and developmental considerations. Integrative and Comparative Biology 48:647-657.

Kuratani, S. 2008b. Evolutionary developmental studies of cyclostomes and the origin of the vertebrate neck. Development, Growth & Differentiation 50:189-194.

Kuratani, S. 2012. Evolution of the vertebrate jaw from developmental perspectives. Evolution & Development 14:76-92.

Kuratani, S., and K. G. Ota. 2008. Primitive versus derived traits in the developmental program of the vertebrate head: views from cyclostome developmental studies. Journal of Experimental Zoology B 310:294-314.

Kuratani, S., N. Horigome, and S. Hirano. 1999. Developmental morphology of the cephalic mesoderm and re-evaluation of segmental theories of the vertebrate

head: evidence from embryos of an agnathan vertebrate, *Lampetra japonica*. Developmental Biology 210:381-400.

Kuratani, S., Y. Nobusada, N. Horigome, and Y. Shigetani. 2001. Embryology of the lamprey and evolution of the vertebrate jaw: insights from molecular and developmental perspectives. Philosophical Transactions of the Royal Society B 356:15-32.

Kuratani, S., T. Ueki, S. Aizawa, and S. Hirano. 1997. Peripheral development of cranial nerves in a cyclostome, *Lampetra japonica*: morphological distribution of nerve branches and the vertebrate body plan. Journal of Comparative Neurology 384:483–500.

Kuratani, S., N. Adachi, N. Wada, Y. Oisi, and F. Sugahara. 2012. Developmental and evolutionary significance of the mandibular arch and prechordal/premandibular cranium in vertebrates: revising the heterotopy scenario of gnathostome jaw evolution. Journal of Anatomy. Published online ahead of print. DOI: 10.1111/j.1469-7580.2012.01505.x

Kuratani, S., Y. Murakami, Y. Nobusada, R. Kusakabe, and S. Hirano. 2004. Developmental fate of the mandibular mesoderm in the lamprey, *Lethenteron japnicum*: comparative morphology and development of the gnathostome jaw with special reference to the nature of the trabecular cranii. Journal of Experimental Zoology B 302:458-468.

Küry, P., R. Connor, E. Pasquale, and S. Guthrie. 2000. Eph receptors and ephrin expression in cranial motor neurons and the branchial arches of the chick embryo. Molecular and Cellular Neuroscience 15:123-140.

Kusakabe, R., and S. Kuratani. 2005. Evolution and developmental patterning of the vertebrate skeletal muscles: perspectives from the lamprey. Developmental Dynamics 234:824-834.

Kusakabe, R., S. Kuraku, and S. Kuratani. 2011. Expression and interaction of muscle-related genes in the lamprey imply the evolutionary scenario for vertebrate skeletal muscle, in association with the acquisition of the neck and fins. Developmental Biology 350:217-227.

Kusakabe, R., M. Takechi, S. Tochinai, and S. Kuratani. 2004. Lamprey contractile protein genes mark different populations of skeletal muscles during development. Journal of Experimental Zoology B 302:121-133.

Lacalli, T. C. 1996. Landmarks and subdomains in the larval brain of *Branchiostoma*: vertebrate homologs and invertebrate antecedents. Israel Journal of Zoology 42:131-146.

Lacalli, T. C. 2001. New perspectives on the evolution of protochordate sensory and locomotory systems, and the origin of brains and heads. Philosophical Transactions of the Royal Society of London B 356:1565-1572.

Lacalli, T. C. 2008a. Head organization and the head/trunk relationship in protochordates: problems and prospects. Integrative and Comparative Biology 48:620-629.

Lacalli, T. C. 2008b. Basic features of the ancestral chordate brain: a protochordate perspective. Brain Research Bulletin 75:319-323.

Lacalli, T. C., N. D. Holland, and J. E. West. 1994. Landmarks in the anterior central nervous system of amphioxus larvae. Philosophical Transactions of the Royal Society of London B 344:165-185.

Lamb, T. D., S. P. Collin, and E. N. Pugh, Jr. 2007. Evolution of the vertebrate eye: opsins, photoreceptors, retina and eye cup. Nature Reviews Neuroscience 8:960-975.

Langecker, T. G., and G. Longley. 1993. Morphological adaptations of the Texas blind catfishes *Trogloglanis pattersoni* and *Satan eurystomus* (Siluriformes: Ictaluridae) to their underground environment. Copeia 1993:976-986.

Lindström, T. 1949. On the cranial nerves of the cyclostomes with special reference to n. trigeminus. Acta Zoologica 30:315-458.

Linnaeus, C. 1758. Systema Naturae per Regna Tria Naturae. Regnum Animale. Laurentii Salvii, Stockholm.

Løvtrup, S. 1977. The Phylogeny of the Vertebrata. Wiley, New York.

Lumsden, A., and R. Keynes. 1989. Segmental patterns of neuronal development in the chick hindbrain. Nature 337:424-428.

Lumsden, A., N. Spawson, and A. Graham. 1991. Segmental origin and migration of neural crest cells in the hindbrain region of the chick embryo. Development 113:1281-1291.

Luther, A. 1938. Die Visceralmuskulatur der Acranier, Cyclostomen, und Fische. A. Acranier, Cyclostomen, Selachier, Holocephalen, Ganoiden und Dipnoer. Pages 468-542 in L. Bolk, E. Göppert, E. Kallius, and W. Lubosch, eds. Handbuch der vergleichenden Anatomie der Wirbeltiere, volume 5. Urban & Schwarzenberg, Berlin.

Maisey, J. G. 1986. Heads and tails: a chordate phylogeny. Cladistics 2:201–256.

Maisey, J. G. 1988. Phylogeny of early vertebrate skeletal induction and ossification patterns. Evolutionary Biology 22:1-36.

Mallatt, J. 1984. Early vertebrate evolution: pharyngeal structure and the origin of gnathostomes. Journal of Zoology 204:169-183.

Mallatt, J. 1996. Ventilation and the origin of jawed vertebrates: a new mouth. Zoological Journal of the Linnean Society 117:329-404.

Mallatt, J. 1997. Shark pharyngeal muscles and early vertebrate evolution. Acta Zoologica 78:279-294.

Mallatt, J. 2008. The origin of the vertebrate jaw: neoclassical ideas versus newer, development-based ideas. Zoological Science 25:990-998.

Mallatt, J., and J. Chen. 2003. Fossil sister group of craniates: predicted and found. Journal of Morphology 258:1-31.

Manni, L., A. Agnoletto, G. Zaniolo, and P. Burighel. 2005. Stomodeal and neurohypophyseal placodes in *Ciona intestinalis*: insights into the origin of the pituitary gland. Journal of Experimental Zoology B 304:324-339.

Manni, L., N. J. Lane, J.-S. Joly, F. Gasparini, S. Tiozzo, F. Caicci, G. Zaniolo, and P, Burighel. 2004. Neurogenic and non-neurogenic placodes in ascidians. Journal of Experimental Zoology B 302:483-504.

Marin, F., and P. Charnay. 2000. Hindbrain patterning: FGFs regulate *Krox20* and *mafB/kr* expression in the otic/preotic region. Development 127:4925-4935.

Marinelli, W., and A. Strenger. 1954. Vergleichende Anatomie und Morphologie der Wirbeltiere. I Lieferung. *Petromyzon marinus* (L). 1-80.

Marinelli, W., and A. Strenger. 1956. Vergleichende Anatomie und Morphologie der Wirbeltiere. II Lieferung. *Myxine glutinosa* (L). 81-172.

Martini, F. H. 1998. The ecology of hagfishes. Pages 57-77 in J. M. Jørgensen, J. P. Lonholt, R. E. Weber, and H. Malte, eds. The Biology of Hagfishes. Chapman, London.

Mazet, F., and S. M. Shimeld. 2005. Molecular evidence from ascidians for the evolutionary origin of vertebrate cranial sensory placodes. Journal of Experimental Zoology B 304:340-346.

Mazet, F., J. A. Hutt, J. Milloz, J. Millard, A. Graham, and S. M. Shimeld. 2005. Molecular evidence from *Ciona intestinalis* for the evolutionary origin of vertebrate sensory placodes. Developmental Biology 282:494-508.

McCauley, D. W., and M. Bronner-Fraser. 2003. Neural crest contributions to the lamprey head. Development 130:2317-2327.

McCauley, D. W., and M. Bronner-Fraser. 2006. Importance of SoxE in neural crest development and the evolution of the pharynx. Nature 441:750-752.

McClearn, D., and D. M. Noden. 1988. Ontogeny of architectural complexity in embryonic quail visceral arch muscles. American Journal of Anatomy 183:277-293.

McMullen, C. A., F. H. Andrade, and S. D. Crish. 2010. Underdeveloped extraocular muscles in the naked mole-rat (*Heterocephalus glaber*). The Anatomical Record 293:918-923.

Minoux, M., G. S. Antonarakis, M. Kmita, D. Duboule, and F. M. Rijli. 2009. Rostral and caudal pharyngeal arches share a common neural crest ground pattern. Development 136:637-645.

Miyake, T., J. D. McEachran, and B. K. Hall. 1992. Edgeworth's legacy of cranial muscle development with an analysis of muscles in the ventral gill arch region of batoid fishes (Chondriichthyes: Batoidea). Journal of Morphology 212:213-256.

Miyashita, T., and A. R. Palmer. In review. Handed hagfish and spiraling larvae: bilateral asymmetry and laterality in chordate evolution. The American Naturalist. 70 MS pp, 3 figures, 1 table, and 2 appendices.

Moody, S. A., and M. B. Heaton. 1983a. Developmental relationships between trigeminal ganglia and trigeminal motoneurons in chick embryos. I. Ganglion development is necessary for motoneuron migration. Journal of Comparative Neurology 213:327-343.

Moody, S. A., and M. B. Heaton. 1983b. Developmental relationships between trigeminal ganglia and trigeminal motoneurons in chick embryos. II. Ganglion axon ingrowth guides motoneuron migration. Journal of Comparative Neurology 213:344-349.

Moody, S. A., and M. B. Heaton. 1983c. Developmental relationships between trigeminal ganglia and trigeminal motoneurons in chick embryos. III. Ganglion perikarya direct motor acon growth in the periphery. Journal of Comparative Neurology 213: 350-364.

Mootoosamy, R. C., and S. Dietrich. 2002. Distinct regulatory cascades for head and trunk myogenesis. Development 129:573-583.

Müller, G. B., and G. P. Wagner. 1991. Novelty in evolution: restructuring the concept. Annual Review of Ecology and Systematics 22:229-256.

Müller, J. 1834. Vergleichende anatomie der Myxinoiden, der Cyclostomen mit durchbohrtem Gaumen. Osteologie und Myologie. Abhandlungen der Königlichen Akademie der Wissenschaften zu Berlin 1834:65-340.

Murakami, Y., K. Uchida, F. M. Rijli, and S. Kuratani. 2005. Evolution of the brain developmental plan: insights from agnathans. Developmental Biology 280:249-259.

Murakami, Y., M. Ogasawara, F. Sugahara, S. Hirano, N. Satoh, and S. Kuratani. 2001. Identification and expression of the lamprey *Pax6* gene: evolutionary origin of the segmented brain of vertebrates. Development 128:3521-3531.

Murakami, Y., M. Ogasawara, N. Satoh, F. Sugahara, S. Hirano, M. Myojin, S. Hirano, and S. Kuratani. 2002. Compartments in the lamprey embryonic brain as revealed by regulatory gene expression and the distribution of reticulospinal neurons. Brain Research Bulletin 57:271-275.

Neal, H. V. 1918. The history of the eye muscles. Journal of Morphology 30:433-453.

Neumayer, L. 1938. Die entwicklung des kopskelettes von *Bdellostoma* St. L. Archivio Italiano di Anatomica e di Embriologia 40(suppl.):1-222.

Nicol, D., and L. Meinertzhagen. 1991. Cell counts and maps in the larval central nervous system of the ascidian *Ciona intestinalis* (L.). Journal of Comparative Neurobiology 309:415-429.

Niederländer, C., and A. Lumsden. 1996. Late emigrating neural crest cells migrate specifically to the exit points of cranial branchiomotor nerves. Development 122:2367-2374.

Noden, D. M. 1978a. The control of avian cephalic neural crest cytodifferentiation. I. Skeletal and connective tissues. Developmental Biology 67:296-312.

Noden, D. M. 1978b. The control of avian cephalic neural crest cytodifferentiation. II. Neural tissues. Developmental Biology 67:313-329.

Noden, D. M. 1983a. The role of the neural crest in patterning of avian cranial skeletal, connective, and muscle tissues. Developmental Biology 96:144-165.

Noden, D. M. 1983b. The embryonic origins of avian cephalic and cervical muscles and associated connective tissues. American Journal of Anatomy 168:257-276.

Noden, D. M. 1984. Craniofacial development: new views on old problems. Anatomical Record 208:1-13.

Noden. D. M. 1986a. Patterning of avian craniofacial muscles. Developmental Biology 116:347-356.

Noden, D. M. 1986b. Origins and patterning of craniofacial mesenchymal tissues. Journal of Craniofacial Genetics and Developmental Biology 2:15-31.

Noden, D. M. 1988. Interactions and fates of avian craniofacial mesenchyme. Development 103:121-140.

Noden, D. M., and P. Francis-West. 2006. The differentiation and morphogenesis of craniofacial muscles. Developmental Dynamics 235:1194-1218.

Noden, D. M., and P. A. Trainor. 2005. Relations and interactons between cranial mesoderm and neural crest populations. Journal of Anatomy 207:575-601.

Northcutt, R. G. 1993. A reassessment of Goodrich's model of cranial nerve phylogeny. Acta Anatomica 148:71–80.

Northcutt, R. G. 2005. The new head hypothesis revisited. Journal of Experimental Zoology B 304:274-297.

Northcutt, R. G. 2008. Historical hypotheses regarding segmentation of the vertebrate head. Integrative and Comparative Biology 48:611-619.

Northcutt, R. G., and C. Gans. 1983. The genesis of neural crest and epidermal placodes: a reinterpretation of vertebrate origins. Quarterly Review of Biology 58:1–28.

Ohtani, K., T. Yao, M. Kobayashi, R. Kusakabe, S. Kuratani, and H. Wada. 2008. Expression of Sox and fibrillar collagen genes in lamprey larval chondrogenesis with implications from the evolution of vertebrate cartilage. Journal of Experimental Zoology B 310:596-607.

Oken, L. 1807. Über die bedeutung der Schädelknochen. Göbhardt, Bamberg.

Ota, K. G., and S. Kuratani. 2010. Expression pattern of two collagen type 2α1 genes in the Japanese inshore hagfish (*Eptatretus burger*) with special reference to the evolution of cartilaginous tissue. Journal of Experimental Zoology B 314:157-165.

Ota, K. G., S. Kuraku, and S. Kuratani. 2007. Hagfish embryology with reference to the evolution of the neural crest. Nature 446:672-675.

Ota, K. G., S. Fujimoto, Y. Oisi, and S. Kuratani. 2011. Identification of vertebra-like elements and their possible differentiation from sclerotomes in the hagfish. Nature Communications 2:373. 6 pp.

Oury, F., Y. Murakami, J.-S. Renaud, M. Pasqualetti, P. Charnay, S.-Y. Ren, and F. M. Rijli. 2006. *Hoxa2*- and rhombomere-dependent development of the mouse facial somatosensory map. Science 313:1408-1413.

Parker, W. K. 1883a. On the skeleton of the marsipobranch fishes. Part I. The myxinoids (*Myxine* and *Bdellostoma*). Philosophical Transactions of the Royal Society of London 174:373-409.

Parker, W. K. 1883b. On the skeleton of the marsipobranch fishes. Part II. *Petromyzon*. Philosophical Transactions of the Royal Society of London 174:411-457.

Pasquale, E. B. 2008. Eph–Ephrin bidirectional signaling in physiology and disease. Cell 133:38–52.

Pasqualetti, M., M. Ori, I. Nardi, and F. M. Rijli. 2000. Ectopic *Hoxa2* induction after neural crest migration results in homeosis of jaw elements in *Xenopus*. Development 127:5367-5378.

Pitsillides, A. A., and D. E. Ashhurst. 2008. A critical evaluation of specific aspects of joint development. Developmental Dynamics 237:2284-2294.

Prin, F., K.-E. Ng, U. Thaker, U. Drescher, and S. Guthrie. 2005. Ephrin-As play a rhombomere-specific role in trigeminal motor axon projections in the chick embryo. Developmental Biology 279:402-419.

Purcell, P., B. W. Joo, J. K. Hu, P. V. Tran, M. L. Calicchio, D. J. O'Connell, R. L. Maas, and C. J. Tabin. 2009. Temporomandibular joint formation requires two distinct hedgehog-dependent steps. Proceedings of the National Academy of Sciences 106:18297-18302.

Purnell, M. A. 1995. Microwear on conodont elements and macrophagy in the first vertebrates. Nature 374:798-800.

Purnell, M. A., and P. H. von Bitter. 1992. Blade-shaped conodont elements functioned as cutting teeth. Nature 359:629-631.

Purnell, M. A., and P. C. J. Donoghue. 1997. Architecture and functional morphology of the skeletal apparatus of ozarkodinid conodonts. Philosophical Transactions of the Royal Society of London B 352:1545-1564.

Randall, D. J. 1972. The respiration. Pages 287-306 in M. W. Hardisty and I. C. Potter, eds. The Biology of Lampreys. Volume 2. Academic Press, New York.

Reichert, H., and A. Simeone. 2001. Developmental genetic evidence for a monophletic origin of the bilateral brain. Philosophical Transactions of the Royal Society of London B 356:1533-1544.

Riedl, R. 1978. Order in Living Organisms. Wiley, New York.

Romer, A. S. 1972. The vertebrate as a dual animal – somatic and visceral. Evolutionary Biology 6:121-156.

Rovainen, C. M. 1996. Feeding and breathing in lampreys. Brain, Behavior and Evolution 48:297-305.

Rovainen, C. M., and M. H. Schieber. 1986. Ventilation of larval lampreys. Journal of Comparative Physiology A 158:91-102.

Ruppert, E. E. 2005. Key characters uniting hemichordates and chordates: homologies or homoplasies? Canadian Journal of Zoology 83:8-23.

Sambasivan, R., and S. Tajbakhsh. 2007. Skeletal muscle stem cell birth and properties. Seminars in Cell and Developmental Biology 18:870-882.

Sambasivan, R., S. Kuratani, and S. Tajbakhsh. 2011. An eye on the head: the development and evolution of craniofacial muscles. Development 138:2401-2415.

Sänger, A. M., and W. Stoiber. 2001. Muscle fiber diversity and plasticity. Pages 187-250 in I. Johnston, ed. Fish Physiology. Volume 18. Academic Press, New York.

von Scheven, G., L. E. Alvares, R. C. Mootoosamy, and S. Dietrich. 2006. Neural tube derived signals and Fgf8 act antagonistically to specify eye versus mandibular arch muscles. Development 133:2731–2745.

Schlosser, G. 2005. Evolutionary origins of vertebrate placodes: insights from developmental studies and from comparisons with other deuterostomes. Journal of Experimental Zoology B 304:347-399.

Schlosser, G. 2008. Do vertebrate neural crest and cranial placodes have a common evolutionary origin? BioEssays 30:659-672.

Schilling, T. F., and C. B. Kimmel. 1997. Musculoskeletal patterning in the pharyngeal segments of the zebrafish. Development 124:2945-2960.

Schilling, T. F., and R. D. Knight. 2001. Origins of anteroposterior patterning and *Hox* gene regulation during chordate evolution. Philosophical Transactions of the Royal Society of London B 356:1599-1613.

Schneider, A. 1879. Anatomie und Entwicklungsgeschichte von *Petromyzon* und Ammocoetes. Pages 85-92 in Beiträge zur vergleichenden Entwicklungsgeschichte der Wirbeltiere. Reimer, Berlin.

Schneider-Manoury, S., T. Seitanidou, P. Charney, and A. Lumsden. 1997. Segmental and neuronal architecture of the hindbrain of *Krox-20* mouse mutants. Development 124:1215-1226.

Schneider-Manoury, S., P. Topilko, T. Seitanidou, G. Levi, M. Cohen-Tannoudji, S. Pournin, C. Babinet, and P. Carney. 1993. Disruption of *Krox20* results in alteration of rhombomeres 3 and 5 in the developin hindbrain. Cell 75:1199-1214.

Sewertzoff, A. N. 1916. Études sur l'évolution des Vertébrés inférieurs. I. Morphologie du squelette et de la musculature de la tête des Cyclostomes. Archives russes d'anatomie, d'histologie et d'embryologie 1:1-104.

Shigetani, Y., F. Sugahara, and S. Kuratani. 2005. A new evolutionary scenario for the vertebrate jaw. BioEssays 27:331-338.

Shigetani, Y., F. Sugahara, Y. Kawakami, Y. Murakami, S. Hirano, and S. Kuratani. 2002. Heterotopic shift of epithelial-mesenchymal interactions in vertebrate jaw evolution. Science 296:1316-1319.

Shu, D., H.-L. Luo, S. Conway Morris, X.-L. Zhang, S.-X. Chen, J. Han, M. Zhu, Y. Li, and L.-Z. Chen. 1999. Lower Cambrian vertebrates from South China. Nature 402:42-46.

Shu, D., S. Conway Morris, J. Han. Z. F. Zhang, K. Yasui, P. Janvier, L. Chen, X. L. Zhang, J. N. Liu, Y. Li, and H. K. Liu. 2003. Head and backbone of the Early Cambrian vertebrate *Haikouichthys*. Nature 421:526-529.

Spater, D., T. P. Hill, R. J. O'Sullivan, M. Gruber, D. A. Conner, and C. Hartmann. 2006. Wnt9a signaling is required for joint integrity and regulation of Ihh during chondrogenesis. Development 133:3039-3049.

Sperry, D. G., and R. L. Boord. 1993. Organization of the vagus in elasmobranchs: its bearing on a primitive gnathostome condition. Acta Anatomica 148:150-159.

Shibukawa, Y., B. Young, C. Wu, S. Yamada, F. Long, M. Pacifici, and E. Koyama. 2007. Temporomandibular joint formation and condyle growth require Indian hedgehog signaling. Developmental Dynamics 236:426-434.

St-Jacques, B., M. Hammerschmidt, and A. P. McMahon. 1999. Indian hedgehog signaling regulates proliferation and differentiation of chondrocytes and is essential for bone formation. Genes & Development 13:2072-2086.

Stensiö, E. A. 1927. The Devonian and Downtonian vertebrates of Spitsbergen. Part I. Family Cephalaspidae. Skrifter om Svalbard og Nordishavet 12:1-391.

Stensiö, E. A. 1932. The Cephalaspids of Great Britain. Trustees of the British Museum, London. 220 pp.

Stensiö, E. A. 1958. Les Cyclostomes fossles ou Ostracodermes. Pages 173-425 in P. P. Grassé, ed. Traité de Zoologie. Volume 13. Masson et Cie, Paris.

Stensiö, E. A. 1964. Les Cyclostomes fossils ou Ostracodermes. Pages 96-383 in J. Piveteau, ed. Traité de Paléontologie, Volume 4. Masson et Cie, Paris.

Stensiö, E. A.1968. The cyclostomes with special reference to the diphyletic origin of the Petromyzontida and the Myxinoidea. Pages 13-71 in T. Ørvig, ed. Current Problems in Lower Vertebrate Phylogeny. Almqvist and Wiksell, Stockholm.

Stockard, C. R. 1906. The development of the mouth and gills in *Bdellostoma stouti*. American Journal of Anatomy 5:481-517.

Stolfi, A., and M. Levine. 2012. Neuronal subtype specification in the spinal cord of a protovertebrate. Development 138:995-1004.

Storm, E. E., and D. M. Kingsley. 1999. GDF5 coordinates bone and joint formation during digit development. Developmental Biology 209:11–27.

Strahan, R. 1958. The velum and the respiratory current of *Myxine*. Acta Zoologica 39:227-240.

Strahan, R. 1963. The behaviour of myxinoids. Acta Zoologica 44:73-102.

Sundin, O. H., and G. Eichele. 1990. A homeodomain protein reveals the metameric nature of the developing chick hindbrain. Genes and Development 4:1267-1276.

Taijbakhsh, S., D. Rocancourt, G. Cossu, and M. Buckingham. 1997. Redefining the genetic hierarchies controlling skeletal myogenesis: Pax-3 and Myf-5 act upstream of MyoD. Cell 89:127-138.

Takio, Y., M. Pasqualetti, S. Kuraku, S. Hirano, F. M. Rijli, and S. Kuratani. 2004. Lamprey *Hox* genes and the evolution of jaws. Nature 429. Published online. 2 pp.

Takio, Y., S. Kuraku, Y. Murakami, M. Pasqualetti, F. M. Rijli, Y. Narita, S. Kuratani, and R. Kusakabe. 2007. *Hox* gene expression patterns in *Lethenteron japonicum* embryos – insights into the evolution of the vertebrate Hox code. Developmental Biology 308:606-620.

Theisen, B. 1973. The olfactory system in the hagfish *Myxine glutinosa*. I. Fine structure of the apical part of the olfactory epithelium. Acta Zoologica 54:271-284.

Thomson, K. S. 1993. Segmentation, the adult skull, and the problem of homology. Pages 36-68 in J. Hanken and B. K. Hall, eds. The Skull. Volume II. Patterns of Structural and Systematic Diversity. The University of Chicago Press, Chicago.

Tjoa, L. T., and U. Welsch. 1974. Electron microscopical observations on Kölliker's and Hatschek's pit on the wheel organ in the head region of amphioxus (*Branchiostoma lanceolatum*). Cell and Tissue Research 153:175-187.

Tortora, G. J., and B. H. Derrickson. 2008. Principles of Anatomy and Physiology (12th edition). Wiley, New York. 1280 pp.

Tosney, K. W. 1978. The early migration of neural crest cells in the trunk region of the avian ambryo: an electron microscopic study. Developmental Biology 62:317-333.

Tosney, K. W. 1982. The segregation and early migration of cranial neural crest cells in the avian embryo. Developmental Biology 89:13-24.

Trainor, P. A., and R. Krumlauf. 2001. *Hox* genes, neural crest cells and branchial arch patterning. Current Opinion in Cell Biology 13:698-705.

Trainor, P. A., L. Ariza-McNaughton, and R. Krumlauf. 2002. Role of the isthmus and FGFs in resolving the paradox of neural crest plasticity and prepatterning. Science 295:1288-1291.

Tretjakoff, D. 1926. Das skelett und die Muskulatur im Kopfe des Flüssneunauges. Zeitschrift für Wissenschaftliche Zoologie 128:267-304.

Tretjakoff, D. 1929. Die schleimknorpeligen Bestandteile in Kopfskelett von Ammocoetes. Zeitschrift für Wissenschaftliche Zoologie 133:470-516.

Tsumaki, N., T. Nakase, T. Miyaji, M. Kakiuchi, T. Kimura, T. Ochi, and H. Yoshikawa. 2002. Bone morphogenetic protein signals are required for cartilage formation and differently regulate joint development during skeletogenesis. Journal of Bone and Mineral Research 17:898-906.

Tsuyama, M., H. Fukuda, and M. Wakita. 1995. A developmental study of the synovial membrane of the rat temporomandibular joint: changes in the three-dimensional configuration during postnatal development. Anatomia Embryologia 192:309-317.

Turner, S., C. J. B. Burrow, H.-P. Schutlze, A. Blieck, W.-E. Reif, C. B. Rexroad, P. Bultynck, and G. S. Nowlan. 2010. False teeth: conodont-vertebrate phylogenetic relationships revisited. Geodiversitas 32:545-594.

Tzahor, E. 2009. Heart and craniofacial muscle development: a new developmental theme of distinct myogenic fields. Developmental Biology 327:273-279.

Tzahor, E., H. Kempf, R. C. Mootoosamy, A. C. Poon, A. Abzhanov, C. J. Tabin, S. Dietrich, and A. B. Lessar. 2003. Antagonists of Wnt and BMP signaling promote the formation of vertebrate head muscle. Genes and Development 17:3087-3099.

Van Valen, L. M. 1982. Homology and causes. Journal of Morphology 173:305-312.

Wada, N., H. Saiga, N. Satoh, and P. W. H. Holland. 1998. Tripartite organization of the ancestral chordate brain and the antiquity of placodes: insights from ascidian *Pax-2/5/8*, *Hox* and *Otx* genes. Development 125:1113-1122.

Wagner, E., and M. Levine. 2012. FGF signaling establishes the anterior border of the *Ciona* neural tube. Development 139:2351-2359.

Wagner, G. P. 1994. Homology and the mechanisms of development. Pages 273-299 in B. K. Hall, ed. Homology: The Hierarchical Basis of Comparative Biology. Academic Press, San Diego.

Wängsjö, G. 1952. The Downtonian and Devonian vertebrates of Spitsbergen. 9. Morphologic and systematic studies of the Spitzbergen cephalaspids. Results of Th. Vogt's Expedition 1928 and the English-Norwegian-Swedish Expedition in 1939. Norsk Polarinstitutt Skrifter 97:1-611.

Weintraub, H. 1993. The MyoD family and myogenesis: redundancy, networks, and thresholds. Cell 75:1241-1244.

van Whijhe, J. W. 1915. Über die Mesodermsegmente und die Entwicklung der Nerven des Selachierkopfes. Verhandelingen der Koninklijke Akademie van Wetenschappen 22:1–50.

Whillis, J. 1940. The development of synovial joints. Journal of Anatomy 74:277-283.

Wicht, H., and T. C. Lacalli. 2005. The nervous system of amphioxus: structure, development, and evolutionary significance. Canadian Journal of Zoology 83:122-150.

Wicht, H., and R. G. Northcutt. 1995. Ontogeny of the head of the Pacific hagfish (*Eptatretus stouti*, Myxinoidea): development of the lateral line system. Philosophical Transactions of the Royal Society of London B 349:119-134.

Wilson, M. V. H., G. F. Hanke, and T. Märss. 2007. Paired fins of jawless vertebrates and their homologies across the "agnathan"-gnathostome

transition. Pages 122-149 in J. S. Anderson and H.-D. Sues, eds. Major Transitions in Vertebrate Evolution. Indiana University Press, Bloomington.

Worthington, J. 1905. Contribution to our knowledge of the Myxinoids. The American Naturalist 39:625-663.

Yalden, D. W. 1985. Feeding mechanisms as evidence for cyclostome monophyly. Zoological Journal of the Linnean Society 84:291-300.

Young, G. C. 1991. The first armoured agnathan vertebrates from the Devonian of Australia. Pages 67-85 in M. M. Chan, Y. H. Liu, and G. R. Zhang, eds. Early Vertebrates and Related Problems of Evolutionary Biology. Science Press, Beijing.

Young, G. C. 2008. Number and arrangement of extraocular muscles in primitive gnathostomes: evidence from extinct placoderm fishes. Biology Letters 4:110-114.

Zhang, G., and M. J. Cohn. 2006. Hagfish and lancelet fibrillar collagens reveal that type II collagen-based cartilage evolved in stem vertebrates. Proceedings of the National Academy of Sciences 103:16829-16833.

Zhang, G., M. M. Miyamoto, and M. J. Cohn. 2006. Lamprey type II collagen and *Sox9* reveal an ancient origin of the vertebrate collagenous skeleton. Proceedings of the National Academy of Science 103:3180-3185.

Zhang, G., B. F. Eames, and M. J. Cohn. 2009. Evolution of vertebrate cartilage development. Current Topics in Developmental Biology 86:15-42.

Zintzen, V., C. D. Roberts, M. J. Anderson, A. L. Stewart, C. D. Struthers, and E. S. Harvey. 2011. Hagfish predatory behaviour and slime defence mechanism. Scientific Reports 1:131. 6 pp.

3.7. TABLES

Table 3-1. Functional groupings of cranial muscles across vertebrates. In the lamprey column, larva indicates muscles that only occur in ammocoetes, whereas adult indicates those that appear during or after metamorphosis. Muscles without notation occur in both ammocoetes and adults. In the gnathostome column, general nomenclature is used to avoid confusion in terminology and designation of homology down to specific muscles. Because of the wide variety of cranial muscles in gnathostomes, a comprehensive analysis of homology within that lineage is beyond the scope of this paper. For recent reviews on this topic, see Anderson (2008); Diogo and Abdala (2010). The terminology for lamprey muscles follows Marinelli and Strenger (1954) and Hardisty and Rovainen (1982). Other sources are cited in the main text.

Table 3-1.

Major functional groups	Hagfish	Lampreys	Gnathostomes
Somatic locomotion	M. parietalis, m. obliquus	M. parietalis	Epaxial and hypaxial muscles
Connection of head to trunk	M. parietalis, m. obliquus	M. epibranchialis, m. hypobranchialis, m. supraocularis Adult: m. cornealis, m. probranchialis, m. subocularis	Cucullaris
Elevation of upper lip/maxillary region	M. tentacularis posterior, m. nasalis, m. subnasalis superficialis et profundus, m. cornual labialis, m. lingual tentacularis, m. nasolingualis, m. palatolabialis	Larva: m. buccalis anterior et superficialis, m. retractor labialis dorsalis et ventralis, m. levaltor labialis ventralis, m. retractor papillaris, m. velocranialis. Adult: m. annularis, m. basilaris, m. tectospinosus anterior et posterior, m. tectolateralis, m. spinocopularis, m. stylotectalis	Levator labialis musculature (Chondrichthyes)
Oropharyngeal constriction	M. constrictor pharyngis, m. palatolingualis profundus, m. palatolabialis	Larva: m. constrictor buccalis Adult: m. apicalis lateralis, m. pharyngicus anterior et posterior, m. protractor oesophagi	Intermandibular muscles
Suspension of lingual apparatus: protraction	M. palatolingualis superficialis, m. cornual lingualis, m. nasolingualis, m. otic lingualis	Adult: m. annuloglossus, m. basilariglossus, m. copuloglossus rectus, m. cornuoglossus	NA

Major functional groups	Hagfish	Lampreys	Gnathostomes
Suspension of lingual apparatus: retraction	M. rectus, m. craniolingualis, m. palatolingualis profundus, m. palatocoronarius, m. constrictor pharyngis pars anterior	Adult: m. copuloglossus obliquus, m. styloapicalis	NA
Lingual and dental apparatus: stabilization	M. retractor lingualis, m. perpendicularis	Adult: m. constrictor cornualis superficialis, m constrictor glossae internus, m. cornuotaenialis	NA
Dental apparatus: retraction	M. retractor dentalis major et lateralis	Adult: m. cardioapicalis, m. tendinoapicalis	Functional analogue: hypoglossal muscles
Dental apparatus: protraction	M. protractor dentalis lateralis et medialis	—	Functional analogue: hypoglossal muscles
Velum: flexion	M. craniovelar posterior	Larva: m. velohyoideus, m. velothyroideus Adult: m. depresser veli	NA
Velum: extension	M. craniovelar anterior dorsalis et ventralis, m. spinovelaris	Adult: m. levator valvulae velaris, m. protractor veli	NA
Suspension of branchial pouches and efferent duct	M. constrictor branchialis	Adult: m. compressor bursae branchialis circularis et obliquus	NA (branchial arch skeletons support the gill lamellae)
Eye movement	—	M. obliquus anterior et posterior, m. rectus anterior, inferior, posterior, et superior	M. obliquus anterior et ventralis, m. rectus anterior, inferior, lateralis, et superior

Major functional groups	Hagfish	Lampreys	Gnathostomes
Constrictors of branchial basket (feeding and respiration in ammocoete larvae; respiration in adults)	—	M. adductor branchialis dorsalis et ventralis, m. constrictor branchialis externus Larva: m. constrictor prebranchialis Adult: m. constrictor branchialis internus, m. interbranchialis	—
Constrictors of branchial cavity	—	—	Dorsal, ventral, and superficial constrictors including interhyoideus, dorsal and lateral interarcuals, branchial adductors.
Jaw levators and adductors	NA	NA	Levators and adductors of mandibular and hyoid arch skeletons; hypobranchial muscles including coracomandibularis, coracoarcual, coracohyoid, and coracobranchial.

Table 3-2. Comparison of vertebrate cranial muscles based on their developmental origin at the onset of myogenesis and differentiation of individual muscles. In the lamprey column, larva indicates muscles that only occur in ammocoetes, whereas adult indicates those that appear during or after metamorphosis. Muscles without notation occur both in ammocoetes and adults. In the gnathostome column, general nomenclature is used to avoid confusion in terminology and designation of homology down to specific muscles. Because a wide variety of cranial muscles in gnathostomes, a comprehensive analysis of homology within that lineage is beyond the scope of this paper. For recent reviews on this topic, see Anderson (2008); Diogo and Abdala (2010). The terminology for lamprey muscles follows Marinelli and Strenger (1954) and Hardisty and Rovainen (1982). Other sources are cited in the main text.

Table 3-2.

Developmental groups	Hagfish	Lampreys	Gnathostomes
Somatic muscle, lateral plate, anterior migration	M. parietalis	M. parietalis, m. epibranchialis, m. supraocularis Adult: m. cornealis, m. probranchialis, m. subocularis	Cucullaris muscles
Somatic muscle, lateral plate, anterior migration along ventral midline	M. obliquus, ?m. rectus	M. hypobranchialis	Hypobranchial and hypoglossal muscles
Prechordal mesoderm; parachordal mandibular domain[1]	—	M. obliquus anterior et posterior, m. rectus anterior, inferior, posterior, et superior	M. obliquus anterior et ventralis, m. rectus anterior, inferior, lateralis, et superior
Upper lip muscles, superficial, anterior migration from anterior mandibular domain	M. tentacularis posterior, m. nasalis, m. cornual labialis et lingualis, m. lingual tentacularis, m. nasolingualis (extended doromedially), m. palatolingualis profundus	Larva: m. buccalis superficialis, m. retractor labialis dorsalis, m. buccalis anterior, m. levator labialis ventralis Adult: m. tectospinosus anterior et posterior, m. tectolateralis, m. basilaris, m. annularis, m. basilariglossus, m. spinocopularis	NA
Upper lip muscles, deep, anterior migration from anterior mandibular domain	M. subnasalis superficialis et profundus, m. palatocoronarius, m. palatolabialis	Larva: m. retractor labialis ventralis, m. retractor papilallis Adult: m. copuloglossus obliquus	NA

Developmental groups	Hagfish	Lampreys	Gnathostomes
Maxillary labial muscles, anterior migration from posterior mandibular domain	NA	NA	Levator labialis musculature (Chondrichthyes)
Lateral plate, superficial mandibular domain	—	Adult: m. stylotectalis, m. constrictor cornualis superficialis, m. cornuoglossus,	M. adductor mandibulae, m. levator palatoquadratus, m. spiracularis (Chondrichthyes) and their homologues
Lateral plate, deep mandibular domain	—	Larva: m. constrictor buccalis, m. velocranialis. Adult: m. pharyngicus anterior et posterior, m. constrictor glossus internus, m. protractor oesophagi, m. depressor veli, m. levator valvulae velaris, m. protractor veli	M. intermandibularis (Chondrichthyes) and its homologues
Deep mandibular domain, posterior migration along pharynx	M. craniovelar anterior dorsalis et ventralis, m. craniovelar posterior, m. spinovelaris	Larva: m. velohyoideus, m. velothiroideus	NA
Superficial mandibular domain, ventral portion, longitudinal migration along ventral midline	M. protractor dentalis lateralis et medialis	Adult: m. annuloglossus, m. cornuotaenialis,?m. copuloglossus rectus	NA

Developmental groups	Hagfish	Lampreys	Gnathostomes
Deep mandibular domain, ventral portion, posterior migration along ventral midline	M. retractor dentalis major et lateralis, m. retractor lingualis, m. perpendicularis	Adult: m. styloapicalis, m. cardioapicalis, m. tendinoapicalis	NA
Visceral, hyoid domain	M, palatolingualis superficialis, m. craniolingualis (superficial), m. otic lingualis (deep)	Larva: m. constrictor prebranchialis Adult: m. sphincter branchialis anterior et posterior, m. constrictor branchialis externus, m. adductor branchiali dorsalis et ventralis (superficial), m. interbranchialis, m. constrictor branchialis internus (deep)	Homologues of m. levator hyoideus, m. interhyoideus (Chondrichthyes)
Post-hyoid pharyngeal domain, branchial arch, superficial	M. constrictor pharyngis	Larva: m. constrictor branchialis dorsalis et ventralis Adult: m. sphincter branchialis anterior et posterior, m. constrictor branchialis externus, m. adductor branchiali dorsalis et ventralis	Homologues of superficial constrictors (Chondrichthyes)
Post-hyoid pharyngeal domain, branchial arch, deep	NA	Adult: m. interbranchialis, m. constrictor branchialis internus	Homologues of interarcuals (Chondrichthyes)
Post hyoid pharyngeal domain, posterior migration	M. constrictor branchialis	NA	NA

Table 3-3. Similarities between specific hagfish cranial muscles recognized in this study and other cranial muscles of lampreys and gnathostomes based on phenotypic criteria. In the gnathostome column, general nomenclature is used to avoid confusion in terminology and designation of homology down to specific muscles. Sources are cited in the main text.

Notations for phenotypic criteria: A= attachment site (cartilage or other connective tissue); N= nerve innervation; M= position with respect to other muscles; P= overall position with respect to anatomical landmarks other than muscles (e.g. pharyngeal diverticulum; brain); V= position with respect to major blood vessels. Upper-case notations indicate close similarity, whereas lower-case notations indicate incomplete similarity. Similarity in attachment site was determined by homology of cartilages (Chapter 2). Similarity in nerve innervation was determined by the proximodistal position of the major motor branch that innervates the muscle. Lower-case notation for nerve innervation indicates that the muscle is innervated by a different motor branch of the same cranial nerve (Figure 3-15; Lindström 1949; Song and Boord 1993; other sources are cited in the main text).

Table 3-3.

Hagfish	Lampreys	Gnathostomes	Notes
M. parietalis	M. parietalis, m. supraocuralis, m. subocularis, m. cornealis, m. probranchialis, m. epibranchialis[A, N, M, P, V]	Cucullaris, epaxial and hypaxial musculature[A, N, M, P, V]	
M. obliquus	M. parietalis, m. hypobranchialis [A, N, M, P, V]	Hypaxial and hypobranchial musculature [a, N, m, P, V]	
M. rectus	M. parietalis [a, N, M, P, V]	Hypaxial and hypobranchial musculature [a, N, m, P, V]	
M. tentacularis posterior	M. basilaris[a, n, M, P]; m. buccalis superficialis[n, M, P]	NA	M. buccalis superficialis is present in ammocoetes
M. nasalis	m. retractor labialis dorsalis[N, M, p]; m. basilaris[a, n, M, P]; m. annularis[n, p]	NA	M. retractor labialis dorsalis is present in ammocoetes
M. palatolingual profundus	M. basilariglossus[a, N, M, P]; m. cornuoglossus[a, N, m, p]; m. levator labialis ventralis[a, n, m, p]	NA	M. levator labialis ventralis is present in ammocoetes
M. cornual lingualis	M. basilariglossus[a, N, M, P]	NA	
M. cornual labialis	M. basilariglossus[N, M, p]; m. tectospinosus posterior[a, n, M, p]; m. buccalis anterior[n, P]	NA	M. buccalis anterior is present in ammocoetes
M. lingual tentacularis	M. spinocopularis[a, N, M, P]; m. tectospinosus anterior and posterior[N, M, p]; m. tectolateralis[n, M, p]; m. retractor papillaris[n, m, p]	NA	M. retractor papillaris is present in ammocoetes

Hagfish	Lampreys	Gnathostomes	Notes
M. nasolingualis	M. tectospinosus anterior and posterior[a, N, M, P]; m. tectolateralis[a, n, M, P]	NA	
M. subnasalis superficialis	M. stylotectalis[n, m, P]; m. tectolateralis[a, N]	NA	
M. subnasalis profundus	M. tectolateralis[a, N, p]; m. pharyngicus anterior[N, m, p]	NA	
M. palatocoronarius	M. pharyngicus posterior[n, M, p]; m. levator valvulae velaris, m. constrictor buccalis, m. retractor labialis ventralis[n, m, p]	M. levator labialis[n, m, p] (Chondrichthyes) and its homologues	M. constrictor buccalis and m. retractor labialis ventralis are present in ammocoetes
M. palatolabialis	M. pharyngicus posterior[a, n, M, p]; m. levator valvulae velaris, m. constrictor buccalis, m. retractor labialis ventralis[n, m, p]	M. levator labialis[n, m, p] (Chondrichthyes) and its homologues	M. constrictor buccalis and m. retractor labialis ventralis are present in ammocoetes
M. craniovelar anterior dorsalis	M. protractor veli, m, velocranialis[a, N, M, P]; m. levator valvulae velaris[a, n, m, p]	NA	M. velocranialis is present in ammocoetes
M. craniovelar anterior ventralis	M. protractor veli, m. velocranialis[a, N, M, P]; m. levator valvulae velaris[a, n, m, p]	NA	M. velocranialis is present in ammocoetes
M. craniovelar posterior	M. depressor veli[a, n, M, P]	NA	
M. spinovelaris	M. protractor veli[a, N, M, p]	NA	
M. protractor dentalis lateralis	M. copuloglossus rectus[a, N, M, P]	NA	
M. protractor dentalis medialis	M. annuloglossus[a, N, M, P]	NA	
M. retractor dentalis lateralis	M. styloapicalis[A, N, M, P]	NA	
M. retractor dentalis major	M. cardioapicalis[a, N, M, P]	NA	

Hagfish	Lampreys	Gnathostomes	Notes
M. retractor lingualis	M. constrictor cornualis superficialis, m. constrictor glossus internus[N, M, p]	M. intermandibularis[n, m, p] (Chondrichthyes) and its homologues	Test of similarity based on lamprey adults
M. perpendicularis	NA	NA	
M. palatolingual superficialis	M. basilariglossus[a, M, P]	NA	
M. craniolingualis	M. cornuoglossus[A, m, P]; m. constrictor branchialis externus[N, m, p]	M. levator hyoideus[N, m, p] (Chondrichthyes) and its homologues	M. cornuotaenialis is innervated by the trigeminal nerve
M. otic lingualis	M. constrictor prebranchialis[a, N, m, P, V]; m. cornuotaenialis[a, m, P, V]; m. constrictor branchialis externus[N, m, p, V]; m. interbranchialis[N, m, p, V]	M. levator hyoideus[a, N, m, P] (Chondrichthyes) and its homologues	M. constrictor prebranchialis is present in ammocoetes; m. cornuotaenialis is innervated by the trigeminal nerve
M. constrictor pharyngis	m. constrictor branchialis externus, m. adductor branchialis dorsalis and ventralis, m. interbranchialis[N, p, V]	Superficial constrictors and interarcuals[N, p] (Chondrichthyes); and their homologues	
M. constrictor branchialis	M. constrictor branchialis externus, m. adductor branchialis dorsalis, m. interbranchialis[a, N, P, V]	Superficial constrictors and interarcuals[a, N, P] (Chondrichthyes); and their homologues	

Table 3-4. Proposed homologies between specific hagfish cranial muscles recognized in this study and those of lampreys and gnathostomes, based on congruence in functional, developmental, and morphological similarities as detailed in Tables 3-1 to 3-3. This is not a comprehensive homology analysis of lamprey or gnathostome cranial muscles, and does not include muscles unique to either or both of the lineages that do not occur in hagfish including extraocular muscles. For detailed discussion and sources, see the main text and Figure 3-16. Notations: —, absent; NA, not applicable.

Table 3-4.

Hagfish	Lampreys	Gnathostomes	Notes
M. parietalis	M. parietalis, m. supraocuralis, m. subocularis, m. cornealis, m. probranchialis, m. epibranchialis	Cucullaris, epaxial and hypaxial musculature	Myomeres in cephalochordates
M. obliquus	M. parietalis, m. hypobranchialis	Hypaxial and hypobranchial musculature	Pterygial muscle in cephalochordates
M. rectus	M. parietalis, m. hypobranchialis	Hypaxial and hypobranchial musculature	Pterygial muscle in cephalochordates
M. tentacularis posterior	—	NA	
M. nasalis	—	NA	
M. palatolingual profundus M. cornual lingualis	M. basilariglossus	NA	
M. cornual labialis	—	NA	
M. lingual tentacularis	?M. spinocopularis	NA	
M. nasolingualis	?M. tectospinosus anterior and posterior	NA	Feeding muscle in osteostracan?
M. subnasalis superficialis	—	NA	
M. subnasalis profundus	—	NA	
M. palatocoronarius	—	—	
M. palatolabialis	—	—	
Velar extensors (m. craniovelar anterior dorsalis and ventralis, m. spinovelaris)	?m. protractor veli; ?m. velocranialis	NA	M. velocranialis is present in ammocoetes
M. craniovelar posterior	M. depressor veli	NA	
M. protractor dentalis lateralis	M. copuloglossus rectus	NA	
M. protractor dentalis medialis	M. annuloglossus	NA	
M. retractor dentalis lateralis	M. styloapicalis	NA	

Hagfish	Lampreys	Gnathostomes	Notes
M. retractor dentalis major	M. cardioapicalis	NA	
M. retractor lingualis	?M. constrictor cornualis superficialis; ?m. constrictor glossus internus	NA; ?M. intermandibularis (Chondrichthyes) and its homologues	Test of similarity based on lamprey adults
M. perpendicularis	—	NA	
M. palatolingualis superficialis	—	—	
M. craniolingualis	—	—	
M. otic lingualis	?M. constrictor prebranchialis; ?m. constrictor branchialis externus; ?m. interbranchialis	?M. levator hyoideus (Chondrichthyes) and its homologues	M. constrictor prebranchialis is present in ammocoetes
M. constrictor pharyngis (anterior portion; glossopharyngeal innervation)		—	
M. constrictor pharyngis (posterior portion; vagus innervation)	NA	NA	
M. constrictor branchialis	?M. constrictor branchialis externus; ?m. adductor branchialis dorsalis; ?m. interbranchialis	?Superficial constrictors and interarcuals (Chondrichthyes); and their homologues	

Table 3-5. Summary and phylogenetic distribution of characters for early vertebrate evolution used in the formulation of Mandibular Siege Hypothesis. Neural crest, placodes, and pharyngeal domains are central to this hypothesis, and various key innovations either pattern head morphology or are patterned into head morphology via interaction with neural crest cells. In the taxonomic columns, the mark "x" indicates presence; "e" indicates uncertain ancestral condition or equivocal evidence. Blank cells represent absence, whereas question mark "?" indicates unknown state.
Taxon abbreviations: CE= cephalochordates; CO= conodonts; GN= gnathostomes; HA= hagfish; HE= hemichordates; LA= lampreys; SG= jawless stem gnathostomes (arandaspids, anaspids, galeaspids, heterostracans, osteostracans, and thelodonts); SV= stem vertebrates (based on *Haikouichthys* and *Myllokunmingia* with consideration of *Haikouella*); UR= urochordates.
Character notations: G= diverticulum of gut endoderm or pharyngeal structure; N= innervated by nerve; NC= contribution from or potential to interact with neural crest-derived ectomesenchyme; ONC= ability or potential to affect path of neural crest cell migration; PC= prechordal; PL= derived from placode; and S= somatic structure. Lower-case characters indicate that the condition is not universal across compared taxa. Sources are cited in the main text. Additional sources for the table that are not cited in the text: Goodrich (1917); Carvey and Cloney (1974); Tjoa and Welsc (1974); Nicol and Meinertzhagen (1991); Chen et al. (1999); Shu et al. (1999, 2003); Holland and Chen (2001); Boorman and Shimeld (2002a, b); Ruppert (2005); Mallatt and Chen (2003).

Characters	HE	CE	UR	SV	HA	LA	CO	SG	GN
Neural crest				e	x	x	?	x	x
Neurogenic ectodermal placodes[N, NC]				e	x	x	?	x	x
Premandibular, mandibular, and hyoid domains[N, NC]				?	x	x	?	x	x
Delineated mandibular domain[N, NC]									x
Jaw[NC]									x
Life history									
Tornarian larva	x								
Tadpole larva			x						
Motile filter-feeding stage		x	x	e		x	?	e	x
Motile macrophagous stage				?	x	x	x	e	x
Sessile adult stage	e		e	?					
Dlx cascade									
Perioral expression of *Edn-2* and *Edn-3*[NC]				?	?	x	?	?	x
Bapx1 expression at lower-lip/velum boundary[NC]				?	?	x	?	?	
Bapx1 expression at jaw joint[NC]				?	?		?	?	x
Duplicated *Dlx*				?	?	x	?	?	x
Dlx code[NC]				?	?		?	?	x
Posterior shift of oral patterning genes and *Dlx* expression domain (*Dlx*-free anterior mandibular domain)[NC]				?	?		?	?	x
Overall body plan									
Pharyngeal slits[ONC]	x	x	x	x	x	x	?	x	x
Skeletal support for pharyngeal arches[nc]		x		e	x	x	?	x	x
Notochord		x	x	x	x	x	x	x	x
Somite[N, ONC]		x	e	x	x	x	x	x	x
Dorsal nerve cord with cerebral ganglion		x	x	x	x	x	?	x	x
Tripartite brain		e	e	?	x	x	?	x	x
Rhombomeres[ONC]				?	x	x	?	x	x

Characters	HE	CE	UR	SV	HA	LA	CO	SG	GN
Somitovisceral differentiation of motor and sensory neurons		x		?	x	x	?	?	x
Unsegmented head mesoderm[N, NC]				?	x	x	?	x	x
Pharyngeal mesoderm[N, NC]				?	x	x	?	x	x
Branchiomeric nerves[NC]				?	x	x	?	x	x
Dorsoventral patterning of pharyngeal arches[NC] (cascade expression of *Dlx* pathway)				?	?	x	?	?	x
Tendons[NC]				?	x	x	?	?	x
Cellular cartilages[NC]				?	x	x	?	x	x
Mineralized dermal skeleton[NC]								x	x
Scales[NC, PL]								x	x
Tooth-like oral apparatus[NC?, PL?]				?	x	x	x	x	
Teeth[NC, PL]									x
Mineralized internal skeleton[NC]									x
Synovial joint[NC]									x
Paraxial skeletal elements derived from sclerotomes (vertebra)				?	x	x	?	x	x
Paired fins[N, S]								x	x
Dorsoventral patterning of somatic body wall[N, S]				?	x	x	?	x	x
Epaxal-hypaxial differentiation[N, S]								x	x
Cucullaris[N, S]								?	x
Hypoglossal muscles[N, S]								?	x
Nasal capsule and potential homologue									
Kölliker's pit[G, N, PC] (secretory)		x							
Nasal capsule[N, NC, ONC, PL]				e	x	x	?	x	x
Pituitary-adenohypophysis homologues									
Proboscis pore[N]	x								
Hatschek's pit[G, N]		x							
Ciliated funnel (olfactory) with asymmetric gland[G, N]			x						
Adenohypophysis[N, NC, ONC, PL]				?	x	x	x	x	x
Rathke's pouch[N, NC, ONC, PL]								?	x

Characters	HE	CE	UR	SV	HA	LA	CO	SG	GN
Ocular structures									
Pigment spot[N]		x							
Ocellus[N]			x						
Eye[N, ONC, PL]				x	x	x	x	x	x
Extraocular muscles[N, PC]				?		x	x	x	x
Balance organs and vestibulocochlear derivatives									
Infundibular organ[N]		x							
Otolith[N]			x						
Otic capsule[NC, ONC, PL]				e	x	x	?	x	x
Number of semicircular canals[N, PL]				?	1	2	?	2	3
Lateral line[N, NC, PL]				?	x	x	?	x	x
Electrosensory receptors[N, PL]						x	?	?	x
Thyroid homologue									
Endostyle[G, N]		x	x	e		x	?	?	
Thyroid[G, N]					x	x	?	?	x
Premandibular domain									
Single nasal aperture[N, NC, PL]				?	x	x	?	x	
Paired nasal apertures[N, NC, PL]								x	x
Preoral nasohypophyseal complex[G, N, NC, PL]				?	x			x	
Postoral nasohypophyseal complex[G, N, NC, PL]				?		x	?	x	
Nasal cavity[N, NC, PL]									x
Trabecula[NC]								?	x
Mandibular-hyoid domains									
Upper lip[N, NC]				?	x	x	?	x	
Lingual apparatus[N, NC]				?	x	x	x	?	
Velum[G]		e		?	x	x	?	e	
Cardinal heart associated with proximal velar contact					x		?	?	
Spiracle[G]								x	x
Motor neurons of trigeminal nerve largely restricted to posterior distal branch (mandibular nerve)[NC]									x

Characters	HE	CE	UR	SV	HA	LA	CO	SG	GN
Pharyngeal/branchial structures									
External gill arch skeleton[NC]				?	?	x	?	x	x
Internal gill arch skeleton[NC]					?		?		x

3.8. FIGURES

Figure 3-1. Overall head anatomy of the northeastern Pacific hagfish *Eptatretus stoutii*. (A-C) The cranial musculature in left lateral view, from superficial to deep parasagittal levels. Muscles (red) with associated tendons (blue) are semi-transparent to show relative positions with respect to cranial landmark tissues underneath. For B and C, muscles are selectively removed from superficial positions to reveal the muscles at deeper levels. For different combination of muscles that help clarify overall muscle configurations, see figures 3-5 through 3-10. (D) The cranial nerves shown with the semi-transparent chondrocranium (white) based on original observation and the description of cranial nerves of the Atlantic hagfish *Myxine glutinosa* by Lindström (1949). Only major branches are represented. The innervation of the vagus nerve is omitted. Motor branches are shaded in red, whereas sensory branches are in pale brown.

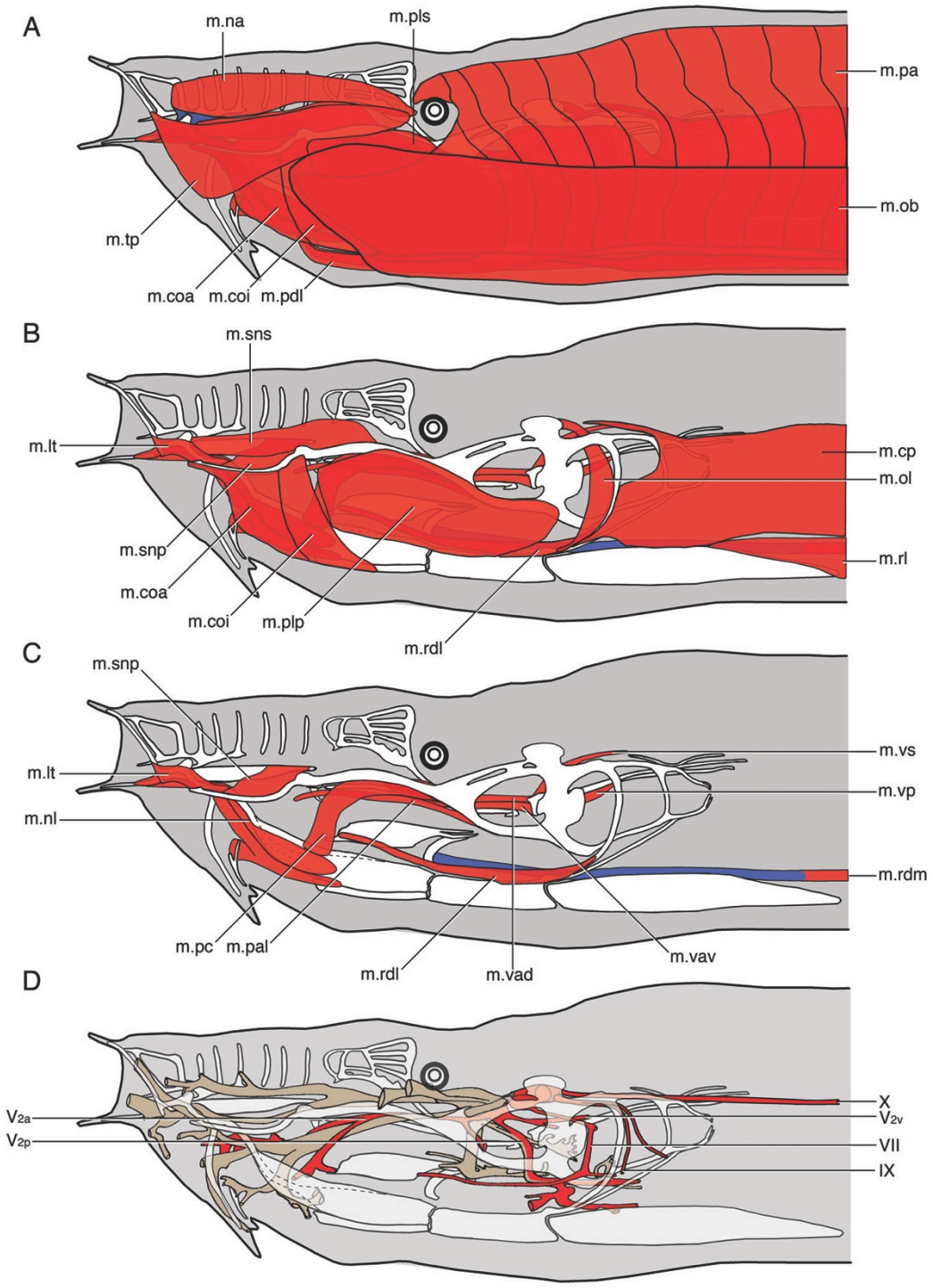
A
m.na
m.pls
m.pa
m.ob
m.tp
m.coa
m.coi
m.pdl
B
m.sns
m.lt
m.cp
m.ol
m.snp
m.rl
m.coa
m.coi
m.plp
m.rdl
C
m.snp
m.vs
m.lt
m.vp
m.nl
m.rdm
m.pc
m.pal
m.vav
m.rdl
m.vad
D
X
V2v
V2a
V2p
VII
IX

Figure 3-1.

Figure 3-2. Comparison of vertebrate head anatomy using lamprey adults. (A-E) The cranial musculature of the lamprey *Lampetra fluvialis* in left lateral view from superficial to successively deeper parasagittal levels. From B through E, muscles (red) with associated tendons (blue) are selectively removed from superficial positions to reveal muscles at deeper levels. (F) Extraocular muscles (red) and associated motor nerves (dark yellow) in the orbit (pale yellow) of *L. fluvialis* in left lateral view. (G) The velar muscles with the associated skeletal elements in dorsal view, with the anterior end oriented upward. (H) The general morphology of the lingual retractors in lampreys. A simplified reconstruction of the retractors of the apical tooth plate of *L. fluvialis* was combined with the lingual apparatus of *Petromyzon marinus* to show an overall configuration of the retractors. Muscles are semi-transparent to show relative positions with respect to cranial landmark tissues underneath. Cartilages and notochord are shaded in grey, with the more superficial with the lighter shade and the deeper with the darker shade. Redrawn based on reconstructions by Johnels (1948; H), Marinelli and Strenger (1954; A-H), Hardisty and Rovainen (1982; A-H).

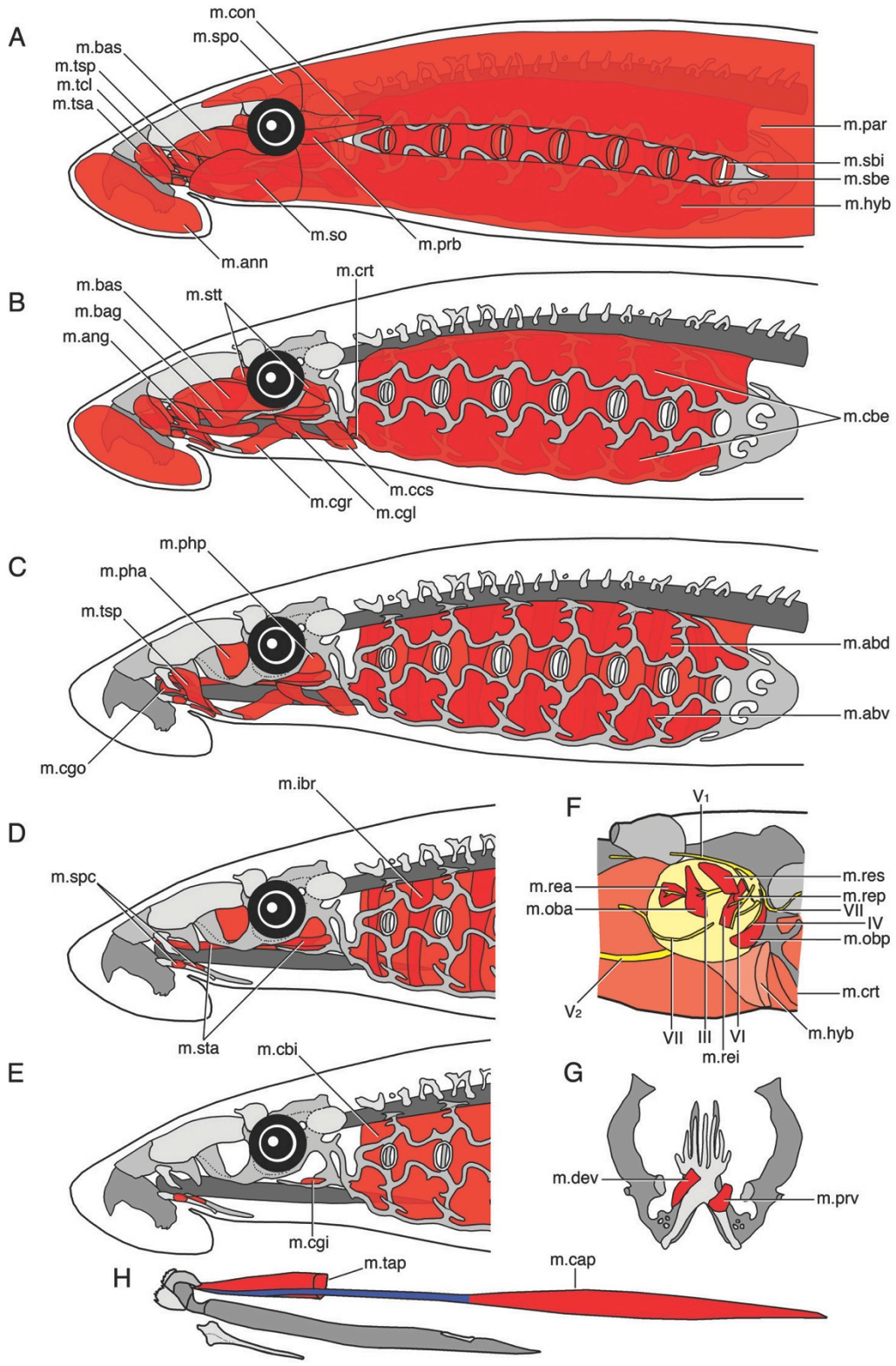
A
m.con
m.spo
m.bas
m.tsp
m.tcl
m.tsa
m.par
m.sbi
m.sbe
m.hyb
m.so
m.prb
m.ann
B
m.crt
m.bas
m.stt
m.bag
m.ang
m.cbe
m.cgr
m.ccs
m.cgl
C
m.php
m.pha
m.tsp
m.abd
m.abv
m.cgo
D
m.ibr
m.spc
m.sta
E
m.cbi
m.cgi
F
V1
m.res
m.rea
m.rep
m.oba
VII
IV
m.obp
m.crt
V2
VII
III
VI
m.hyb
m.rei
G
m.dev
m.prv
H
m.tap
m.cap

Figure 3-2.

Figure 3-3. Comparison of the vertebrate head anatomy using lamprey ammocoetes larva. (A-D) The generalized reconstruction of the cranial musculature (red) in left lateral view from superficial to successively deeper parasagittal levels. From B through D, muscles are successively removed from superficial positions to reveal muscles at deeper levels. Muscles are semi-transparent to show relative positions with respect to cranial landmark tissues (white) underneath. The notochord is shaded black. Specimens not to scale. Redrawn after reconstructions by Tretjakoff (1927, 1929), Damas (1935), Johnels (1948), and Hardisty and Rovainen (1982).

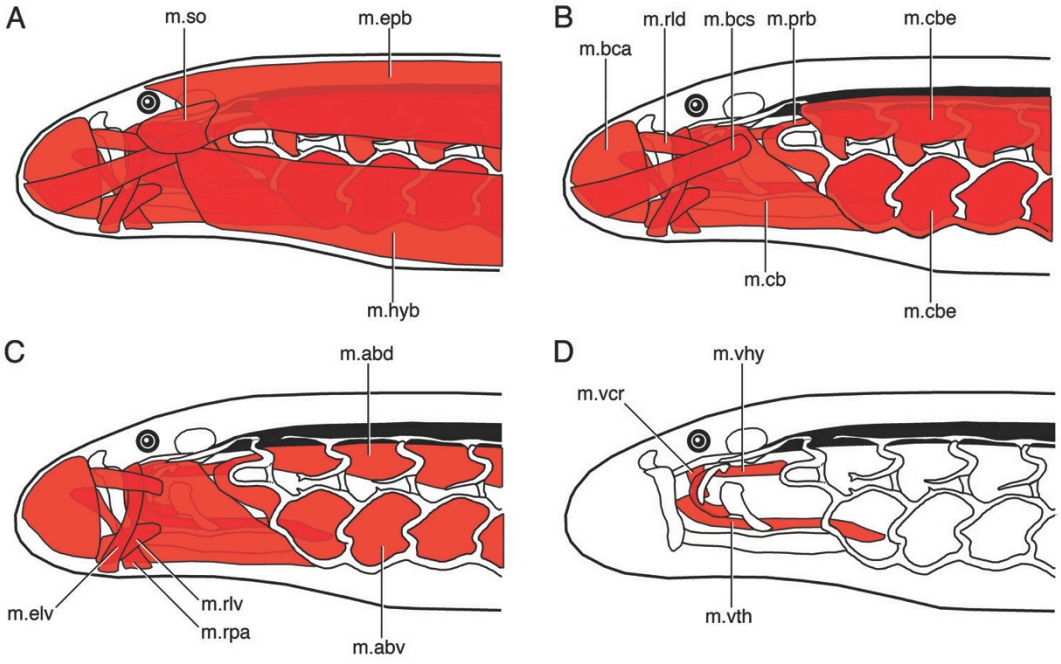
A
m.so
m.epb
m.hyb
B
m.rld
m.bcs
m.prb
m.cbe
m.bca
m.cb
m.cbe
C
m.abd
m.elv
m.rlv
m.rpa
m.abv
D
m.vhy
m.vcr
m.vth

Figure 3-3.

Figure 3-4. Vertebrate head anatomy and muscles (various shades of red) illustrated using a chondrichthyan, the dogfish *Squalus acanthias*. (A) Cranial muscles in left lateral view. (B) General morphology and nomenclature of cranial muscles in vertebrates; left lateral view. (C) Cranial muscles in ventral view. On the left side, superficial muscles are partially removed to reveal deeper muscles. Specimens not to scale. Different shades of muscles simply indicate individual muscles. Reproduced from Mallatt (1997) with shading added.

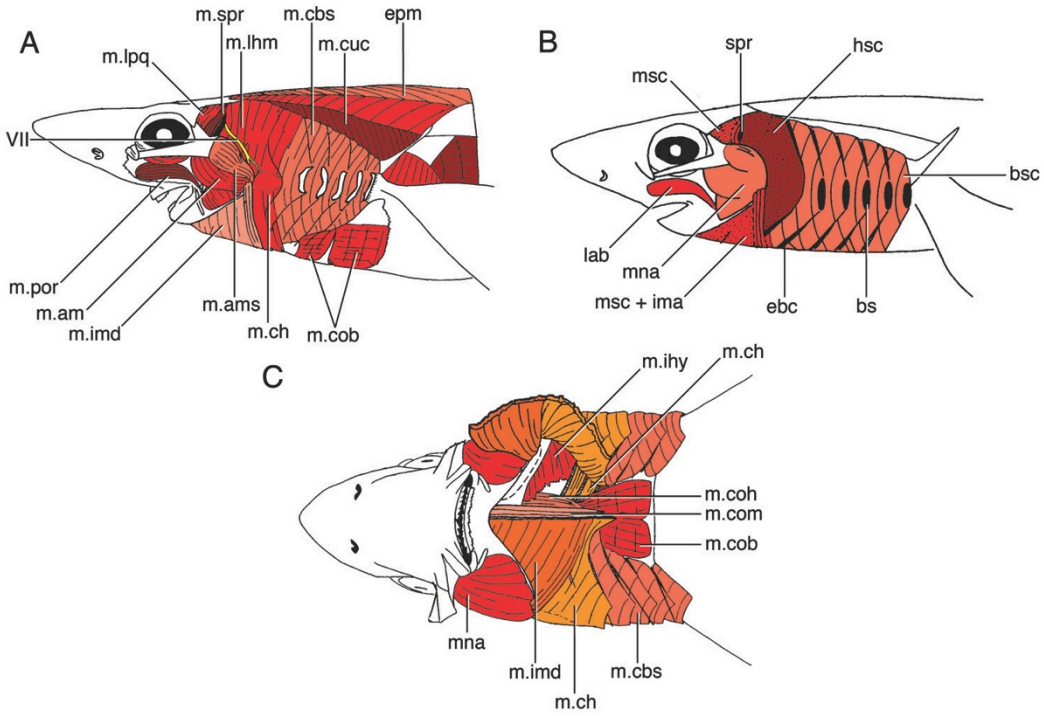
A
m.spr
m.cbs
epm
m.lhm
m.cuc
m.lpq
VII
m.por
m.am
m.imd
m.ams
m.ch
m.cob
B
spr
hsc
msc
bsc
lab
mna
msc + ima
ebc
bs
C
m.ihy
m.ch
m.coh
m.com
m.cob
mna
m.imd
m.cbs
m.ch

Figure 3-4.

Figure 3-5. Somatic and superficial cranial muscles (red) with associated tendons (blue) of the hagfish *Eptatretus stoutii*. (A) The head in left lateral view, with deeper cranial muscles removed to show topographical relationship with the chondrocranium (white). (B) The head in dorsal view, with deeper cranial muscles removed for clarity. On the left side, muscles are semi-transparent to reveal position with respect to the chondrocranium. On the right side, muscles are opaque as in living individuals. Horizontal bars indicate positions of the sections labeled accordingly. (C-G) Left halves of transverse sections of the head, showing somatic and superficial cranial muscles with respect to other cranial structures. Sections were stained with eosin and hematoxylin. Section locations are marked in B.

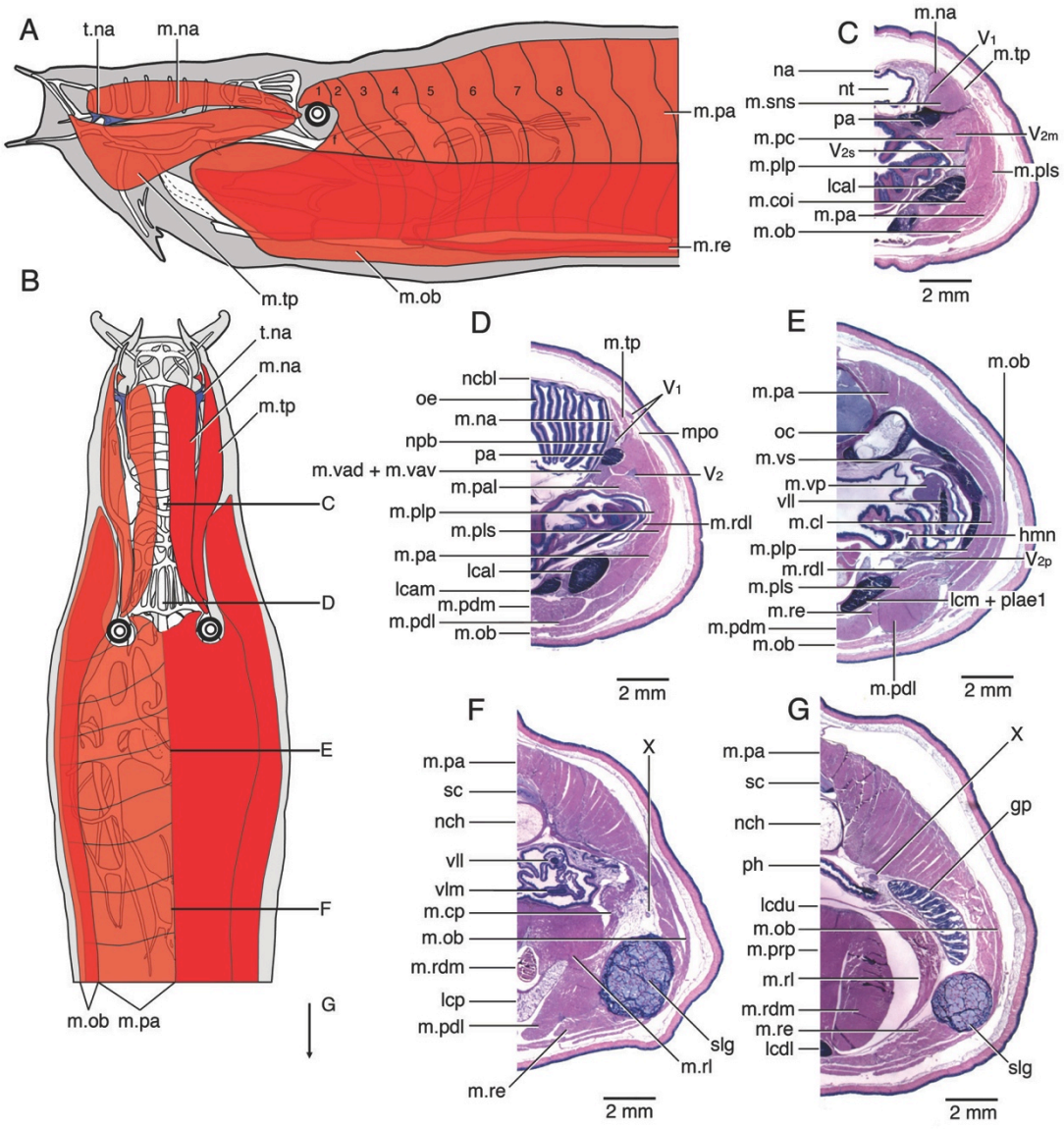
A
t.na
m.na
1
2
3
4
5
6
7
8
m.pa
m.re
m.tp
m.ob
B
t.na
m.na
m.tp
C
D
E
F
G
m.ob
m.pa
C
m.na
V1
m.tp
na
nt
m.sns
pa
m.pc
V2s
V2m
m.plp
m.pls
lcal
m.coi
m.pa
m.ob
2 mm
D
m.tp
ncbl
V1
oe
m.na
mpo
npb
pa
m.vad + m.vav
V2
m.pal
m.plp
m.rdl
m.pls
m.pa
lcal
lcam
m.pdm
m.pdl
m.ob
2 mm
E
m.ob
m.pa
oc
m.vs
m.vp
vll
m.cl
hmn
m.plp
V2p
m.rdl
m.pls
lcm + plae1
m.re
m.pdm
m.ob
m.pdl
2 mm
F
X
m.pa
sc
nch
vll
vlm
m.cp
m.ob
m.rdm
lcp
m.pdl
slg
m.rl
m.re
2 mm
G
X
m.pa
sc
gp
nch
ph
lcdu
m.ob
m.prp
m.rl
m.rdm
m.re
lcdl
slg
2 mm

Figure 3-5.

Figure 3-6. Facial muscles (red) with associated tendons (blue) of the hagfish *Eptatretus stoutii* in left lateral view (A-D). Muscles are in different combinations from Figure 3-1 to describe their overall configuration, and their relation to the chondrocranium (white). From B through D, muscles are successively removed from superficial positions to reveal muscles at deeper levels.

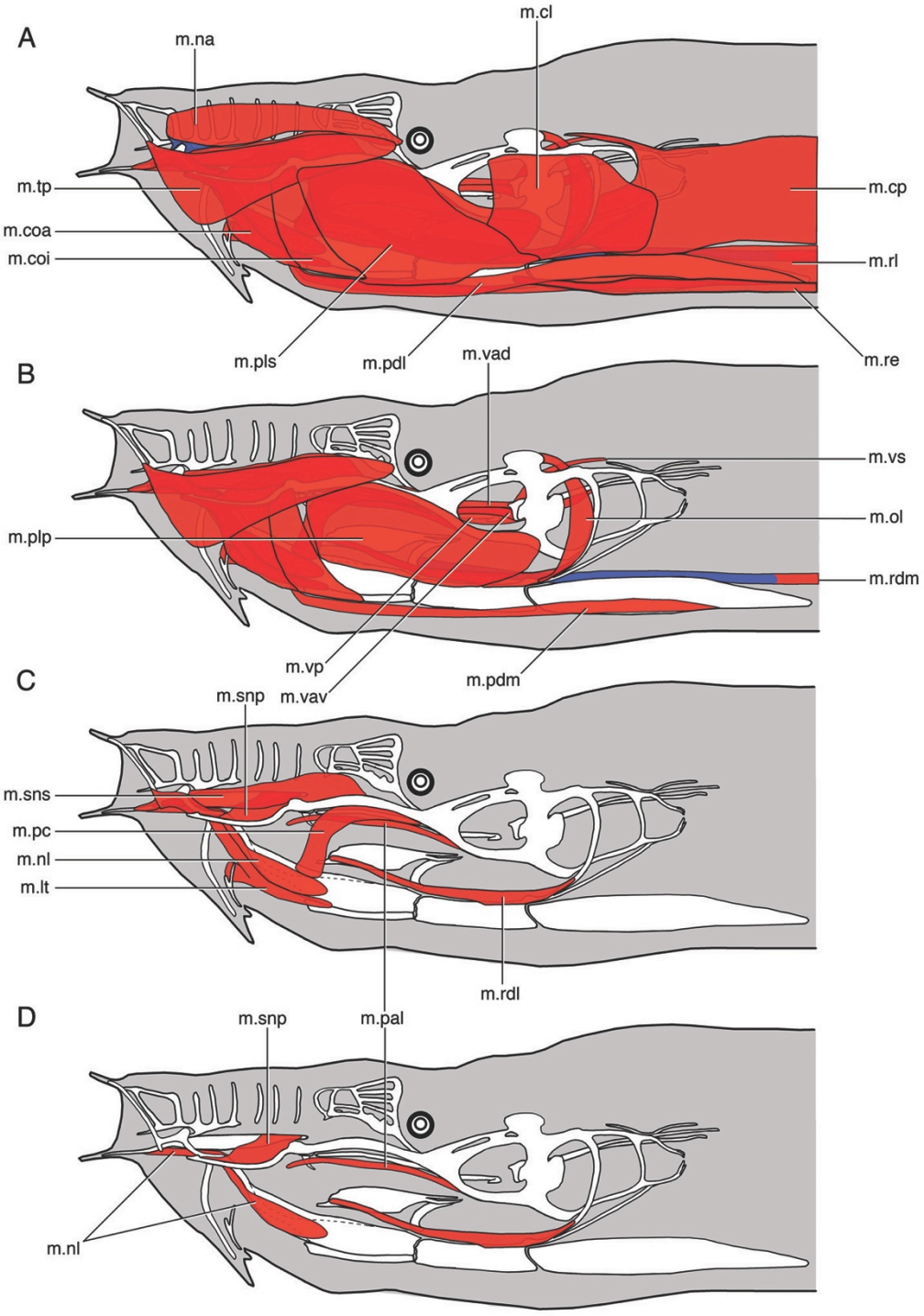
A
m.na
m.cl
m.tp
m.coa
m.coi
m.cp
m.rl
m.re
m.pls
m.pdl
B
m.vad
m.vs
m.ol
m.plp
m.rdm
m.vp
m.vav
m.pdm
C
m.snp
m.sns
m.pc
m.nl
m.lt
m.rdl
D
m.snp
m.pal
m.nl

Figure 3-6.

Figure 3-7. Mid to deep muscles in the snout of the hagfish *Eptatretus stoutii*. (A) The head in dorsal view, with the nasal tube and other muscles in the periphery removed for clarity. Cartilages are shaded in grey, with the more superficial with the lighter shade and the deeper with the darker shade. Alphabetical single-letter labels indicate position of sections labeled with the same letter. (B-D) Left halves of transverse sections stained with eosin and hematoxylin. Sections B-D are all to the same scale.

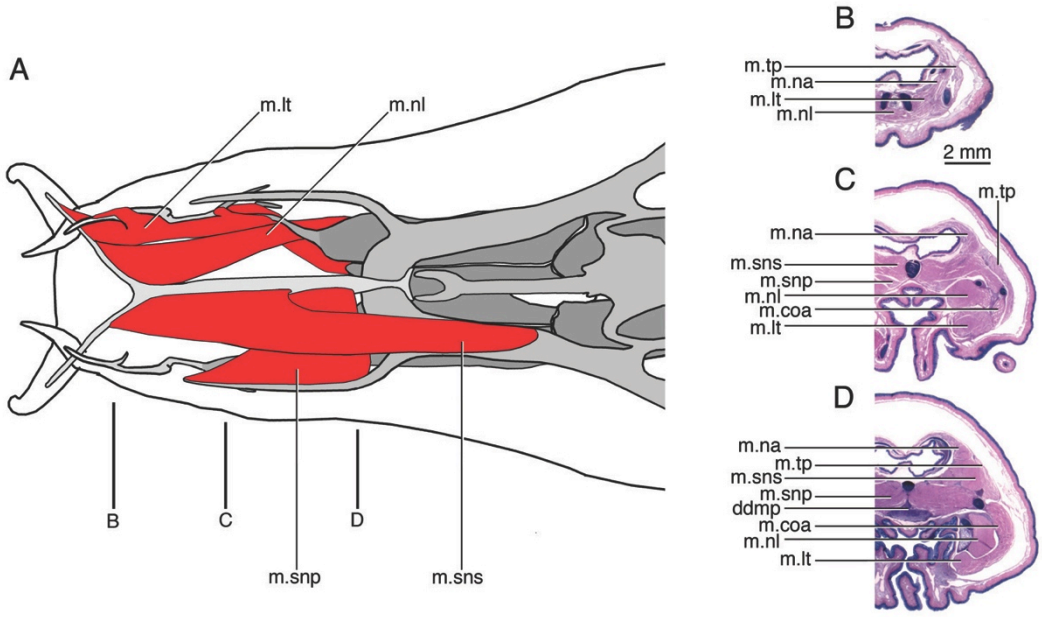
A
m.lt
m.nl
B
C
D
m.snp
m.sns
B
m.tp
m.na
m.lt
m.nl
2 mm
C
m.tp
m.na
m.sns
m.snp
m.nl
m.coa
m.lt
D
m.na
m.tp
m.sns
m.snp
ddmp
m.coa
m.nl
m.lt

Figure 3-7.

Figure 3-8. Velar muscles of the hagfish *Eptatretus stoutii*. (A) The head in left lateral view, showing the velar muscles (red) relative to the chondrocranium (white). Vertical lines indicate positions of sections for C-E. (B) The chondrocranium (stippled) in dorsal view, with the anterior end oriented toward left. The right half shows attachment sites of various cranial muscles (semi-transparent red), whereas the left half shows reconstruction of the velar muscles (red). (C-E) Left halves of transverse sections of the head, showing the velar muscles with respect to other cranial structures. Sections were stained with eosin and hematoxylin. Positions of the sections are marked in A. Sections C-E are all to the same scale.

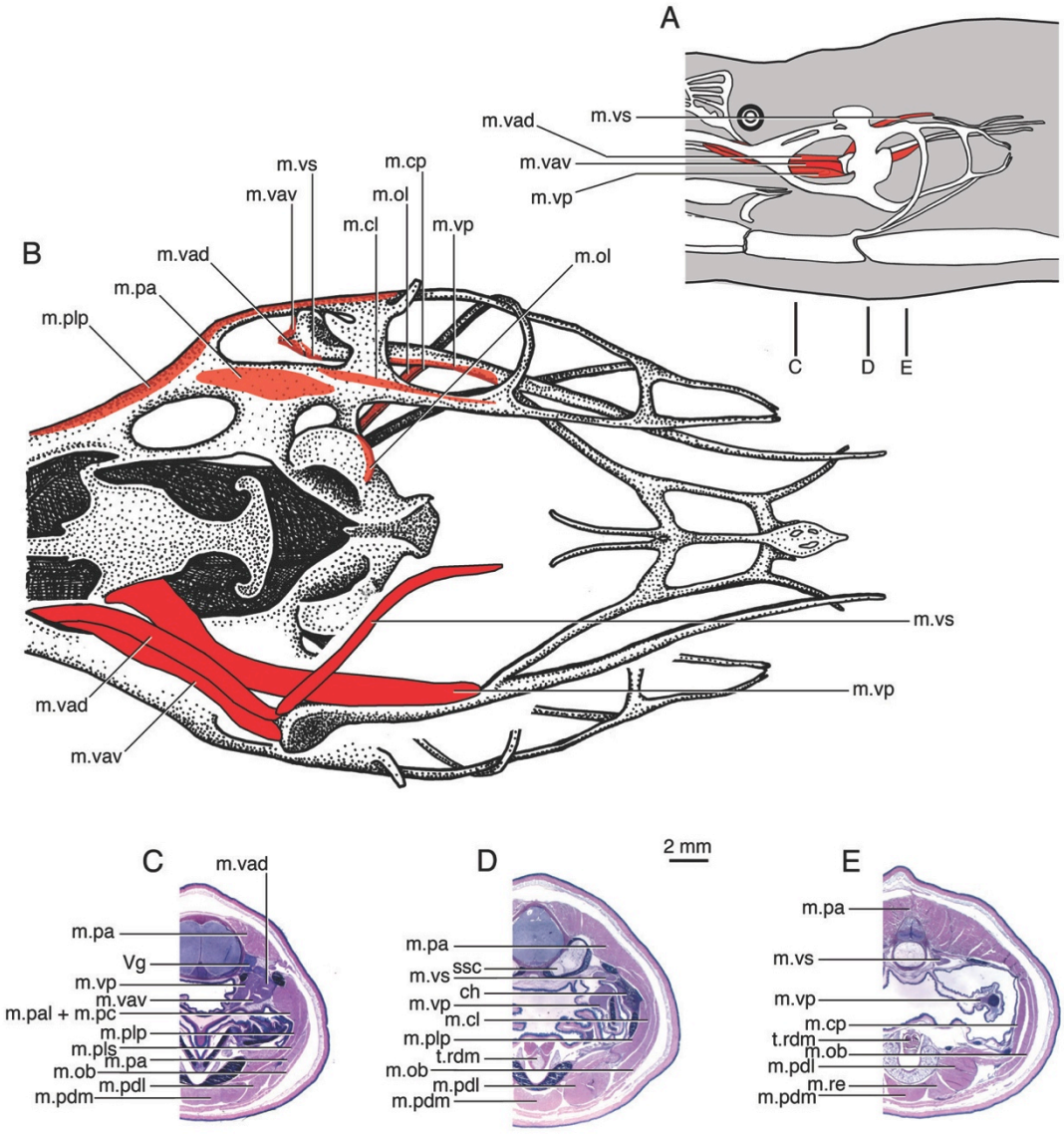
A
m.vad
m.vs
m.vav
m.vp
C
D
E
B
m.vs
m.cp
m.vav
m.ol
m.cl
m.vp
m.vad
m.ol
m.pa
m.plp
m.vs
m.vp
m.vad
m.vav
C
m.vad
m.pa
Vg
m.vp
m.vav
m.pal + m.pc
m.plp
m.pls
m.pa
m.ob
m.pdl
m.pdm
D
2 mm
m.pa
m.vs
ssc
ch
m.vp
m.cl
m.plp
t.rdm
m.ob
m.pdl
m.pdm
E
m.pa
m.vs
m.vp
m.cp
t.rdm
m.ob
m.pdl
m.re
m.pdm

Figure 3-8.

Figure 3-9. The distal lingual complex and branchial series of the hagfish *Eptatretus stoutii* in left lateral view, successively revealing deeper structures (A-C). M. constrictor pharyngis and connective tissues for the distal lingual complex from the branchial region are omitted for clarity. M. retractor lingualis (lighter red) wraps around the distal lingual complex, and m. perpendicularis (darker red) attaches to both the upper and lower distal lingual cartilages concealed in lateral view by the muscle itself. Tendon for m. retractor dentalis major is shaded blue. The morphology of m. constrictor branchialis is simplified because of large individual variation. Redrawn from Ayers and Jackson (1901).

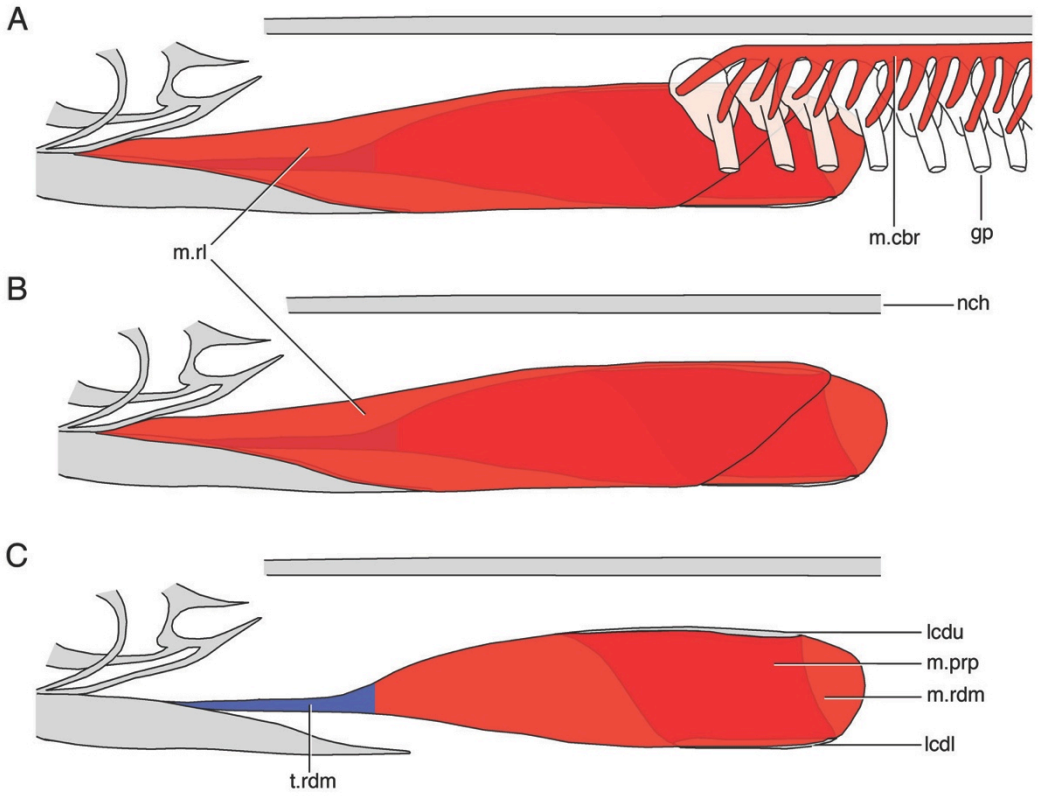

Figure 3-9.

Figure 3-10. Sites of muscle attachment (semi-transparent red) to the chondrocranium (stippled) of the hagfish *Eptatretus stoutii*. (A) A reconstructed chondrocranium in left lateral view, showing muscle attachments as labeled. (B) The anterior and middle segments of the lingual apparatus in ventral (B_1) and dorsal (B_2) views, with the anterior end oriented toward left. The right half shaded in gray indicates ventral surface, whereas the unshaded left half shows the dorsal surface. (C) The snout region of the chondrocranium in dorsal view, with the anterior end oriented toward left. The right half (upper) shows attachment sites for m. lingual tentacularis and m. nasolingualis, whereas the left half (lower) shows attachment sites for m. subnasalis superficialis and profundus. The nasal tube is removed for clarity. (D) The dental apparatus in dorsal view, with the anterior end oriented upward. Tooth plates are reconstructed on the left side, and attachment sites are shown along the midline and on the right side. Blue indicates sites of tendon attachment. With the exception of m. retractor dentalis lateralis, the illustrations show only attachment sites to cartilage.

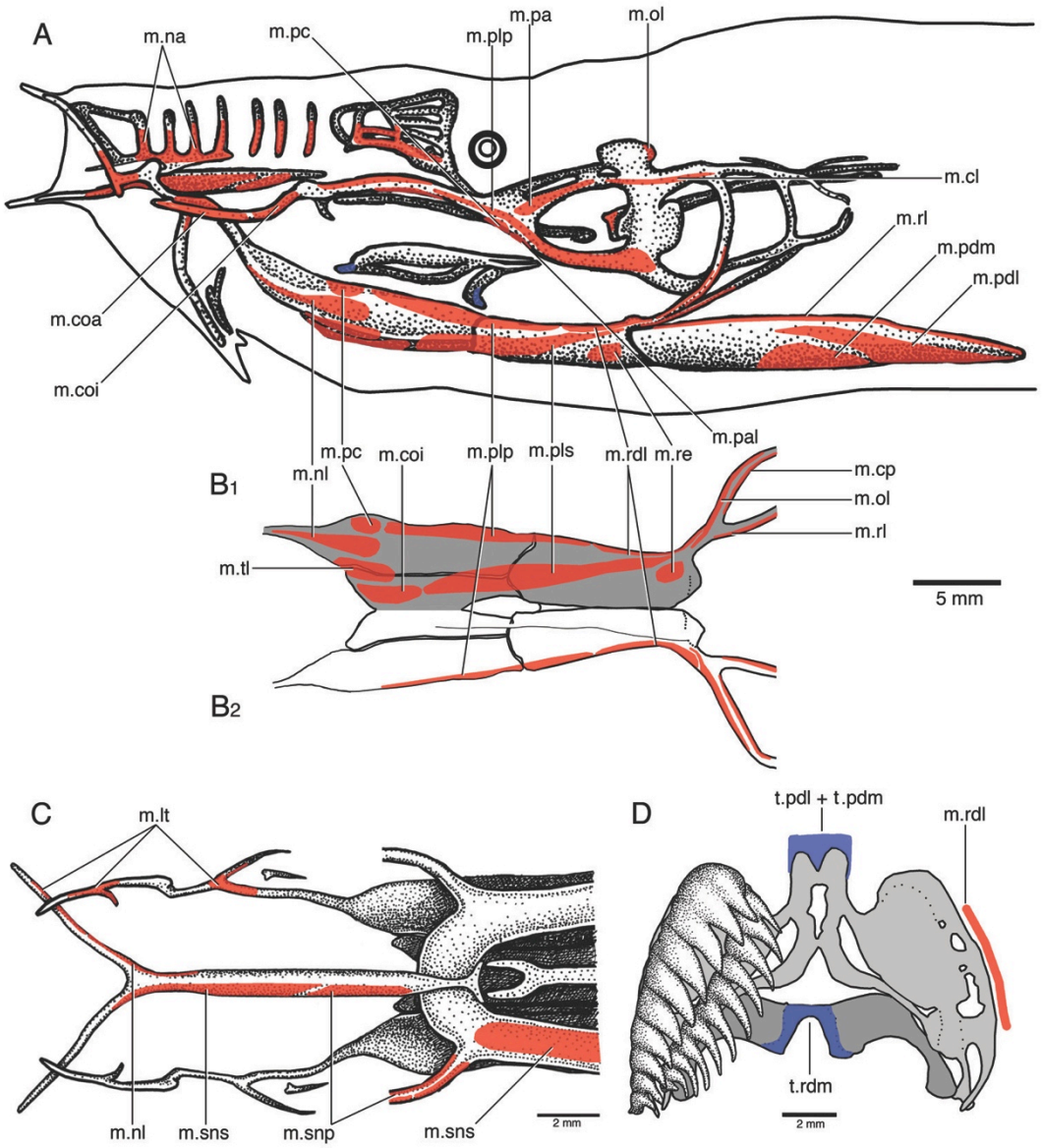
A
m.na
m.pc
m.plp
m.pa
m.ol
m.cl
m.rl
m.pdm
m.pdl
m.coa
m.coi
m.pal
B1
m.pc
m.coi
m.plp
m.pls
m.rdl
m.re
m.nl
m.cp
m.ol
m.rl
m.tl
5 mm
B2
C
m.lt
m.nl
m.sns
m.snp
m.sns
2 mm
D
t.pdl + t.pdm
m.rdl
t.rdm
2 mm

Figure 3-10.

Figure 3-11. Histological sections of cranial muscules of the hagfish *Eptatretus stoutii*. (A) A histological section of m. parietalis showing red (rf), intermediate (if), and white (wf) fibres along with capillaries (cap), perpendicular to orientation of the fibres. Red fibres are indicated by an arrowhead. (B) A histological section of m. craniovelar anterior dorsalis perpendicular to the orientation of the fibres. Red fibres that exclusively make up the velar muscles are smaller in diameter than those that occur elsewhere in the hagfish, with rich lipid content (appearing more blue in eosin and hematoxylin staining), and within an open blood sinus. (C) A histological section of m. retractor lingualis perpendicular to the orientation of the fibres. The lingual retractors and protractors consist of white fibres only. (D) A histological section of m. cornual lingualis parallel to the orientation of the fibres, showing longitudinal sections of white fibres. All specimens were stained with eosin and hematoxylin.

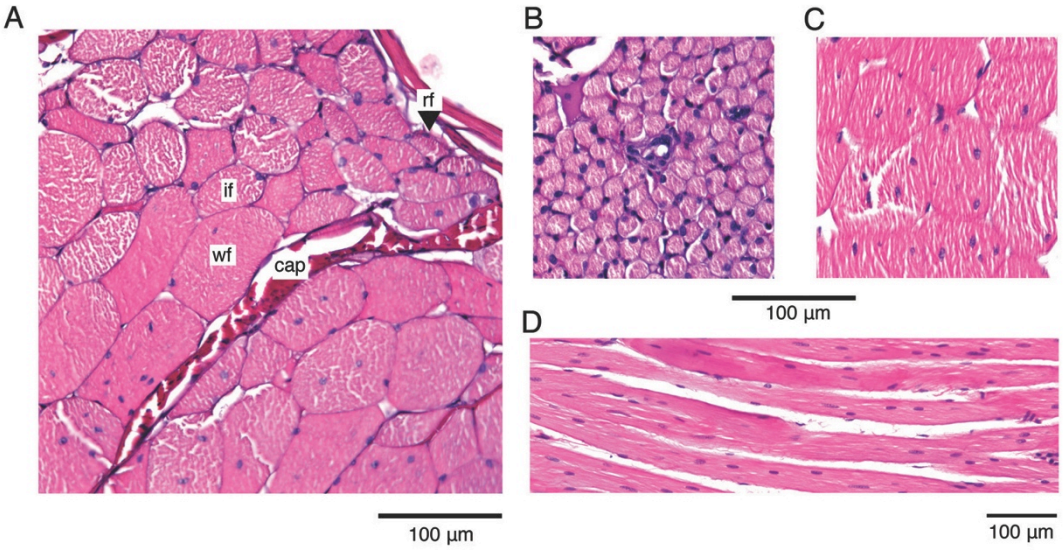

Figure 3-11.

Figure 3-12. Cranial muscles (red) of an embryo of the Atlantic hagfish *Myxine glutinosa*, between stages I and II of Neumayer (1938). (A) Superficial and deep cranial muscles (red) and associated tendons (blue) reconstructed with the oropharyngeal and nasohypophyseal structures (grey). Note that the branchial series is more proximal than in adults, and that neither the nasohypophyseal aperture nor mouth has opened. (B) The lingual retractors and m. constrictor pharyngis reconstructed with skeletal elements (grey) in the same embryo. Redrawn from Holmgren (1946).

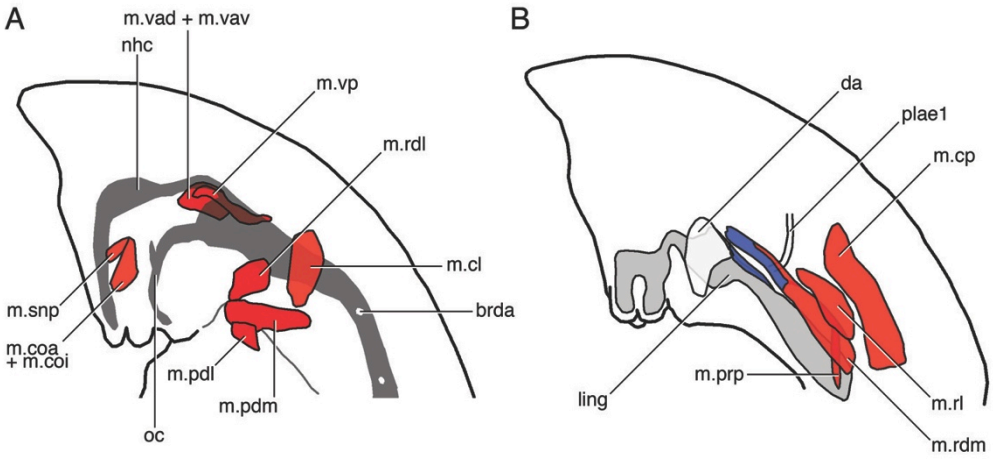
A
m.vad + m.vav
nhc
m.vp
m.rdl
m.cl
brda
m.snp
m.coa
+ m.coi
m.pdl
m.pdm
oc
B
da
plae1
m.cp
ling
m.prp
m.rl
m.rdm

Figure 3-12.

Figure 3-13. Suspension of the lingual apparatus and muscle antagonism in the head of the hagfish *Eptatretus stoutii*. (A-C) The muscles involved in suspension of the lingual apparatus are shaded with colours that indicate pairs of antagonizing muscles. Superficial muscles are successively removed from A to C to reveal the configuration of antagonizing muscles. Antagonists are at similar parasagittal positions.

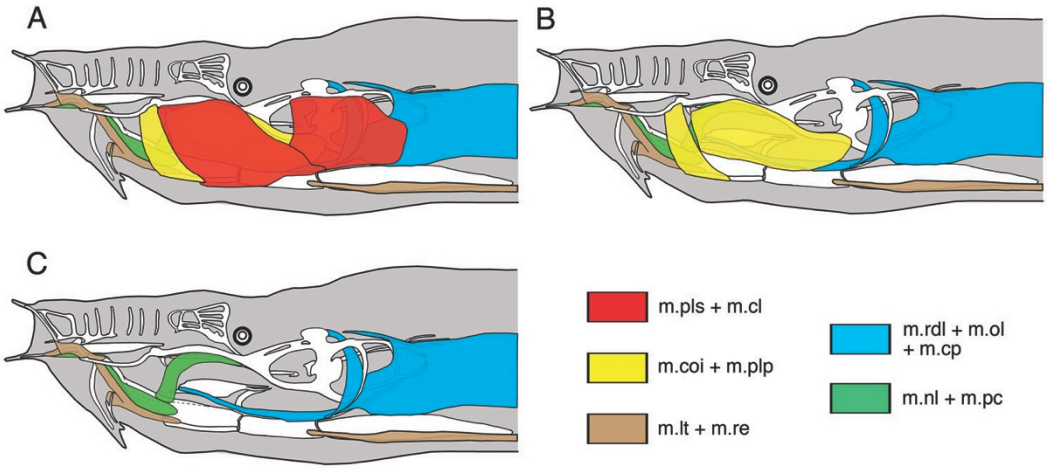

Figure 3-13.

Figure 3-14. Cardinal heart (ch) and proximal velar contact in the hagfish *Eptatretus stoutii* as a possible precursor of synovial joints in gnathostomes. (A) Transverse section of the proximal velar contact, showing the cardinal heart between the lateral velar cartilage (vll) and the velar process of the visceral plate (vlp). Inset boxes indicate subsequent close-up panels. (B) The ligamentous wall of cardinal heart (lig) is continuous with the perichondrium of the lateral velar cartilage. (C) The perichondrium forms the boundary of the cardinal heart. B and C illustrate conditions mimicking a synovial joint capsule in gnathostomes.

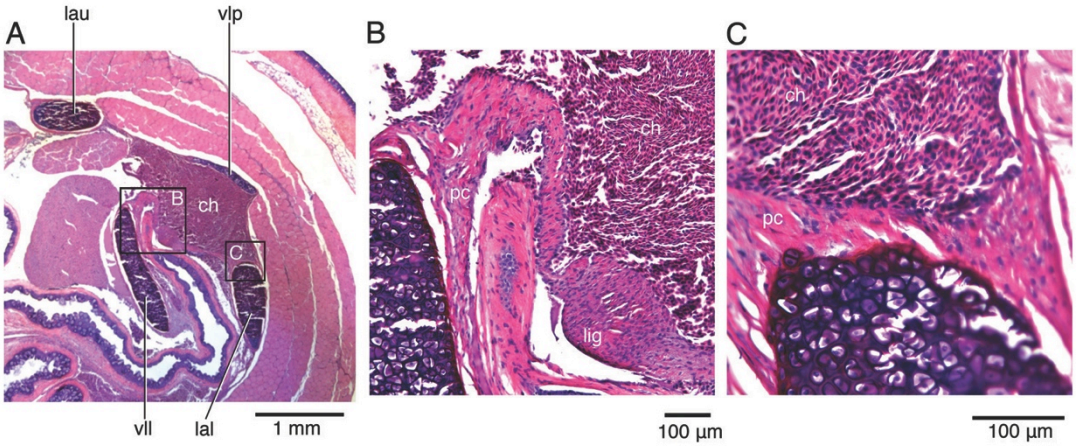

Figure 3-14.

Figure 3-15. Nerve innervation of cranial muscles of hagfish (A-E), lamprey (F-K), and gnathostomes (L, M). All figures are left lateral view except G (dorsal) and M (ventral). (A-D) Cranial muscles of the hagfish *Eptatretus stoutii* shaded according to nerve innervation (as indicated by the color legend), showing successively deeper muscles within the head and their relation to the chondrocranium (white). (E) The distal lingual complex and branchial series of *E. stoutii*, shaded according to nerve innervation. M. retractor lingualis and m. retractor dentalis major (illustrated in B, C) are omitted for clarity. (F) The lingual apparatus and retractors of the lamprey *Lampetra fluvialis*, shaded according to nerve innervation. (G) The velar skeleton (grey) and associated muscles of *L. fluvialis*, shaded according to nerve innervation. (H-K) Cranial musculature of *L. fluvialis* shaded according to nerve innervation, showing successively deeper muscles within the head relative to the cranial skeleton (various shades of grey). (L) Cranial muscles of the dogfish *Squalus acanthias*, shaded according to nerve innervation. The labial muscles of some chondrichthyans receive innervation by the maxillary branch, whereas almost all muscles in the mandibular domain of gnathostomes are innervated by the mandibular branch. Although *S. acanthias* does not receive maxillary innervation for its labial muscles, the green shade in the front part represents those exceptional cases of maxillary innervation (e.g., holocephalans; Mallatt 1996). For details, see main text. (M) The cranial musculature of *S. acanthias*, shaded according to nerve innervation. Note the somatic hypobranchial muscles (m.cob, m.coh, m.com) in place of the lingual apparatus in cyclostomes. For labels of individual muscles, see original figures respectively. F-K redrawn after Johnels (1948; F), Marinelli and Strenger (1954; F-K), Hardisty and Rovainen (1982; F-K). L and M reproduced after Mallatt (1997) with colour shading added.

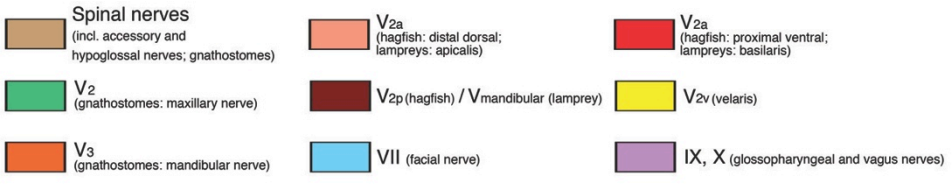

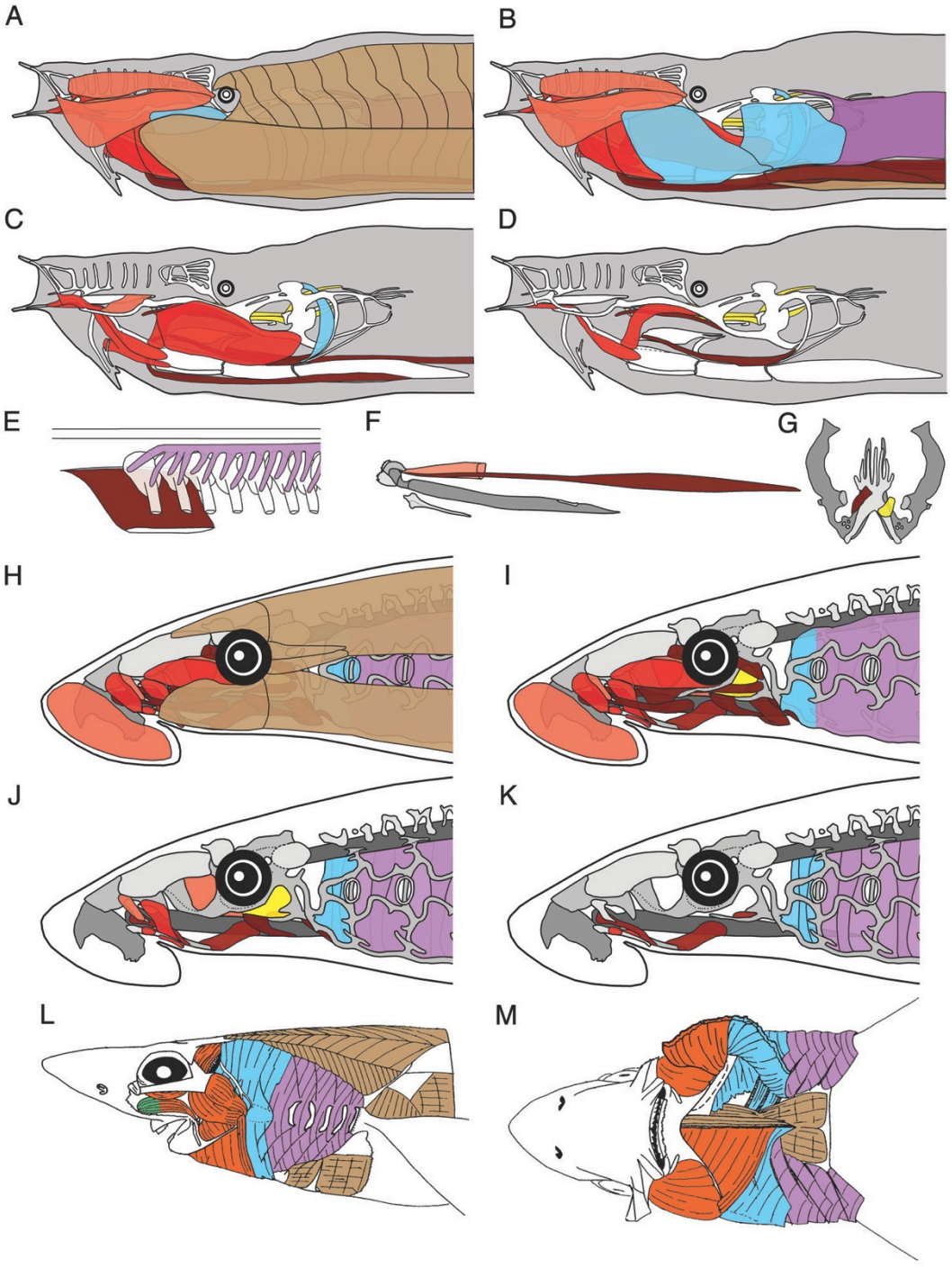

Figure 3-15.

Figure 3-16. Summary of proposed muscle homologies among hagfish (A-E), lamprey (F-K), and gnathostomes (L, M). Potential homologues are shaded with the same colour (i.e., colour code only to indicates potential homology). For labels of individual muscles, see Table 3-4 and the original figures. All figures are left lateral view except G (dorsal) and M (ventral). (A-D) Cranial musculature of the hagfish *Eptatretus stoutii* shaded according to potential homology, showing successively deeper muscles within the head and their relation to the chondrocranium (white). (E) The distal lingual complex and branchial series of *E. stoutii* in left lateral view, shaded according to potential homology. M. retractor lingualis and m. retractor dentalis major (illustrated in B, C) are omitted for clarity. (F) The lingual apparatus and retractors of the lamprey *Lampetra fluvialis*, shaded according to potential homology. (G) The velar skeleton and its associated muscles of *L. fluvialis*, shaded according to potential homology. (H-K) The cranial musculature of *L. fluvialis* shaded according to potential homology, showing successively deeper muscles within the head relative to the cranial skeleton (various shades of grey). The cranial musculature of the dogfish *Squalus acanthias*, shaded according to potential homology. F-K redrawn after Johnels (1948; F), Marinelli and Strenger (1954; F-K), Hardisty and Rovainen (1982; F-K). L and M reproduced after Mallatt (1997) with colour shading added.

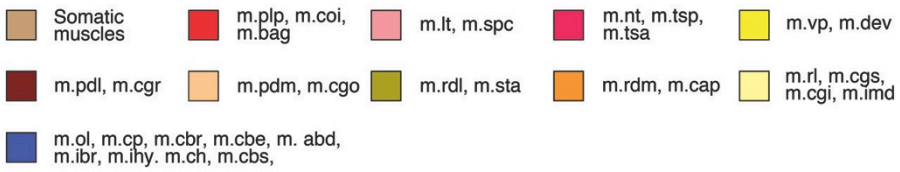

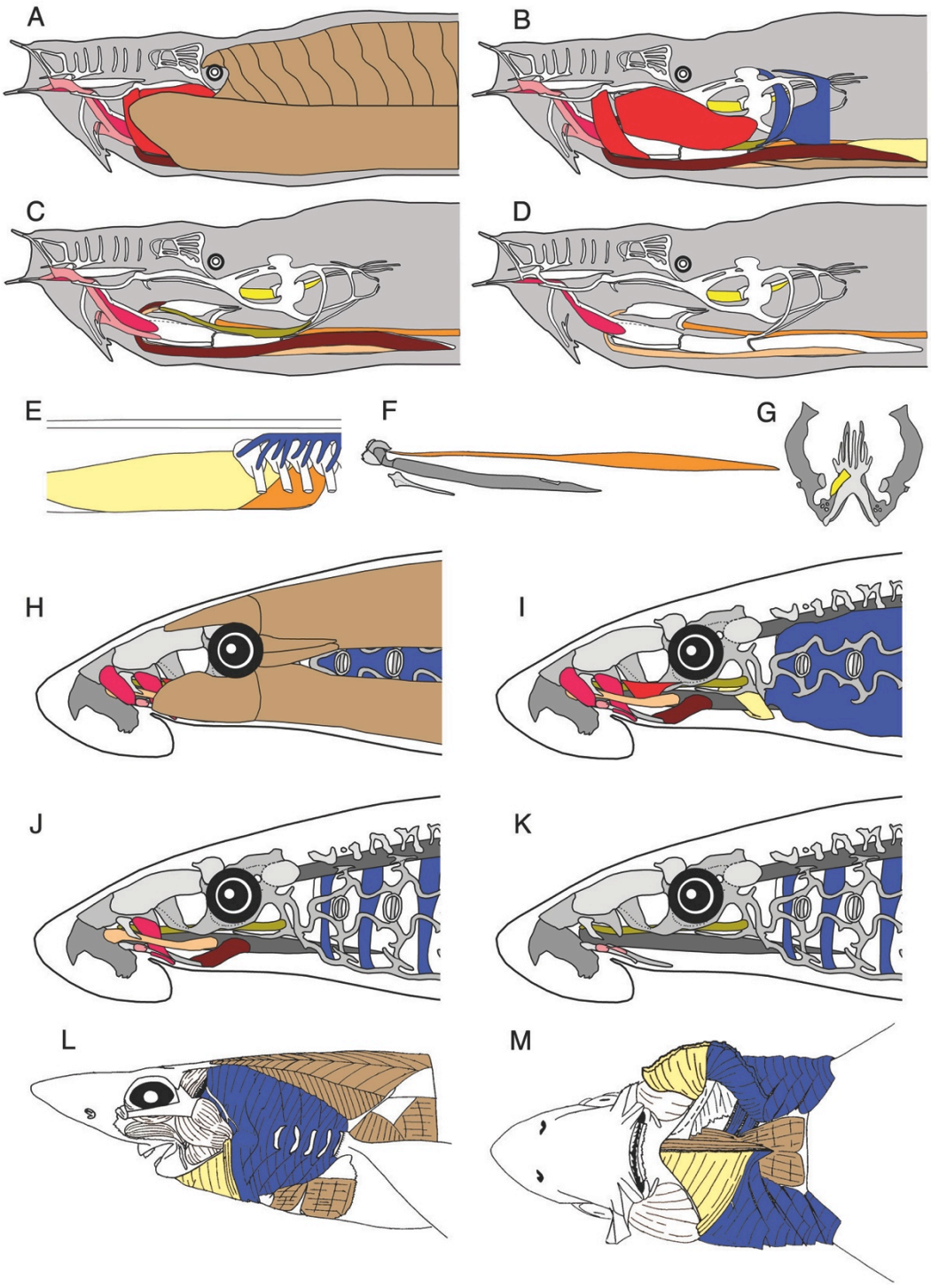

Figure 3-16.

Figure 3-17. Development and evolution of the vertebrate head as a basis for the Mandibular Siege Hypothesis. All drawings are left lateral view.

(A) Generalized vertebrate embryo based on a common elasmobranch, the dogfish *Squalus*. Dark dots indicate motor ganglia (numbered according to cranial nerves: III-VII, IX, X). An ellipse with a dark outline indicates a placode. Ganglia for VII, IX, and X form under the epibranchial placodes. Trigeminal ganglion (V) forms from the trigeminal placode. In gnathostome embryos, the olfactory placodes (olp) are paired and separate from the hypophyseal placode (Rathke's pouch, rap). So crest cells around the eye vesicle dorsally (preoptic crest cells) and ventrally (postoptic crest cells) meet here, forming the trabecula (Kuratani 2012). In hagfish and lamprey, these placodes are a single midline structure.

Grey indicates mesoderm, which interdigitates with gut endoderm (ps, pharyngeal slits).

Light brown shades the neural tube, whereas dark brown shades the mid- and forebrain. The hindbrain forms rhombomeres (r1 to r7), and from certain segments neural crest cells migrate as ectomesenchyme populations (shaded in semi-transparent shades according to pharyngeal domain; e.g., green shades the premandibular domain, red shades the mandibular domain, and light blue shades the hyoid domain).

The distribution of ectomesenchyme depends on the presence of mesoderm, divisions by the gut endoderm, and positions of placodes. Cranial nerves (indicated by darker, thick lines of the same colour within ectomesenchyme populations) follow the distribution of the ectomesenchyme. In gnathostomes, the maxillary process (max) develops with the maxillary branch of the trigeminal nerve (V_2). In the hyoid and post-hyoid domains, pretrematic and posttrematic branches form in the branchiomeric nerves (VII, IX, X).

The ectomesenchyme populations express collinear *Hox* genes (red bars) in the rhombomeres from which they migrate, and establish the pharyngeal *Hox* code. Note that the mandibular domain has no *Hox* expression. In gnathostomes, pharyngeal arches are dorsoventrally patterned by *Dlx* (orange bars), which is a prerequisite for patterning the branchial skeleton and jaw (Depew et al. 2001).

(B) The model for the segmented vertebrate head of a hypothetical ancestor by Goodrich (1918). Note one-to-one relationships among the nerves, mesoderm derivatives, and endoderm derivatives. This illustration depicts Goodrich's view that the neural tube, mesoderm, and endoderm are correspondingly metameric (thereby having full pharyngeal arches from the premandibular domain posteriorly), which now has little support but continues to influence developmental and morphological views of vertebrate head anatomy (Kuratani 2004a; see A). Yellow semi-transparent shade indicates the extent of the mandibular domain. The myotomes are longitudinally striated. The nerves are shaded black, whereas the sclerotomes are stippled. The cartilaginous visceral arches, otic capsule, and nasal capsules are represented by dotted outlines.

Labels for this panel: I-VI, gill slits; 1-11, somites, prootic from 3 forwards, and metaotic from 4 ackwards; a, auditory nerve; ab, abducens nerve; ac, otic capsule; ah, anterior head-cavity; c, ocelom in lateral plate mesoblast; C.R., limit of cranial region; f, facial nerve; gl, Glosso-pharyngeal nerve; ha, hyoid cartilaginous arch; hvt, hypoglossal muscles from myotomes of somites 6, 7, 8; hy, hypoglossal complex nerve; la, lamina antotica; M, mouth; m^2, second metaotic myotome; m^6, Sixth meta-otic myotome; ma, mandibular cartilaginous arch; mb, muscle-bud to pectoral fin; nc, nasal capsule, continuous with.trabecula behind; aa^1 and aa^2, first and second occipital arches of segments 6 and 7; om, oculomotor nerve; prf, profundns nerve; sol, schyrotome of segment 10. sp^1, vestigial dorsal root and ganglion

of first spinal nerve; sp^2, second spinal; t. trochlear nerve; tr, trigeminal nerve; v, complex root of vagus nerve; vgi, vestigial dorsal root and ganglion of segment 7; vc_1, ventral coelom extending up each visceral bar; V.R., limit of visceral region; vr_6, ventral nerve-root of segment 6, supplying second metaotic myotome and hypoglossal muscle.

(C-E) The mandibular domain, including some cranial muscles (red) and skeletal elements (white in C, grey in D) in various vertebrate heads. Yellow indicates an expected distribution of mandibular ectomesenchyme based on Goodrich (1918, 1930) and conventional comparative zoological understanding of the vertebrate head (delineated by the trigeminal foramen, hyomandibular pouch, and hypophyseal fenestra). Note that both hagfish and lampreys extend the mandibular domain along the pharynx and between the premandibular and hyoid domains longitudinally, well beyond the normal range of the mandibular domain in gnathostomes confined by the trabecula, spiracle, hypobranchial muscles, and other structures. (C) Head of the hagfish *Eptatretus stoutii* with muscles innervated by the motor component of the trigeminal nerve. (D) Head of the lamprey *Lampetra fluvialis* with muscles innervated by the motor component of the trigeminal nerve. (E) Head of the dogfish *Squalus acanthias* with muscles innervated by the motor component of the trigeminal nerve.

A redrawn after Northcutt (2008) and Kuratani (2012); B reproduced from Goodrich (1918); and C reproduced after Mallatt (1997), shading added. Illustrations not to scale.

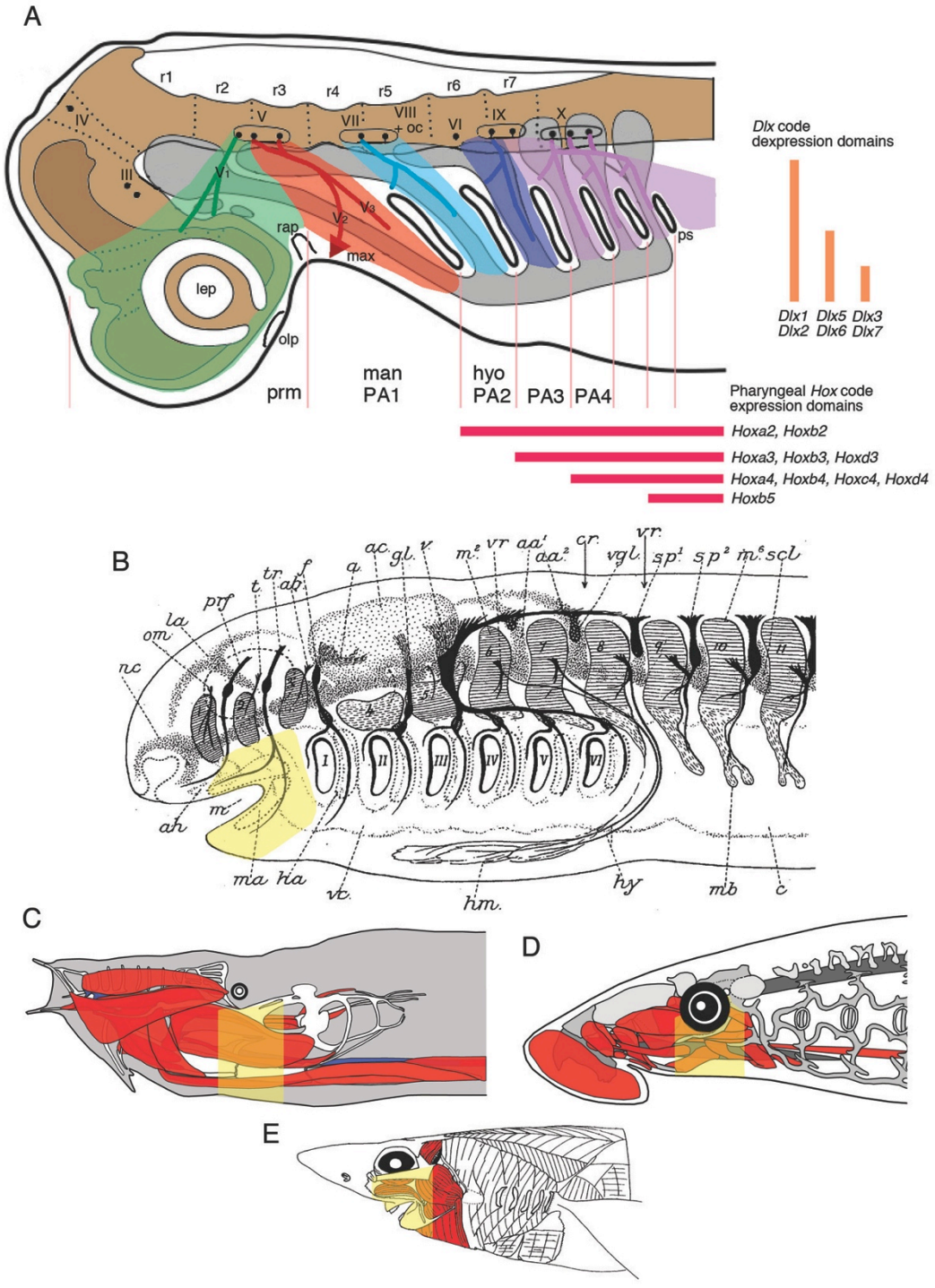
A
r1
r2
r3
r4
r5
r6
r7
IV
V
VII
VIII
+ oc
VI
IX
X
III
V1
V2
V3
rap
max
lep
olp
ps
prm
man
PA1
hyo
PA2
PA3
PA4
Dlx code
dexpression domains
Dlx1 Dlx5 Dlx3
Dlx2 Dlx6 Dlx7
Pharyngeal Hox code
expression domains
Hoxa2, Hoxb2
Hoxa3, Hoxb3, Hoxd3
Hoxa4, Hoxb4, Hoxc4, Hoxd4
Hoxb5
B
C
D
E

Figure 3-17.

Figure 3-18. Early vertebrate evolution as reconstructed according to the Mandibular Siege Hypothesis. Blue lines represent cyclostome monophyly, whereas red lines show relationships based on cyclostome paraphyly. Triangle in each lineage indicates presence of the numbered traits. Important characters are mapped onto the phylogenetic tree. Question marks (?) in front of characters indicate uncertain timing of appearance in the phylogenetic tree. In the two lists of prerequisites, a question mark means that it remains uncertain whether the character appeared before that point in the three as a key innovation or occurred after that point (in which case the character is not a prerequisite) and an X indicates that the character occurs in outgroups. Question marks on characters mapped along lineages indicate either circumstantial evidence or uncertainty of the trait being present in that lineage. Relationships among stem gnathostomes follow Javiner (2007).

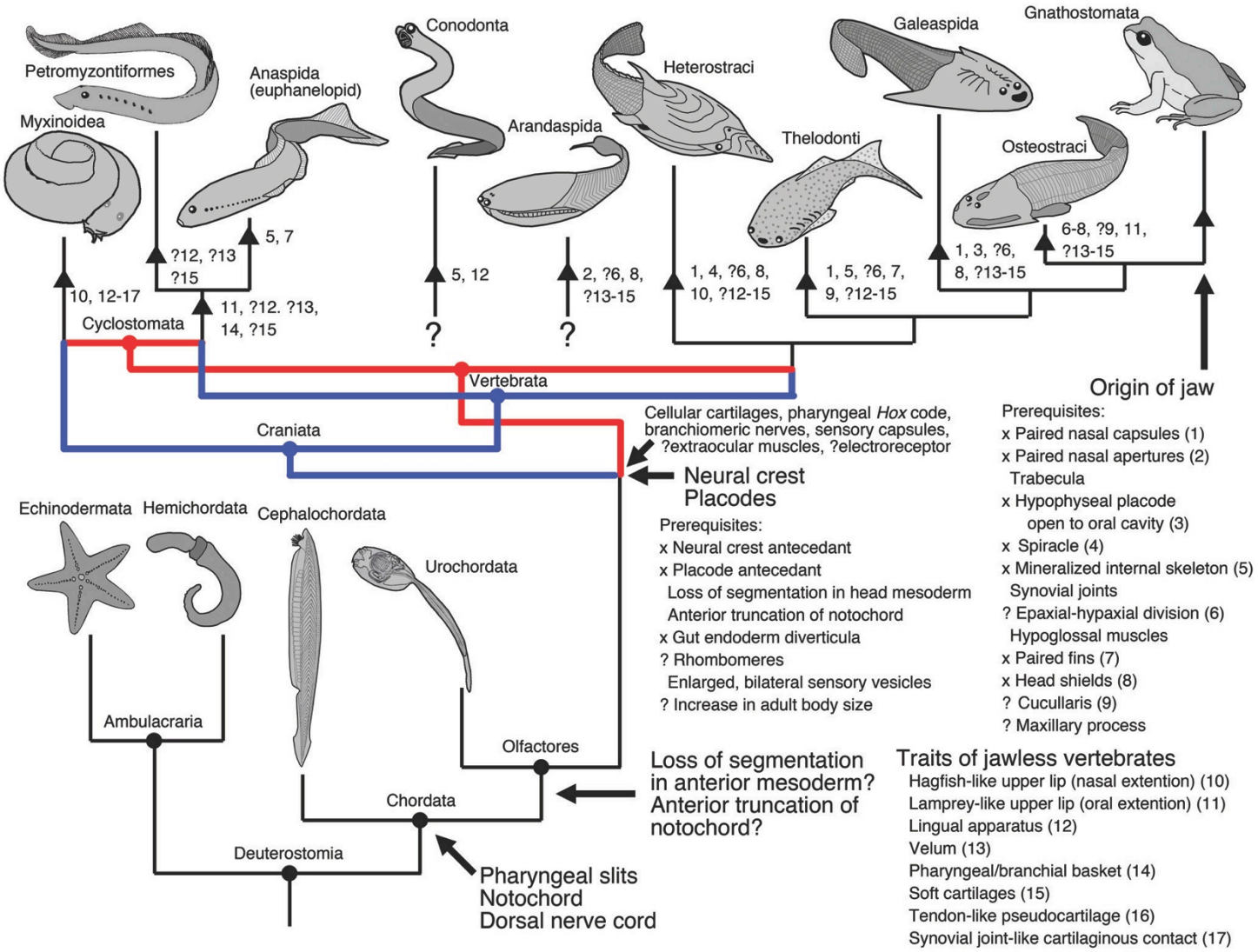
Petromyzontiformes
Myxinoidea
Anaspida
(euphanelopid)
Conodonta
Arandaspida
Heterostraci
Galeaspida
Thelodonti
Osteostraci
Gnathostomata
10, 12-17
?12, ?13
?15
5, 7
11, ?12. ?13,
14, ?15
5, 12
2, ?6, 8,
?13-15
1, 4, ?6, 8,
10, ?12-15
1, 5, ?6, 7,
9, ?12-15
1, 3, ?6,
8, ?13-15
6-8, ?9, 11,
?13-15
Cyclostomata
Vertebrata
Craniata
Origin of jaw
Cellular cartilages, pharyngeal Hox code,
branchiomeric nerves, sensory capsules,
?extraocular muscles, ?electroreceptor
Neural crest
Placodes
Prerequisites:
x Neural crest antecedant
x Placode antecedant
Loss of segmentation in head mesoderm
Anterior truncation of notochord
x Gut endoderm diverticula
? Rhombomeres
Enlarged, bilateral sensory vesicles
? Increase in adult body size
Prerequisites:
x Paired nasal capsules (1)
x Paired nasal apertures (2)
Trabecula
x Hypophyseal placode
open to oral cavity (3)
x Spiracle (4)
x Mineralized internal skeleton (5)
Synovial joints
? Epaxial-hypaxial division (6)
Hypoglossal muscles
x Paired fins (7)
x Head shields (8)
? Cucullaris (9)
? Maxillary process
Echinodermata
Hemichordata
Cephalochordata
Urochordata
Ambulacraria
Olfactores
Chordata
Deuterostomia
Loss of segmentation
in anterior mesoderm?
Anterior truncation of
notochord?
Pharyngeal slits
Notochord
Dorsal nerve cord
Traits of jawless vertebrates
Hagfish-like upper lip (nasal extention) (10)
Lamprey-like upper lip (oral extention) (11)
Lingual apparatus (12)
Velum (13)
Pharyngeal/branchial basket (14)
Soft cartilages (15)
Tendon-like pseudocartilage (16)
Synovial joint-like cartilaginous contact (17)

Chapter 4 – Phylogenetic Analysis of Early Vertebrates: General Discussion and Conclusion

Eye of newt, and toe of frog,
Wool of bat, and tongue of dog,
Adder's fork, and blind-worm's sting,
Lizard's leg, and owlet's wing, —
For a charm of powerful trouble,
Like a hell-broth boil and bubble.

William Shakespeare (1606), The Tragedy of Macbeth

4.1. INTRODUCTION

The previous chapters extensively explored phylogenetic relationships of cyclostomes with an emphasis on hagfish anatomy. Despite the breadth of new anatomical information that illuminates the early evolution of numerous vertebrate characters, the question of cyclostome monophyly versus paraphyly remains. New morphological data presented in this thesis so far do indicate plesiomorphic conditions near the root of the vertebrate tree, but support or reject neither phylogenetic hypothesis. Two special conditions account for this curious outcome. First, the fossil record does not provide enough information to break down frustratingly long branches leading to living representatives of the early vertebrate radiation, hagfish, lampreys, and gnathostomes. Myxinoidea, the lineage of hagfish, does not have stem taxa that are morphologically intermediate between living hagfish and other vertebrates. Petromyzontiformes, the lineage of lampreys, is likely a sister group of the extinct naked anaspids such as *Euphanerops* (Janvier 1996a, 2007; Janvier and Arsenault 2002, 2010), but their affinity with the rest of Anaspida is uncertain. Many fossil jawless vertebrate lineages are placed along the main stem of the vertebrate tree leading to gnathostomes, and as such, these taxa form stem lineages that potentially document evolutionary transitions toward the origin of the

jaw. However, their relationships are highly unstable, and putative gnathostome-like characters distribute in a mosaic pattern among the lineages (comprehensive reviews by Janvier 1996b, 2007; Chapter 3). For example, conodonts may either represent one lineage of the total group Gnathostomata (Donoghue et al. 2000) or fall outside Vertebrata (Turner et al. 2010), even though these two studies used the same set of characters with slightly different coding methods. Coupled with incomplete preservation of soft tissues in fossil forms, and coupled with decay patterns that partly parallel phylogenetic hierarchy during taphonomic transformations (Sansom et al. 2010), it is extremely challenging to resolve character incongruence that results from long branch lengths. As a result, the seemingly rudimentary eye, lateral line, and vestibular apparatus of hagfish (Fernholm and Holmberg 1975; Wicht and Northcutt 1995; Braun and Northcutt 1997; Jørgensen et al. 1998; Collin 2007) are each equally likely to be retention of plesiomorphic conditions or secondary degeneration of apomorphic conditions.

The second challenge that has not been addressed fully in previous phylogenetic discussion is the hierarchical nature of homology (Figure 4-1). For example, cartilaginous and muscular homologues between hagfish and lampreys are phylogenetically uninformative (chapters 2 and 3). This paradox results from the fact that criteria for morphological homology cannot be applied to hagfish, lampreys, and gnathostomes for many of the potential hagfish-lamprey homologues identified in this thesis. The muscles in the lingual apparatus are similar between hagfish and lampreys and likely represent homologies (Yalden 1985; Chapter 3). On the other hand, criteria for that putative homology include attachment to the lingual apparatus and innervation by the posterior distal branch of the trigeminal nerve. Gnathostomes have no structural equivalent of the cyclostome lingual apparatus (Chapter 2), and the gnathostome configuration of the trigeminal nerve differs from that of cyclostomes (Lindström 1949). Regardless of whether or not the same muscle (or the same muscle progenitor population) is conserved among these animals, the criteria for homology are inapplicable. So the morphological homology simply does not exist (Figure 4-1, coding row 3), although the homologue itself may be conserved at

different levels (e.g., a homologous cell population with different developmental fate). This should never be confused with an alternative, hypothetical state in which the lingual apparatus or similar configuration of the trigeminal nerve exists, but none of the muscles are present (Figure 4-1, coding row 2). Therefore, homology of the lingual muscles is a subset of the homology of the lingual apparatus, and the state for gnathostomes for this character is inapplicable ("-"), rather than absent ("0"). Vertebrate outgroups do not have the mandibular domain in which the apparatus occurs. So they are coded as inapplicable for this character as well. The lingual apparatus was likely present in stem gnathostomes, but no information whatsoever is available as to the morphology of protractors and retractors. These taxa are coded with unknown/missing ("?"). As a result, this character distribution is computationally uninformative (Figure 4-1, coding row 3). The lingual apparatus is likely a plesiomorphic condition, but the muscular homologues in the apparatus are uninformative unless outgroup taxa root the character. In other words, if an outgroup taxon possessed a lingual apparatus but no muscular homologues, the basal state is rooted at the base of vertebrates as absence ("0"). Only then would the muscle homologues set apart hagfish and lampreys from gnathostomes, although stem gnathostomes still may shift into the cyclostome clade or remain along the main stem. Consequently, these characters cannot recover cyclostome monophyly exclusive to hagfish and lampreys.

This methodological challenge highlights a profound effect of the breaking of homology. Because neither cephalochordates nor urochordates have the vertebrate head with a mandibular domain, the lingual apparatus of cyclostomes cannot be compared to any structure in either of the lineages. The structure is not simply absent in the latter animals; the homology is inapplicable. On the other hand, the lingual apparatus cannot be compared to a gnathostome jaw. The jaw depends on the heterotopic shift of *Dlx* expression domain (Shigetani et al. 2002, 2005; Kuratani 2012) so the mandibular domain housing the lingual apparatus or jaw has radically transformed across the jawless-jawed boundary. Such heterotopy is phylogenetically

informative, but not for the jaw or lingual apparatus. Again, the homology cannot be applied across the boundary.

Such a cascade of homologues dramatically reduces the number of characters of potential phylogenetic significance. Paradoxically, however, the reduction of redundant phylogenetic information presents a partial solution to the underestimated effect of secondary loss, one of the major weaknesses of the morphological data set in cladistics (Figure 4-2). For example, the absence of hair cells in the inner ear of hagfish may represent retention of a plesiomorphy or a secondary loss (Khonsari et al. 2009: character 38 and 39). Traditional morphological analysis would favour the former hypothesis, because hair cells are also absent in cephalochordates and urochordates as well. However, these outgroup taxa do not have the inner ear system in which the hair cells occur in vertebrates. Therefore, the proper coding in accordance with the hierarchy of homology would be inapplicable for the outgroups. This coding revision would result in uncertainty of a basal state. Even though the analysis does not favour one hypothesis over its alternative and cannot resolve relationships with this character alone, it does not impose a particular assumption on the tree where support is equivocal.

With these two caveats in mind, this final chapter delivers a revised phylogenetic analysis of basal vertebrates. A decay analysis dilutes a seemingly strong signal for cyclostome monophyly using microRNA (miRNA) data (Heimberg et al. 2010). With revisions to previous morphological phylogenetic analysis, a new parsimony analysis proposes phylogenetic relationships among basal vertebrates. Finally, results of these analyses highlight the need to revise the systematic definition of vertebrates (currently defined as the common ancestor of lampreys and gnathostomes and all its descendants).

4.2. MATERIALS AND METHODS

4.2.1. Decay analysis of miRNA data

A decay analysis of Heimberg et al.'s (2010) miRNA data set was performed using PAUP version 4.20 (Swofford 2002). All characters and taxa from Heimberg et al.'s miRNA analysis were included, and character type and assumptions (normal Dollo) were retained from the original data set. The number of steps required to collapse a node was determined by a heuristic search for trees with the best score plus successively added steps. For example, if the best tree for the data set had a tree length of 100, the heuristic search was set to look for trees with 101 steps or shorter. Any node that collapses under strict consensus of recovered trees (tree length of 100 or 101) has a decay index of one. In other words, it takes one extra step to collapse that node. This was repeated with successively added steps. The decay analysis was performed on Heimberg et al.'s (2010) data matrix of 19 taxa (outgroups: *Drosophila* and *Capitella*) and 190 characters, using PAUP* 4.0b10 (Swofford 2002).

4.2.2. Phylogenetic analysis of early vertebrate lineages

A revised phylogenetic analysis in large part depends on the morphological and physiological data set compiled by Donoghue et al. (2000) and Khonsari et al. (2009) and revised by Heimberg et al. (2010) and Turner et al. (2010) (Appendix 4-1). Taxon sampling was increased to 21 operational taxonomic units beyond the living chordates used by Heimberg et al. (2010): Cephalochordata (coding mainly based on *Branchiostoma*), Urochordata (coding mainly based on *Ciona*), Yunnanozoidea (coding mainly based on *Haikouella*), Myllokunmingidae (coding mainly based on *Haikouichthys*), Myxinoidea (hagfish), two genera of Petromyzontiformes (lampreys: *Lampetra* and *Petromyzon*), Euconodonta, Heterostraci (including potential stem heterostracans such as *Athenaegis* and *Astraspis*), Arandaspida, Anaspida, *Euphanerops* ('naked' anaspid), Thelodonti (coding based on both *Loganelia* and furcacaudiforms), Pituriaspida, Galeaspida, Osteostraci, Elasmobranchii (coding mainly based on *Squalus*), bichir (*Polypterus*),

lungfish (*Ceratodus*), coelacanth (*Latimeria*), and salamander (*Ambystoma*). To incorporate miRNA data, the data set included the two lamprey genera. These genera code identically for all phenotypic characters, but differ in miRNA characters (Heimberg et al. 2010). Heimberg et al.'s miRNA characters were coded for the Cephalochordata (*Branchiostoma*), Urochordata (*Ciona*), Myxinoidea (*Myxine*), the two lamprey genera, and Elasmobranchii (*Squalus*).

As for other characters, Heimberg et al.'s (2010) data set was adopted. As Heimberg et al. (2010) excluded characters that are only meaningful among fossil lineages, the omitted characters were reincorporated based on Turner et al.'s (2010) revision of Donoghue et al.'s (2000) data set to elucidate interrelationships of extinct taxa. The coding of each character was checked against the principle of character independence. Characters that are potentially related to each other functionally, developmentally, or anatomically were compared for perfect or almost perfect correlation in distributions of plesiomorphic and apomorphic conditions. Examples include all characters coding for feeding apparatus (functional correlation), cartilages (developmental correlation), or morphology dependent on a particular body plan such as the branching pattern of the trigeminal nerve within the mandibular domain (anatomical correlation). For example, all branchiomeric nerves depend on the presence of epibranchial placodes to form a ganglion. Therefore, without the neural crest, placode, and interaction between them, non-vertebrate chordates cannot have morphological homologues of the vertebrate branchiomeric nerves, at least based on morphological information alone. Therefore, the absence of these nerves in non-vertebrate chordates should be coded as inapplicable, because the absence is just a subset of the absence of the neural crest and placodes already incorporated in the data set. Unless more than one taxon with neural crest and epibranchial placodes lacks one or more of the branchiomeric nerves, all of the characters are phylogenetically uninformative and subject to exclusion from the analysis.

Plesiomorphic conditions were replaced with the inapplicable state ("-") where homology or the morphological basis for the homology does not apply. Character definitions were modified for those that contain more than one statement

of homology, so that the statement of homology is explicit and singular for each character (Brazeau 2011). For example, Donoghue et al.'s (2000) character 69 (dentine: 0, absent; 1, methodentine; 2, orthodentine) was split into two characters: one describes presence or absence of dentine, and the other specifies either methodentine or orthodentine (characters 118 and 119, this analysis). For the latter two characters, any taxon that scores for the absence of dentine was coded inapplicable. In another example, the character for the velum only applies to the pharyngeal structure for ventilation powered by muscles (character 82, this analysis) because the homology of the velum between cyclostomes and cephalochordates is uncertain (Chapter 2).

Once the character set was complete, phylogenetically uninformative characters that were either constant or autapomorphic were excluded. After revision of Heimberg et al.'s (2010) coding, the following characters were either constant or phylogenetically uninformative (due to autapomorphy), and were therefore excluded: 3, 7, 10, 12, 14, 16, 17, 19, 20, 25, 28, 29, 35-37, 40-43, 45, 49, 51, 53, 55, 56, 58, 59, 61, 63, 64, 71, 73, 74, 77, 79, 85, 87, 89, 92, 95, 97. 98, 101, 104-108, 113-115, 118, 122, 133, 134, 144, 156, 160, 168, 170, 174, 176, and 180. Heimberg et al.'s character 6 was excluded because of redundancy with their character 4, and their character 33 for redundancy with their character 32. Additional characters from Turner et al. (2010) were included only if they were phylogenetically informative under the scheme of the current analysis (Appendix 4-1; characters with citation for Turner et al. 2010).

The maximum parsimony analysis was performed on the resulting data matrix of 21 taxa and 335 characters (Appendix 4-2), using PAUP* 4.0b10 (Swofford 2002). Cephalochordata and Urochordata were outgroups. As for the characters, 145 out of the 335 characters were phenotypic characters and unordered. The rest (190 characters) were based on presence and absence of miRNA families and designated as normal Dollo so as to prohibit independent acquisitions of the same miRNA families (Heimberg et al. 2010). The parsimony analysis ran with phenotypic data alone first (145 characters), and then with all characters combined (335 characters).

The same procedure was repeated for just the living taxa in the data set. Decay indices were calculated for the first two analyses using all taxa. Trees were recovered using heuristic search and swapped using the multiple TBR (tree bisection-reconnection) method. Characters transformations were optimized for ACCTRAN (accelerated transformation) first and then for DELTRAN (delayed transformation).

4.3. RESULTS

4.3.1. Decay analysis of miRNA tree

A decay analysis of Heimberg et al.'s (2010) tree based on miRNA data showed that the clade Cyclostomata had the weakest support in the data set with a decay index of 2 (Figure 4-3). In other words, it takes an increase of two steps from the shortest tree to find trees that do not support this clade. The support value is substantially lower than those for the clades such as Gnathostomata, Osteichthyes, Olfactora, Protostomia (each with a decay index of 6), Actinopterygii (with a decay index greater than 6 but smaller than 10), Petromyzontiformes (a decay index between 16 and 20), Vertebrata, and Aves (each with a decay index greater than 20). The value is not significantly lower than those for the Reptilia (with a decay index of 2), Ambulacraria, Tetrapoda, Theria (each with a decay index of 3), or Mammalia (with a decay index of 4). However, the clades Reptilia and Tetrapoda are poorly constrained taxonomically, each lacking potential basal taxa (turtles and lissamphibians, respectively). Strength of support for each clade varies substantially, and there appears to be little correlation between morphological disparity and a number of unique miRNA families. The Petromyzontiformes accumulated a large number of unique miRNA families, and the lineage would be susceptible to long branch attraction should independent evolution of miRNA families be possible.

4.3.2. Phylogenetic analysis of early vertebrate lineages

The maximum parsimony analysis recovered cyclostomes as a paraphyletic or polyphyletic assemblage, both with phenotypic data only (Figure 4-4A) and with

phenotypic plus miRNA data (Figure 4-4B). The paraphyletic cyclostomes persisted even when fossil taxa were removed from the analysis, both with phenotypic data only and with phenotypic plus miRNA data (Figure 4-5A). With phenotypic data alone (Figure 4-4A), hagfish formed a clade with euconodonts at a position more basal than all other vertebrate taxa except for the yunnanozoan *Haikouella*, whereas lampreys fell in a clade with *Euphanerops* nested within a larger clade with anaspids and thelodonts as successive sister groups. Pituriaspids, galeaspids, and osteostracans all fell into an assemblage of successive stem lineages with respect to gnathostomes, with heterostracans and arandaspids forming a clade just outside this assemblage. Elasmobranchs, bichirs, and lungfish collapsed into a polytomy with a clade of coelacanths and salamanders, but this was due to the instability of bichirs. It was equally parsimonious to recover bichirs as a sister group to lungfish, elasmobranchs, or the clade (lungfish + (coelacanth + salamander)), accounting for all the variations of the three most parsimonious trees found in the heuristic search. The deletion of *Haikouella* or euconodonts did not impact the rest of the tree, but deletion of myllokunmingiids substantially altered the topology of the most parsimonious trees (Figure 4-5B). The deletion pulled hagfish, eucoodonts, lampreys, *Euphanerops*, and anaspids stem-ward. These taxa form a stem assemblage in that order, and the rest of fossil jawless vertebrate lineages collapsed into a large polytomy.

With the inclusion of miRNA data (Figure 4-4B), hagfish, euconodonts, and myllokunmingiids collapsed into a polytomy, just outside another polytomy among lampreys, *Euphanerops*, and the rest of vertebrates. Here, the similarity in miRNA data pulled both hagfish and lampreys stem-ward. Anaspids were recovered more basal than other fossil jawless vertebrate lineages, but the rest collapsed into a large polytomy.

For both the phenotypic data and the phenotypy plus miRNA data, decay indices were uniformly low (Figures 4-4 A, B). Most nodes were supported by an index of 1, whereas lampreys were united by an index of 2. Gnathostomes received the strongest support, followed by the node for the total group Vertebrata.

4.4. DISCUSSION

4.4.1. Critical analysis of miRNA data and cyclostome monophyly

Heimberg et al.'s (2010) analysis using miRNA set a landmark in a long-standing debate on cyclostome relationships. Previously, the signal for cyclostome paraphyly from morphological data sets had been ruled stronger than the signal for cyclostome monophyly based on molecular data sets (Near 2009). Characters based on miRNA differ from most other molecular data types in that each gene is coded as present or absent just like morphological or physiological characters, because miRNA sequences are short and highly conservative (Peterson et al. 2009; Christodoulou et al. 2010). Due to the regulatory functions of miRNAs, loss of miRNA genes is supposedly rare (Heimberg et al. 2008, 2010). Heimberg et al. (2010) first demonstrated that paraphyletic cyclostomes are only one step shorter than monophyletic cyclostomes in a revised phylogenetic analysis of morphological and physiological characters. Then they revealed that miRNA data unambiguously support cyclostome monophyly, with four unique miRNAs only found in hagfish and lampreys. This miRNA evidence convinced some paleontologists who had been staunch defenders of cyclostome paraphyly (Janvier 2010).

The decay analysis showed that it takes only two extra steps to collapse cyclostome monophyly into a polytomy among hagfish, lampreys, and gnathostomes. Despite Heimberg et al.'s (2010) insistence on the strong support from miRNA for cyclostome monophyly, support for the monophyletic Cyclostomata is much weaker than for Vertebrata or Gnathostomata. For cyclostomes to be paraphyletic, the four miRNAs unique to hagfish and lampreys must have been lost along the main stem leading to gnathostomes, or, in an extremely unlikely event, independently evolved in hagfish and lampreys. Simultaneously, two out of the four steps were presumably compensated for by reduced steps in the predicted evolution of other miRNA families. Significantly, even in Heimberg et al.'s (2010) analysis, loss of miRNA was not a rare event. Under their optimization, the following losses occurred (number in parentheses is the number of lost families): Gnathostomata, *Branchiostoma*, and

Petromyzon (1); Chondrichthyes and Osteichthyes (2); Olfactora (4); and *Ciona* (8). In addition, six miRNA families cannot be identified for hagfish, and two for *Lampetra*. Therefore, at least one miRNA family was lost just within Petromyzontiformes, and more losses are predicted for many of the long branches. If the morphological phylogeny was ruled out because the tree supporting cyclostome paraphyly was just a step shorter than the one supporting cyclostome monophyly (Heimberg et al. 2010), it would be equally risky to accept the miRNA tree showing cyclostome monophyly two steps shorter than cyclostome paraphyly.

Heimberg et al. (2010) argued that the large number of miRNA families unique to gnathostomes is likely involved in regulatory functions specific to that clade, implying that increased regulatory complexity played a role in the origin of gnathostomes. The regulatory complexity in gnathostomes also suggests that the loss of miRNA families along the main stem to gnathostomes is unlikely, further lending support for the four miRNA families unique to hagfish and lampreys as synapomorphies. However, the assumption of increased complexity preceding gnathostome origins is too simplistic. Gnathostome mandibular morphology is only possible when the cyclostome-like mandibular morphology is spatially inhibited from expanding and differentiating (Chapter 3). This would have accompanied the loss of cyclostome-specific regulatory functions, in addition to the acquisition of gnathostome-specific regulatory functions. Furthermore, phylogenetic and phenotypic distances between living cyclostomes and gnathostomes should be considered. There is no evidence that the gnathostome-specific miRNA families immediately preceded the origin of gnathostomes. The morphological diversity of extinct jawless vertebrates is so great that it could overwhelm that of any given stem assemblage within gnathostomes if measured by major bauplän characters such as paired fins, number of branchial arches, and skeletal tissues that remain constant among gnathostomes. Just like in gene duplications predicted to occur between cyclostomes and gnathostomes, miRNA families could have appeared and disappeared anywhere along the long main stem. A whole-genome duplication event preceded a common ancestor of hagfish, lampreys, and gnathostomes (Kuraku et al.

2009). In the case of *Dlx* genes, the duplication crucial for the gnathostome *Dlx* code occurred even before cyclostomes (Kuraku et al. 2010). In addition, the consequence of functional duplications of miRNA remains poorly known, even though it is a likely event along a long stem of a phylogenetic tree. Such functional duplication would facilitate either loss or modification of paralogues. It is also possible that the four miRNA families unique to hagfish and lampreys were plesiomorphies lost along the main stem leading to gnathostomes.

At any rate, the application of miRNA data to phylogenetics has only recently begun (Heimberg et al. 2008, 2010; Peterson et al. 2009; Christodoulou et al. 2010). Mechanisms behind acquisition and loss of a miRNA family have yet to be elucidated, and likelihood of independent acquisitions and losses have yet to be constrained and measured with fine phylogenetic resolution. Therefore, it is premature at this point to place too much confidence in the seemingly conservative nature of miRNA data, and it is risky to accept cyclostome monophyly uncritically based on miRNA data alone.

4.4.2. Phylogenetic analysis of early vertebrate lineages

The revised phylogenetic analysis (Figures 4-4, 4-5) follows the trend of analyses based on phenotypic data sets in supporting cyclostome paraphyly when only living taxa are considered. With fossil taxa included, the most parsimonious interpretation of the phenotypic data supports cyclostome polyphyly. Polyphyly is reminiscent of traditional views in which hagfish and lampreys were set apart from each other with intervening lineages of fossil vertebrates along the main stem (Janvier 1978, 1981; Janvier and Blieck 1979) or within the clade Cyclostomata (Stensiö 1927, 1932, 1958, 1964, 1968). The phylogenetic distribution suggests that at least lampreys may represent an independent loss of paired fins and mineralized scales. On the other hand, recent phylogenetic trees tend to place hagfish and lampreys as successive stem lineages, with a possible inclusion of *Euphanerops* (Hardisty 1982; Forey 1984; Gagnier 1993; Janvier 1993, 1996a, 2007; Donoghue et al. 2000; Turner et al. 2010). A stem-ward pull of hagfish and lampreys is likely to

result from constrained plesiomorphic states. The absence of derived vertebrate characters in non-vertebrate chordates (coded as such) root the state for hagfish and lampreys as a plesiomorphy at the base of vertebrates. In this phylogenetic analysis, however, many of these characters were coded as inapplicable to non-vertebrate chordates, if the characters have no morphological basis to be expressed in these animals. Therefore, only the distribution of states amongst vertebrate taxa determines the most parsimonious relationships within that clade.

The signal from the phenotypic data set overwhelms that from the miRNA data. The addition of miRNA data did not recover a monophyletic Cyclostomata. However, it altered the topology of fossil lineages. Because miRNA families were coded as absent or present (Heimberg et al. 2010), and because more miRNAs are absent in non-vertebrate chordates than in vertebrates, these data are expected to pull hagfish and lampreys stem-ward just like a conventional phenotypic data set for a parsimony analysis. The net result is a loss of resolution to relationships among stem gnathostomes. The strict consensus of the most parsimonious trees based on phenotypic and miRNA data provides almost no information on evolutionary transitions along the main stem leading to gnathostomes.

The decay indices show that the support for each node tends to be low. Most nodes collapse by an increase of just one step to the shortest tree length (Figure 4-4). A relatively high retention index (RI) suggests that the lack of phylogenetic information, and not high homoplasy, accounts for the instability. Each of the fossil vertebrate taxa represents a highly specialized long branch (Janvier 1993, 1996b, 2007, 2008). Much of the morphological variation among them is autapomorphic to a specific lineage. Autapomorphic characters are subject to exclusion from this analysis, and therefore do not contribute to resolution of relationships. On the other hand, the higher consistency index (CI) for the combined phenotypic and miRNA data together than for the phenotypic data alone is inflated by autapomorphies in the miRNA data. Good support for vertebrates and gnathostomes results from a large number of synapomorphies for each clade. Given the instability of stem lineages, increased character sampling for internal nodes between the nodes of vertebrates and

gnathostomes will improve phylogenetic resolution in this data set. Because much of the basal vertebrate diversity has long been extinct, this requires further sampling and refinement of morphological data.

4.4.3. Systematic definition of vertebrates

Although the phylogenetic analysis presented here supports the view that hagfish are more basal than lampreys and other extinct vertebrate lineages, the support is relatively low. As most branches collapse with an increase of one step to tree length, a future analysis of phenotypic data will likely alter the topology dramatically, including the basal position of hagfish. Phylogenetic analyses based on molecular data, be it miRNA or more conventional sequence data, will certainly test cyclostome para-/poly- phyly. Therefore, the consensus tree for this thesis (Figure 4-6) should be taken with a grain of salt. A more critical problem with the instability is the systematic terminology of vertebrates between the Vertebrata and Craniata. Janvier (1978, 1981) defined the current usage of both with a node-based criterion: Vertebrata as a common ancestor between lampreys and gnathostomes and all its descendants; and Craniata as a common ancestor between hagfish and gnathostomes and all its descendants. As reviewed in Chapter 1, these two terms converge onto the same node with cyclostome monophyly. In this case of redundancy, the term Vertebrata takes the precedence over the term Craniata.

The terminology raises the stake of resolving the root of vertebrates unnecessarily high. Namely, cyclostome paraphyly could give hagfish a status as a vertebrate sister group. There is mounting evidence that hagfish do share features of the vertebrate body plan in neural crest, sclerotomal differentiations, and highly integrated head anatomy (Ota et al. 2007, 2011; Kuratani and Ota 2008a; this thesis). Hagfish do differ from vertebrates in numerous skeletal and muscular characters. Some characters appear primitive (e.g., absence of branchial arches and extraocular muscles), but the antiquity of these characters cannot be easily tested because cephalochordates or urochordates typically lack comparable structures (Chapters 2 and 3). Many other differences (e.g., a large number of muscles suspending a lingual

apparatus) may have functional explanations, and are best attributed to the long branch length of the Myxinoidea (Chapters 2 and 3).

It could be well argued that hagfish are vertebrates as conventionally and morphologically recognized. Even in the case of cyclostome paraphyly, the morphological disparity that sets apart craniates and vertebrates is much smaller than the difference between non-vertebrate chordates and vertebrates. Finally, the debate is ongoing whether various vertebrate-like fossil taxa such as conodonts, yunnanozoans, and myllokunmingiids are true vertebrates or non-vertebrate craniates (Chen et al. 1995, 1999; Janvier 1996b, 2007; Shu et al. 1996, 1999, 2003a, b; Donoghue et al. 2000; Holland and Chen 2001; Mallatt and Chen 2003; Turner et al. 2010). With the exception of yunannozoans, these authors unanimously regard these fossil taxa as closer to vertebrates than to cephalochordates or urochordates. If the phylogenetic positions for hagfish and lampreys are unstable and similarly basal, it is rather futile to contend whether the animal in question falls into a craniate grade or a vertebrate grade.

In both the general and scientific literature, the term Vertebrata has much wider usage than the term Craniata. Hagfish, conodonts, myllokunmingiids, and yunnanozoans are all treated within a loose category of general vertebrates in both a treatise and textbook (Janvier 1996b, 2007; Kardong 2006). So the terminological distinction of craniates and vertebrates is in the domain of semantics, and the body plan shared by hagfish, lampreys, and gnathostomes will continue to be regarded as a vertebrate body plan. These circumstances call for a revision of the phylogenetic definition of vertebrates and craniates. Given that the basal part of the vertebrate phylogenetic tree is unstable, and given that the term Vertebrata has precedence over and significantly wider usage than the term Craniata, it is desirable to stabilize Vertebrata over Craniata.

For these reasons, I propose to change the systematic definition of the Vertebrata from a node-based one to a stem-based one:

> Vertebrata: the first common ancestor of the northeastern Pacific hagfish (*Eptatretus stoutii*) and zebrafish (*Danio rerio*), which is neither an ancestor of an amphioxus (*Branchiostoma lanceolatum*) nor of a vase tunicate (*Ciona intestinalis*), and all descendants of that ancestor.

With this stem-based definition, the total group Vertebrata encompasses living and fossil taxa closer to hagfish and zebrafish than to neither of cephalochordates nor urochordates, whereas the crown group Vertebrata consists of the last common ancestor of hagfish and zebrafish and all its descendants. Because the clade Vertebrata has precedence over the same clade Craniata, the latter is a junior subjective synonym of the former.

4.5. FUTURE DIRECTIONS

A number of novel insights presented in this thesis call for further investigation. The description of tooth plate histology predicts a possible scenario for the replacement of tooth plates (Chapter 2). The replacement pattern has not been observed, and it remains to be tested whether the pokal cells deposit the keratinous tooth plate or an unknown mechanism is involved. None of the sections showed two layers of the keratinous tooth plate. So the keratin must be synthesized after or shortly before shedding of an old tooth plate. A test will require histological observations and cell labeling of pokal cells from their precursor state across the replacement event. The histological similarity between tendons and Type 2 cartilages in hagfish (Chapter 2) has profound implications for the evolutionary origin of vertebrate tendons and cartilages. The histological characters of both tissues can be rigorously compared using immunohistochemical techniques beyond just superficial comparison of sections prepared for general light microscopical observations. An improved morphological understanding of the musculoskeletal system of hagfish suggests a possible precursor of a synovial joint, a character unique to gnathostomes (Chapter

3). A possible link between the proximal velar contact in hagfish and a synovial joint (particularly a jaw joint) in gnathostomes should be carefully evaluated anatomically and developmentally. An immunohistochemical approach will be crucial to test that hypothesis.

The development of the hagfish chondrocranium and cranial musculature is poorly documented, even though the tissue origin, timing of appearance, and mode of differentiation may provide crucial information for taxonomic comparison and an analysis of homology. Hagfish embryos can provide that information, and contribute to a comparative analysis of other morphological variation among hagfish, lampreys, and gnathostomes. Unfortunately, the availability of hagfish embryos is severely limited. Only one laboratory has succeeded in obtaining embryos under captive conditions (Ota et al. 2007; Kuratani and Ota 2008b; Ota and Kuratani 2008), and wild-caught embryos are rare (Ota and Kuratani 2006). With the potential to resolve the plesiomorphic state of vertebrates via comparison with lamprey and gnathostome embryology, the acquisition of hagfish embryos under captivity remains a prize worth risking failure.

A new model for the origins of vertebrates and gnathostomes via spatial confinement of the mandibular domain (the Mandibular Siege Hypothesis; Chapter 3) will immensely benefit from embryological information. The hypothesis of a spatial regulation of the pharyngeal domains offers a number of predictions that need to be tested with molecular genetic evidence and with experimental embryology. The main prediction worth testing would be positive correlation of genetic defects related to mandibular morphology and other structures predicted by the Hypopthesis to confine the mandibular domain (e.g., spiracle, Rathke's pouch). Indeed, the loss of function of the *Dlx* code in mutant mice results in defects of the hypoglossal muscles as well as the mandibular masticatory muscles (Heude et al. 2010). The molecular landscape of gene expression along the gut endoderm in lamprey and hagfish embryos will test whether and how a spatial regulation of pharyngeal domains depends on epigenetic interactions in the embryonic environments in these animals. Selective ablation of cell populations in the periphery of the mandibular domain may

partly alter the developmental fate of the nearby mandibular population of ectomesenchyme. Such an experimental embryological approach need not exclusively focus on hagfish and lamprey embryos, as it is theoretically possible with vertebrate model taxa such as zebrafish.

At the same time, the post-hatching ontogeny of hagfish also remains poorly understood. Small hagfish with body lengths of 100 to 150 mm are occasionally caught in Barkley Sound (personal data). These individuals are approximately twice the body length of a hatchling (based on the long circumference of a sterile egg capsule; personal observation). A detailed morphological comparison of these juveniles to adults may reconstruct the post-hatching ontogeny of hagfish.

Beyond hagfish, the anatomy of lampreys requires an update. There are more monographic treatments for hagfish than for lampreys. The lamprey literature since the latter half of the 20th century has heavily relied on Marinelli and Strenger (1954), which falls short in providing detailed anatomical data beyond gross morphology and in providing information on taxonomic comparison within lampreys. Lampreys undergo far more dramatic metamorphosis and are arguably morphologically more diverse than hagfish (Hardisty 1979; Renaud 2011). A muscle-by-muscle, cartilage-by-cartilage description of lampreys would yield a similarly large, if not larger, number of novel insights into early vertebrate evolution. The cyclostome-like oral apparatus of anuran tadpoles (Chapter 2) also calls for anatomical, developmental, and systematic treatment. The development of the keratinous teeth, muscle organization, and subsequent remodeling could provide an insight about evolutionary transitions from jawless to jawed feeding structures.

Anatomical information on hagfish and lampreys could improve resolution of early vertebrate phylogeny only if these insights were extended to include fossil taxa (this chapter). Nothing would improve the phylogeny more than identification of correlates of the soft tissue anatomy in fossil jawless vertebrate lineages. New technology such as micro X-ray computed tomography has become increasingly accessible, and the internal anatomy of fossil vertebrates can now be examined in unprecedented detail. The comparative morphological approach applied here to

hagfish and lampreys provides a number of correlates that can be used to identify associated soft tissue (Chapters 2 and 3). This approach should be combined with fine-scale observations on fossils to increase the number of comparative morphological characters to help reveal the interrelationships of early vertebrate lineages.

4.6. GENERAL CONCLUSIONS

The two chapters of comparative morphological treatment of the head anatomy of hagfish (Chapters 2 and 3) and the phylogenetic comparison (this chapter) present a comprehensive morphological revision of the most basal living vertebrate, hagfish. A detailed comparison with lampreys and gnathostomes identified a number of homologues and provides a framework for further morphological comparison with extinct jawless vertebrate lineages. Hagfish share more homologues with lampreys than with gnathostomes in the chondrocranium and cranial musculature. However, these homologues do not necessarily support a sister-group relationship between hagfish and lampreys. Some of the homologues — such as the lingual apparatus and velum — were likely present in extinct stem gnathostome lineages, and thus represent symplesiomorphies. Many morphological structures present in hagfish and lampreys, including the lingual apparatus, velum, and associated muscles, are simply not comparable into the origin of gnathostomes, because of extensive remodeling of the mandibular domain across that boundary. Therefore, these characters cannot resolve whether hagfish and lampreys are sister groups or paraphyletic to one another.

Some morphological variation in hagfish chondrocrania is potentially taxonomically significant. This includes the number of nasal arches, the shape of suprapharyngeal processes of the velar cartilage, and development of pharyngolingual arches. The description presented here extensively revises anatomical terminology for cartilage and muscle, and provides an interpretation of

developmental accounts by early authors (e.g., Dean 1899; von Kupffer 1900; Stockard 1906; Neumayer 1938; Holmgren 1946).

The description also identified a possible precursor of a synovial joint in the proximal velar contact of hagfish and highlighted a morphological similarity between Type2 cartilages and tendons as a possible intermediate stage documenting the origin of either tendons or cartilages. These potentially archaic states, and other characters that appear to be primitive (e.g., the absence of extraocular muscles), may pull the position of hagfish stem-ward outside the lamprey + gnathostome clade. However, these seemingly primitive states are not necessarily shared with non-vertebrate chordates such as cephalochordates or urochordates, because these animals lack the morphological basis necessary to identify homologous structures. So the homology breaks down not only at the origin of gnathostomes, but also at the origin of vertebrates.

A revised phylogenetic analysis found weak but unequivocal support for a basal position of hagfish with respect to lampreys. Conodonts may represent a sister group to hagfish, whereas lampreys may fall in the clade of jawless vertebrates including anaspids and thelodonts. This would make cyclostomes polyphyletic. The recent evidence for cyclostome monophyly based on miRNA data was critically evaluated, and I argue that the strength of support by miRNA data for cyclostome monophyly may be an overestimate. Similar levels of support for cyclostome monophyly, paraphyly, and polyphyly leave the root of vertebrates highly unstable under the current definition. The node-based definition for the Vertebrata was therefore revised into a more stable, stem-based version as: “the first common ancestor of the northeastern Pacific hagfish (*Eptatretus stoutii*) and zebrafish (*Danio rerio*), which is neither an ancestor of an amphioxus (*Branchiostoma lanceolatum*) nor of a vase tunicate (*Ciona intestinalis*), and all descendants of that ancestor.” Molecular inference for the early vertebrate evolution lacks phylogenetic resolution because of the wide variety of fossil taxa along the main stem of the vertebrate tree. On the other hand, morphological evidence has not provided enough characters useful to elucidate interrelationships of early vertebrate lineages. Little is certain as

to the prospect of resolving early vertebrate phylogeny, but one thing is clear about the molecule-morphology conflict: no matter how much molecular evidence accumulates for cyclostome monophyly, ultimately it is morphological evidence that reveals interrelationships of early vertebrates, so long as fossils fill in the wide gaps among living lineages across the tree.

A morphological comparison among living and fossil vertebrate taxa led to the formulation of a new scenario for early vertebrate evolution (the Mandibular Siege Hypothesis; Chapter 3). Under this new hypothesis, the mandibular domain as a serial homologue of branchial arches is a derived gnathostome trait. The pharyngeal domains resulted from the invention of the neural crest and establishment of a variety of tissue interactions during development. The latter was allowed by a number of morphological prerequisites such as pharyngeal slits, rhombomeres, placodes, and the lack of segmentation in the cephalic mesoderm. Although a classic comparative morphological approach variably designated each pharyngeal domain as a serial homologue within the category of pharyngeal arches, the new hypothesis regards each domain as a field of ectomesenchyme delimited by other tissues, particularly the derivatives of the gut endoderm such as pharyngeal slits. The mandibular domain appeared as a domain that fills the gap between the preoral premandibular domain and the branchiomeric hyoid and post-hyoid domains. It shows a high degree of differentiation among early vertebrate lineages including hagfish and lampreys. For the mandibular domain to co-opt the heterotopic and dorsoventrally patterned *Dlx* code and evolve a functional jaw, it required spatial confinement between the premandibular and hyoid domains and ‘defaulting’ into a domain serially homologous with the branchiomeric pharyngeal arches. A morphological comparison identified a number of characters that variably and independently allowed such spatial regulation, such as diplorhiny, the spiracle, and hypoglossal muscles. These characters appear to have evolved in a mosaic pattern among stem gnathostome linages. Coupled with a possible precursor in hagfish for a synovial joint, a morphological survey indicates that these specializations coincided at the origin of gnathostomes, and this likely facilitated the evolution of the jaw.

4.7. LITERATURE CITED

Braun, C. B., and R. G. Northcutt. 1997. The lateral line system of hagfishes (Craniata: Myxinoidea). Acta Zoologica 78:247-268.

Brazeau, M. D. 2011. Problematic character coding methods in morphology and their effects. Biological Journal of the Linnean Society 104:489-498.

Chen, J.-Y., D.-Y. Huang, and C.-W. Li. 1999. An Early Cambrian craniate-like chordate. Nature 377:720-722.

Chen, J.-Y., J. Dzik, G. Edgecombe, L. Ramsköld, and G.-Q. Zhou. 1995. A possible Early Cambrian chordate. Nature 377:720-722.

Christodoulou, F., F. Raible, R. Tomer, O. Simakov, K. Trachana, S. Klaus, H. Snyman, G. J. Hannon, P. Bork, and D. Arendt. 2010. Ancient animal microRNAs and the evolution of tissue identity. Nature 463:1084-1088.

Collin, S. P. 2007. Nervous and sensory systems. Fish Physiology 26:121-179.

Dean, B. 1899. On the embryology of *Bdellostoma stouti*. A general account of myxinoid development from the egg and segmentation to hatching. Pages 220-276 in Festschrift zum 70ten Geburststag Carl von Kupffer. Gustav Fischer Verlag, Jena.

Donoghue, P. C. J., P. L. Forey, and R. J. Adridge. 2000. Conodont affinity and chordate phylogeny. Biological Review 75:191-251.

Fernholm, B., and K. Holmberg. 1975. The eyes in three genera of hagfish (*Eptatretus*, *Paramyxine*, and *Myxine*) — a case of degenerative evolution. Vision Research 15:253-259.

Forey, P. L. 1984. Yet more reflections on agnathan-gnathostome relationships. Journal of Vertebrate Paleontology 4:330-343.

Gagnier, P.-Y. 1993. *Sacabambaspis janvieri*, Vertébré ordovicien de Bolivie. 2. Analyse phylogéenétique. Annales de Paléontologie (Vertébrés) 79:119-166.

Hardisty, M. W. 1979. Biology of the Cyclostomes. Chapman and Hall, London. 428 pp.

Hardisty, M. W. 1982. Lampreys and hagfishes: analysis of cyclostome relationships. Pages 165-250 in M. W. Hardisty and I. C. Potter, eds. The Biology of Lampreys. Volume 4B. Academic Press, London.

Heimberg, A. M., R. Cowper-Sal-lari, M. Sémon, P. J. C. Donoghue, and K. J. Peterson. 2010. microRNAs reveal the interrelationships of hagfish.

Lampreys, and gnathostomes and the nature of the ancestral vertebarate. Proceedings of the National Academy of Sciences 107:19379-19383.

Heimberg, A. M., L. F. Sempere, V. N. Moy, P. C. J. Donoghue, and K. J. Peterson. 2008. MicroRNAs and the advent of vertebrate morphological complexity. Proceedings of the National Academy of Sciences 105:2946-2950.

Heude, É., K. Bouhali, Y. Kurihara, H. Kurihara, G. Couly, P. Janvier, and G. Levi. 2010. Jaw muscularization requires *Dlx* expression by cranial neural crest cells. Proceedings of the National Academy of Sciences 107:11441-11446.

Holland, N. D., and J. Chen. 2001. Origin and early evolution of the vertebrates: new insights from advances in molecular biology, anatomy, and palaeontology. BioEssays 23:142-151.

Holmgren, N. 1946. On two embryos of *Myxine glutinosa*. Acta Zoologica 27:1-90.

Janvier, P. 1978. Les nageoires paires des Ostéostracés et la position systématique des Céphalaspidomorphes. Annales de Paléontologie (Vertébrés) 64:113-142.

Janvier, P. 1981. The phylogeny of the Craniata, with particular reference to the significance of fossil 'agnathans'. Journal of Vertebrate Paleontology 1:121-159.

Janvier, P. 1993. Patterns of diversity in the skull of jawless fishes. Pages 131-188 in J. Hanken and B. K. Hall, eds. The Skull. Volume II. Patterns of Structural and Systematic Diversity. The University of Chicago Press, Chicago.

Janvier, P. 1996a. The dawn of the vertebrates: characters versus common ascent in the rise of current vertebrate phylogenies. Palaeontology 39:259-287.

Janvier, P. 1996b. Early Vertebrates. Oxford Monographs on Geology and Geophysics, 33. Clarendon Press, Oxford. 393 pp.

Janvier, P. 2007. Homologies and evolutionary transitions in early vertebrate history. Pages 57-121 in J. S. Anderson and H. D. Sues, eds. Major Transitions in Vertebrate Evolution. Indiana University Press, Bloomington.

Janvier, P. 2008. Early jawless vertebrates and cyclostome origins. Zoological Science 25:1045-1056.

Janvier, P. 2010. microRNAs revive old views about jawless vertebrate divergence and evolution. Proceedings of the National Academy of Sciences 107:19137-19138.

Janvier, P., and M. Arsenault. 2002. Calcification of early vertebrate cartilage. Nature 417:609.

Janvier, P., and M. Arsenault. 2007. The anatomy of *Euphanerops longaevus* Woodward, 1900, an anaspid-like jawless vertebrate from the upper devonian of Miguasha, Quebec, Canada. Geodiversitas 29:143-216.

Janvier, P., and A. Blieck. 1979. New data on the internal anatomy of the Heterostraci (Agnatha), with general remarks on the phylogeny of the Craniota. Zoologica Scripta 8:287-296.

Jørgensen, J. M., M. Shichiri, and F. A. Geneser. 1998. Morphology of the hagfish inner ear. Acta Zoologica 79:251-256.

Kardong, K. V. 2006. Vertebrates: Comparative Anatomy, Function, Evolution. 4th edition. McGraw-Hill, Boston. 782 pp.

Khonsari, R. H., B. Li, P. Vernier, R. G. Northcutt, and P. Janvier. 2009. Agnathan brain anatomy and chordate phylogeny. Acta Zoologica 90:52-68.

von Kupffer, C. 1900. Studien zur vergleichenden Entwicklungsgeschichte des Kopfes der Kranioten. 4 heft: Zur Kopfentwicklung von *Bdellostoma*. Verlag von J. F. Lehmann, Muchen. 86 pp.

Kuraku, S., A. Meyer, and S. Kuratani. 2009. Timing of genome duplications relative to the origin of the vertebrates: did cyclostomes diverge before or after? Molecular Biology and Evolution 26:47-59.

Kuraku, S., Y. Takio, F. Sugahara, M. Takechi, and S. Kuratani. 2010. Evolution of oropharyngeal patterning mechanisms involving *Dlx* and *endothelins* in vertebrates. Developmental Biology 341:315-323.

Kuratani, S. 2012. Evolution of the vertebrate jaw from developmental perspectives. Evolution & Development 14:76-92.

Kuratani, S., and K. G. Ota. 2008a. Primitive versus derived traits in the developmental program of the vertebrate head: views from cyclostome developmental studies. Journal of Experimental Zoology B 310:294-314.

Kuratani, S., and K. G. Ota. 2008b. Hagfish (Cyclostomata, Vertebrata): searching for the ancestral developmental plan of vertebrates. BioEssays 30:167-172.

Lindström, T. 1949. On the cranial nerves of the cyclostomes with special reference to n. trigeminus. Acta Zoologica 30:315-458.

Mallatt, J., and J. Chen. 2003. Fossil sister group of craniates: predicted and found. Journal of Morphology 258:1-31.

Marinelli, W., and A. Strenger. 1954. Vergleichende Anatomie und Morphologie der Wirbeltiere. I Lieferung. *Petromyzon marinus* (L). 1-80.

Near, T. J. 2009. Conflict and resolution between phylogenies inferred from molecular and phenotypic data sets from hagfish, lampreys, and gnathostomes. Journal of Experimental Zoology B 312:749-761.

Neumayer, L. 1938. Die entwicklung des kopskelettes von *Bdellostoma* St. L. Archivio Italiano di Anatomica e di Embriologia 40(suppl.):1-222.

Ota, K. G., and S. Kuratani. 2006. The history of scientific endeavors towards understanding hagfish embryology. Zoological Science 23:403-418.

Ota, K. G., and S. Kuratani. 2008. Developmental biology of hagfishes, with a report on newly obtained embryos of the Japanese inshore hagfish, *Eptatretus burger*. Zoological Science 25:999-1011.

Ota, K. G., S. Kuraku, and S. Kuratani. 2007. Hagfish embryology with reference to the evolution of the neural crest. Nature 446:672-675.

Ota, K. G., S. Fujimoto, Y. Oisi, and S. Kuratani. 2011. Identification of vertebra-like elements and their possible differentiation from sclerotomes in the hagfish. Nature Communications 2:373. 6 pp.

Peterson, K., M. R. Dietrich, and M. A. McPeek. 2009. MicroRNAs and metazoan macroevolution: insights into canalization, complexity, and the Cambrian explosion. BioEssays 31:736-747.

Renaud, C. B. 2011. Lampreys of the world. An annotated and illustrated catalogue of lamprey species known to date. Food and Agriculture Organization Species Catalogue for Fishery Purposes 5:1-109.

Sansom, R. S., S. E. Gabbott, and M. A. Purnell. 2010. Non-random decay of chordate characters causes bias in fossil interpretation. Nature 463:797-800.

Shigetani, Y., F. Sugahara, and S. Kuratani. 2005. A new evolutionary scenario for the vertebrate jaw. BioEssays 27:331-338.

Shigetani, Y., F. Sugahara, Y. Kawakami, Y. Murakami, S. Hirano, and S. Kuratani. 2002. Heterotopic shift of epithelial-mesenchymal interactions in vertebrate jaw evolution. Science 296:1316-1319.

Shu, D., X. Zhang, and L. Chen 1996. Reinterpretation of *Yunnanozoon* as the earliest known hemichordate. Nature 380:428-430.

Shu, D., S. Conway Morris, Z.-F. Zhang, J.-N. Liu, J. Han, L. Cheng, X.-L. Zhang, K. Yasui, and L. Young. 2003a. A new species of yunnanozoan with implications for deuterostome phylogeny. Science 299:1380-1384.

Shu, D., H.-L. Luo, S. Conway Morris, X.-L. Zhang, S.-X. Chen, J. Han, M. Zhu, Y. Li, and L.-Z. Chen. 1999. Lower Cambrian vertebrates from South China. Nature 402:42-46.

Shu, D., S. Conway Morris, J. Han. Z. F. Zhang, K. Yasui, P. Janvier, L. Chen, X. L. Zhang, J. N. Liu, Y. Li, and H. K. Liu. 2003b. Head and backbone of the Early Cambrian vertebrate *Haikouichthys*. Nature 421:526-529.

Stensiö, E. A. 1927. The Devonian and Downtonian vertebrates of Spitsbergen. Part I. Family Cephalaspidae. Skrifter om Svalbard og Nordishavet 12:1-391.

Stensiö, E. A. 1932. The Cephalaspids of Great Britain. Trustees of the British Museum, London. 220 pp.

Stensiö, E. A. 1958. Les Cyclostomes fossles ou Ostracodermes. Pages 173-425 in P. P. Grassé, ed. Traité de Zoologie. Volume 13. Masson et Cie, Paris.

Stensiö, E. A. 1964. Les Cyclostomes fossils ou Ostracodermes. Pages 96-383 in J. Piveteau, ed. Traité de Paléontologie, Volume 4. Masson et Cie, Paris.

Stensiö, E. A.1968. The cyclostomes with special reference to the diphyletic origin of the Petromyzontida and the Myxinoidea. Pages 13-71 in T. Ørvig, ed. Current Problems in Lower Vertebrate Phylogeny. Almqvist and Wiksell, Stockholm.

Stockard, C. R. 1906. The development of the mouth and gills in *Bdellostoma stouti*. American Journal of Anatomy 5:481-517.

Swofford, D. L. 2002. PAUP: Phylogenetic Analysis Using Parsimony (and Other Methods). Version 4.0b10. Sinaeur Associates, Sunderland, Massachusetts.

Turner, S., C. J. Burrow, H.-P. Schultze, A. Blieck, W.-E. Reif, C. B. Rexroad, P. Bultynck, and G. S. Nowlan. 2010. False teeth: conodont-vertebrate phylogenetic relationships revisited. Geodiversitas 32:545-594.

Wicht, H., and R. G. Northcutt. 1995. Ontogeny of the head of the Pacific hagfish (*Eptatretus stouti*, Myxinoidea): development of the lateral line system. Philosophical Transactions of the Royal Society of London B 349:119-134.

Yalden, D. W. 1985. Feeding mechanisms as evidence for cyclostome monophyly. Zoological Journal of the Linnean Society 84:291-300.

4.8. FIGURES

Figure 4-1. The hierarchical nature of homology and phylogenetic signal in a character. The table at the top shows the distribution of characters on which muscles for the lingual apparatus depend and different coding methods for that character. The tree at the bottom shows possible relationships of early vertebrate lineages and chordate outgroups. Coding methods 1 and 2 are common in previous phylogenetic data sets. A proper coding (3) renders the character phylogenetically uninformative.

Characters						
Mandibular domain			X	X	(X)	X
Lingual apparatus			X	X	(?/X)	
Jaw						X
Muscles associated with lingual apparatus						
1. Coding based on simple absence/presence	0	0	1	1	(?/0/1)	0
2. Coding based on absence/presence if morphological basis for homology (e.g. homologous branching pattern of nerves that innervate the structure) exists within the mandibular domain.	-	-	1	1	(?/0/1)	0
3. Coding based on absence/presence with no morphological basis for homology	-	-	1	1	(?/0/1)	-

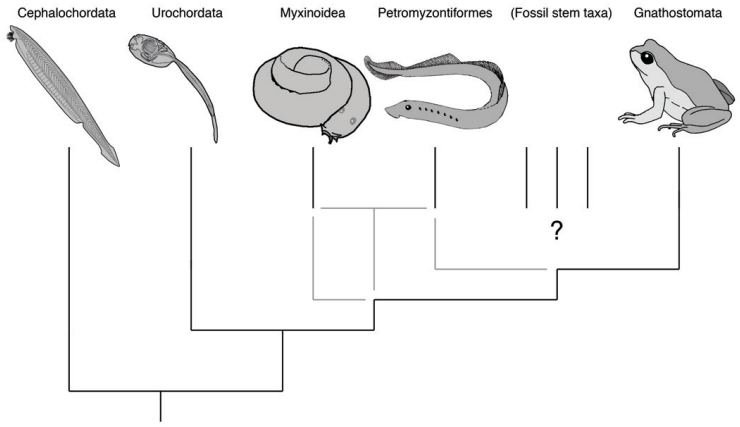

Figure 4-1.

Figure 4-2. The hierarchical nature of homology and phylogenetic signal in a character. A homology breaks down at the origin of vertebrates. The table at the top shows the phylogenetic distribution of inner ear and hair cells and different coding methods for the presence of hair cells. The tree at the bottom shows possible relationships of early vertebrate lineages and chordate outgroups. Coding method 1 is common in previous phylogenetic data sets. With a proper coding (2), a basal state in the common ancestor of hagfish, lampreys, and gnathostomes is uncertain. Therefore, the character is phylogenetically uninformative.

Characters						
Inner ear			x	x	(x)	x
Hair cells			x	x	(?/x)	x
Coding of hair cells						
1. Coding based on simple absence/presence	0	0	0	1	(?)	1
2. Coding based on absence/presence as dependent on absence/presence of inner ear	-	-	0	1	(?)	1

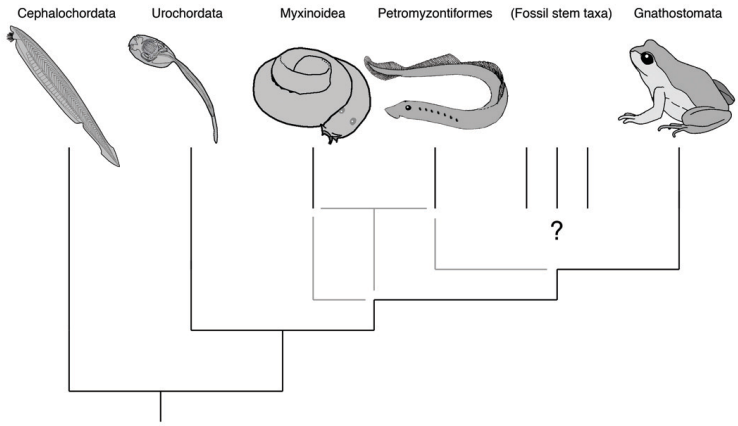

Figure 4-2.

Figure 4-3. Decay analysis of Heimberg et al.'s (2010) tree based on miRNA data. The tree topology follows Heimberg et al.'s hypothesis. Numbers in red are decay indices for that branch, which indicates the number of extra steps to the total tree length required to collapse the branch in a strict consensus tree. Cyclostomata and Reptilia have the lowest support in the tree.

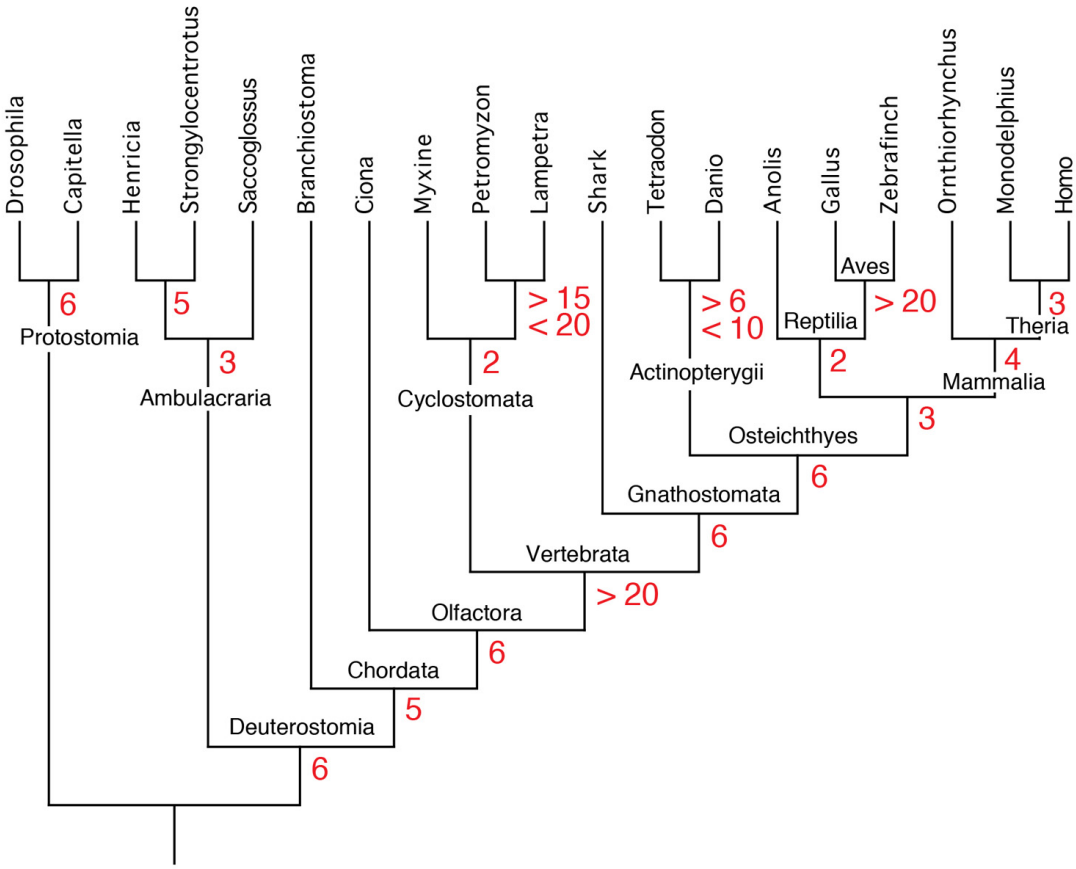
Drosophila
Capitella
Henricia
Strongylocentrotus
Saccoglossus
Branchiostoma
Ciona
Myxine
Petromyzon
Lampetra
Shark
Tetraodon
Danio
Anolis
Gallus
Zebrafinch
Ornthiorhynchus
Monodelphius
Homo
6
Protostomia
5
3
Ambulacraria
Deuterostomia
6
Chordata
5
Olfactora
6
Vertebrata
> 20
Gnathostomata
6
Osteichthyes
6
Actinopterygii
> 6
< 10
Cyclostomata
2
> 15
< 20
Aves
Reptilia
2
> 20
Mammalia
4
Theria
3
3

Figure 4-3.

Figure 4-4. Results of a maximum parsimony analysis of characters for the Chordata. (A) Strict consensus tree of the 3 shortest trees based on phenotypic data. (B) Strict consensus tree of the 176 shortest trees based on phenotypic and miRNA data. Trees were rooted by collapsing outgroups into a polytomy so that they are paraphyletic with respect to the ingroup (therefore the root was removed). Numbers in red are decay indices, and boxes show tree statistics. Phylogenetic abbreviations for this figure only: CI, consistency index; HI, homoplasy index; MPT, most parsimonious (shortest) trees; RC, rescaled consistency index; RI, retention index. A crown group is the clade defined at the node by two or more living lineages. Total group includes all the stem taxa closer to the crown group than to other crown groups in the tree.

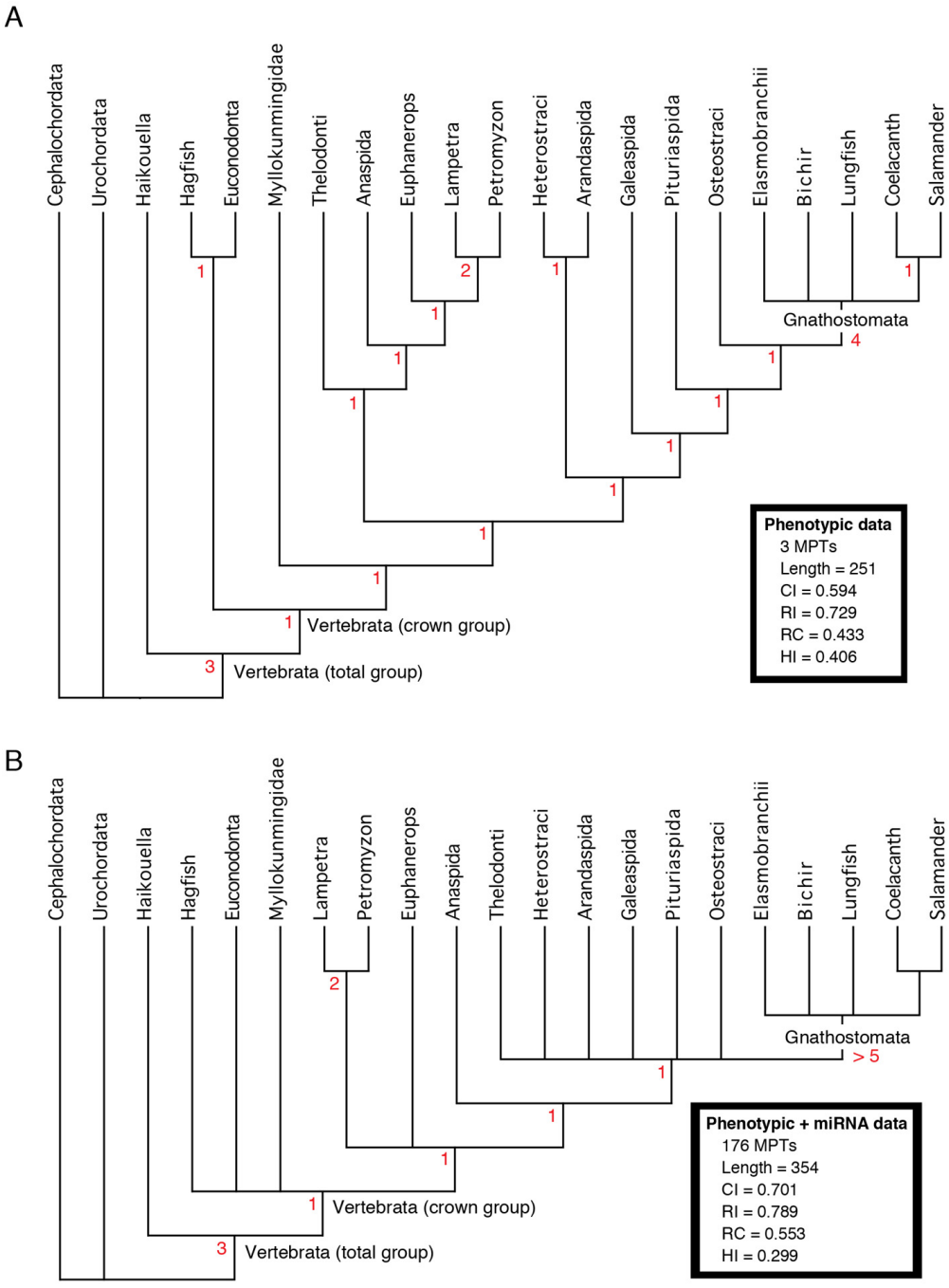
A
Cephalochordata
Urochordata
Haikouella
Hagfish
Euconodonta
Myllokunmingidae
Thelodonti
Anaspida
Euphanerops
Lampetra
Petromyzon
Heterostraci
Arandaspida
Galeaspida
Pituriaspida
Osteostraci
Elasmobranchii
Bichir
Lungfish
Coelacanth
Salamander
Gnathostomata
4
Vertebrata (crown group)
Vertebrata (total group)
3
Phenotypic data
3 MPTs
Length = 251
CI = 0.594
RI = 0.729
RC = 0.433
HI = 0.406
B
Cephalochordata
Urochordata
Haikouella
Hagfish
Euconodonta
Myllokunmingidae
Lampetra
Petromyzon
Euphanerops
Anaspida
Thelodonti
Heterostraci
Arandaspida
Galeaspida
Pituriaspida
Osteostraci
Elasmobranchii
Bichir
Lungfish
Coelacanth
Salamander
Gnathostomata
> 5
Vertebrata (crown group)
Vertebrata (total group)
3
Phenotypic + miRNA data
176 MPTs
Length = 354
CI = 0.701
RI = 0.789
RC = 0.553
HI = 0.299

Figure 4-4.

Figure 4-5. Results of a sensitivity analysis to the maximum parsimony analysis of the Chordata. (A) A single most parsimonious tree (tree length= 289) recovered in the maximum parsimony analysis of living vertebrate taxa in the data set based on phenotypic and miRNA data. (B) Strict consensus of 36 the shortest trees (tree length= 241) recovered in the maximum parsimony analysis of all taxa with exclusion of myllokunmingiids, based on phenotypic and miRNA data. The exclusion of myllokunmingiids altered the topology dramatically, pulling lampreys stem-ward and dissolving the thelodont-anaspid-lamprey clade into the main stem leading to gnathostomes. Relatively derived jawless vertebrate lineages collapsed into a large polytomy. The trees were rooted by collapsing outgroups into a polytomy so that they are paraphyletic with respect to the ingroup (therefore the root was removed).

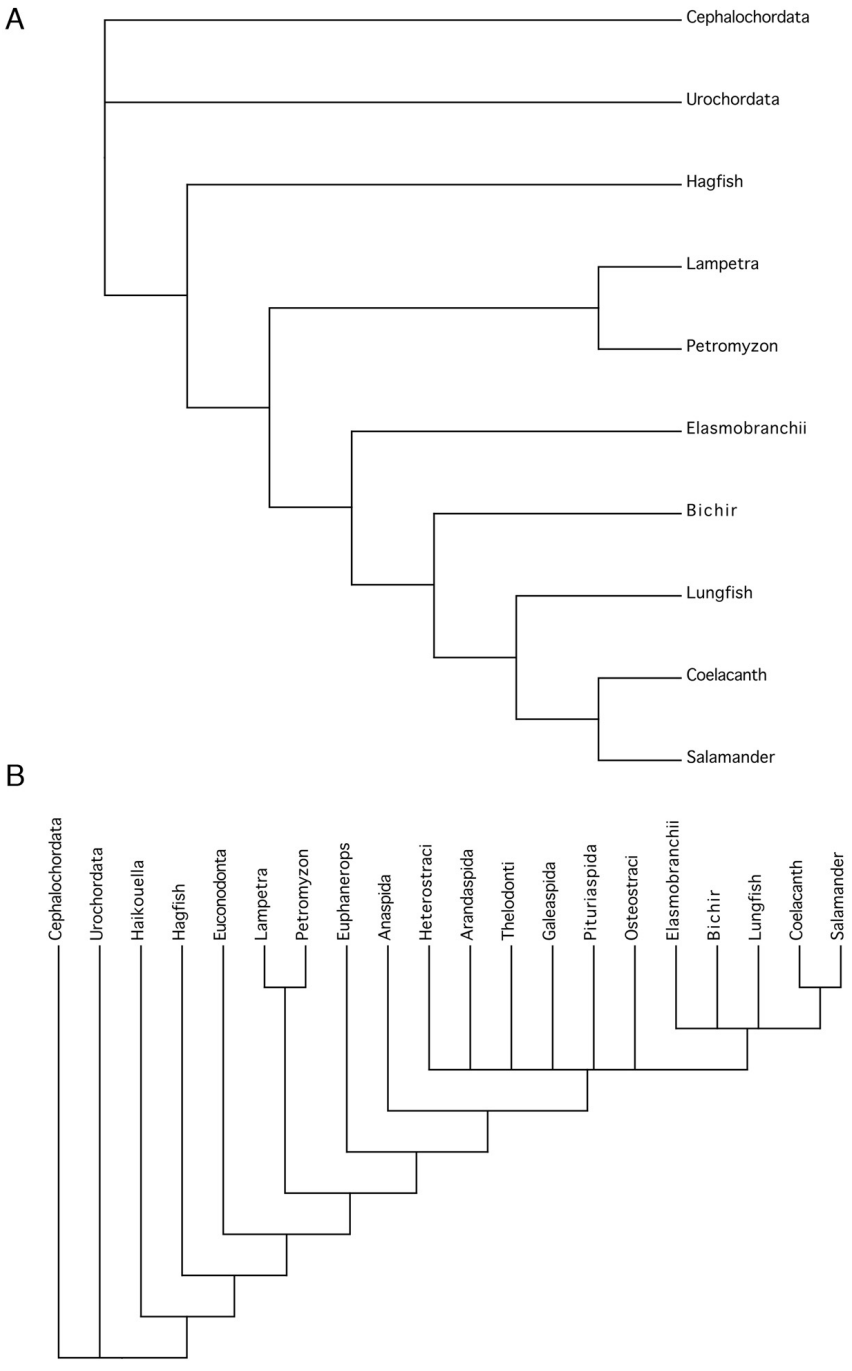
A
Cephalochordata
Urochordata
Hagfish
Lampetra
Petromyzon
Elasmobranchii
Bichir
Lungfish
Coelacanth
Salamander
B
Cephalochordata
Urochordata
Haikouella
Hagfish
Euconodonta
Lampetra
Petromyzon
Euphanerops
Anaspida
Heterostraci
Arandaspida
Thelodonti
Galeaspida
Pituriaspida
Osteostraci
Elasmobranchii
Bichir
Lungfish
Coelacanth
Salamander

Figure 4-5.

Figure 4-6. Deuterostome phylogeny showing relationships of early vertebrate lineages as supported in this phylogenetic analysis. Relationships of ambulacrarians and non-vertebrate chordates are based on the consensus (Swalla and Smith 2008). 'Naked' anaspids are represented by *Euphanerops*.

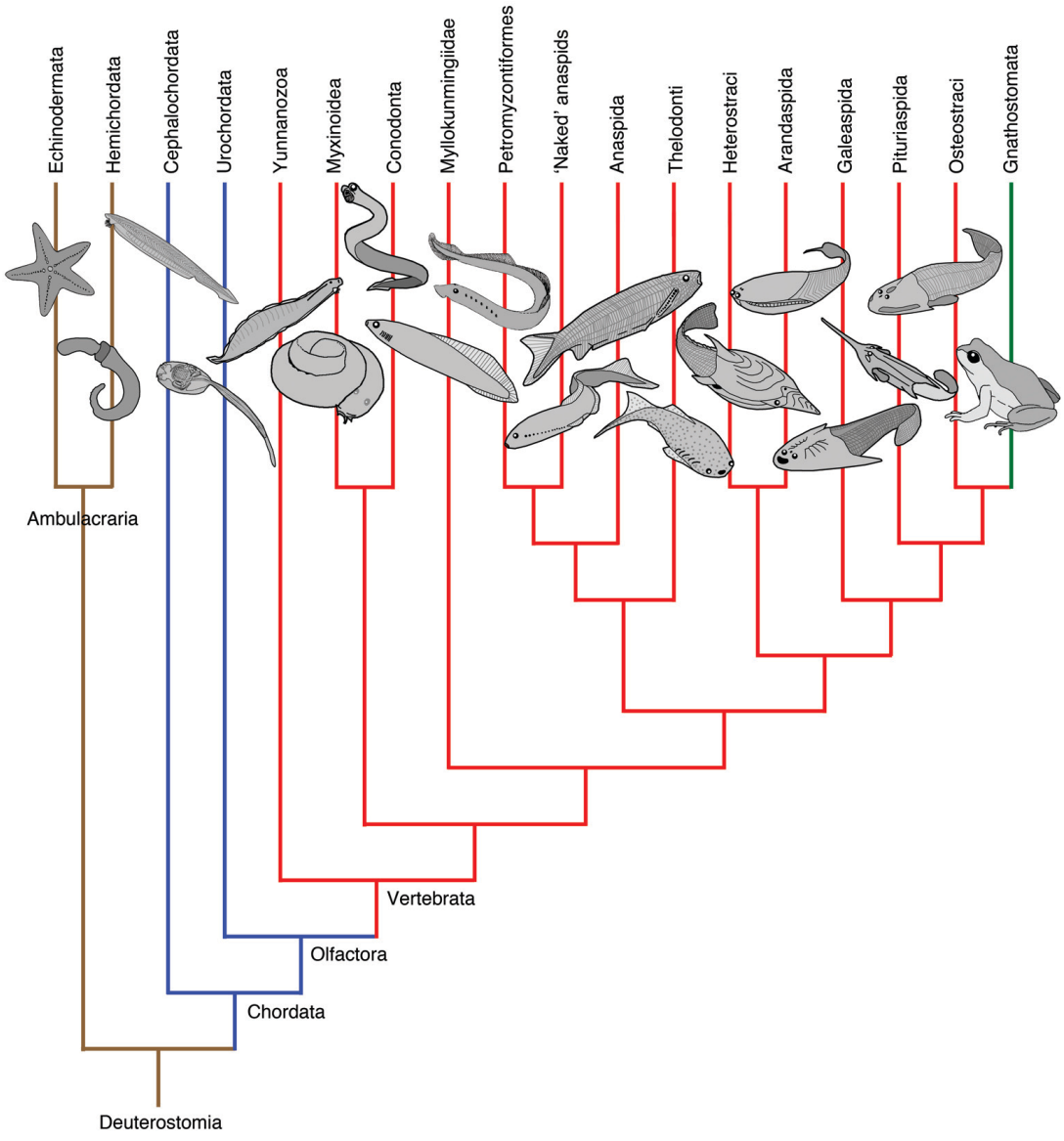
Echinodermata
Hemichordata
Cephalochordata
Urochordata
Yunnanozoa
Myxinoidea
Conodonta
Myllokunmingiidae
Petromyzontiformes
'Naked' anaspids
Anaspida
Thelodonti
Heterostraci
Arandaspida
Galeaspida
Pituriaspida
Osteostraci
Gnathostomata
Ambulacraria
Vertebrata
Olfactora
Chordata
Deuterostomia

Figure 4-6.

Appendix 4-1. Character Descriptions

Overall body plan

1. Neurulation by fusion of neural plate folds (absent = 0, present = 1) (Khonsari et al. 2009; Heimberg et al. 2010).
2. Neural crest (absent = 0, present = 1) (Khonsari et al. 2009; Heimberg et al. 2010). Note: *Ciona* is coded as absent for this character (see Discussion in Chapter 3).
3. Body shape (elongate, anguiliform = 0, dorsoventrally compressed = 1, transversely compressed = 2, fusiform/conical = 3). New character.
4. Position of nasohypophyseal opening (terminal = 0, dorsal = 1) (Donoghue et al. 2000; Turner et al. 2010).
5. Nasohypophyseal duct (absent = 0, present = 1) (Khonsari et al. 2009; Heimberg et al. 2010).
6. Paired nasal capsules (absent = 0, present = 1) (Khonsari et al. 2009; Heimberg et al. 2010). Character definition modified.
7. Paired nostrils (absent = 0, present = 1). New character.
8. Mouth position (ventral = 0, terminal = 1) (Donoghue et al. 2000; Turner et al. 2010).
9. Forward migration of postotic myomeres (absent = 0, present = 1) (Donoghue et al. 2000; Heimberg et al. 2010).
10. Horizontal septum in trunk myomeres (absent = 0, present = 1) (Donoghue et al. 2000; Heimberg et al. 2010).
11. Preoral gut diverticula (absent = 0, present = 1). New character.

Neural characters

12. Olfactory bulbs (absent = 0, present = 1) (Khonsari et al. 2009; Heimberg et al. 2010).
13. Pedunculated olfactory bulbs (absent = 0, present = 1) (Khonsari et al. 2009; Heimberg et al. 2010).

14. Terminal nerve (absent = 0, present = 1) (Khonsari et al. 2009; Heimberg et al. 2010).
15. Two eyes (absent = 0, present = 1) (Khonsari et al. 2009; Heimberg et al. 2010).
16. Lens placode (absent = 0, present = 1). A hagfish lacks a lens, but a lens placode occurs during development (Kuratani and Ota 2008).
17. Retina (absent = 0, present = 1) (Khonsari et al. 2009; Heimberg et al. 2010).
18. Lateral line system (absent = 0, present = 1) (Khonsari et al. 2009; Heimberg et al. 2010).
19. Recurrent ramus of the anterior lateral line nerve (absent=0, present = 1) (Khonsari et al. 2009; Heimberg et al. 2010).
20. Spiracular organs (absent = 0, present = 1) (Khonsari et al. 2009; Heimberg et al. 2010).
21. Lateral line neuromast cupulae (absent = 0, present = 1) (Khonsari et al. 2009; Heimberg et al. 2010).
22. Internal taste buds (absent = 0, present = 1) (Khonsari et al. 2009; Heimberg et al. 2010).
23. Electroreceptors (absent = 0, present = 1) (Khonsari et al. 2009; Heimberg et al. 2010).
24. Numerous electroreceptive regions on epithelium (absent = 0, present = 1) (Khonsari et al. 2009; Heimberg et al. 2010).
25. Endolymphatic organ (absent = 0, present =1). New character.
26. External opening of the endolymphatic duct (absent = 0, present = 1) (Khonsari et al. 2009; Heimberg et al. 2010).
27. Semicircular canals (absent = 0, present = 1) (Khonsari et al. 2009; Heimberg et al. 2010).
28. Horizontal semicircular canal (absent = 0, present = 1). New character.
29. Statoliths composed of calcium phosphate (absent = 0, present = 1) (Khonsari et al. 2009; Heimberg et al. 2010).
30. Hair cells in the inner ear with cupulae (absent = 0, present = 1) (Khonsari et al. 2009; Heimberg et al. 2010).

31. Mesencephalic trigeminal nucleus (absent=0, present=1) (Khonsari et al. 2009; Heimberg et al. 2010).
32. Fusion of the profundal nerve ganglion with the trigeminal ganglion (absent = 0, present = 1) (Khonsari et al. 2009; Heimberg et al. 2010).
33. Superficial ophthalmic trigeminal ramus (absent = 0, present = 1) (Khonsari et al. 2009; Heimberg et al. 2010).
34. Fusion of the maxillary trigeminal ramus with the buccal ramus of the anterolateral lateral line nerve (absent = 0, present = 1) (Khonsari et al. 2009; Heimberg et al. 2010).
35. Division of the facial nerve into pharyngeal, pre-, and posttrematic branches (absent = 0, present = 1) (Khonsari et al. 2009; Heimberg et al. 2010).
36. Hypodermal and dermal nerve plexi (absent = 0, present = 1) (Khonsari et al. 2009; Heimberg et al. 2010).
37. Viscero-sensory nerves (absent = 0, present = 1) (Khonsari et al. 2009; Heimberg et al. 2010).
38. Single glossopharyngeal ganglion (absent=0, present=1) (Khonsari et al. 2009; Heimberg et al. 2010).
39. Cardiac innervation (absent = 0, present = 1) (Khonsari et al. 2009; Heimberg et al. 2010).
40. Abducent nerve with retractor bulbi innervation (absent = 0, present = 1) (Khonsari et al. 2009; Heimberg et al. 2010).
41. Ciliary ganglion (absent = 0, present = 1) (Khonsari et al. 2009; Heimberg et al. 2010).
42. Extracranial ciliary ganglion (absent = 0, present = 1) (Khonsari et al. 2009; Heimberg et al. 2010).
43. Hypobranchial nerve (absent = 0, present = 1) (Khonsari et al. 2009; Heimberg et al. 2010).
44. Ventral branch of spinal ganglionated nerves contributes to the hypobranchial nerve (absent = 0, present = 1) (Khonsari et al. 2009; Heimberg et al. 2010).
45. Hypobranchial nerve formed by the fusion of the ventral branches of intracranial

nonganglionated postvagal nerves and the ventral branches of spinal ganglionated nerves (absent = 0, present = 1) (Khonsari et al. 2009; Heimberg et al. 2010).

46. Cerebellar primordia (absent = 0, present = 1) (Khonsari et al. 2009; Heimberg et al. 2010).
47. Hypothalamus (absent = 0, present = 1) (Khonsari et al. 2009; Heimberg et al. 2010).
48. Hypophysis (absent = 0, present = 1) (Khonsari et al. 2009; Heimberg et al. 2010).
49. Adenohypophysis (develops from a combined nasohypophyseal placode = 0, develops from a discrete hypophyseal placode = 1) (Khonsari et al. 2009; Heimberg et al. 2010).
50. Median eminence (absent = 0, present = 1) (Khonsari et al. 2009; Heimberg et al. 2010).
51. Superficial isthmic nucleus (absent = 0, present = 1) (Khonsari et al. 2009; Heimberg et al. 2010).
52. Preoptic area with magno- and parvocellular parts (absent = 0, present = 1) (Khonsari et al. 2009; Heimberg et al. 2010).
53. Tectum (absent = 0, present = 1) (Khonsari et al. 2009; Heimberg et al. 2010).
54. Less than five tectal laminae (absent = 0, present = 1) (Khonsari et al. 2009; Heimberg et al. 2010).
55. Thalamus (absent = 0, present = 1) (Khonsari et al. 2009; Heimberg et al. 2010).
56. Overlap of the areas with tectal and retinal projections in the dorsal thalamus (absent = 0, present = 1) (Khonsari et al. 2009; Heimberg et al. 2010).
57. Protrusion of the dorsal thalamus into the third ventricle (absent = 0, present = 1) (Khonsari et al. 2009; Heimberg et al. 2010).
58. Pineal organ (absent = 0, present = 1) (Donoghue et al. 2000; Turner et al. 2010).
59. Saccus vasculosus (absent = 0, present = 1) (Khonsari et al. 2009; Heimberg et al. 2010).
60. Pretectum (absent = 0, present = 1) (Khonsari et al. 2009; Heimberg et al. 2010).
61. Epithalamus (absent = 0, present = 1) (Khonsari et al. 2009; Heimberg et al.

2010).

62. Paraphysis (absent = 0, present = 1) (Khonsari et al. 2009; Heimberg et al. 2010).
63. Telencephalon (absent = 0, present = 1) (Khonsari et al. 2009; Heimberg et al. 2010).
64. Extensive median septum ependymal (absent = 0, present = 1) (Khonsari et al. 2009; Heimberg et al. 2010).
65. Subpallium (absent = 0, present = 1) (Khonsari et al. 2009; Heimberg et al. 2010).
66. Pallium (absent = 0, present = 1) (Khonsari et al. 2009; Heimberg et al. 2010).
67. Dorsal and ventral roots of the spinal nerves (remain unjoined = 0, join outside the nerve cord = 1) (Khonsari et al. 2009; Heimberg et al. 2010).
68. Ribbon-shaped spinal cord (absent = 0, present = 1) (Khonsari et al. 2009; Heimberg et al. 2010).
69. Blood supply in the spinal cord (absent = 0, present = 1) (Khonsari et al. 2009; Heimberg et al. 2010).
70. Regularly decreasing spinal cord diameter along the anteroposterior axis (absent = 0, present = 1) (Khonsari et al. 2009; Heimberg et al. 2010).
71. Müller cells (absent = 0, present = 1) (Khonsari et al. 2009; Heimberg et al. 2010).
72. Mauthner cells (absent = 0, present = 1) (Khonsari et al. 2009; Heimberg et al. 2010).
73. Choroid plexi (absent = 0, present = 1) (Khonsari et al. 2009; Heimberg et al. 2010).
74. Oligodendrocytes (absent = 0, present = 1) (Khonsari et al. 2009; Heimberg et al. 2010).
75. Astroglia (absent = 0, present = 1) (Khonsari et al. 2009; Heimberg et al. 2010).
76. Anastomotic capillary network in the brain (absent = 0, present = 1) (Khonsari et al. 2009; Heimberg et al. 2010).

Respiratory and circulatory characters

77. Pouch-shaped gills (absent = 0, present = 1) (Donoghue et al. 2000; Heimberg et al. 2010).
78. Elongate branchial series (more than 10 gill pouches/slits = 0, fewer than 10 = 1) (Donoghue et al. 2000; Heimberg et al. 2010).
79. Opercular flaps associated with gill openings (absent = 0, present = 1) (Donoghue et al. 2000; Heimberg et al. 2010).
80. Endodermal gill lamellae (absent = 0, present = 1) (Donoghue et al. 2000; Heimberg et al. 2010).
81. Gill lamellae with filaments (absent = 0, present = 1) (Donoghue et al. 2000; Heimberg et al. 2010).
82. Muscular-powered velum in mandibular domain (absent = 0, present = 1). Character definition modified.
83. Distinct stomach within digestive tract (absent = 0, present = 1) (Donoghue et al. 2000; Heimberg et al. 2010).
84. Subcutaneous open blood sinus (present = 0, absent = 1). Character definition modified.
85. Paired dorsal aortae (absent = 0, present = 1) (Donoghue et al. 2000; Heimberg et al. 2010).
86. Large lateral head vein (absent = 0, present = 1) (Donoghue et al. 2000; Heimberg et al. 2010).
87. Pulmonary vein (absent = 0, present = 1) (Donoghue et al. 2000; Heimberg et al. 2010).
88. Lymphocyte-based recombinatorial system of anticipatory immunity (absent = 0, present = 1) (Donoghue et al. 2000; Heimberg et al. 2010).
89. Lymphocytes (with variable lymphocyte receptor (VLR) antigen receptors = 0, true lymphocytes with T and B antigen receptors = 1) (Donoghue et al. 2000; Heimberg et al. 2010).

Skeletal characters

90. Skeletal differentiation of sclerotomes (absent = 0, present = 1). New character.
91. Dorsal arcualia (absent = 0, present = 1) (Heimberg et al. 2010). Heimberg et al. (2010) coded this character as present in hagfish. However, if the sclerotomal condensation in hagfish is to be compared to arcualia, the hagfish elements correspond to ventral arcualia (Ota et al. 2011). Either way, the sclerotomal elements of hagfish migrate to support the caudal fin and do not retain their para-, infra-, or supra-chordal positions. Therefore, these are not conventional arcualia as identified in vertebrates. It is possible to introduce two new characters (sclerotomal condentations, dorsal; and sclerotomal condensations, ventral) to group hagfish together with other vertebrates. The characters would be coded inapplicable for any taxon that does not have skeletal differentiation of sclerotomes, and the morphology of the sclerotomal condensation in *Haikouella* is uncertain (coded as "?"). As a result, the character for dorsal sclerotomal condensation would be phylogenetically uninformative (absence autapomorphic to hagfish), and the one for ventral sclerotomal condensation would be constant (present in all taxa for which the character can be coded). Therefore, these characters do not merit inclusion in the analysis under the current taxonomic sampling.
92. Ventral arcualia (absent = 0, present = 1) (Heimberg et al. 2010).
93. Dorsal fin: separate dorsal fin (absent = 0, present = 1) (Donoghue et al. 2000; Heimberg et al. 2010).
94. Anal fin separate (absent = 0, present = 1) (Donoghue et al. 2000; Heimberg et al. 2010).
95. Fin ray supports (absent = 0, present = 1) (Donoghue et al. 2000; Heimberg et al. 2010).
96. Paired fins (absent = 0, present = 1). New character.
97. Pectoral fins (absent = 0, present = 1) (Donoghue et al. 2000; Heimberg et al. 2010).
98. Pelvic fins (absent = 0, present = 1) (Donoghue et al. 2000; Heimberg et al.

2010).

99. Tail shape (no distinct lobes developed = 0, distinct lobes present = 1). Character definition modified.
100. Tail shape (ventral lobe much larger than dorsal = 0, dorsal lobe much larger than ventral = 1, dorsal and ventral lobes almost equally developed = 2). Unordered. Character definition modified.
101. Chordal disposition relative to tail development (isochordal = 0, hypochordal = 1, hyperchordal = 2) (Donoghue et al. 2000; Heimberg et al. 2010).
102. Ability to synthesize creatine phosphatase (absent = 0, present = 1) (Donoghue et al. 2000; Heimberg et al. 2010).
103. Visceral arches fused to the neurocranium (absent = 0, present = 1) (Donoghue et al. 2000; Heimberg et al. 2010).
104. Relative position of the pharyngeal skeleton to the gills and associated vasculature (lateral = 0, medial = 1) (Donoghue et al. 2000; Heimberg et al. 2010).
105. Keratinous teeth (absent = 0, present = 1) (Donoghue et al. 2000; Heimberg et al. 2010).
106. Trematic rings (absent = 0, present = 1) (Donoghue et al. 2000; Heimberg et al. 2010). Modified. Hagfish do not have trematic rings.
107. Annular cartilage (absent = 0, present = 1)
108. Lingual apparatus (absent = 0, present = 1). Character definition modified.
109. Longitudinally aligned tooth rows providing transverse bite (absent = 0, present = 1) (Donoghue et al. 2000; Heimberg et al. 2010).
110. Jaws (absent = 0, present = 1) (Donoghue et al. 2000; Heimberg et al. 2010).
111. Braincase with lateral walls (absent = 0, present = 1) (Donoghue et al. 2000; Heimberg et al. 2010).
112. Occiput enclosing vagus and glossopharyngeal. Enclosure of cranial nerves IX and X and glossopharyngeal and vagus nerves (absent = 0, present = 1) (Donoghue et al. 2000; Heimberg et al. 2010).
113. Collagenous matrix as skeletal support (entirely acellular = 0, cellular

cartilage = 1). Character definition modified.

114. Cellular cartilage (soft and hard = 0, hard only = 1). New character.
115. Perichondral bone (absent = 0, present = 1) (Donoghue et al. 2000; Heimberg et al. 2010).
116. Calcified cartilage (absent = 0, present = 1) (Donoghue et al. 2000; Heimberg et al. 2010).
117. Calcified dermal skeleton (absent = 0, present = 1). Character definition modified.
118. Dentine (absent = 0, present = 1). Character definition modified.
119. Types of dentine (methodentine = 0, orthodentine = 1). Character definition modified.
120. Enamel/oid (absent = 0, present = 1) (Donoghue et al. 2000; Heimberg et al. 2010).
121. Spongy aspidin (absent = 0, present = 1) (Donoghue et al. 2000; Turner et al. 2010).
122. Lamellar aspidin (absent = 0, present = 1) (Donoghue et al. 2000; Turner et al. 2010).
123. Three-layered exoskeleton (absent = 0, present = 1) (Donoghue et al. 2000; Turner et al. 2010).
124. Cancellar layer in exoskeleton with honey-comb shaped cavities (absent = 0, present =1) (Donoghue et al. 2000; Turner et al. 2010).
125. Scales or denticles (absent = 0, present = 1). Character definition modified.
126. Scales or denticles, morphology (single odontode = 0, polyodontode = 1). Character definition modified.
127. Scales or denticles, morphology (diamond-shaped = 0, rod-shaped = 1) (Donoghue et al. 2000; Turner et al. 2010).
128. Oak-leaf shaped tubercles (absent = 0, present =1) (Donoghue et al. 2000; Turner et al. 2010).
129. Oral plates (absent = 0, present =1) (Donoghue et al. 2000; Turner et al. 2010).

130. Denticles in pharynx (absent = 0, present = 1) (Donoghue et al. 2000; Turner et al. 2010).
131. Dermal head covering (absent = 0, present = 1) (Donoghue et al. 2000; Turner et al. 2010).
132. Dermal head covering (micromeric = 0, large plates = 1) (Donoghue et al. 2000; Turner et al. 2010).
133. Large dermal plates (paired = 0, unpaired = 1) (Donoghue et al. 2000; Turner et al. 2010).
134. Massive endoskeletal head shield (does not cover gills = 0, covers gills dorsally = 1) (Donoghue et al. 2000; Turner et al. 2010).
135. Sclerotic ossicles (absent = 0, present = 1) (Donoghue et al. 2000; Heimberg et al. 2010).

Physiological characters

136. Hemoglobins (exist as monomers when oxygenated and form complex dimeric or tetrameric aggregates when deoxygenated = 0, exist as stable tetramers = 1) (Donoghue et al. 2000; Heimberg et al. 2010).
137. High blood pressure (absent = 0, present = 1) (Donoghue et al. 2000; Heimberg et al. 2010).
138. Hyperosmoregulation (absent = 0, present = 1) (Donoghue et al. 2000; Heimberg et al. 2010).
139. Pituitary control of gametogenesis (absent = 0, present = 1) (Donoghue et al. 2000; Heimberg et al. 2010).
140. Spleen (absent = 0, present = 1) (Donoghue et al. 2000; Heimberg et al. 2010).
141. Separate endocrine and exocrine pancreas (absent = 0, present = 1) (Donoghue et al. 2000; Heimberg et al. 2010).
142. A cells (absent = 0, present = 1) (Donoghue et al. 2000; Heimberg et al. 2010).
143. B cells (absent = 0, present = 1) (Donoghue et al. 2000; Heimberg et al.

2010).

Reproductive characters

144. Male gametes shed directly through the coelom (absent = 0, present= 1) (Donoghue et al. 2000; Heimberg et al. 2010).

145. Larval phase (absent = 0, present = 1) (Donoghue et al. 2000; Heimberg et al. 2010).

Appendix 4-2. Data Matrix of Phenotypic Characters

Lampreys are split into *Lampetra fluvialis* and *Petromyzon marinus* when miRNA data are included. These two genera code identically for all phenotypic characters.

	1	2	3	4	5	6	7	8	9	10	11	12	13	14	15	16	17
Cephalochordata	0	0	2	-	0	-	-	0	-	-	1	0	-	-	0	0	0
Urochordata	1	0	-	-	0	-	-	-	0	-	1	0	-	-	0	0	0
Yunnanozoa	?	?	2	?	?	?	?	0	0	?	?	?	?	?	1	?	?
Myllokummingiidae	?	?	2	0	1	1	0	?	0	?	?	?	0	?	1	?	?
Hagfish	1	1	0	0	1	0	0	0	0	1	1	1	0	0	1	0	1
Lamprey	0	1	0	1	1	0	0	1	0	1	0	1	0	0	1	1	1
Euconodonta	?	1	0	?	?	?	?	1	0	?	?	?	?	?	1	?	?
Heterostraci	?	1	1	0	1	1	0	0	?	?	?	1	0	?	1	?	?
Arandaspida	?	1	1	0	1	1	1	1	?	?	?	?	?	?	1	?	?
Anaspida	?	1	2	1	1	0	0	1	?	?	?	1	?	?	1	?	?
Euphanerops	?	1	2	1	1	?	0	1	?	?	?	?	?	?	1	?	?
Thelodonti	?	1	?	0	1	1	0	1	?	?	?	1	?	?	1	?	?
Pituriaspida	?	1	1	?	1	?	0	0	?	?	?	?	?	?	1	?	?
Galeaspida	?	1	1	1	1	1	0	0	?	?	?	1	0	?	1	?	?
Osteostraci	?	1	1	1	1	0	0	1	?	?	?	1	0	?	1	?	?
Chondrichthyes	1	1	3	1	0	1	1	1	1	0	0	1	1	1	1	1	1
Bichir	0	1	1	1	0	1	1	1	1	0	0	1	0	1	1	1	1
Lungfish	1	1	1	1	0	1	1	1	1	0	0	1	1	1	1	1	1
Coelacanth	1	1	2	1	0	1	1	1	1	0	0	1	1	0	1	1	1
Salamander	1	1	-	1	0	1	1	1	1	0	0	1	1	1	1	1	1

Appendix 4-2 (cont.)

	18	19	20	21	22	23	24	25	26	27	28	29	30	31	32	33	34
Cephalochordata	0	-	0	-	0	0	-	0	-	0	-	0	0	-	-	-	-
Urochordata	0	-	1	-	0	0	-	0	-	0	-	0	0	-	-	-	-
Yunnanozoa	?	?	0	?	?	?	?	?	?	?	?	?	?	?	?	?	?
Myllokummingiidae	?	?	0	?	?	?	?	?	?	?	?	?	?	?	?	?	?
Hagfish	1	0	0	0	0	0	-	1	0	1	0	1	0	0	1	0	0
Lamprey	1	1	0	0	1	1	1	1	0	1	0	1	1	0	1	1	0
Euconodonta	?	?	?	?	?	?	?	?	?	?	?	?	?	?	?	?	?
Heterostraci	?	?	1	?	?	?	?	1	0	1	0	?	?	?	?	?	?
Arandaspida	?	?	0	?	?	?	?	1	0	1	?	?	?	?	?	?	?
Anaspida	1	?	0	?	?	?	?	1	0	1	?	?	?	?	?	?	?
Euphanerops	?	?	0	?	?	?	?	1	0	1	?	?	?	?	?	?	?
Thelodonti	?	?	0	?	?	?	?	1	?	1	0	?	?	?	?	?	?
Pituriaspida	?	?	1	?	?	?	?	1	0	1	?	?	?	?	?	?	?
Galeaspida	1	?	0	?	?	?	?	1	0	1	0	?	?	?	?	1	?
Osteostraci	1	?	0	?	?	?	?	1	1	1	0	?	?	?	?	1	?
Chondrichthyes	1	0	0	1	1	1	1	1	1	1	1	0	1	1	0	1	1
Bichir	1	0	1	1	1	1	0	1	0	1	1	0	1	1	0	1	1
Lungfish	1	1	1	1	1	1	0	1	1	1	1	0	1	1	1	1	1
Coelacanth	1	0	0	1	1	1	0	1	0	1	1	0	1	1	0	0	1
Salamander	1	0	0	1	1	1	1	1	1	1	1	0	1	1	0	1	1

Appendix 4-2 (cont.)

	35	36	37	38	39	40	41	42	43	44	45	46	47	48	49	50	51
Cephalochordata	-	1	0	-	0	-	0	-	0	-	-	0	0	0	-	-	-
Urochordata	-	1	0	-	1	-	0	-	0	-	-	0	0	0	-	-	-
Yunnanozoa	?	?	?	?	?	?	?	?	?	?	?	?	?	?	?	?	?
Myllokummingiidae	?	?	?	?	?	?	?	?	?	?	?	?	?	?	?	?	?
Hagfish	0	1	1	1	0	-	0	-	0	-	-	0	1	1	0	0	0
Lamprey	0	1	1	1	1	0	0	-	?	0	0	1	1	1	0	0	0
Euconodonta	?	?	?	?	?	?	?	?	?	?	?	?	?	?	?	?	?
Heterostraci	?	?	1	?	?	?	?	?	?	?	?	?	?	1	0	?	?
Arandaspida	?	?	?	?	?	?	?	?	?	?	?	?	?	?	?	?	?
Anaspida	?	?	?	?	?	?	?	?	?	?	?	?	?	?	0	?	?
Euphanerops	?	?	?	?	?	?	?	?	?	?	?	?	?	?	0	?	?
Thelodonti	?	?	?	?	?	?	?	?	?	?	?	?	?	?	0	?	?
Pituriaspida	?	?	?	?	?	?	?	?	?	?	?	?	?	?	0	?	?
Galeaspida	?	1	1	?	?	?	?	?	?	?	?	?	?	1	1	?	?
Osteostraci	?	1	1	?	?	?	?	?	?	?	?	?	?	1	0	?	?
Chondrichthyes	1	0	1	1	1	0	1	1	1	1	1	1	1	1	1	1	0
Bichir	1	0	1	1	1	0	1	1	1	1	1	1	1	1	1	1	0
Lungfish	1	0	1	1	1	0	1	1	1	1	0	1	1	1	1	1	1
Coelacanth	1	0	1	0	1	1	1	0	1	0	0	1	1	1	1	1	1
Salamander	1	0	1	0	1	1	1	0	1	1	0	1	1	1	1	1	0

Appendix 4-2 (cont.)

	52	53	54	55	56	57	58	59	60	61	62	63	64	65	66	67	68
Cephalochordata	-	0	-	0	-	-	0	0	0	0	-	0	0	0	0	0	-
Urochordata	-	0	-	0	-	-	0	1	0	0	-	0	0	0	0	-	-
Yunnanozoa	?	?	?	?	?	?	?	?	?	?	?	?	?	?	?	?	?
Myllokummingiidae	?	?	?	?	?	?	?	?	?	?	?	?	?	?	?	?	?
Hagfish	?	1	1	1	-	-	0	0	1	1	0	1	0	1	1	1	1
Lamprey	0	1	0	1	?	?	1	0	1	1	1	1	0	1	1	0	1
Euconodonta	?	?	?	?	?	?	?	?	?	?	?	?	?	?	?	?	?
Heterostraci	?	?	?	?	?	?	1	?	?	1	?	?	?	?	?	?	?
Arandaspida	?	?	?	?	?	?	1	?	?	1	?	?	?	?	?	?	?
Anaspida	?	?	?	?	?	?	1	?	?	1	?	?	?	?	?	?	?
Euphanerops	?	?	?	?	?	?	1	?	?	?	?	?	?	?	?	?	?
Thelodonti	?	?	?	?	?	?	?	?	?	?	?	?	?	?	?	?	?
Pituriaspida	?	?	?	?	?	?	?	?	?	?	?	?	?	?	?	?	?
Galeaspida	?	1	?	?	?	?	1	?	?	1	?	1	?	?	?	?	?
Osteostraci	?	1	?	?	?	?	1	?	?	1	?	1	?	?	?	?	?
Chondrichthyes	0	1	0	1	1	0	1	1	1	1	0	1	0	1	1	1	0
Bichir	1	1	0	1	1	0	1	1	1	1	1	1	1	1	1	1	0
Lungfish	1	1	1	1	1	1	1	0	1	1	1	1	1	1	1	1	0
Coelacanth	1	1	1	1	0	1	1	1	1	1	1	1	1	1	1	1	0
Salamander	1	1	0	1	0	0	1	0	1	1	1	1	0	1	1	1	0

Appendix 4-2 (cont.)

	69	70	71	72	73	74	75	76	77	78	79	80	81	82	83	84	85
Cephalochordata	0	1	0	0	0	1	0	0	0	0	0	1	0	-	0	0	1
Urochordata	0	0	0	0	0	?	?	0	0	0	0	0	0	-	0	0	0
Yunnanozoa	?	?	?	?	?	?	?	?	1	0	0	?	?	-	0	?	?
Myllokummingiidae	?	?	?	?	?	?	?	?	1	1	0	?	?	?	0	?	?
Hagfish	1	1	0	0	0	0	1	1	1	0	0	1	0	1	0	0	1
Lamprey	0	1	0	1	1	0	0	0	1	1	0	1	1	1	0	1	0
Euconodonta	?	?	?	?	?	?	?	?	?	?	?	?	?	?	?	?	?
Heterostraci	?	?	?	?	?	?	?	?	1	1	0	?	?	1	?	?	?
Arandaspida	?	?	?	?	?	?	?	?	1	1	0	?	?	?	?	?	?
Anaspida	?	?	?	?	?	?	?	?	1	0	0	?	?	?	?	?	?
Euphanerops	?	?	?	?	?	?	?	?	1	0	0	?	?	?	0	?	?
Thelodonti	?	?	?	?	?	?	?	?	1	1	0	?	?	?	1	?	?
Pituriaspida	?	?	?	?	?	?	?	?	?	?	?	?	?	?	?	?	?
Galeaspida	?	?	?	?	?	?	?	?	1	0	0	?	?	1	?	?	?
Osteostraci	?	?	?	?	?	?	?	?	1	1	0	?	?	1	?	?	0
Chondrichthyes	1	1	1	1	1	1	1	1	0	1	0	0	1	0	1	1	1
Bichir	1	1	0	1	1	1	1	1	0	1	1	0	1	0	1	1	1
Lungfish	1	1	0	1	1	1	1	1	0	1	1	0	1	0	0	1	1
Coelacanth	1	0	1	1	1	1	1	1	0	1	1	0	1	0	1	1	1
Salamander	1	0	0	1	1	1	1	1	0	1	1	0	1	0	1	1	1

Appendix 4-2 (cont.)

	86	87	88	89	90	91	92	93	94	95	96	97	98	99	100	101	102
Cephalochordata	0	0	0	-	0	-	-	0	0	0	0	0	-	0	-	0	0
Urochordata	0	0	0	-	0	-	-	0	0	0	0	0	-	0	-	0	0
Yunnanozoa	?	?	?	?	1	0	0	0	0	0	0	0	-	0	-	0	?
Myllokummingiidae	?	?	?	?	1	1	1	1	0	0	0	0	-	0	-	?	?
Hagfish	0	0	1	0	1	0	0	0	0	1	0	0	-	0	-	1	1
Lamprey	0	0	1	0	1	1	0	1	1	1	0	0	-	1	1	1	1
Euconodonta	?	?	?	?	?	?	?	0	0	1	0	0	-	0	-	1	?
Heterostraci	?	?	?	?	?	?	?	0	0	1	0	0	-	0	-	0	?
Arandaspida	?	?	?	?	?	?	?	0	0	?	0	0	-	1	2	1	?
Anaspida	?	?	?	?	1	1	1	0	1	1	0	0	1	1	0	1	?
Euphanerops	?	?	?	?	1	1	1	1	1	1	0	0	1	1	0	1	?
Thelodonti	?	?	?	?	?	?	?	1	1	1	1	0	0	1	2	1	?
Pituriaspida	?	?	?	?	?	?	?	?	?	?	1	?	0	?	?	?	?
Galeaspida	1	?	?	?	1	1	1	0	0	?	0	0	-	?	?	?	?
Osteostraci	1	0	?	?	1	1	1	1	0	?	1	0	0	0	-	2	?
Chondrichthyes	1	0	1	1	1	1	1	1	0	1	1	1	0	1	1	2	1
Bichir	1	0	1	1	1	1	1	1	1	1	1	1	0	0	-	2	1
Lungfish	1	1	1	1	1	1	1	1	0	1	1	1	1	0	-	1	1
Coelacanth	1	1	1	1	1	1	1	1	1	1	1	1	1	1	2	0	1
Salamander	1	1	1	1	1	1	1	0	0	0	1	1	-	0	-	0	1

Appendix 4-2 (cont.)

	103	104	105	106	107	108	109	110	111	112	113	114	115	116	117	118	119
Cephalochordata	-	0	-	0	-	-	-	-	0	-	0	-	0	0	0	-	-
Urochordata	-	-	-	0	-	-	-	-	0	-	0	-	0	0	0	-	-
Yunnanozoa	?	0	?	0	0	-	?	-	0	-	?	?	0	0	0	-	-
Myllokummingiidae	?	0	?	?	0	?	?	0	0	-	?	?	0	0	0	-	-
Hagfish	1	0	1	0	0	1	1	0	0	-	1	0	0	0	0	-	-
Lamprey	1	0	1	1	1	1	1	0	1	0	1	0	0	0	0	-	-
Euconodonta	?	?	0	0	0	1	1	0	0	-	?	?	0	0	0	-	-
Heterostraci	1	0	0	?	0	1	0	0	1	0	?	?	0	0	1	1	0
Arandaspida	?	?	?	?	0	?	?	0	?	?	?	?	0	0	1	0	-
Anaspida	?	0	?	?	0	?	?	0	?	?	?	?	0	?	1	0	-
Euphanerops	1	0	?	?	1	1	?	0	?	?	1	?	0	1	0	-	-
Thelodonti	?	?	?	?	0	?	?	0	?	?	?	?	0	0	1	1	0
Pituriaspida	?	?	?	?	0	?	?	0	?	?	?	?	1	0	1	?	?
Galeaspida	1	0	?	?	0	?	?	0	1	1	1	?	1	0	1	0	-
Osteostraci	1	0	0	?	0	?	0	0	1	1	1	?	1	0	1	1	0
Chondrichthyes	0	1	0	0	0	0	0	1	1	1	1	1	0	1	1	1	1
Bichir	0	1	0	0	0	0	0	1	1	1	1	1	1	0	1	1	1
Lungfish	0	1	0	0	0	0	0	1	1	1	1	1	1	0	1	1	1
Coelacanth	0	1	0	0	0	0	0	1	1	1	1	1	1	0	1	1	1
Salamander	0	-	0	0	0	0	0	1	1	1	1	1	1	0	1	1	1

Appendix 4-2 (cont.)

	120	121	122	123	124	125	126	127	128	129	130	131	132	133	134	135	136
Cephalochordata	0	-	-	-	-	0	-	-	-	0	-	0	-	-	-	-	?
Urochordata	0	-	-	-	-	0	-	-	-	0	-	0	-	-	-	-	?
Yunnanozoa	-	0	0	-	-	0	-	-	-	0	-	0	-	-	-	0	?
Myllokummingiidae	-	0	0	-	-	0	-	-	-	0	-	0	-	-	-	0	?
Hagfish	-	0	0	-	-	0	-	-	-	0	-	0	-	-	0	0	0
Lamprey	-	0	0	-	-	0	-	-	-	0	-	0	-	-	0	0	0
Euconodonta	-	0	0	-	-	0	-	-	-	0	-	0	-	-	?	0	?
Heterostraci	0	1	1	1	1	1	1	(0/1)	1	1	0	1	1	1	0	0	?
Arandaspida	0	1	1	1	1	1	1	1	1	1	0	1	1	1	0	1	?
Anaspida	0	0	0	0	0	1	1	1	0	1	0	1	0	0	0	0	?
Euphanerops	0	0	0	0	0	0	-	-	-	0	-	0	-	0	1	0	?
Thelodonti	1	0	0	0	0	1	0	0	0	0	1	1	0	0	0	0	?
Pituriaspida	?	?	?	?	?	?	?	?	?	?	?	1	1	1	1	0	?
Galeaspida	0	0	1	0	0	1	0	0	0	1	0	1	1	0	1	1	?
Osteostraci	0	0	0	1	0	1	1	0	0	1	0	1	1	0	1	1	?
Chondrichthyes	1	0	0	1	0	1	1	0	0	0	1	1	1	0	0	0	1
Bichir	1	0	0	1	0	1	1	0	0	0	1	1	1	0	0	0	1
Lungfish	1	0	0	1	0	1	1	0	0	0	0	1	1	0	0	0	1
Coelacanth	1	0	0	1	0	1	1	0	0	0	0	1	1	0	0	1	1
Salamander	1	0	0	1	0	1	0	-	-	-	0	1	1	0	0	1	1

Appendix 4-2 (cont.)

	137	138	139	140	141	142	143	144	145
Cephalochordata	0	0	-	-	-	0	0	-	1
Urochordata	0	0	-	-	-	0	0	-	1
Yunnanozoa	?	?	?	?	?	?	?	?	?
Myllokummingiidae	?	?	?	?	?	?	?	?	?
Hagfish	0	0	1	0	1	0	1	1	0
Lamprey	1	1	1	0	1	0	1	1	1
Euconodonta	?	?	?	?	?	?	?	?	?
Heterostraci	?	?	?	?	?	?	?	?	?
Arandaspida	?	?	?	?	?	?	?	?	?
Anaspida	?	?	?	?	?	?	?	?	?
Euphanerops	?	?	?	?	?	?	?	?	?
Thelodonti	?	?	?	?	?	?	?	?	?
Pituriaspida	?	?	?	?	?	?	?	?	?
Galeaspida	?	?	?	?	?	?	?	?	?
Osteostraci	?	?	?	?	?	?	?	?	?
Chondrichthyes	1	1	1	1	0	1	1	0	0
Bichir	1	1	1	1	0	1	1	0	0
Lungfish	1	1	1	1	0	1	1	0	0
Coelacanth	1	1	1	1	0	1	1	0	0
Salamander	1	1	1	1	0	1	1	0	1